INFORMATION TO USERS

This manuscript has been reproduced from the microfilm master. UMI films the text directly from the original or copy submitted. Thus, some thesis and dissertation copies are in typewriter face, while others may be from any type of computer printer.

The quality of this reproduction is dependent upon the quality of the copy submitted. Broken or indistinct print, colored or poor quality illustrations and photographs, print bleedthrough, substandard margins, and improper alignment can adversely affect reproduction.

In the unlikely event that the author did not send UMI a complete manuscript and there are missing pages, these will be noted. Also, if unauthorized copyright material had to be removed, a note will indicate the deletion.

Oversize materials (e.g., maps, drawings, charts) are reproduced by sectioning the original, beginning at the upper left-hand corner and continuing from left to right in equal sections with small overlaps.

Photographs included in the original manuscript have been reproduced xerographically in this copy. Higher quality 6" x 9" black and white photographic prints are available for any photographs or illustrations appearing in this copy for an additional charge. Contact UMI directly to order.

ProQuest Information and Learning
300 North Zeeb Road, Ann Arbor, MI 48106-1346 USA
800-521-0600

DISSERTATION

MOLECULAR AND PHYLOGENETIC ANALYSES OF A CALCIUM/CALMODULIN-REGULATED MICROTUBULE MOTOR PROTEIN FROM DIVERSE PHOTOSYNTHETIC EUKARYOTES

Submitted by

Salah Esmat Abdel-Ghany

Biology Department

In partial fulfillment of the requirements

For the Degree of Doctor of Philosophy

Colorado State University

Fort Collins, Colorado

Spring 2001

Bell & Howell Information and Learning Company
300 North Zeeb Road
P.O. Box 1346
Ann Arbor, MI 48106-1346

COLORADO STATE UNIVERSITY

March 21, 2001

WE HEREBY RECOMMEND THAT THE DISSERTATION PREPARED UNDER OUR SUPERVISION BY SALAH ESMAT ABDEL-GHANY ENTITLED MOLECULAR AND PHYLOGENETIC ANALYSES OF A CALCIUM/CALMODULIN-REGULATED MICROTUBULE MOTOR PROTEIN FROM DIVERSE PHOTOSYNTHETIC EUKARYOTES BE ACCEPTED AS FULFILLING IN PART REQUIREMENTS FOR THE DEGREE OF DOCTOR OF PHILOSOPHY.

Committee on Graduate Work

Rajinder T. Ram

Advisor

Department Head

ABSTRACT OF DISSERTATION

MOLECULAR AND PHYLOGENETIC ANALYSES OF A CALCIUM/CALMODULIN-REGULATED MICROTUBULE MOTOR PROTEIN FROM DIVERSE PHOTOSYNTHETIC EUKARYOTES

The kinesin -like calmodulin (CaM) binding protein (KCBP), a minus end-directed microtubule (MT) motor protein was previously cloned and characterized from dicot species. Like other members of the kinesin superfamily, KCBP has three domains (tail, stalk, and motor). KCBP is unique among all known kinesin-like proteins (KLPs) in having a myosin tail homology 4 domain and talin-like domain (present in some myosin) and a calmodulin-binding domain (CBD). The activity of KCBP has been shown to be negatively regulated by Ca^{2+}/CaM. Genetic studies have indicated a role for KCBP in trichome morphogenesis. In addition, immunolocalization and microinjection studies with KCBP-specific antibody suggest a role for KCBP in plant cell division. Orthologs of KCBP have not been found in the completely sequenced genome of *Drosophila melanogaster*, *Caenorhabditis elegans*, and *Saccharomyces cerevisiae*. The involvement of KCBP in plant-specific functions and its absence in animals and fungi suggest that KCBP is a plant-specific motor protein. To investigate the origin and evolution of KCBP, I used various molecular approaches to clone and characterize KCBP orthologs from phylogenetically diverse photosynthetic species, including *Zea mays* (maize), a highly evolved flowering plant; *Picea abies* (spruce), a representative member of gymnosperms; a *Stichococcus*, a member of charaphyte algae, which are thought to be

primitive living photosynthetic eukaryotes. Analyses of the structural organization of KCBP genes have shown that KCBP with its characteristic domains is conserved among all studied organisms, suggesting its origin along with or prior to the evolution of plastids. KCBP in all studied organisms is detected by affinity-purified KCBP antibody to the CBD, suggesting the topology conservation of their CBDs. The C-terminal region of KCBP with the motor domain and CBD was cloned into expression vectors and the fusion protein from these constructs was bound to CaM in the presence of Ca^{2+}. Chelation of Ca^{2+} abolished CaM interaction with KCBP. Although the coding sequences of KCBP are highly conserved, the number, length, and the position of intervening sequences are highly diverged. DNA blot analysis showed that KCBP is a single copy gene in all studied organisms, suggesting that this gene could be used in phylogenetic analysis to study the relationship among photosynthetic eukaryotes.

Salah E. Abdel-Ghany
Department of Biology
Colorado State University
Fort Collins, CO. 80523
Spring 2001

ACKNOWLEDGMENT

First and foremost I would like to express my gratitude to my God for every thing and particularly for giving me this great opportunity to work with this wonderful committee and in between those wonderful people in Dr. Reddy's lab. Dr. Reddy, nothing is enough to tell about your intelligent guidance, support, encourage, kindness and optimism. I feel very grateful and proud to be your student. Special thanks go to Dr. Paul Kugrens for continuous help and answering my questions. I also want to acknowledge Dr. Steve Stack, Dr. Rajinder Ranu for serving on my committee and for the assistance they have given to me.

For those wonderful people in our lab, Drs. Irene Day, Farida Safadi, Maxim Golovkin, Vaka Reddy, Gul-Shad Ali, Yu-Lin Kao, and Tyler Thomas, I will never forget your help, company and the wonderful days that we spent together.

I also would like to express my sincere thanks to all Professors, Drs. and friends in Faculty of Science, Zagazig University, Egypt, particularly Prof. Yassin El-Ayouty for his uncountable help at the beginning of my graduate study, Dr. Mahmoud Desouky, Alaa said and Aymn El-Haddad for the best company I have.

Financial assistance from the Egyptian Government, Ministry of High Education is gratefully acknowledgment.

And finally, thanks Father and Mother, for providing us with every thing that really helped us in this world.

DEDICATION

To

My father and the memory of my father-in-low

My two mothers

My Brother and sister

My wife whose encouragement and love kept

me going from start to finish

And my lovely kids

Hadeel and Ahmad

For letting me see the joy and wonder of the life

TABLE OF CONTENTS

LIST OF FIGURES

List of Tables

CHAPTER 1

INTRODUCTION

INTRODUCTION

I. CYTOSKELETON AND MOLECULAR MOTORS

Much of cell behavior and architecture depends on the directed transport of macromolecules, membranes, chromosomes, organelles, and vesicles within the cytoplasm. Many of these processes depend on a complex interaction between linear polymers referred to as the cytoskeleton and a specialized class of cytoskeleton-associated protein called motor proteins. The cytoskeleton is a highly dynamic network that reorganizes continuously as the cell changes shape, divides or responds to hormonal and environmental signals and so the cytoskeleton provides the driving force for cells to move and divide (Reddy, 2001). The cytoskeleton of eukaryotes is made of three types of filaments: microfilaments (actin filaments), intermediate filaments, and microtubules (MTs). As the names suggest, the diameter of the intermediate filaments (10 nm) is intermediate between microfilament (5-9 nm) and MTs (25 nm). The cytoskeletal elements are connected to one another by cytoskeletal-associated proteins (actin-binding proteins and MT-associated proteins, MAPS) (Yang *et al.*, 1996; Fuchs and Cleveland, 1998; Hirokawa, 1998; Mermall *et al.*, 1998; Reddy, 2001).

The molecular motors fall into three families of proteins: (i) myosins, which move toward the plus end of actin filaments; (ii) kinesins, which are either plus-end-directed or minus-end-directed MT motors; and (iii) dyneins, which are minus-end-directed MT motors (Hirokawa, 1998; Mermall *et al.*, 1998; Brown, 1999). These proteins convert the chemical energy released from hydrolysis of nucleotide triphosphate (ATP or GTP) into kinetic energy for movement along a cytoskeletal polymer. Thus motor proteins act as molecular vehicles

that travel along the cytoskeletal net work to transport cargo in various forms including vesicles, organelles, chromosomes, and cytoskeletal elements (Mountain and Compton, 2000).

A. Actin cytoskeleton and Myosin motors

The actin cytoskeleton is a dynamic structure, which is involved in a variety of cellular activities. In plants, actin filaments are presumed to play essential roles in many important processes including cell division, cell elongation, establishment of cytoplasmic organization, cytoplasmic streaming, pathogen response, tropism, and pollen tube growth (Kost *et al.*, 1998). A number of actin-based motors called myosins have been characterized from a number of eukaryotes. Myosins are a diverse class of related proteins that share a common domain with actin and ATP-binding sites (Fig 1). Each molecule of myosin consists of two heavy chains (HCs) and four light chains (LCs). Each HC is typically constructed of three functional subdomains. (i) a highly conserved motor domain at the N-terminus with actin- and ATP-binding sites. (ii) a neck domain that binds light chain or calmodulin (CaM), and (iii) a non-conserved tail domain which serves to anchor and position the motor domain and to interact with specific cargo (Seiler *et al.*, 2000; Reddy, 2001). Light chains and CaM bind to a helical sequence in the neck region termed the IQ motif with the consensus sequence IQXXXRGXXXR (Wolenski *et al.*, 1993; Wolenski, 1995). The number of IQ motifs in different myosins can vary between zero and six. Phylogenetic analysis based upon the motor domain groups myosins into 15 distinct classes. To date no class of myosins appears to be universally expressed in all tested phyla (Seiler *et al.*, 2000). Myosins are regulated by multiple mechanisms including Ca^{2+}/CaM regulation and protein phosphylation (for more information, see the recent review by (Reddy, 2001). Myosins are responsible for

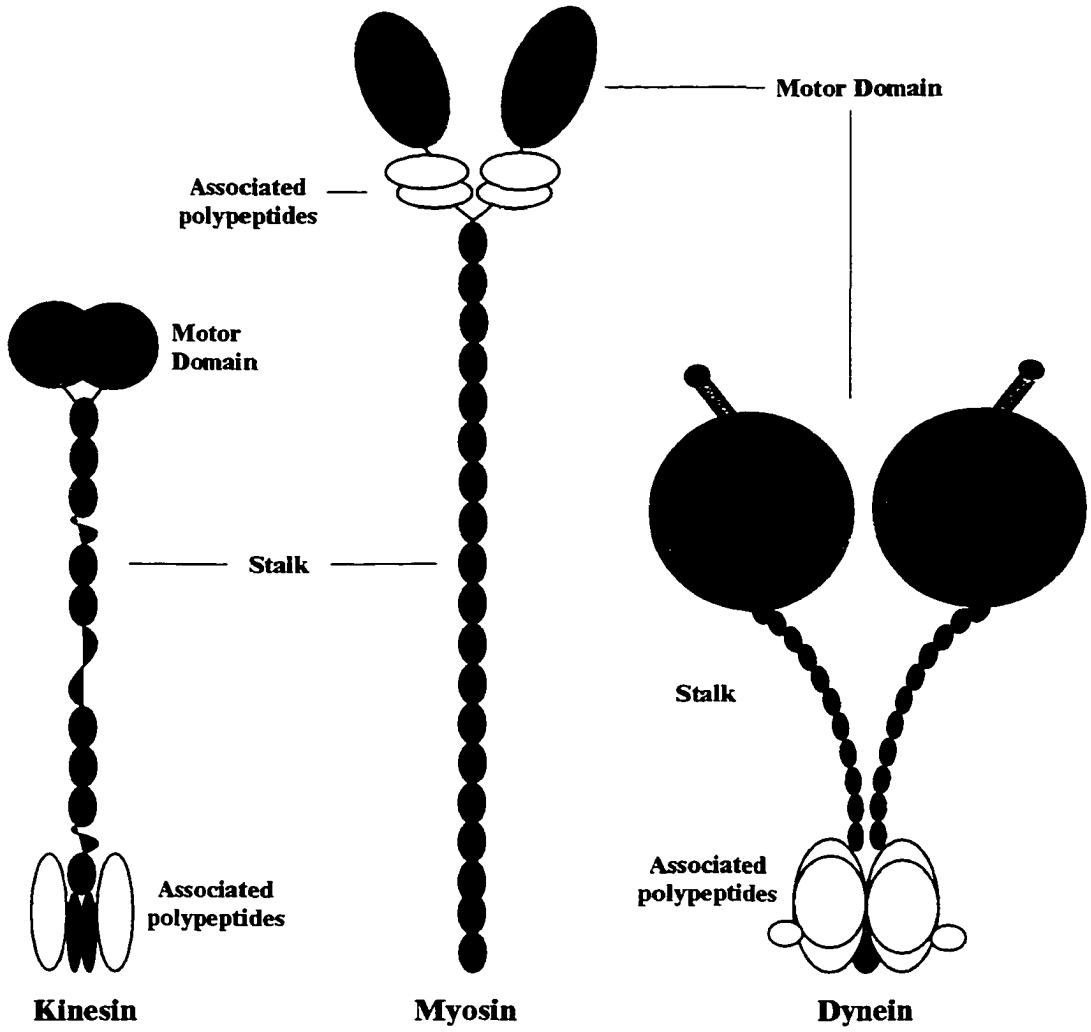

Fig. 1 **Schematic diagram of three classes of molecular motors.** The microtubule-based motors, conventional kinesin and cytoplasmic dynein, are on either side of the actin-based motor, myosin. All three motors consist of two heavy chains that form a dimer, and associated light chains. Heavy chains: the catalytic domans are shown in red and the stalk, which forms coiled-coils are shown in blue. The four light chains associated with skeletal muscle myosin, the two light chains associated with conventional kinesin, and the light-intermediate and light chains of dynein are all shown in white. Microtubule binding sites which are a part of the catalytic core of conventional kinesin and myosin, extend from the dynein head like 'antennae'. Figure modified from Woehlke and Schliwa, 2000, and prepared by Thomas *et al.*, 2000.

a variety of motile phenomena including cell growth, cell movement, transport of vesicles and organelles, cytokinesis, RNA transport, phagocytosis, organelle transport, and signal transduction (Mooseker and Cheney, 1995; Wolenski, 1995; Mermall *et al.*, 1998; Walker *et al.*, 2000).

B. Microtubules and MT-based motors

MTs are ubiquitous non-covalent polar cytoskeletal polymers composed of heterodimers of α-and β-tubulin. Tubulin dimers assemble head-to-tail to form 13 linear protofilaments that comprise the wall of the hollow MT cylinder. Due to this head-to-tail assembly of asymmetrical tubulin subunits, MTs have an intrinsic polarity in which one end (the plus end) elongates 2-3 times faster than the other (minus end). Recent evidence indicates that the plus end is crowned by β-tubulin and that the minus end is crowned by α-tubulin (Mitchison, 1993; Fan *et al.*, 1996). MTs exist in dynamic equilibrium with tubulin subunits, growing and shrinking by addition or loss of tubulin dimers from the ends of the MTs (Kirschner and Mitchison, 1986). Individual MTs switch stochastically between phases of slow growth and fast shrinking so that in a MT population some will be growing and some will be shrinking, a property known as "dynamic instability" (Mitchison and Kirschner, 1984; Walker *et al.*, 1988). The transition from elongation to rapid shortening is termed catastrophe, whereas the reverse is termed rescue (Walker *et al.*, 1988). These two distinct morphogeneic features of MTs are central to many biological functions such as cell division, morphogenesis, motility, gravisensing and cellulose deposition in plants (Gunning, 1982). In addition to being dynamic polymers, the surface of the MTs polymer serves as a track on which motor proteins of the dynein and kinesin superfamilies transport cargoes throughout the cell.

B-1. Dyneins

Dyneins are large multi-component MT-based molecular motors involved in many fundamental cellular processes including vesicular transport, mitosis, and ciliary/flagellar beating. All dyneins have ATP-ase activity and move along MT toward the minus end. Phylogenetic analysis groups dyneins into three subfamilies: the cytoplasmic dynein; and the outer and inner arm axonemal dyneins (Mountain and Compton, 2000). This genetic grouping correlates with the cellular functions of the proteins. Cytoplasmic dynein consists of two heavy chains (HCs), three intermediate chains (ICs), and four light intermediate chains (LCs) (Fig 1). The intermediate and light intermediate chains associate with a protein complex called dynactin which assist in binding dynein to its cargo (Hirokawa, 1998). Dyneins motor activity is regulated by many mechanisms including direct phosphorylation/dephosphorylation of the HCs, phosphorylation of ICs and LCs, and ligands associated with HCs (King, 2000).

B-2. Kinesin superfamily

Members of the kinesin superfamily are responsible for a variety of intracellular MT-based transport functions, including organelle transport, chromosome movement during mitosis and meiosis, maintenance of endoplasmic reticulum and intermediate filament distribution, spindle formation and elongation, flagellar growth and positioning of developmental morphogenesis (Leopold *et al.*, 1992; Goldstein, 1993; Sawin and Endow, 1993; Bloom and Endow, 1994; Brady, 1995; Barton and Goldstein, 1996; Endow and Komma, 1996; Robb *et al.*, 1996).

(i) Structure of conventional kinesin

Conventional kinesin, the first kinesin identified, was first isolated from the squid optic lobe as an ATPase responsible for fast axonal transport in giant axons of the squid, *Loligo pealei*. Kinesin was subsequently purified and demonstrated to move unidirectionally on MTs toward the more dynamic plus ends (Brady, 1985; Vale *et al.*, 1985). Biochemical studies of the native kinesin revealed that it is a tetramer consisting of two heavy chains (KHC) and two light chains (KLC) (Bloom *et al.*, 1988; Kuznetsov *et al.*, 1988). Sequence analysis, expression studies (Yang *et al.*, 1989), and electron microscopic and crystallographic studies of kinesin heavy chains (Sack *et al.*, 1997; Sablin *et al.*, 1998; Sablin, 2000; Vale *et al.*, 2000) suggested that the molecule has three domains (Fig 2A): (i) a globular motor domain (~350 amino acids) at the amino terminus of the heavy chain with conserved ATP- and MT-binding sites, (ii) a central stalk region that facilitates dimer formation through an extended α-helical coiled-coil, (iii) and a globular carboxy-terminal tail domain that interacts with light chains and vesicles (Vale and Goldstein, 1990; Yang *et al.*, 1990). Detailed analyses of structure, sequence, and expression strongly suggest that the motor domain itself is composed of two major elements (Vale *et al.*, 2000). One element is the "catalytic core" (~320 amino acid residues) which is conserved throughout the kinesin superfamily. The second element is the "neck region" (~45 amino acids) that emerges from the C-terminus of the catalytic core and includes two distinct parts. The first 10 residues "nick linker" is conserved among all amino-terminal, plus-end motors, and a subsequent "neck coiled-coil region" is conserved selectively among the conventional kinesin subfamily (Kozielski *et al.*, 1997; Vale *et al.*, 1997; Vale *et al.*, 2000). Although kinesin heavy chains appear to be highly conserved in terms of primary amino acid sequence and structural

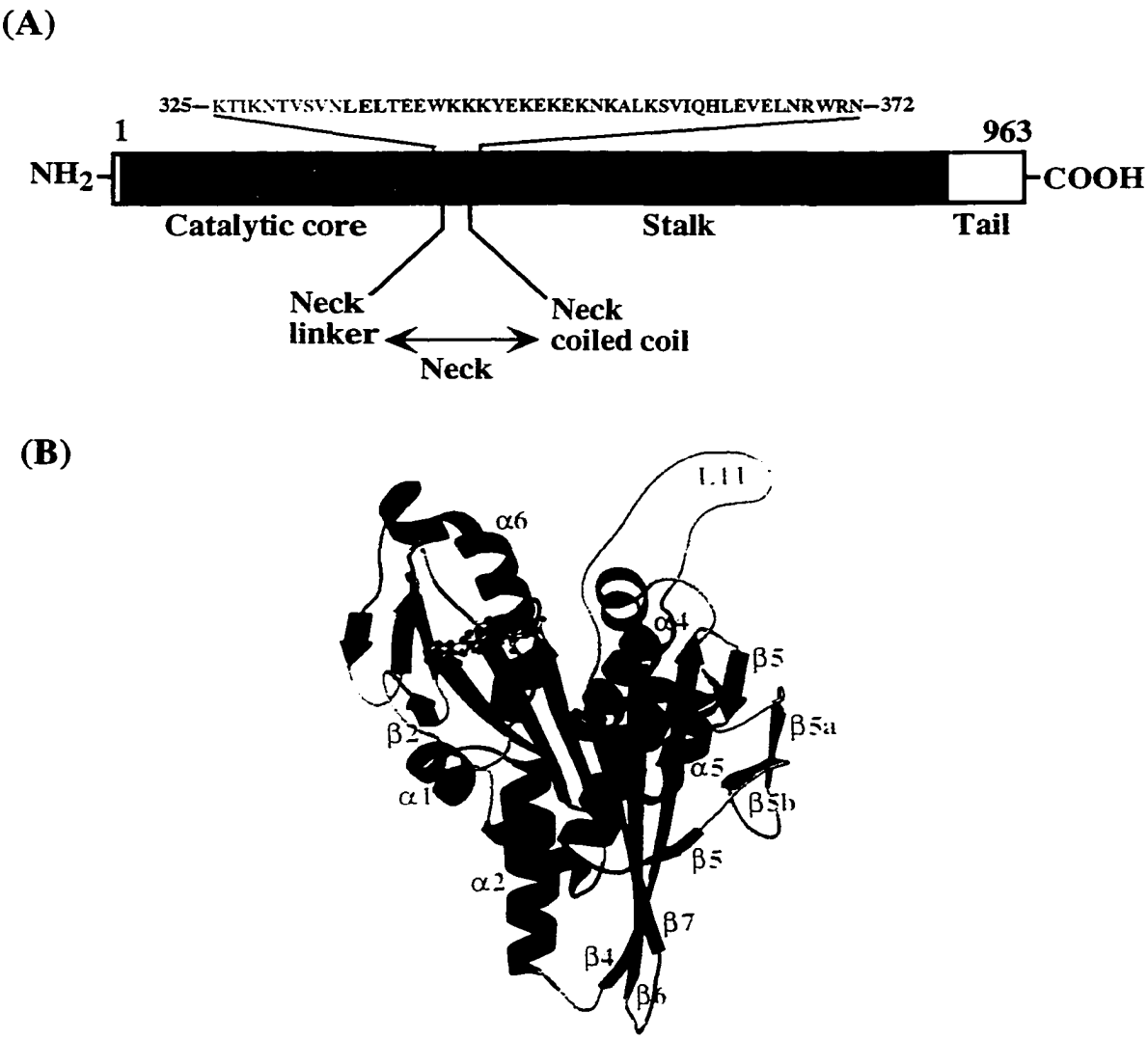

Fig. 2 **Domain organization and crystal structure of human conventional kinesin.** (A) Conventional kinesin domain organization. The polypeptide chain forms four domains. A catalytic core (shown in red), contains both ATP-and MT-binding sites and is highly conserved among all kinesins. A class-conserved neck region (~45 residues) which includes two distinct parts: neck linker (~10 residues) (shown in green) that is highly conserved among all N-terminal motors, and neck coiled-coil (shown in black) that is conserved selectively among the conventional kinesin subfamily. The non-conserved stalk region is shown in blue (B) Crystal structure of human kinesin motor domain in which the β-strands are shown in green, α-helices in purple, and loops in cyan. The ADP is shown as a ball-and-stick figure. The catalytic core of kinesin motor domain is composed of eight parallel strands of β-sheets that are flanked on each side by three α-helices and a small lobe composed of a three-stranded-β sheet (Kull *et al.*, 1996).

features, light chains of kinesin show considerable diversity (Bloom and Endow, 1994). Evidence from electron microscopy and biochemical studies suggests that the C-termini of light and heavy chains associate with membrane bound organelles (Hirokawa *et al.*, 1989; Gauger and Goldstein, 1993; Rahman *et al.*, 1998), suggesting that the specificity of a kinesin for its particular cargo resides in the C-terminus of the heavy and light chains.

(ii). Kinesin subfamilies

During the last decade, genetic, biochemical, and genome sequence projects have led to the identification of over 260 kinesin-like proteins (KLPs) from all the major eukaryotic kingdoms: protists, fungi, plants, and animals (Moore and Endow, 1996; Goldstein and Philip, 1999; Reddy, 2001). The completed genome sequence of *Saccharomyces cerevisiae*, *Caenorhabditi elegans*, *Drosophila melanogaster* and *Arabidopsis thalania* revealed six, nineteen, twenty-four, and fifty-eight different kinesins-like proteins respectively (Reddy and Day, 2001). Although all kinesins and KLPs are related in that both have a conserved motor domain, KLPs show considerable variation in the location of the motor domain and motility properties. Outside the motor domain, KLPs share little or no sequence similarity to the kinesin heavy chain or to each other (Bloom and Endow, 1994).

Phylogenetic analysis of the motor domain of kinesin proteins has shown that most members of the kinesin superfamily can be placed into one of ten subfamilies (Table1) (Kim and Endow, 2000). However, some KLPs (orphans) do not fall into these ten subfamilies and could represent prototypes of additional subfamilies. Members of each subfamily, in addition to having more closely related motor domain sequences, usually share a common domain organization, exhibit sequence similarity outside the motor domain and have similar motility properties and cellular functions. One of these ten subfamilies (a C-terminal

Table 1. Kinesin subfamilies and their functions

Kinesin subfamily	Motor polarity[b]	Function
BimC	Plus	Cell division (required for spindle pole separation, centrosome separation, bipolar spindle formation and maintanance)
Kip2	ND[a]	ND[a]
Chromokinesin/KIF4	Plus	Cell division (binds DNA, required for chromosomes congression to plate, spindle stabilization)
C-terminal motor	Minus	Cell division (spindle formation and integrity, karyogamy and trichome morphogenesis)
KHC	Plus	Intracellular transport of membrane-binded vesicles and organelles.
KRP58/95	Plus	Anterograde vesicle transport, flagellar - assembly and maintenance
MCAK/KIF2	Plus	Vesicle transport and cell division (separation of sister centromeres, chromosome congression, poleward chromosome movement, and regulation of microtubule dynamics)
MKLP1	Plus	Anaphase B spindle elongation, position of midbody for cytokinesis, pole formation, centosome separation, and bipolar spindle formation
Unc104	Plus	Vesicle and organelle transport
Ungrouped	Plus	Cell division and flagellar beating

[a] Not determined

[b] Based on *in vitro* motility assays of representative members of the particular subfamily (From Goldstein, 1999; Reddy, 2001)

subfamily) posses C-terminal motor domain with minus-end motility whereas the N-terminal subfamilies are plus-end motors (McDonald and Goldstein, 1990; Walker *et al.*, 1990; Endow *et al.*, 1994a; Kuriyama *et al.*, 1995). Six subfamilies have been shown to be involved in some aspects of cell division, three subfamilies are involved in organelle/vesicle transport and one subfamily (MCAK/KIF2 subfamily) is involved in both vesicle transport and cell division (Moore and Endow, 1996). Since the focus of my research is on a KLP that belongs to the C-terminal subfamily, a summary of the work that has been done with some members of this subfamily follows

(a) C-terminal subfamily

The *Drosophila melanogaster* non-claret disjunction (DmNcd), *Saccharomyces cerevisia* kinesin-related protein (ScKar3) and *Arabidopsis thaliana* kinesin-like CBD (AtKCBP) are the most extensively characterized members of the C-terminal subfamily. C-terminal motors have been found in fungi, plants, and animals, and multiple members of this subfamily exist in some species. Members of the C-terminal subfamily have a C-terminal motor domain, a basic, proline-rich N-terminal tail, and a central stalk that forms the coiled-coil domain. Ncd was the first kinesin shown to move towards the minus ends of MTs (Walker *et al.*, 1990). Ncd is implicated in organizing/focusing MTs activity required for pole formation since null mutants show multi-polar and diffuse spindles (Hatsumi and Endow, 1992). Ncd motor also function in meiosis II spindle assembly in oocytes by recruiting or anchoring δ-tubulin to the spindle and stabilizing newly nucleated MTs (Endow and Waligora, 1998). Truncated Ncd protein that includes only the N-terminal tail is capable of cross-linking MTs in ATP-independent manner (Chandra and Endow, 1993).

Kar3, a meiotic motor, was identified in yeast mutants that are defective in karyogamy, where it facilitates the movement of zygotic nuclei toward one another (inward-directed movement) (Endow et al., 1990; Meluh and Rose, 1990). Kar3 shows the unusual ability of destabilizing MTs at their minus ends (Endow et al., 1994b), an effect that can be suppressed by treatment of cells with the MT destabilizing drug, benomyl (Saunders et al., 1997). Beside Kar3 and Ncd, three other C-terminal motor kinesins, AtKCBP, CgCHO2, and SpoPkl1, have been shown to be minus-end motors (Pidoux and Cande, 1993; Kuriyama et al., 1995; Song et al., 1997) and perform similar roles in spindle pole function in plants, vertebrate cells, and fission yeast respectively

(iii) Crystal structure of kinesin motor domain

Kinesin motor domain, ~350 amino acid, is the smallest molecular motor domain when compared to that of myosin (~850 amino acids) and dynein (~1000 amino acids). During the last few years, the structure of the motor domain of several kinesins have been solved by X-ray diffraction. The conformational variability among all of them is concentrated in six areas, most of which are functionally important either in MT binding or in linking the core motor to the stalk (Sack *et al.*, 1999). The crystal structure of the human conventional kinesin motor domain, for example, (amino acids 1-349) complexed with MgATP is determined (Kull *et al.*, 1996). The catalytic core (amino acids 7-325) is composed of eight strands of β-sheets, mostly parallel, that are flanked on each side by three α-helices and a small lobe composed of a three-stranded β-sheets (Fig 2B). The first β-strand (β1) marks the point at which sequence conservation begins among all motors of the superfamily with consensus sequence "I/VXVXXRXRP". Sequence conservation throughout the superfamily terminates by the end of the last helix (α6) with the consensus

sequence "ETXXTLXFAXR" (Vale *et al.*, 2000). The phosphate-binding loop (P-loop) (amino acids 84-92) lies towards the front side in the upper part of the motor domain and is identical in structure to the P-loops of adenylate kinase, transducin, GTPases, Ras, RecA, and myosin, while the ATP-binding site lies on the rear surface. The catalytic core is followed by a neck linker region, composed of two short β strands (β9 and β10, residues 325-338), and the neck coiled-coil which is composed of one helix (α7, residues 339-370). These two secondary structural elements are connected by short loops. Dimerization is usually achieved by the coiled-coil interaction between the two neck helices α7 (Sack *et al.*, 1999).

Although kinesins and myosins do not have any amino acid sequence similarities seven of the eight core β strands (β5 being the exception) and all six major helices of the kinesin motor domain are superimposable with corresponding elements in the myosin motor domain in the area around the P-loop (Fig 3A&B) indicating that these two motor classes may have evolved from a common ancestor (Kull *et al.*, 1998). In addition to the structural overlap, they are identical to the G-protein in the mechanism by which the two "switches" sense whether NTP or NDP is present in P-loop, and influence the protein conformation (Mountain and Compton, 2000). The size difference in the motor domain of the two motors is likely due to genetic insertions in a common ancestor of the kinesin and myosin families. Myosin has two larger insertions compared to kinesin: residues 270-450 (insertion 1), which correspond to a smaller insertion in kinesin (amino acids 138-173) and residues 506-649 (insertion 2), which correspond to L12 in kinesin (amino acid 272-280) (Fig 3C) (Kull *et al.*, 1996).

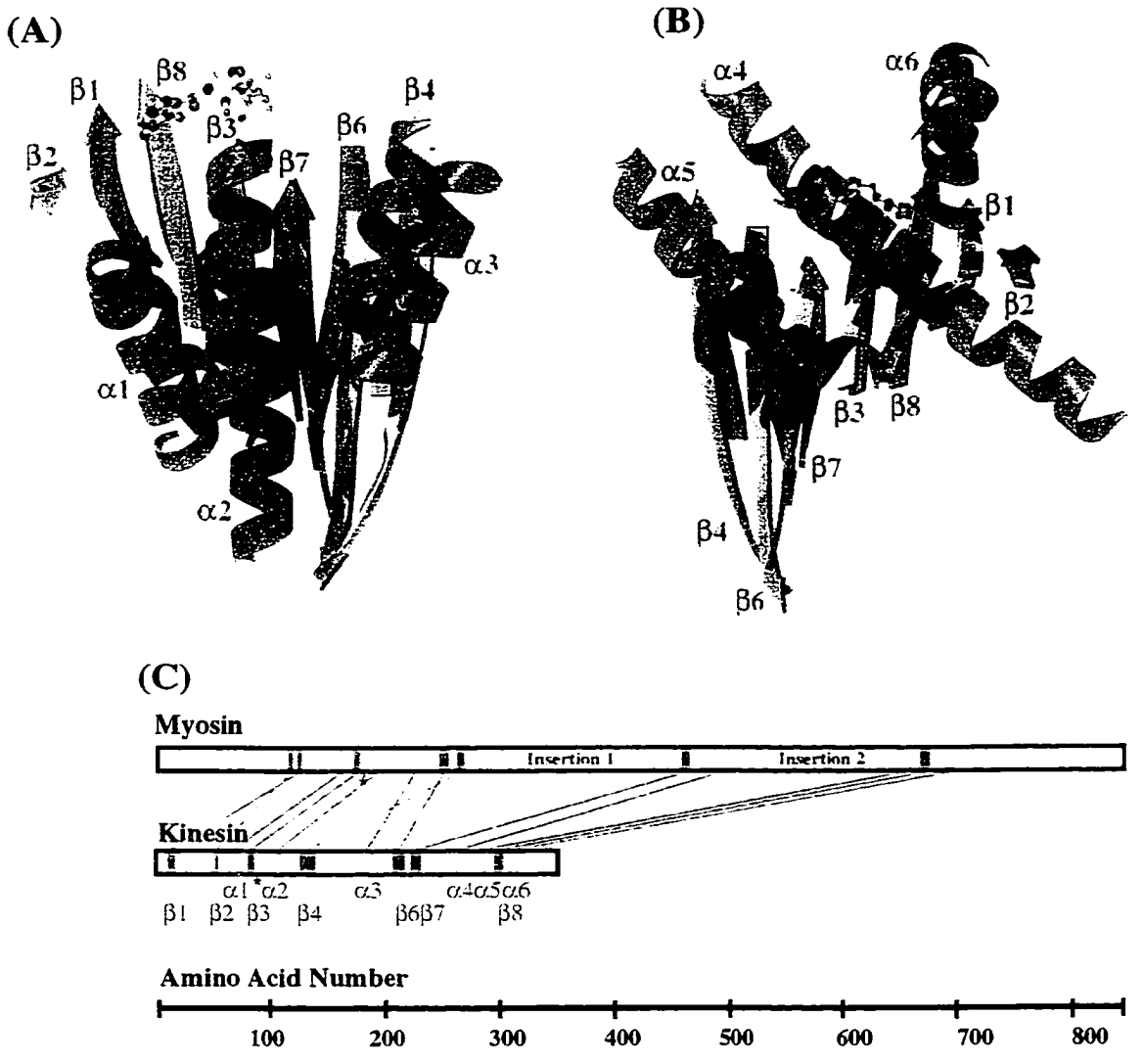

Fig. 3 **Comparison of kinesin motor domain structure with myosin motor domain.** The overlap was achieved by aligning nine α-carbon atoms in the P-loops of the two structures. (A) Front view of the molecule, showing overlapping β-sheets and the three front α-helices. (B) Rear view of the molecule showing overlapping β-sheets and the three rear α-helices. β-sheets are shown in yellow for kinesin and in green for myosin. α- helices are shown in blue for kinesin and purple for myosin. (C) Placement of corresponding sructural elements in the linear sequence of kinesin and myosin. Helices and strands are shown in purple and green, respectively. Insertions in the core motor domain are shown in yellow. In myosin,these insertions contain elements that interact with actin. Lines connect overlapping structural elements; broken lines indicates structural elements that are in a different relative location in the primary sequence; asterisks indicate the position of the P-loops. (from Kull *et al.*, 1996).

(iv). Determinants of kinesin directionality

Kinesins have been classified based on the directionality of their movement (towards the plus or minus end of MTs), the position of the motor domain in the polypeptide chain (N-terminal, internal, or C-terminal), and the polypeptide chain composition (monomers, homodimers, heterodimers, trimers, tetramers, etc.) (Sack *et al.*, 1999).

All of the C-terminal motors, for which motility has been determined, are minus-end-directed, while the N-terminus motors, as conventional kinesin, are plus-end-directed kinesin (Endow, 1999). The directionality of the internal kinesins has not been determined. However, they may not be traditional transport motors, but instead act as ATP-dependent MT depolymerizing agents (Vale *et al.*, 1997; Desai *et al.*, 1999). Based on three-dimensional models of monomeric and dimeric kinesin and Ncd bound to MTs, it was concluded that the neck region, not the conserved catalytic core, is responsible for directionality of the motor. Motility studied with truncated and chimeric kinesins have indicated that the direction of motion is not determined by the catalytic core, but rather by the adjacent neck region (Stewart *et al.*, 1993; Vale, 1996; Case *et al.*, 1997; Henningsen and Schliwa, 1997; Endow and Waligora, 1998). Additional domains (e.g. coiled-coil and hinge regions) most certainly augment motility in terms of velocity or processivity. Mutagenesis studies in the neck region of conventional kinesin and Ncd also indicated that the neck region serves as a mechanical amplifier for motility via coupling the ATP hydrolysis and energy into directional motion along the MT (Vale *et al.*, 2000). Additionally, the directed movement requires interaction of the neck and motor core. Endow and Higuchi, (2000) showed that a single amino acid change in the neck region of Ncd (a minus-end motor) caused the motor to move with the wild-type velocities towards the plus or minus end directions. Also mutation of a motor core

residue that touches the neck residues in crystal structures resulted in movement in both directions. Sequence analysis of the conserved neck regions generates a phylogenetic tree that is similar to the one produced using the entire catalytic domain suggesting that the catalytic cores and necks have co-evolved (Case *et al.*, 2000).

B-3. Plant kinesins and KLPs

Compared with animal cells and fungi, little is known about KLPs in plants (Asada and Collings, 1997). However there are ample reasons to assume that KLPs are ubiquitous in plants and perform similar functions as in other systems and some plant-specific functions. For example, aside from the organization and operation of the mitotic apparatus, motor protein-related activities may govern the directed accumulation of secretory vesicles necessary for tip growth in root hairs and pollen tubes, the deposition of localized wall thickenings in a variety of cell types, and formation of the cell plate during cytokinesis (Liu *et al.*, 1996). In addition, plants contain several unique MT arrays such as the preprophase band and phragmoplasts that may require unique KLPs (Staehelin and Hepler, 1996; Granger and Cyr, 2001).

To date, nine kinesin-like proteins have been characterized at the molecular level from plants (Reddy, 2001). The first indication for the presence of MT-dependent motors in plants came with the finding that phragmoplast MTs in BY-2 cells could translocate with respect to each other in the presence of ATP or GTP (Asada *et al.*, 1991). Subsequently, using a monoclonal antibody raised against the kinesin heavy chain from bovine brain, a 100 kDa pollen kinesin homologue (PKH) from tobacco pollen tube was identified and partially characterized (Tiezzi *et al.*, 1992; Cai *et al.*, 1993). By immunocytochemical analysis using antibodies against conventional kinesin (Cai *et al.*, 1993), PKH was colocalized with MTs in

the apex of pollen tube, a place rich in Golgi-vesicles (Tiezzi *et al.*, 1992). Biochemical studies have shown that the 100 kDa polypeptide retained some kinesin properties, such as MT-activated ATPase activity, and ATP-sensitive MT binding ability (Cai *et al.*, 1993). A kinesin-related protein has also been isolated from a Golgi vesicles-enriched fraction from *Corylus avellana* pollen (Liu *et al.*, 1994).

125 kDa and 120 kDa MT motor proteins with plus-end-directed motor activity were isolated from phragmoplasts of tobacco BY-2 cells (Asada and Shibaoka, 1994). TKRP125 (tobacco kinesin-related polypeptide of 125 kDa) was shown to co-localize with cortical MTs in the S phase, preprophase band MTs in prophase, the spindle in metaphase and anaphase, and the phragmoplast during telophase and cytokinesis, (Asada *et al.*, 1997). Immunoblots of synchronized BY-2 cells showed cell-cycle dependent expression of TKRP125, with a low level in the S phase and increased in G2 reaching the highest levels in the M phase, but no detectable expression in G1. TKRP125 is closely related to Eg5 of *Xenopus* and other BimC subfamily KLPs.

Very recently, in a MT cosedimentation experiment, a MT-based motor protein was characterized from tobacco pollen tubes (Cai *et al.*, 2000). The purified 90 kDa motor protein induced MTs to glide *in vitro* and co-fractionated with MT-activated ATPase activity. The 90-kDa ATP-MAP cross-reacted specifically with a peptide antibody directed against a highly conserved region in the motor domain of the kinesin superfamily. In immunolocalization studies, the 90 kDa motor protein bound to organelles associated with MTs in the cortical region of the pollen tube, suggesting an organelle transport role for this protein in the pollen tube (Cai *et al.*, 2000). Recently, another plus-end motor, DcKRP120-2,

belong to Bim-C subfamily was cloned from carrot cells and strongly decorates the phragmoplast mid-line where the plus-end of MTs overlap (Barroso *et al.*, 2000).

(i) *Arabidopsis* kinesin-like proteins (AtKLPs)

Using primers corresponding to conserved regions of the kinesin motor domain, a kat gene family (katA, katB, katC, katD, and katE) encoding kinesin-like proteins in *Arabidopsis thaliana* has been characterized (Mitsui *et al.*, 1993; Mitsui *et al.*, 1994; Tamura *et al.*, 1999). Using antibodies against two peptides in the MT binding domain, KatA (89kDa) protein has been shown to be a minus-end directed motor and localized to the mitotic spindle and the phragmoplast (Liu *et al.*, 1996). Similar protein has been found in tobacco BY-2 cells and carrot suspension culture. The predicted secondary structure of the KatA, KatB, and KatC proteins indicate the presence of long α helical coiled-coil region with heptad repeats (Mitsui *et al.*, 1993; Mitsui *et al.*, 1994). However, the predicted secondary structure of KatD revealed the lack of an α-helical coiled-coil structure suggesting that KatD may function as a monomeric motor. The central region of the KatD polypeptide shares sequence similarity to the motor domain of kinesin heavy chain. The amino-terminal region of KatD shares marked sequence similarity with the calponin homology domain, whereas the ~240-residue carboxy-terminal region shows no significant homology to other known proteins. KatD is a flower-specific motor protein suggesting that KatD may function in transport or cytoskeleton organization in pollen (Tamura *et al.*, 1999).

Recently, an phragmoplast-associated kinesin-related protein (AtPAKRP1) has been cloned and characterized from *Arabidopsis* (Lee and Liu, 2000). Immunolocalization studies showed that AtPAKRP1, an amino-terminal KLP, associates with MT arrays in a cell-cycle dependent manner. AtPAKRP1 was shown to accumulate along MTs towards the spindle

midline during late anaphase and telophase and once the phragmoplast MT array was established, AtPAKRP1 was localized to MTs near the future cell plate. Similar localization pattern has been shown in dividing rice root cells (Lee and Liu, 2000). In phylogenetic analyses based on the motor domain sequence, AtPAKRP1 was divergent from *Arabidopsis* KLPs and also divergent from major kinesin/KLP subfamilies but was most closely related to an ungrouped XlKLP1 from *Xenopus levis*. Another candidate of the *Arabidopsis* KLPs, KCBP, was the focus of this research

Arabidopsis thaliana genome is the first plant genome and the fifth eukaryotic organism after *Saccharomyces cerevisiae* (Goffeau *et al.*, 1996), *Saccharomyces pombe*, *Caenorhabditis elegans* (Consortium, 1998), *Drosophila melanogaster* (Adam, 2000), to be completely sequenced. Using the motor domain of the plant kinesin, KCBP, *Arabidopsis* database (**www.*Arabidopsis*.org/agi.html/**) was searched using BLASTP and TBLASTN programs (Reddy and Day, 2001). Fifty-eight sequences that contain a kinesin-like motor domain were identified (AtKLPs) (Table 2). As a percentage of genes, AtKLPs represents 0.23% of the total genes as compared to 0.1%, 0.17%, 0.11%, and 0.18% in *S. cerevisiae*, *S. pombe*. *C. elegans* and *D. melanogaster* respectively. The 58 AtKLPs are distributed on all five *A. thaliana* chromosomes. The *Arabidopsis* KLPs have been analyzed by the domain prediction program SMART (Reddy and Day, 2001). In addition to the motor domain and coiled-coil domain (CC), which are present in most of them (56 AtKLPs), many of the AtKLPs contain other predicted domains (Fig 4). Six of the KLPs have a calponin homology domain (CH domain) which is an actin-binding domain. Three KLPs contain putative Armadillo/beta-cateinin-like repeats that form a superhelix of helices and mediate protein interaction. Three KLPs have transmembrane domains. Five KLPs contain spectrin repeats

Table 2. *Arabidopsis thaliana* kinesin-like proteins.

No.	Gene/protein name	Motor location	# of aa	Protein ID	# of introns	Chr No.	Motility	Cellular localization	Other Domains	References
1	AtKatA (F7J7)	C-terminal	793	1170619	8	4	Minus[a]	Mitotic MT arrays	CC	(Mitsui *et al.*, 1993; Liu *et al.*,1996)
2	AtKatB (T24A18)	C-terminal	745	1170620	15	4	ND	ND	CC	(Mitsui *et al.*, 1994)
3	AtKatC (F5F14)	C-terminal	754	1170621	15	5	ND	ND	CC	(Mitsui *et al.*, 1994)
4	AtKatD (F2P16)	Internal[b]	987	3421378	17	5	ND	ND	CH	(Tamura *et al.*, 1999)
5	AtKCBP (K14B20)	C-terminal	1259	237101	20	5	Minus	PPB, spindle, Spindle poles, Phragmoplast	CC, MyTH4 Talin-like, CBD, PEST	(Reddy *et al.*, 1996; Oppenheimer *et al.*, 1997)
6	AtKRP125a (F3G5)	N-terminal	1022	4056495	17	2	ND	ND	CC	AtDB
7	AtKRP125b (F9C22)	N-terminal	1056	4510356	22	2	ND	ND	CC	AtDB
8	AtKRP125c (T8O18)	N-terminal	1076	4580395	18	2	ND	ND	CC,RhoGEF	AtDB
9	Atd13205w (FCA1)	N-terminal	959	2244790	9	4	ND	ND	CC	AtDB
10	AtT19F6.3	N-terminal	995	2262101	12	4	ND	ND	CC	AtDB
11	AtT32N15.10	Internal[b]	767	2392771	14	3	ND	ND	CC	AtDB
12	AtT30B22.20	Internal[b]	861	2529677	14	2	ND	ND	CC,CH	AtDB
13	AtT12M4.14	Internal[b]	1032	3249113	18	1	ND	ND	CC,CH	AtDB
14	AtT5A14.3	N-terminal	887	4204259	9	1	ND	ND	CC	AtDB
15	AtT9I22.5	Internal[b]	1068	4314358	18	2	ND	ND	CC	AtDB
16	AtF19H22.50	N-terminal	834	4539314	11	4	ND	ND	CC	AtDB
17	AtF19H22.150	N-terminal	1121	4539324	22	4	ND	ND	CC,TM	AtDB
18	AtF3K23.6	N-terminal	581	4567265	9	2	ND	ND	CC	AtDB
19	AtF3K23.14	N-terminal	857	4567271	18	2	ND	ND	CC, TM	AtDB
20	AtF8K7.17	N-terminal	909	5263326	22	1	ND	ND	CC	AtDB
21	AtF28P10.150	N-terminal	1070	5541717	20	3	ND	ND	CC, ARM	AtDB
22	AtF14P13.9	Internal	897	6056195	16	3	ND	ND	CC,CH	AtDB
23	AtF14P13.22	N-terminal	459	6056206	11	3	ND	ND	CC	AtDB
24	AtF24D7.17[1]	Internal	1056	6456171	19	1	ND	ND	CC,CH	AtDB
25	AtZCF125[2]	N-terminal	823	6526979	17	1	ND	ND	CC,TOP4c,	AtDB
26	AtT9C5.240	N-terminal	813	6561941	14	3	ND	ND	CC	AtDB
27	AtF25P22.28[3]	C-terminal	1050	6692749	17	1	ND	ND	CC,MA	AtDB
28	AtF15I118.10	C-terminal	1162	6714287	17	1	ND	ND	CC	AtDB
29	AtF15H18.12	N-terminal	1003	6714288	11	1	ND	ND	CC	AtDB
30	AtF24M12.190	N-terminal	968	6782245	13	3	ND	ND	CC	AtDB

31	AT4g05190 (C17L7)	C-terminal	777	7267279	17	4	ND	ND	CC,HR1	AtDB
32	AtF16L2.60	N-terminal	1058	7339486	21	3	ND	ND	CC,MA	AtDB
33	AtT1E22.130	N-terminal	664	7406433	10	5	ND	ND		AtDB
34	AtMAA21.110	N-terminal	439	7573331	11	3	ND	ND	CC	AtDB
35	AtT15B3.190	N-terminal	1229	7594566	20	3	ND	ND	CC	AtDB
36	AtF11C1.80	N-terminal	1075	7630025	21	3	ND	ND	CC	AtDB
37	AtF7K15.60	N-terminal	932	7649361	13	3	ND	ND	FH2,CC	AtDB
38	AtF12B17.180	N-terminal	1273	7671456	22	5	ND	ND	CC	AtDB
39	AtF22M8.8	N-terminal	885	8570446	18	1	ND	ND	CC,ARM, TOPEU1	AtDB
40	AtPAKRP[4] (FCA0)	N-terminal	1292	8745333	24	4	ND	Spindle midzone Phragmoplast	CC	[Lee and Liu, 2000] AtDB
41	AtF5011.15	N-terminal	895	8778646	16	1	ND	ND	CC,ARM	AtDB
42	AtT20H2.17	N-terminal	923	8778993	21	1	ND	ND	AAA	AtDB
43	AtMGL6.9	Internal	799	9229563	12	3	ND	ND	CC	AtDB
44	AtMGD8.20	N-terminal	2158	9229980	30	3	ND	ND	CC,SPEC,TM	AtDB
45	AtK13E13.17	N-terminal	2756	9280323	34	3	ND	ND	CC,SPEC	AtDB
46	At MAL21.18	N-terminal	1103	9293972	16	3	ND	ND	CC	AtDB
47	AtMSL1.9	Internal	706	9294452	12	3	ND	ND	CC	AtDB
48	AtMDB19.16	N-terminal	1268	9294524	14	3	ND	ND	CC,HR1	AtDB
49	AtMDH9.19	N-terminal	1087	9759485	9	5	ND	ND		AtDB
50	AtMNA5.20	N-terminal	1264	9759626	22	5	ND	ND	CC	AtDB
51	AtF25I16.11	N-terminal	703	9795601	3	1	ND	ND	CC	AtDB
52	AtT21B14.15[5]	N-terminal	956	10092474	22	3	ND	ND	CC	AtDB
53	AtMSL3.5	N-terminal	1335	10177316	24	5	ND	ND	CC	AtDB
54	AtK1L20.9	N-terminal	1037	10177425	13	5	ND	ND	CC	AtDB
55	AtK1013.11	Internal[b]	967	10177775	19	5	ND	ND	CC,CH	AtDB
56	AtF15M7.20	N-terminal	997	10178123	22	5	ND	ND	CC	AtDB
57	AtMCA23.16	N-terminal	1032	10177918	22	5	ND	ND	CC	
58	AtT9N14.6	Internal[b]	1195	10645376	17	1	ND	ND	CC, SPEC	AtDB

[1]also called AtF2K11.1, [2]also called AtT30E16.9, [3]also called F2P9.27, [4]genomic prediction Atd13115c, [5]also called AtMEC18.15, [a]by indirect assay, [b]Although the motor is in the middle, it groups into C-terminal family; CC - coiled coil, CH - calponin homology domain, MyTH4 - domain present in myosin tail region, Talin-like -- talin-like domain found in some myosins and band 4.1 superfamily, CBD – calmodulin binding domain, PEST-Motif rich in proline, glutamine, serine and threonine residues, TM - transmembrane segment, RhoGEF – guanine nucleotide exchange factor for Rho/Rac/Cdc42-like GTPases, ARM – Armadillo/beta-catenin-like repeats, MA - Methyl-accepting chemotaxis-like domains (chemotaxis sensory transducer), HR1 – Protein kinase C-related kinase homology region 1 homologues, FH 2- Formin Homology 2 Domain, TOPEUc - DNA Topoisomerase I (eukaryota), TOP4c - DNA Topoisomerase IV, SPEC – spectrin repeats. ND- not determined (From Reddy and Day, 2001).

Fig. 4 **Schematic diagram of all *Arabidopsis* kinesin-like proteins (KLPs).** *Arabidopsis* database was searched with the conserved motor domain of the plant kinesin, KCBP, using BLASTP and TBLASTN. The 58 KLPs have been analyzed by domain prediction program, SMART. Motor domain, coiled-coil domain, calponin homology domain, and armadillo/beta-catenin-like repeats are color coded as in the key. Myosin tail homology4 (MyTH4), talin-like domain , and calmodulin-binding domain (CBD) characteristic for KCBP are shown in purple, green, and black respectively. RhoGEF, guanine nucleotide exchange factor for Rho/Rac/Cdc-42-like GTPase; Spec, spectrin repeat; HRI, Protein kinase C-related kinase homology region 1 homologues; FH2, Formin homology 2 domain. Different domains are drown to scale. (Modified from Reddy and Day, 2001).

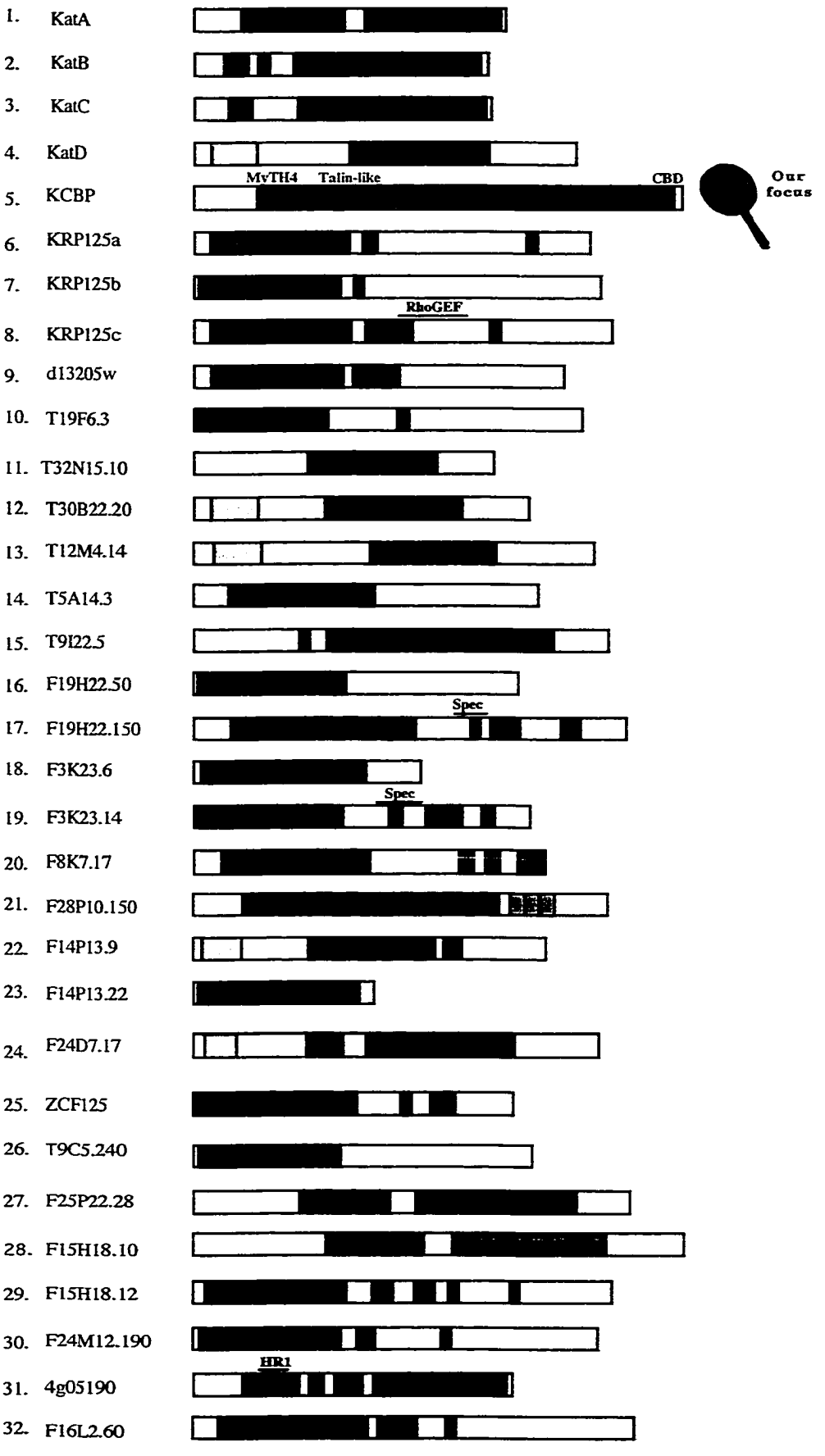

Fig. 4

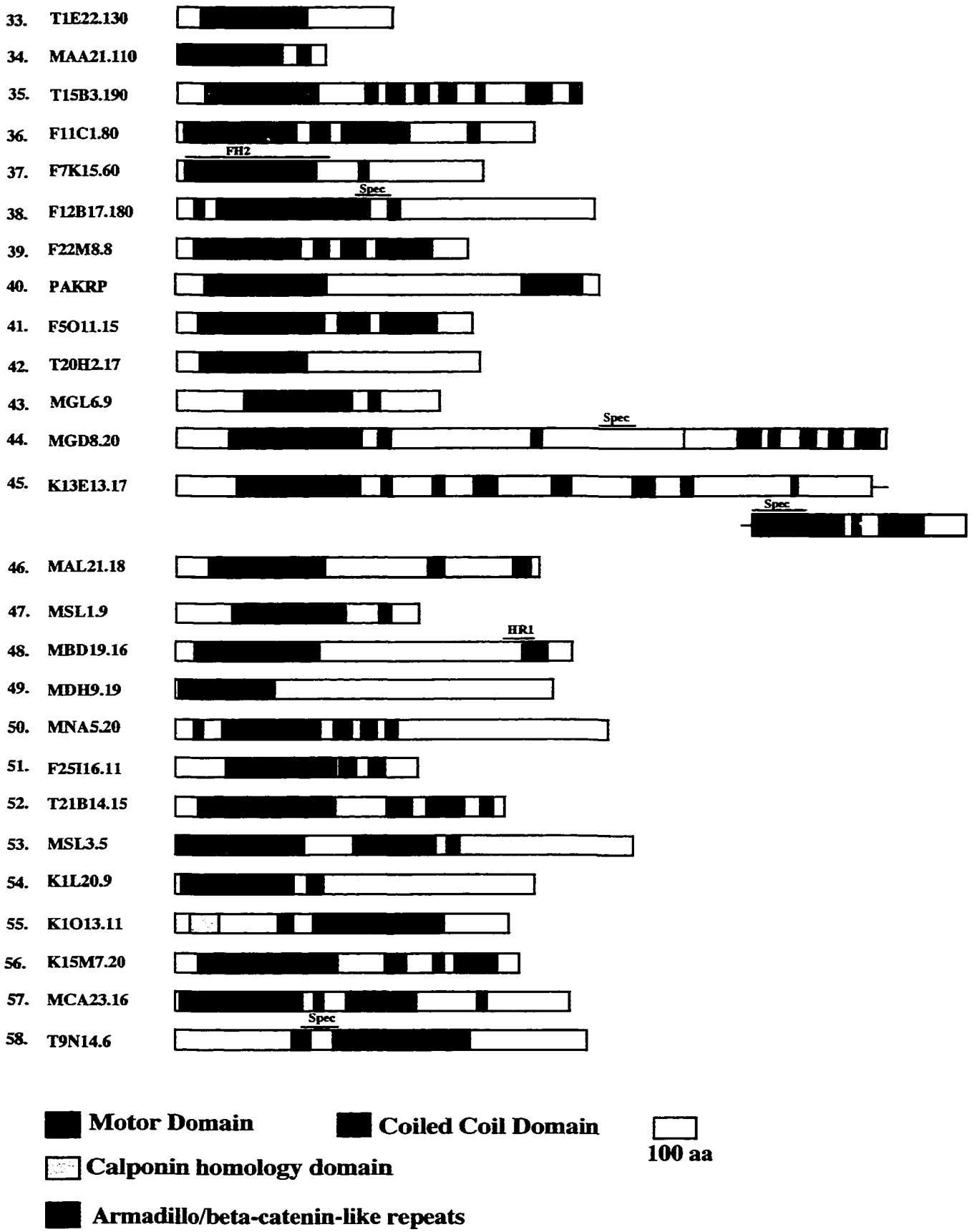

(SPEC). One KLP (KCBP) has a CaM-binding domain (CBD) (Reddy *et al.*, 1996a; Reddy *et al.*, 1998), and a myosin tail homology-4 (MyTH4) and talin-like domain characteristic of myosin.

In phylogenetic analyses, the 58 AtKLPs fall into seven of the ten recognized subfamilies of KLPs (Table 3 and Fig 5). *Arabidopsis* does not have any Kip2, KRP85/95, or Unc104/KIF1 type of KLPs subfamilies. Twenty-five AtKLPs do not fall into any subfamily and in many cases a group of AtKLPs forms a branch within the major subgroup in which they fall, suggesting that there are some families unique to *Arabidopsis* and also may be unique to plants. Nineteen AtKLPs fall into the C-terminal group including some KLPs that have internal motor domain like KatD. The C-terminal and BimC subfamilies are the only ones having at least one representative in each of the five completely sequenced organisms (Table 3). Out of the 58 AtKLPs, only six KLPs have been reported in the literature.

(ii) Kinesin-like Calmodulin-Binding Protein (KCBP)

KCBP: Structural features

In a protein-protein interaction-based screening of *Arabidopsis* expression library using labelled CaM as a probe, a cDNA encoding a novel kinesin-like CBD was isolated (Fordham-Skelton *et al.*, 1994; Reddy *et al.*, 1996a). *Arabidopsis* KCBP (AtKCBP) consists of 1261 amino acids (140 kDa protein) (Fig 6A). The C-terminal region of KCBP (-350 amino acids) has the motor domain typical of kinesin superfamily members and showed the higher sequence similarities with KIFC3 similarity (43% identity and 56% similarity), a C-terminal motor (Reddy and Reddy, 1999). The KCBP motor domain contains the conserved motifs present in all KLPs, including ATP- and MT-binding sites. Outside the motor domain, AtKCBP contains a globular domain in the N-terminus and a putative coiled-coil

Table 3. Number of KLPs in each subfamily in the completely sequenced genomes of five eukaryotic organisms[a].

Subfamily	*A. thaliana*	*D. melanogaster*	*C.elegans*	*S. pombe*	*S .cerevisiae*
BimC	4	1	1	1	2
Kip2	NR	NR	NR	NR	1
Chromokinesin	3	2	1	NR	NR
C-terminal	19	1	4	2	1
KHC	1	1	1	NR	NR
KIP3	2	1	NR	2	1
KRP58/95	NR	2	2	NR	NR
MCAK/KIF2	2	2	1	NR	NR
MKLP1	2	1	1	NR	NR
Unc104	NR	4	3	NR	NR
Ungrouped	25	9	5	4	1
Total	58	24	19	9	6

- [a] Modified from Reddy and Day, (2001)
- NR = not represented according to our phylogenetic analysis.

Fig. 5 **Phylogenetic tree of kinesin superfamily based upon the conserved motor domain.** The amino acid sequences of 171 kinesins and KLPs were retrieved from *Arabidopsis thaliana* database (www.arabidopsis.org/agi.html), NCBI (http://www.ncbi.nlm.nih.gov:80/entrez/query.fcgi?db=Protein), and kinesin home page (http:www.blocks.fhcrc.org/~kinesin/). The phylogenetic tree was obtained using the PAUP (v.4.0b2) maximum parsimony program, with random stepwise addition and tree bisection-reconnection (TBR) branch swapping. The tree built from 500 replicates and rooted using the most diverged kinesin, ScSmy1 as an outgroup protein. Abbreviations of sequences are as follows: *Aspergillus nidulans* (An): AnBIMC, AnKLPA; *Arabidopsis thaliana* (At): AtKRP125b, AtKRP125a, AtF16L2.60, AtKRP125c, At4g05190, AtKATA, AtKATB, AtKATC, AtF12B17.180, AtMNA5.20, AtT9I22.5, AtT9N14.6, AtF14P13.9, AtF15H18.10, AtF25P22.28, AtF24D7.17, AtK1013.11, AtKATD, AtT12M4.14, AtT30B22.20, AtT32N15.10, AtMSL3.5, AtKCBP, AtT5A14.3, AtT1E22.130, Atd13205w, AtT20H2.17, AtMAA21.110, AtF22M8.8, AtF5011.15, AtF28P10.150, AtMGL6.9, AtMSL1.9, AtF25I16.11, AtT9C5.240, AtF11C1.80, AtMCA23.16, AtF15M7.20, AtT21B14.15, AtF8K7.17, AtF19H22.150, AtF3K23.14, AtF14P13.22, AtZCF125, AtF15H18.12, AtF7K15.60, AtF19H22.50, AtF3K23.6, AtF24M12.190, AtK1L20.9, AtT19F6.3, AtMDH9.19, AtK13E13.17, AtMGD8.20, AtT15B3.190, AtMAL21.18, AtMDB19.16, AtPAKRP; *Bombyx mori* (Bm): BmKRP; *Cenorhabditis elegang* (Ce): , CeF23B12.8, CeKLP, CeC41G7.2, CeMO1E11, CeWO2B12, CeLF22F4, CeF20C5, CeOSM3, CeUNC104, CeLR144, CeKHC, CeMO3D4.1, CeK11d9.C, CeTO1G1, CeY43F4B, CeC06G3.2, CeLC33H5; *Cylinderotheca fusiformis* (Cf): CfDSK1; *Cricetulus griseus* (Cg): CgCHO2 , CgCHO1 , CgMCAK , Ggchrkin; *Chlamydomonas reinhardtii* (Cr): CrKLP1 , CrFLA10; *Dictyostelium discoideum* (Dd): Ddk7; *Drosophila melanogaster* (Dm): DmKHC, Dm38B, Dmklp3A, DmKlp73, DmKLP61F, DmKlp67A, DmKlp68D, DmNCD, Dm-NOD, DmPACKLP; *Gallus gallu* (Gg): Ggchrkin; *Homo sapiens* (Hs): HsATSV, HsbKIF1C, HsCENPE, HsCHO2, HsCMKRP, HsKHC, HsKid, HsKIF3, HsKIF3B, HsKIF3C, HsKIF4, HsKIFC3, HsKin2, HsKSP, HsMCAK, HsMKLP1, HsnKHC, HsxKHC; *Leishmania chagasi* (Lc): LcKIN; *Leishmania major*: (Lm): LmKIN; *Loligo pealii* (Lp): LpKHC; *Mus musculus* (Mm): MmKHC, MmKHCS, MmKHCx, MmKIF1A, MmKIF1B, MmKIF2, MmKIF3A, MmKIF3B, MmKIF3C, MmKIF4, MmKIF5c, MmKIFC1, MmKIFC2, MmKlp174; *Morone saxatilis* (Ms): MsFKIF2; *Neurospora crassa* (Nc): NcKHC; *Nectria haematococca* (Nh): NhKin1; *Nicotiana tabacum* (Nt): NtKCBP, NtKRP125; *Solanum tuberosum* (St): StKCBP; *Rattus norvegicus* (Rn): RnKIF1B, RnKIF1D, RnKIF3C, RnKRP2; *Saccharomyces cerevisiae* (Sc): ScVII607, ScCIN8, ScKAR3, ScKIP1, ScKIP2, ScKIP3, ScSMY1; *Strongylocentrotus purpuratus* (Sp): SpKHC, SpKIN2A, SpKIN95, SpKinesinC; *Schizosaccharomyces pombe* (Sp): SpoBC2F12.13, SpoBC649.01C, SpoCUT7, SpoKLP2, SpoPKL1; *Syncephalastrum racemosum* (Sy): SyKin1; *Ustilago maydis* (Um): UmKin1, UmKin2; *Xenopus laevis* (Xl): XlCTK1, XlCTK2, XlEg5, XlEg52, XlKCM1, XlKCM2, Xlklp1, Xlklp2, XlKlp3. (Modified from Reddy and Day, 2001).

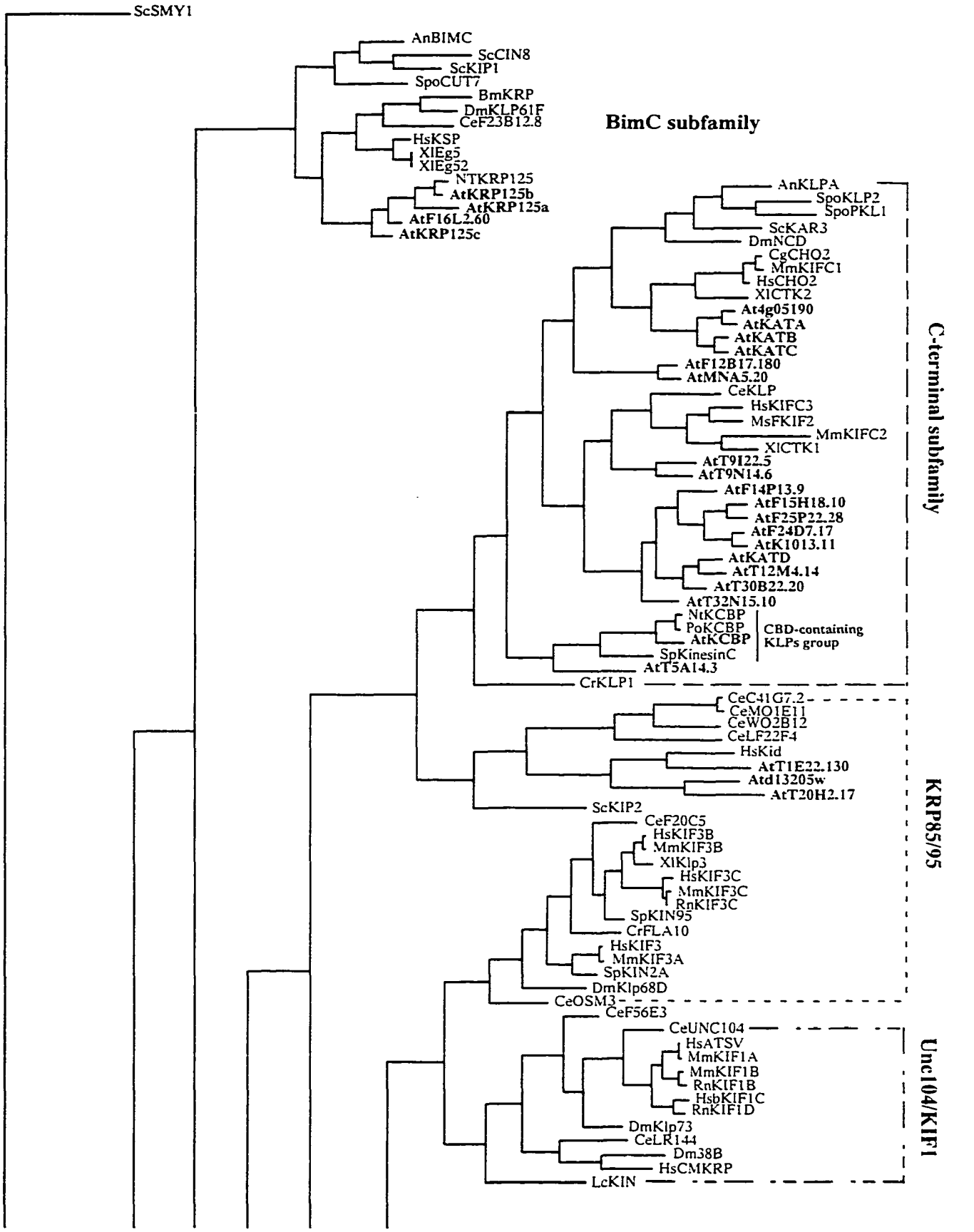

Fig. 5 continue

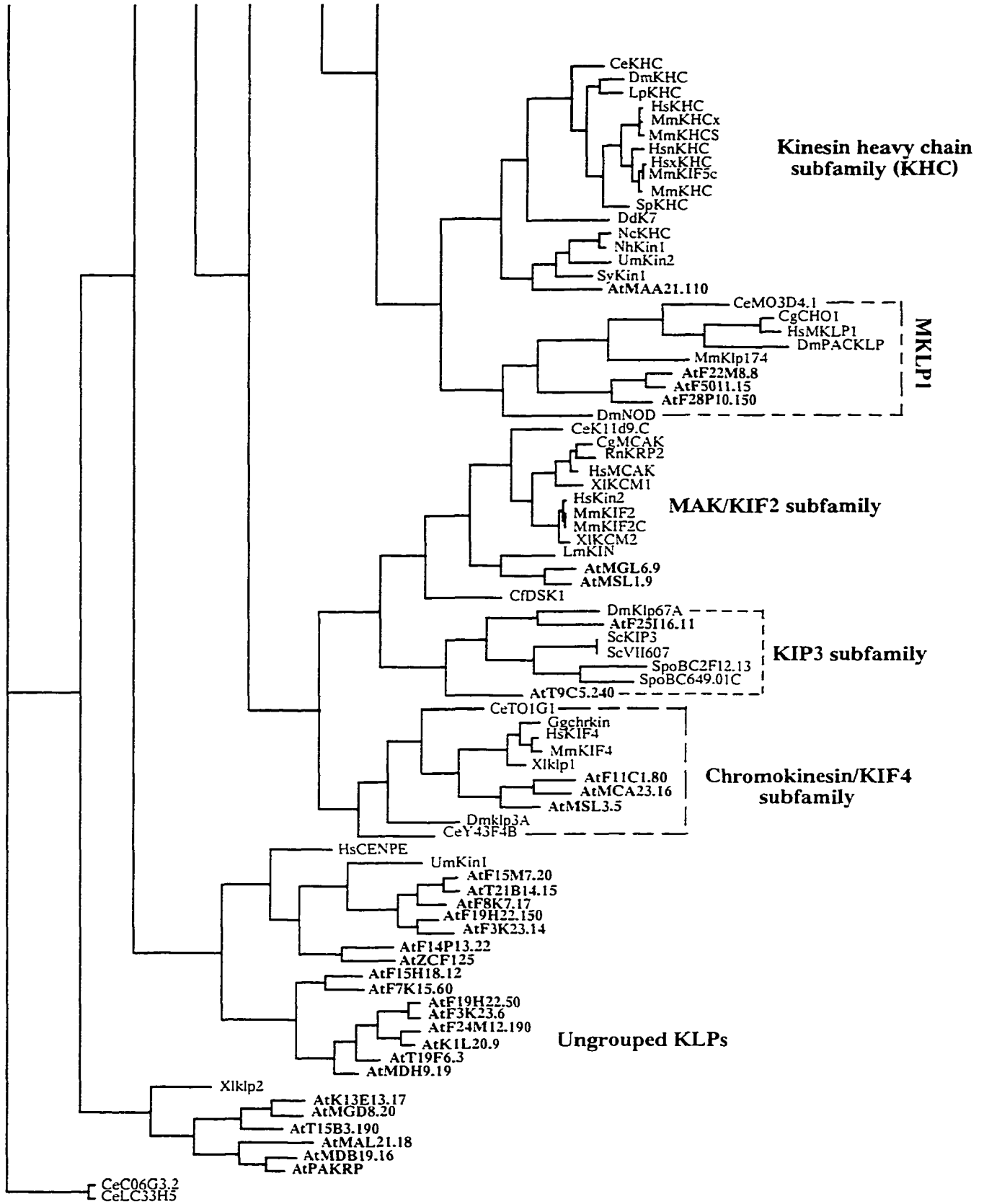

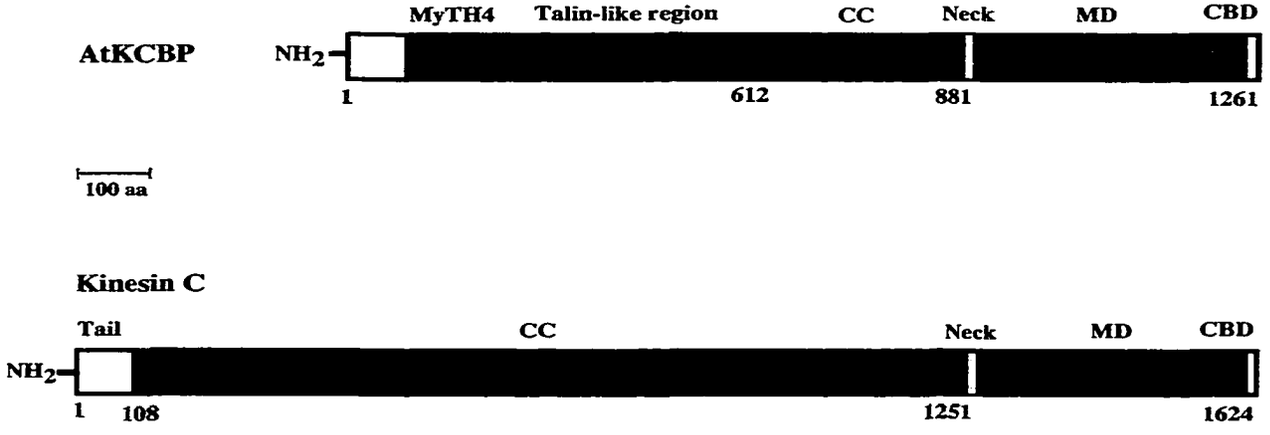

Fig. 6 **Comparision of the structural features of *Arabidopsis* KCBP and sea urchin kinesin C.** Kinesin C is a calmodulin-binding domain (CBD)-containing KLP. In phylogenetic analysis kinesin C grouped with KCBPs from dicot plants within the C-terminal subfamly of KLPs.CBD of kinesin C shares 35% sequence identity to the KCBP CBD. Outside the motor domain, kinesin C does not share any sequence similarity to KCBP. CC of kinesin C spans about 70 % of the protein compared to 20 % in KCBP. Kinesin C does not have myosin homology4 (MyTH4) (shown in cyan) or talin-like regions (shown in green) characteristic to KCBP, myosin VIIa and X. Different domains are drawn to sale. CC, coiled-coil region (shown in blue). MD, motor domain (shown in red). CBD, calmodlin-binding domain (shown in black). Neck regions are shown in yellow. Numbers indicate the amino acid residue.

region in the middle (amino acids residues 610-890). Further analysis of KCBP showed that it may be a rapidly turn over protein (Reddy *et al.*, 1996b). AtKCBP is a single gene in the genome (Reddy *et al.*, 1996b; Oppenheimer *et al.*, 1997) and contains 21 exons and 20 introns. Exons 1-9 contained the coding region for the tail domain. The coiled-coil region is encoded by exon 10-15, and the conserved motor domain is encoded by exons 16-20. The CaM-binding domain unique to KCBP is encoded by the last exon. In contrast, Ncd, another C-terminal KLP from *Drosophila*, has 2 short exons, one in the tail region, the second in the coiled-coil region, and none in the motor domain (Endow *et al.*, 1990). KCBP is expressed in all plant organs and that the mRNA levels vary, with the highest expression in actively dividing cells (Reddy *et al.*, 1996b).

A homologue of AtKCBP from potato and tobacco (Reddy *et al.*, 1996b; Wang *et al.*, 1996), showed identical structural organization suggesting that KCBP is ubiquitous and conserved in dicot plants. KCBP specific antibodies directed against the CBD have detected a protein of expected size in two monocot species (*Haemanthus* endosperm and *Tradescanta* stamen hair cells,) (Smirnova *et al.*, 1998; Vos *et al.*, 2000). In phylogenetic analysis, KCBP from different plant species forms a unique group within the C-terminal subfamily of KLP (Reddy, 2001). A KCBP homologue has not been found in the completely sequenced genomes of *S. cerevisia*, *C.elegans*, and *Drosophila* suggesting that KCBP is unique to plants (Reddy, 2001). However, recently a CaM-binding KLP called kinesin-C, a member of the C-terminal subfamily, has been isolated from sea urchin (Rogers *et al.*, 1999). The CaM-binding region of Kinesin-C shares 35% identity with the KCBP. Outside the motor domain there is no sequence similarity between kinesin-C and KCBP suggesting that KCBP and kinesin-C are two distinct CaM-binding kinesins. The coiled-coil region spans about 20% of

the KCBP, however, in kinesin-C, the coiled-coil region spans about 70% of the protein (Fig 6B).

KCPB is unique and a molecular hybrid

Analysis of the 58 KLPs in the *Arabidopsis* genome sequence database with SMART program for domain prediction (Reddy and Day, 2001) and also comparison with all known KLPs showed that KCBP, unlike other known KLPs, has two unique features, suggesting that it is a new member of the kinesin superfamily. First, KCBP contains a CaM-binding domain that is mapped to a 23 amino acids stretch located near the C-terminus of the protein (Reddy *et al.*, 1996b). This CBD does not bear any sequence similarity to the CaM-binding IQ repeats of the myosin.

CaM, a Ca^{2+}-binding regulatory protein, is known to play a pivotal role in Ca^{2+} signaling in eukaryotes. CaM is ubiquitous and is considered to be multifunctional because of its ability to interact and regulate the activity of a number of other proteins known as CaM-binding proteins (CaMBPs) (Poovaiah *et al.*, 1987; Poovaiah and Reddy, 1993; Snedden and Fromm, 1998; Zielinski, 1998; Reddy, 2001). CaMs are stretches of 16-35 amino acids which form an α-helical wheel representation and show a segregation of basic and polar residues on one side and hydrophobic amino acids on the other side (James *et al.*, 1995). Upon binding, Ca^{2+} CaM becomes activated via a conformational change and is able to regulate the activity of its target proteins.

Among motor proteins, the heavy chain of unconventional myosins binds CaM. The IQ motifs in myosins, unlike most CaM-binding proteins, bind CaM in the absence of Ca^{2+}. Ca^{2+} induces the dissociation of CaM light chains from myosins resulting in inhibition of motility (Hasson and Mooseker, 1995). On the other hand CBD of KCBP binds CaM in the

presence of Ca^{2+} and this binding inhibits the interaction with the MT (Song *et al.*, 1997). Therefore, Ca^{2+} stops the motility of KCBP and myosins by two very different mechanisms. In *in vitro* experiments KCBP binds to bovine CaM and 3 CaM isoforms of *A rabidopsis* CaM (CaM-2, 4, and 6) (Reddy *et al.*, 1999). CaM2 has the highest affinity among all the CaM isoforms tested. Kinesin C has CBD at the C-terminus and is shown to bind to a calmoduilin-affinity column in a Ca^{2+}-dependent fashion (Rogers *et al.*, 1999) .

The amino-terminal tail (aa 121-612) another interesting unique feature of KCBP, which has not been found in any known members of the kinesin superfamily, showed significant sequence similarities to the myosin tail homology 4 (MyTH4) and talin-like region present in myosin VIIa and X (29% identity and 49% similarity in the MyTH4 domain and 29% identity and 49% similarity in the talin-like region of *Homo sapiens* myosin VIIa) (Fig 7) (Chen *et al.*, 1996; Reddy *et al.*, 1996b; Reddy and Reddy, 1999). Therefore, KCBP appears to be a molecular hybrid consisting of a motor domain from MT-based motors and a tail region of some actin-based motors. The tail of myosin VIIa has two long repeats (~460 amino acids per repeat) and that of myosin X has one repeat (Chen *et al.*, 1996). Each repeat contains a MyTH4 domain (~110 aa) and a talin-like (~350 aa) domain. MyTH4 domain and the talin-like regions exist singly in some myosins. Kinesin C does not have talin or MyTH4 domains (Fig 6). The functional significance of MyTH4 and talin-like region is not known.

Ca^{2+}/CaM regulation

Bacterial expression of KCBP motor domain with part of the coiled-coil region forms a dimer revealing that the coiled-coil region is involved in dimerization (Deavours *et al.*, 1998b). In blot overlay assay, the motor domain of KCBP binds tubulin subunits in a concentration-dependent manner (Narasimhulu *et al.*, 1997) and exhibits MT –stimulated

Fig. 7 **Schematic diagrams and alignment of *Arabidopsis* KCBP, human KIFC3, and Myosin VIIa tail regions**. Stars and plus symbols indicate identical and similar amino acids, respectively. Dashes indicate gaps, introduced into sequence for alignment. Numbers at left indicate amino acid residue. (A) Alignment of KCBP and KIFC3 head domains. (B) Alignment of KCBP tail region with the two repeats of MyoVIIa tail region. (C) Schematic diagram of MyoVIIa, KCBP, and KIFC3 proteins. Color representation is as follows: cyan = myosin tail homology 4 regions, green = talin-like domain, red = conserved motor domain of KCBP and KIFC3, blue = coiled-coil region, pink = motor domain of MyoVIIa, and black = calmodulin binding domain (CBD) characteristic for KCBP.

A)

```
860 AQLAELEILYKEEQVLRKRYYNTIEDMKGKIRVYCRIRPLNEKESSERE--KQMLTTVDEFTVEHPWKDDKRKQHIYDR AtKCBP
279 NQ--ELLRKYRRELQLRKKCHNELVRLKGNIRVIARVRPVTKEDGEGPEATNAVTFDADDDSIIHLLHKGKPVSFELDK HsKIFC3

937 VFDMRASQDDIFEDTKYLVQSAVDGYNVCIFAYGQTGSGKTSTIYGHESNPGLTPRATKELFNILKRDSKRFSFSLKAY AtKCBP
356 VFSPQASQQDVFQEVQALVTSCIDGFNVCIFAYGQTGAGKTYTMEGTAENPGINQRALQLLFSEVQEKASDWEYTITVS HsKIFC3

1016 MVELYQDTLVDLLLPKSARRLKLEIKKDSTGMVFVENVTTIPISTLEELRMILERGSERRHVSGTNMNEESSRSHLILS AtKCBP
 435 AAEIYNEVLRDLLGKEPQEKLEIRLCPDGSGQLYVPGLTEFQVQSVDDINKVFEFGHTNRTTEFTNLNEHSSRSHALLI HsKIFC3

1095 VVIESIDLQTQSAARGKLSFVDLAGSERVKKSGSAGCQLKEAQSINKSLSALGDVIGALSSGNQHIPYRNHKLTMLMSD AtKCBP
 514 VTVRGVDCSTGLRTTGKLNLVDLAGSERVGKSGAEGSRLREAQHINKSLSALGDVIAALRSRQGHVPFRNSKLTYLLQD HsKIFC3

1174 SLGGNAKTLMFVNVSPAESNLDETYNSLLYASRVRTIVNDPSKH 1217 AtKCBP
 593 SLSGDSKTLMVVQVSPVEKNTSETLYSLKFAERVRSVELGPGLR 636 HsKIFC3
```

B)

```
 121 PIPTSLLK--INSDLVSRATKL-FHLILKYMGVDSSDRSTPPSLDERIDLVGKLFKKTLKRVELRDELFAQISKQTRHN AtKCBP
1116 ------LKK--KSKLTEEVTKRL-HDGESTVQGNSMLEDRPTSNLEKLHFI---IGNGILRPALRDEIYCQISKQLTHN HsMyoVIIa
1713 PLKQALLKKLLGSEELSQEACLAFIAVLKYMGDYPSKRTRSV-N----ELTDQIFEGPLKAEPLKDEAYVQILKQLTDN HsMyoVIIa

 197 PDRQYLIKAWELMYLCASSMPPSKDIGGYLSEYIHNVAHDATIEPDAQVLAVNTLKALKRSIKAGPRHTTPGREEIEAL AtKCBP
1183 PSKSSYARGWILVSLCVGCFAPSEKFVKYLRNFIH-----G-GPP-GY--APYCEERLRRTFVSGTRTQPPSWLELQAT HsMyoVIIa
1787 HIRYSEERGWELLWLCTGLFPPSNILLPHVQRFLQSRKHC----P----LAIDCLQRLQKALRNGSRKYPPHLVEVEAI HsMyoVIIa

 276 L-TGRKLTTIVFFLDETFEEISYDMATTVSDAVE-VAGTIKLSAFSSFSLFECRKVVSSSKSSDPGNEEYIGLDDNKYI AtKCBP
1253 K-SKKPIMLPVTFMDGTTKTLLTDSATTAKELCNALADKISLKDRFGFSLY----IALFDKVSSLGSGSDHVMDAISQC HsMyoVIIa
1858 QHKTTQIFHKVYFPDDTDEAFEVESSTKAKDFCQNIATRLLLKSSEGFSLF----VKIADKVLSVPENDFF-FDFVRHL HsMyoVIIa

 353 GDLLAEFKAIKD-----------RNK--GEILHCKLVFKKKLFRESDEAVTDLMFVQLSYVQLQHDYLLGNYPVGRG- AtKCBP
1327 -EQYAKEQGAQE-----------RN---A---PWRLFFRKEVFTPWHSPSEDNVATNLIYQQVVRGVKFGEYRCEKED HsMyoVIIa
1932 TDWIKKARPIKDGIVPSLTYQVFFMKKLWTTTVPGK-----------DPMADSIF---HYYQELPKYLRGYHKCTRE- HsMyoVIIa

 417 DAAQLCALQILVGIGFVNSPESCIDWTSLLERFLP-RQIAITRAKREW-ELDILARYRSMENVTKDDARQQFLRILKAL AtKCBP
1387 DLAELASQQYFVDYGSEMILERLL---NLVPTYIPDREITPLKTLEKWAQLAIAAHKKGIYAQRRTDA-QK 1453 HsMyoVIIa
1995 EVLQLGAL--IYRVKFEEDKSYFPSIPKLLRELVP-QDLIRQVSPDDW+KRSIVAYFNKHAGKSKEEAKLAFLKLIFKW HsMyoVIIa

 494 PYGNSVFFSVRKIDDPIGLLPGRIILGINKRGVHFFRPVPKEYLHSAELRDIMQFGSSNTAVFFKMRVAGVLHIFQFET AtKCBP
2070 PTFGSAFFE--QTTEPN--FPEILLIAINKYGVSLIDPKTKDILTTHPFTKISNWSSGNT--YFHITI-GNL-VR---- HsMyoVIIa

 573 KQGEEI-CVA-LQTHINDVMLRRY-SKARSAANSLVNGDISCS 612 AtKCBP
2137 --GSKLLCETSLGYKMDDLLTS-YISQMLTAM-SKQRGSRSGK 2175 HsMyoVIIa
```

MyTH4

Talin-like region

C)

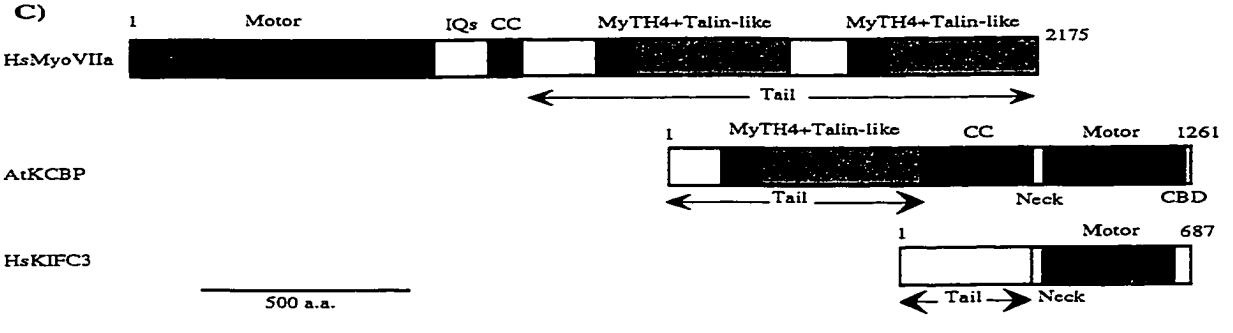

ATPase activity (Deavours *et al.*, 1998b). Cosedimentation assays with MTs indicate that the N terminus region of KCBP has an ATP-independent MT-binding site (Song *et al.*, 1997). An ATP-independent MT-binding site is also present in the tail domain of Ncd, Kar3, and kinesin heavy chain (Meluh and Rose, 1990; Navone *et al.*, 1992; Chandra *et al.*, 1993).

In vitro motility studies, blot overlay assays, pelleting assays, and MT bundling, are four independent sets of experiments that provided insight into Ca^{2+}/CaM regulation of KCBP association with MTs. *In vitro* motility studies with GST-KCBP that consists partly of a coiled-coil region (~70 residues), the entire motor domain and CBD shows movement along MTs towards their minus end. However, KCBP preincubated with bovine CaM and Ca^{2+} does not bind or translocate MT but MTs are observed floating in solution (Song *et al.*, 1997). KCBP binds to tubulin subunits in the presence of either Ca^{2+} or CaM alone, but in the presence of Ca^{2+}/CaM, KCBP dissociates from MTs. This Ca^{2+}/CaM regulation of KCBP interaction with MT was abolished in the presence of antibodies raised against CBD. Additionally, a bacterially expressed construct, which is missing the CBD, has the ability to bind MTs but is insensitive to Ca^{2+}/CaM (Narasimhulu *et al.*, 1997; Narasimhulu and Reddy, 1998). Ca^{2+}/CaM prevents the MT binding in a cosedimentation assay and inhibits MT-stimulated ATPase activity (Deavours *et al.*, 1998a). In an MT bundling experiment, the C-terminal and N-terminal tail of KCBP promote bundling of MTs into cables, indicating that there are two regions within KCBP that are directly capable of MT bundling (Kao *et al.*, 2000). Ca^{2+}/CaM disassociates preformed KCBP-MT rigor complexes formed in the presence of AMP-PNP (Kao *et al.*, 2000). Together, these results indicate the functional importance of CBD on the regulation of KCBP affinity and the effect of Ca^{2+}/CaM on the motor affinity for MTs. The proposed scenario is that cytosolic Ca^{2+} increased in response to

some signals binds CaM, and the activated CaM interacts with CBD of KCBP thereby reducing the affinity of motor to MTs, and preventing its interaction with MTs.

KCBP functions

Immunolocalization, antibody injection studies, yeast two-hybrid screening, and genetic analysis have provided insights into cellular functions of KCBP (Bowser and Reddy, 1997; Oppenheimer *et al.*, 1997; Smirnova *et al.*, 1998; Day *et al.*, 2000), and (Thomas, 2001). Affinity purified KCBP-Ab recognizes a single polypeptide (molecular mass 140 kDa) in protein gel blots of total protein extracts from *Arabidopsis* seedlings and suspension cells and tobacco BY-2 suspension cells. KCBP-Ab does not cross-react with other CBDs from potato, suggesting that the antibody is specific to KCBP and does not recognize other CBDs (Bowser and Reddy, 1997).

(a) Cell division

High levels of KCBP mRNA in meristematic and suspension cultures (Reddy *et al.*, 1996a; Reddy *et al.*, 1996b) suggest that KCBP has a role(s) in cell division. Cell division in plant cells differs from that in animal cells in the following aspects. (1) In late G2, just prior to prophase, cortical MTs rearrange to form a band of MTs called the preprophase band (PPB), that encircles the cell just below the cell membrane (Gunning and Wick, 1985; Baskin and Cande, 1990; Goddard *et al.*, 1994). PPB determines the location of the future cell plate (Torres-Ruiz and Jurgens, 1994; Traas *et al.*, 1995). (2) Bipolar spindles are formed in absence of well-defined centrosomes, which are MT organizing centers in animals (Smirnova and Bajer, 1994; Franklin and Cande, 1999). (3) Cytokinesis occurs via the formation of a cell plate that expands centrifugally between daughter nuclei (Staehelin and Hepler, 1996; Sylvester, 2000). Formation and growth of a cell plate between daughter nuclei is controlled

by the phragmoplast which consists of two sets of MTs and actin with their plus ends interdigitating on the equatorial plane (Hepler and Jackson, 1968; Euteneur *et al.*, 1982; Wick, 1991).

In immunolocalization studies with *Arabidopsis* suspension cells, KCBP colocalizes with MTs in metaphase cells to either side of the chromosomes. In late anaphase, KCBP was associated with the interzone between separating chromosomes, and between the daughter nuclei in cytokinetic cells except in the midzone where a slightly unstained region was observed (Bowser and Reddy, 1997). Similar patterns of staining were observed in tobacco BY-2 cells. In BY-2 cells, the KCBP-Ab and β tubulin-Ab colocalize to the preprophase band also. In synchronized BY-2 cells, KCBP was abundant in M-phase cells and declined as the cells entered interphase. Localization of KCBP in *Haemanthus* also showed localization to mitotic MT arrays with some differences. KCBP appears first in association with the prophase spindles (Smirnova *et al.*, 1998). During metaphase, KCBP decorates MTs of kinetochore-fibers on either side of chromosomes. By mid-anaphase, the protein redistributes and accumulates at the spindle pole regions. In telophase, KCBP relocates towards the phragmoplast and cell plate.

Microinjection studies of KCBP into living stamen hair cells of *Tradescantia virginiana* during all phases of cell division also supports the roles of KCBP in cell division (Vos *et al.*, 2000). Ca^{2+}/CaM inhibit the interaction of KCBP with MTs. However, in the presence of antibodies to CBD, the regulation is abolished (Narasimhulu and Reddy, 1998) and so the injection of these antibodies is thought to activate KCBP constitutively (Vos *et al.*, 2000). The outcome of the antibody injections depends on the timing of the injections. The injections with KCBP-Ab differentially affect specific phases during cell division but not the

cytoplasmic streaming or cell viability during interphase. Microinjection of KCBP-Ab during late prophase results in the premature breakdown of the nuclear envelope and early onset of prometaphase. However, these cells subsequently arrest in late prometaphase or metaphase and do not enter anaphase. Instead, the chromosomes became disoriented throughout the center of the cell. Injection of KCBP-Ab into late metaphase or early anaphase cells does not affect anaphase morphology and transition time. On the other hand, injection of KCBP-Ab during mid-anaphase causes aberrant formation of the phragmoplast and cell plate, and completion of cytokinesis is delayed or inhibited.

Localization of KCBP in the phragmoplast suggests the involvement of KCBP in phragmoplast function and/or cell plate formation. The polarity of MTs and microfilaments in the phragmoplast (Euteneur *et al.*, 1982; Staehelin and Hepler, 1996) indicated that plus-end motors are likely to be involved in the transport of vesicles to the cell plate. TKRP125, a plus-end motor, localizes to the phragmoplast and is shown to be involved in phragmoplast organization (Asada *et al.*, 1997). KCBP, a minus-end motor, is not likely to be involved in transporting vesicles to the cell plate since the MTs are oriented with their plus ends facing the cell plate. One intriguing possible function of KCBP could be recycling of Golgi vesicles membranes from the expanding cell plate, a process which would require a minus-end directed motor protein (Reddy, 2001). Furthermore, KCBP may also be involved in forming the phragmoplast by cross-linking MTs, a property associated with C-terminal motors in yeast and animals (McDonald and Goldstein, 1990; Chandra *et al.*, 1993; Endow *et al.*, 1994b). The finding that the amino-terminus of KCBP possesses a functional ATP-insensitive MT-binding site and the ability of KCBP to bundle MTs support this idea (Narasimhulu and Reddy, 1998; Kao *et al.*, 2000). Localization of KatA, a minus-end motor,

in the phragmoplast (Liu *et al.*, 1996) suggests that it may also perform similar functions to KCBP but without Ca^{2+}/CaM regulation.

(b) Morphogenesis

The final shape of a plant cell is the result of a precisely guided cell wall expansion. The plant cytoskeleton is known to play a pivotal role in determining the direction of cell wall expansion, in part by controlling the orientation of the microfibrils (Giddings and Staehelin, 1991; Fowler and Quatrano, 1997; Nicol and Hofte, 1998). Trichomes are specialized cell types that are present on the surface of nearly all land plants (Johnson, 1975). However, the morphology and pattern of trichomes vary greatly depending on the species. In *Arabidopsis*, wild type trichomes have a genetically defined shape consisting of a stalk topped by three or four branches (Oppenheimer *et al.*, 1997). The process of trichome development is complex and over 40 genes regulate their spacing, density, and morphology in *Arabidopsis* (Oppenheimer, 1998; Szymanski *et al.*, 2000).

ZWICHEL (*ZWI*) gene encodes KCBP and the *zwichel* (*zwi*) mutant is characterized by trichomes with a short stalk and only two branches suggesting a role for KCBP in trichome morphogenesis (Oppenheimer *et al.*, 1997). It is hypothesized that KCBP participates in reorganizing and/or stabilizing the MT array prior to branch initiation. In an elegant study, Mathur and Chua, (2000) tested this hypothesis by treating *zwichel* mutants, expressing GFP-MT-associated protein4 fusion protein, with the MT stabilizing drug, taxol. Taxol-stabilization of MTs in *zwichel* mutants leads to the initiation of new branch points Mathur and Chua, (2000). Furthermore, trichomes treated with oryzalin, a MT destabilizing drug, do not undergo trichome branching (Mathur *et al.*, 1999). Several alleles of *zwi* have been characterized (Oppenheimer *et al.*, 1997). Three of them have been described below

and all of them are recessive. The T-DNA insertion in the *zwi*-5002 mutant is located between the ATP-binding and the putative MT-binding regions of the motor domain. This insertion is likely to result in a ZWI product without the motor activity. The T-DNA insertion in the *zwi*-4673 mutant is located approximately 2 kb downstream from the polyadenylation site, suggesting that the regulatory elements may have been affected in this mutant. The third allele (zwi-9310-7), the strongest phenotype, was generated by fast neutron mutagenesis, and contained an insertion of about 500 bp of DNA at the N-terminal tail. Analysis of *zwi*-3 by RT-PCR and subsequent sequencing of the resulting cDNA revealed that the *zwi* protein is truncated at the amino acid position 522 and lacks the coiled-coil region and the motor domain. The truncation is due to a novel 5' splice donor in intron 8 resulting in a new reading frame with stop codon in exon 9.

Interestingly, all *zwi* mutants appear to grow normally with only the defect in trichome morphogenesis (Oppenheimer *et al.*, 1997; Krishnakumar and Oppenheimer, 1999). The lack of a phenotype in other tissue suggests that either ZWI is nonessential or another motor with overlapping function may substitute for KCBP function in other tissues. Functional redundancy amongst KLPs has been reported in other non-plant system (Goldstein and Philip, 1999). Similar to ZWI, the lack of Ncd in *Drosophila* causes a defect in meiosis, whereas most mitotic divisions are not affected (Yamamoto *et al.*, 1989). In all the *zwi* mutants the N-terminal region of the protein is not affected. This raises the possibility that the N-terminal region of KCBP may perform some functions in cells other than trichomes whereas trichome development requires the full-length protein (Reddy, 2001). In a suppressor screen with *zwi*-3 mutant, Krishnakumar and Oppenheimer, (1999) isolated three extrageneic suppressors, *suz1*, *suz2*, and *suz3* (suppressors of *zwichel*-3) that rescued

trichome number defect but not the short stalk defect. The failure of the suppressors to rescue the stalk defect may be due to the inability of the suppressors to completely rescue *zwi*-3 mutant or the stalk height may be regulated separately from branch initiation, and these two processes may require different levels of KCBP function, or different functions of the KCBP protein (Krishnakumar and Oppenheimer, 1999). Also, the branch-position function of KCBP may be regulated by a different set of interactions and SUZ proteins may play no role in branch position. Another hypothesis is that the trichome position may require motor function that is lacking in *zwi*-3 mutants. Both of *suz1* and *suz2* mutants are completely recessive, but the *suz3* mutation is weakly dominant (Krishnakumar and Oppenheimer, 1999). All three suppressors were found to be allele-specific and belong to the group of "interactional suppressors" in which particular alleles of one gene are suppressed by the suppressor mutation. Genetic studies have shown that SUZ2 may interact not only with ZWI but also with FURCA1, a gene involved in trichome branching. The *suz1 zwi*-3 double mutants are male sterile due to a defect in pollen germination and pollen tube growth, suggesting a role for these genes in pollen germination and tube growth (Krishnakumar and Oppenheimer, 1999). These suppressor studies suggest that at least three gene products likely interact with the tail region of KCBP. Using the yeast two-hybrid method to screen an *Arabidopsis* expression library with the tail of KCBP, the N-terminal tail region of KCBP has been found to interact with a plant-specific protein kinase, KIPK (KCBP-Interacting Protein Kinase) (Day *et al.*, 2000). Coprecipitation assays confirmed KCBP/KIPK interaction. The association of KIPK with KCBP suggests regulation of KCBP or KCBP-associated proteins by phosphorylation and/or KCBP is involved in targeting KIPK to proper cellular function (Reddy, 2001). Recently, in similar screening, (Thomas, 2001) identified and characterized a

small Ca^{2+}-binding protein, KIC (Kinesin Interacting Centrin-like protein) that interacts with the motor domain of KCBP (Thomas, 2001). KIC was found to interact with KCBP *in vitro* in a Ca^{2+}-independent manner, to bind to phenyl sepharose column in the presence of Ca^{2+}, to exhibit heat stability, and to be expressed predominately in leaf, fruit and flower tissues.

II. MOLECULAR PHYLOGENY OF PLANTS

Molecular phylogenetics is the study of evolutionary relationship among organisms or genes by a combination of molecular biology and statistical techniques. The molecular approach to systematics was initiated by using serological cross-reactions to study the phylogenetic relationships among various groups of animals. The advent of various recombinant DNA techniques and the development of the polymerase chain reaction (PCR) have made molecular systematic studies even easier, resulting in an unprecedented high level of activity in phylogenetic reconstruction. During the past 10-15 years, molecular phylogenetics has dramatically reshaped our view of organismal relationships and evolution. This impact has been manifested at all taxonomic levels, from species to kingdom. For example, molecular studies have revealed that charaphyte green algae are the closest relatives of the land plants (Graham, 1993; Kranz *et al.*, 1995) and suggested that *Amborella*, a single species of which lives on the South Pacific island of New Caledonia, is the first branching angiosperm lineage (Mathews and Donoghue, 1999; Soltis *et al.*, 1999; Barkman *et al.*, 2000) and contradicts the anthophyte hypothesis (Doyle, 1998) in which the closest living relatives of angiosperms are believed to be the gentales, a small and enigmatic group of gymnosperms. About a year ago, the New York Times reported that "evolutionary biologists have at least answered a question so difficult that Darwin himself called it the "abominable mystery"

(Yoon, 1999). Actually the article referred to a consensus, based on molecular data, that *Amborella* and water lilies are at the base of the flowering plants.

Among the genes and gene families that have been extensively used for molecular evolution are the actins and actin gene families in addition to ribosomal RNA genes. These studies are focused on the origin, evolution, intron position, and domain consevation of the genes (Shah *et al.*, 1983; Bagavathi and Malathi, 1996; Bhattacharya and Weber, 1997; Bhattacharya *et al.*, 1998; An *et al.*, 1999; Keeling *et al.*, 1999). These studies have revealed that there are at least 25 intron positions distributed at different locations in the coding regions of actin genes in a wide range of organisms from yeast to humans (Bagavathi and Malathi, 1996). Furthermore, these data suggest that the numerous introns found in all actins are of ancient origin and that they are highly conserved although the coding sequences are not (Shah *et al.*, 1983), suggesting a possible functional significance of introns in present day actin genes (Bagavathi and Malathi, 1996).

Other criteria for determining the evolutionary relationships between proteins showing little or no sequence similarity is the secondary structure topology, comparison of functional domains, and active site chemistry (Kull *et al.*, 1998). Motor proteins of the kinesin and myosin superfamilies are examples of such group of proteins. Both types of motors hydrolyze ATP to generate force for their movement on cytoskeletal elements. Recent studies have shown surprising structural similarities between the motor domains of kinesin and myosins, although there is no amino acid sequence similarity (Kull *et al.*, 1996). This raises an important question: Did the members of kinesin and myosin superfamilies evolve from a common ancestor through divergent evolution or from separate proteins through independent pathways (Convergent evolution)?. Structure topology and active site

chemistry studies have shown that kinesin and myosin and possibly G proteins are directly related via divergent evolution from a common core nucleotide-binding motif (Kull *et al.*, 1998). The sequence similarities between the tails of KCBP and myosin VIIa and X support the hypothesis that the molecular motors have evolved from a common ancestral protein.

Origin of plastids and evolution of photosynthetic eukaryotes

Plant molecular evolution has been dominated by studies of plastids (the organelles in which photosynthesis occurs). Phylogenetic analyses have revealed that they arose aeons ago from bacteria that set up home within unicellular eukaryotic organisms (Palmer, 2000). It was first proposed that there were five independent origins of plastids from different photosynthetic bacteria (Mereschkowsky, 1910), but now it is widely agreed that plastids originated only once (Cavalier-Smith, 1987; Cavalier-Smith, 1995; Kohler *et al.*, 1997; Martin and Herrmann, 1999). Photosynthetic eukaryotes have two fundamentally different types of plastids. Primary plastids, the double-membrane-bound products of a symbiotic relationship between eukaryotic cells and cyanobacteria (Palmer, 2000) and are found in green algae, land plants, red algae, and the glaucophytes such as, *Cyanophora paradoxa* (Bhattacharya and Medlin, 1998) (Fig 8). Secondary plastids were acquired by the subsequent uptake of one of these primary phototrophs by a second eukaryotes and these plastids are recognized by the presence of extra plastid membranes (Keeling *et al.*, 1999). There are two lines of secondary symbiogenesis (Cavalier-Smith, 2000). The first occurred with a red algal endosymbiont to produce the chromophytes (a collective term for algae with chlorophyll c), including dinoflagellates, sporozoans, cryptomonads, and chromobiotes. The second occurred with a green algal endosymbiont to generate euglenoid and chlorarachnean

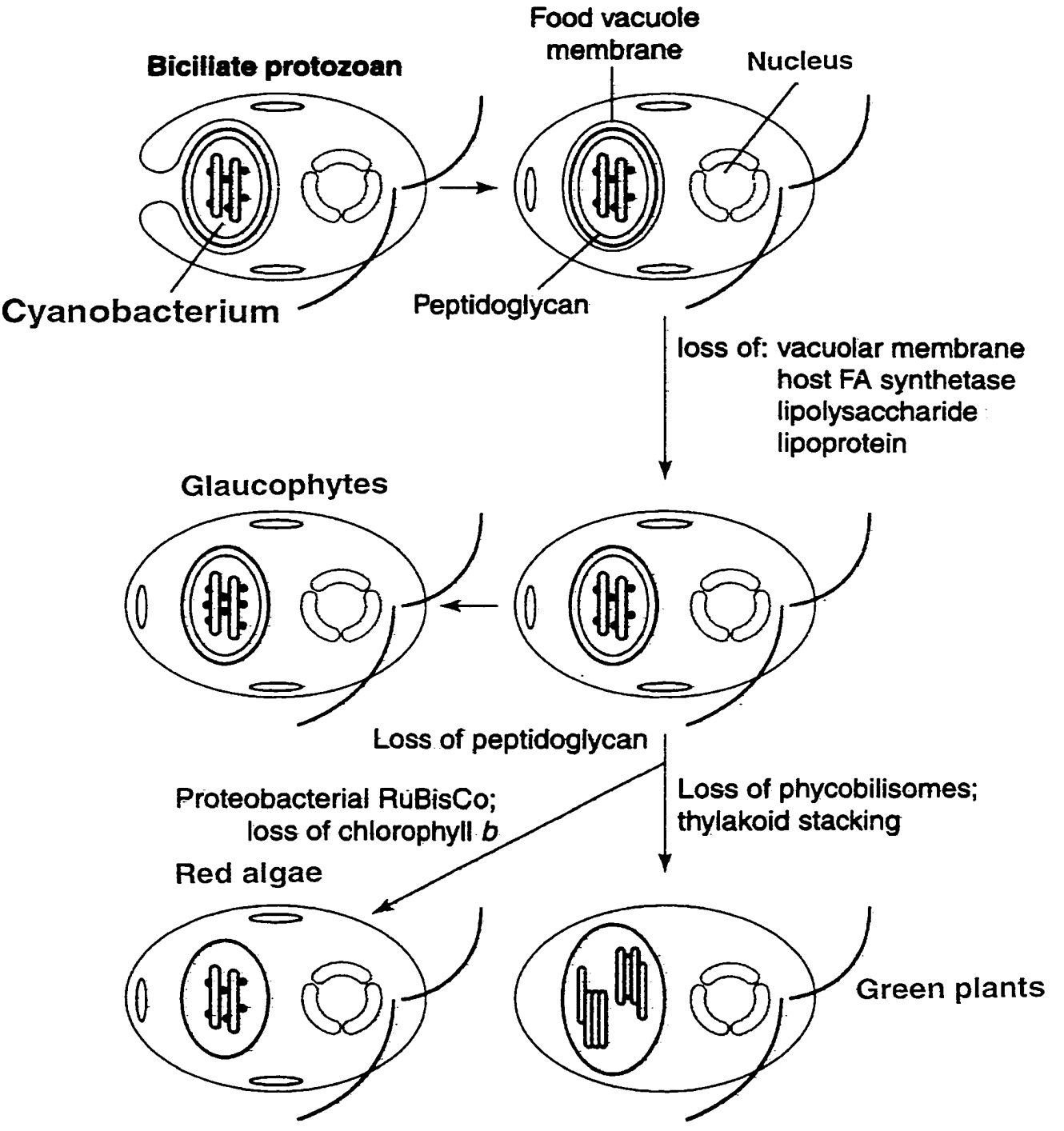

Fig. 8 The symbiotic origin of plastids. Plastids arose monophyletically from a cyanobacterium with phycobilins and chlorophyll a and b that was phagocytosed by a biciliate protozoan host that convert it to organelles. Some of the cyanobacterium genes were transferred to the host during the course of the evolution. In the ancestral plant, the food vacule membrane was lost. Therefore, plant plastids have only a double envelope. Green plant lost phycobilisomes and evolved thylakoids, whereas red algae and glaucophyta lost chlorophyll b, possibly independently. Modified from Cavalier-Smith, (2000).

algae (Cavalier-Smith, 2000). In both cases the endosymbiont genome was reduced and genes were transferred to the host nucleus (Bhattacharya and Medlin, 1995; Gilson and McFadden, 1996).

Red algae and glaucophytes (collectively termed biliphytes because they retained the ancestral cyanobacterial phycobilisomes and unstacked thylakoids) have plastids that closely resemble cyanobacteria, whereas the ancestor of the angiosperms lineage, which includes green algae, bryophytes, and vascular plants lost phycobilisomes and evolved stacked thylakoids (Cavalier-Smith, 1982). Evidence from plastid genes (Martin, 1998) and retention of a bacterial cell wall by glaucophyte plastids (termed cyanelles) supports the hypothesis that glaucophytes represent the first branch of plastid evolution.

It is well established that the land plants are monophyletic and that "bryophytes" are the most primitive land plants (Graham, 1993; Mishler, 1994; Kenrick and Crane, 1997) and evolved at least 450 million years ago (Waters and Vierling, 1999). Molecular data currently support the monophyletic origin of gymnosperms, which evolved from ferns about 300 MYA (Goremykin *et al.*, 1996; Samigullin *et al.*, 1999; Soltis *et al.*, 1999). Angiosperms are evolved from gymnosperms and then diverged into monocots and dicots (Wolfe *et al.*, 1989) (Paterson *et al.*, 1996). Molecular evidence from mitochondrial and plastid genomes support the evolution of flowering plants from non-flowering seed plants and also demonstrate that *Ambroella*, water lilies (Nymphaeales) and *Austrobaileya* represent the first stages of angiosperm evolution. These molecular data are supported by physiological and anatomical data such as self-incompatibility, carpel closure, and structure of vessels. Similar evidence also was obtained from nuclear genes such as the homeobox gene family, MADS-box gene family and phytochromes gene-pair (*PHYA*, *PHYB/D*, *PHYC*, and *PHYE).* MADS-box

genes in flowering plants encode transcription factors that control both flower meristem formation and organ identity in the developing flower. Homologues of these genes have been found in the Norway spruce, a gymnosperm, (Tandre *et al.*, 1995). Some of these genes are expressed only in the male and female strobili and control the identity of the sexual organs. The four phytochrome genes were found in most angiosperms examined, whereas only two gene lineages (PHYC and PHYB/D) related to these genes are known from other seed plants (Mathews and Donoghue, 1999). However, there is little agreement as to when angiosperms arose or even from which branch of the gymnosperms they originated (Wolfe *et al.*, 1989). The fossil record of the flowering plants extends back at least 130 million years (Donoghue and Doyle, 2000), however several lines of molecular evidences do not rule out an earlier origin of the angiosperms, approximately 200 million years ago (Graham and Olmstead, 2000).

The divergence between monocots and dicots represents a major event in higher plant evolution, yet the date of this occurrence has remained enigmatic for over a century. Using two independent approaches, the rate of synonyous and nonsynonymous nucleotide substitution with plastid DNA sequence, led to an estimation of the monocot-dicot divergence at 200 million years ago with an uncertainty of about 40 million years. This supports the theory that angiosperms existed for a considerable period of time before coming to dominate the Earth's flora (Wolfe *et al.*, 1989). This estimate is also supported by analysis of the nuclear genes that encode large (26S) and small (18S) subunit ribosomal RNAs. In other controversial estimates based on the nuclear gene, glyceraldehyde-3-phosphate dehydrogenase (called *gapC* in plants), monocots and dicots diverged about 320 million

years ago, which is long before angiosperms appeared in the fossil record (Martin *et al.*, 1989).

Although monocot and dicot genes and gene families are derived from a single ancestral origin, many of their nuclear and organelle genes show considerable variation in their copy number, conserved motifs, and transcription regulation. For example, analysis of the consensus sequences of the mitochondrial promoter around the transcription initiation sites exhibits several differences between monocot and dicot mitochondria (Fey and Marechal-Drouard, 1999). These consensus sequences are highly conserved in dicots, while they show more plasticity in monocots. Furthermore, analysis of the small single-copy (SSC) region of the plastid genome of the non-photosynthetic flowering plant, *Epifagus virginiana,* showed that there were differences among dicots, monocots, and bryophytes (Wolfe *et al.*, 1992). A protein of 1738 codons in *Epifagus virginiana* is equivalent to a single open reading frame (ORF) of 1901 codons in tobacco (dicot), to a severely truncated pseudogene in rice (monocot), and to two genes of 1068 and 464 codons in *Marchantia* (Bryophyta). Other examples came from the nuclear genes of the catalase gene family (Frugoli *et al.*, 1998). Monocot and dicot plants have three catalase genes, *CAT1*, *CAT2*, and *CAT3,* and they have conserved introns in novel positions as well as lost introns. This was explained by gene duplication before divergence of monocots and dicots followed by intron loss and gain (Frugoli *et al.*, 1998). Similar observations were made for the actin gene family in angiosperms (Moniz de Sa and Drouin, 1996).

Phylogenetic analyses of kinesin and myosin superfamilies are used to classify them into subfamilies. However, the origin and evolution of any particular member of the kinesin superfamily has not been investigated. Therefore it will be of interest to study the origin,

evolution and gene structure of KCBP, a unique motor protein, among phylogenetically *diverged* species. KCBP, a plant-specific KLP, has been studied extensively in the dicot plant, *Arabidopsis*. KCBP is unique among all known KLPs in having CBD at the C-terminal region and MyTH4 and talin-like region in the N-terminal region. Kinesin C, CBD-containing KLP, has been cloned from sea urchins. Outside the motor domain, kinesin C does not show any sequence similarity to KCBP. A homologue of KCBP has not been found in the completely sequenced genomes of *S.cerevisia*, *C.elegans*, and *Drosophila*, suggesting that it is unique to plants. One major objective of this research was to investigate the origin of KCBP and to test whether KCBP co-evolved with the formation of phragmoplasts or if it is ubiquitous in all photosynthetic eukaryotes. A second purpose of this research was to investigate the gene structure, exon/intron organization, intron position, and domain conservation and function of KCBP among different photosynthetic eukaryotes, ranging from a most primitive photosynthetic, unicellular eukaryotes, to highly evolved monocots. Using different molecular approaches, such as PCR and library screening, KCBP homologs were cloned and characterized from representative species of phylogenetically *diverged* groups, including monocotyledons (*Zea mays*), gymnosperms (*Picea abies*), a green alga (*Stichococcus*) and the endosymbiotic glaucophyte *Cyanophora paradoxa*. The results show that the coding regions of KCBP are highly conserved among phylogenetically diverged organisms. However, the gene structure, size and organization of introns/exons, and GC content are highly variable. Two unique domains of KCBP, the MyTH4 and talin-like regions and the CBD are also conserved in all KCBPs. The data also suggest a tendency for reduction in the number of introns per coding sequence throughout the course of evolution. The CBD is interrupted by an extra intron in green algae and glaucophyta, which is not

present in the angiosperms. KCBP in all tested organisms is recognized by polyclonal KCBP-Ab that was raised against the CBD of *Arabidopsis* KCBP.

KCBP is negatively regulated by Ca^{2+}/CaM, and the KCBP mutant (*zwi*) has unbranched trichomes or trichomes with two only branches. Therefore, it is of interest to manipulate the cytosolic Ca^{2+} level using ionophores and ionomyceins to investigate the resulting phenotypes. The results show high cytosolic Ca^{2+} produces different levels of *zwi* phenotypes in addition to phenotypes of other trichome mutants.

CHAPTER 2

MATERIALS AND METHODS

MATERIALS AND METHODS

I. Materials

Cyanophora paradoxa Korschikoff and *Stichococcus bacillaris* were grown in sterilized lake water enriched with Algo-Gro concentrate solution (Carolina Biological Co., Burlington, NC) at 18 ^{0}C in a 16:8 h light/dark cycle. After 10 days, cells were collected by centrifugation and kept at –80 ^{0}C for DNA, RNA and protein extraction.

Cyanophora paradoxa cDNA library prepared in pBluescript vector was kindly provided by Dr.Wolfgang Loeffelhardt, Universitat Wein, Vienna, Austria.

A spruce cDNA library, in Lambda gt10, was prepared from female strobilus RNA. This library was provided by Dr. Annika Sundas, Uppsala University, Uppsala, Sweden.

Spruce (*Picea abies* L. Karst) seeds, kindly provided by Dr. Peter Hedley, Scottish Crop Research Institute, Invergowire, UK, were germinated and grown on moist vermiculite in a growth chamber at 25 ^{0}C for 3 weeks in white light (16 h light, 8 h dark). Seedlings were collected and stored at –80 ^{0}C until use.

A maize genomic library prepared from young maize seedlings in the Lambda EMBL3-3SP6/T7 vector was purchased from Clonetech. Other genomic DNA libraries used to isolate KCBP were as described later.

A. Cloning of KCBP from phylogenetically *diverged* species

A-1 Cloning of KCBP from monocotyledons (*Zea mays*), ZmKCBP

(i). Screening of a maize genomic library

A maize genomic library was prepared from maize seedlings. The DNA was partially digested with *Sau3*A, size fractionated, and cloned into the *BamH*I site of the EMBL-3SP6/T7 vector (CLONTECH). For primary screening, approximately 5 X 10^5 recombinant plaques were plated on 15 cm plates at a density of about 40,000 pfu per plate using NZCYM medium {one liter contains 5 g NaCl, 2 g $MgSO_4.7\ H_2O$, 5 g yeast extract, 10 g NZ amine (casein hydrolysate), 15 g agar, pH 7.5} and *E. coli* XLI-blue MRA (Stratagene) as the host strain Sambrook *et al.*, (1989). The plates were incubated at 37 °C for 8 hours until clear plaques were visible, then chilled at 4 °C for at least 1 hour. Plaques were lifted on duplicate Hybond-N^+ (Amersham) membranes according to the manufacturer's instructions. The phage DNA was denatured for 2 min in denaturing solution (1.5 M NaCl, 0.5 M NaOH), followed by neutralization for 5 min in neutralization solution (1.5 M NaCl, 0.5 M Tris-HCl, pH 8.0). Membranes were rinsed in 2X SSC (2X= 0.3 M NaCl, 0.03 M sodium citrate) buffer for 5 min and then dried at room temperature for 10 min. The DNA was fixed on membranes by exposing to UV light in a Stratalinker (Stratagene), followed by baking in an oven for 1 hour at 60 ^{0}C. Membranes were incubated in pre-hybridization solution (0.5 M sodium phosphate and 0.7% w/v SDS) for three hours at 60 ^{0}C and then in a hybridization solution [pre- hybridization solution with a ^{32}P-labelled PCR-amplified 812-bp cDNA of *Arabidopsis* KCBP containing the coding region for the motor and CaM-binding domains (Reddy *et al.*, 1996b) for 18 hours. Radioactive probe was synthesized with an oligolabelling kit from Amersham using nanonucleotide random primers. After hybridization, membranes were washed in 2X SSC containing 0.1 % SDS (w/v) at room temperature followed by

washing for 15 min each at 60 ^{0}C in 1X SSC containing 0.1 % SDS (w/v) and 0.1X SSC containing 0.1 % SDS (w/v). Membranes were wrapped with Saran wrap, exposed to X-ray film and developed using X-ray film processor (AFP Imaging Corp). Fourteen putative positive clones were picked and put in 1 ml of SM (5.8 g NaCl, 0.977 g MgSO4, 0.1 g gelatin, 50 ml 1 M Tris-HCl pH 7.5, and water to 1 liter) plus 50 µl of chloroform. After elution for one hour at room temperature, serial dilutions were made of each sample (1:100, 1:1000, and 1:10,000) and 10 µl was added to XL1-blue cells and plated on 9 cm plates. Pfu in each plate were counted and aliquots containing about 1000 pfu were used for second screening (Fig 9). Plaques lifting and hybridization was done as above and two positive plaques were picked from each plate and placed in 1 ml SM plus 50 µl chloroform. The positives were confirmed by a third round of screening.

Phage DNA isolation

Phage DNA was isolated using the PEG precipitation method (Chisholm, 1989):

- 100 ml of NZCYM medium was inoculated with 100 µl of XLI-Blue MRA cells and grew to an $O.D_{600}$ of about 0.2-0.3
- Cells were spun down at 4 ^{0}C and resuspended in 10 mM $MgSO_4$ to a final OD of 1.0
- 10-100 µl of eluted phages were added to 500 µl of host cells and incubated at 38 ^{0}C for 30 min for adsorption
- The preadsorbed phage was added to 50 ml of NZCYM in 250 ml Erlenmeyer flasks, grown at 38 ^{0}C for 12-16 hour with gentle shaking (200 rpm) until complete lysis occurred, and then 100 µl chloroform was added with continous shaking for an extra hour

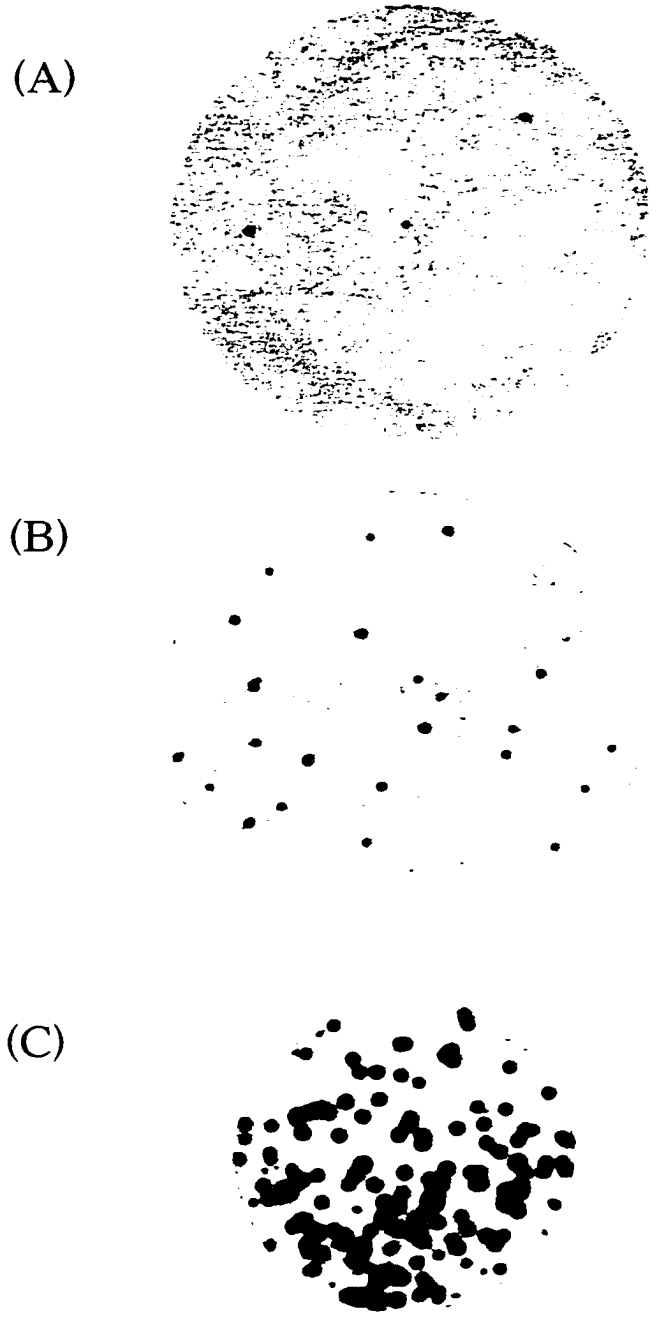

Fig. 9 **Screening of maize genomic library.** Maize genomic library was screened with ^{32}P-labelled 812-bp PCR-amplified cDNA of *Arabidopsis* KCBP that contained the coding region for the domain and calmodulin-binding domains. 5X10^5 pfu were screened and 14 putative positives clones were picked and purified by two additional rounds of screening. A,B, and C represent the first, second, and third screening, respectively.

- 370 µl of nuclease solution {50 mg DNase 1 (Sigma), 50 mg RNase A(Sigma) in 10 ml of 50% glycerol, 30 mM sodium acetate, pH 6.8} were added, incubated at 37 ^{0}C for one hour, 3 g of NaCl was added, and mixed gently until dissolved
- After spinning for 20 min at 7,000 rpm using Sorvall HS-4 rotor at 4 ^{0}C, 5 g of polyethylene glycol (6,000-8,000 molecular weight) was added, gently dissolved by mixing, and kept on ice for at least one hour
- Centrifuged as before, suspended in 500 µl of SM, transferred to microfuge tube and extracted with chloroform
- To the aqueous phase 20 µl of 0.5 M EDTA, 5µl of 20% SDS, and 10 µl of proteinase K (2.5 mg/ml) was added and incubated at 65 ^{0}C for 30 min
- The solution was extracted once with an equal volume of phenol and once with an equal volume of chloroform. Then one seventy µl of 6 M ammonium acetate was added to the aqueous phase and the DNA was precipitated by adding 700 µl of isopropanol
- The mixture was spun down for 15 min in a microfuge at 4 ^{0}C
- The pellet was washed with 70% ethanol, dried in Speed Vac and dissolved in a small volume of TE (100-300µl).

Subcloning

Restriction analysis, together with Southern blotting using probes from both 3' and 5' ends of *Arabidopsis thaliana* (AtKCBP) indicated that two clones (clone 6 and 13) contained the complete gene. Digestion of clones with *SalI*/*EcoR*I and *XbaI*/*Sal*I yielded 6 kb and 7 kb hybridizing fragments, respectively. Digested fragments were separated on a 0.8% agarose gel the DNA was isolated by low-melting point (L.M.P.) agarose method (Falson, 1992). A window was prepared in the gel in front of the fragment. A 1% solution of L.M.P. agarose

(Life Technologies) was poured in the window around the gel piece containing the DNA and kept at 4 ^{0}C for 15 min. DNA was run into the L.M.P. agarose and then the gel pieces containing DNA were excised under long wavelength UV light. Equal volume of TE (10 mM Tris-HCl, pH 8.0, 1 mM EDTA) buffer was added and the mixture was kept at 65 ^{0}C to melt the agarose. After cooling to room temperature an equal volume of equilibrated phenol was added, vortexed, and centrifuged for 3 min at 12,000 rpm. One-tenth volume of 4 M LiCl was added to the supernatant, and the mixture was placed on ice for 3 min, centrifuged for 5 min as above and the supernatant was collected. Then 2.5 volumes of 95% cold ethanol and 1 µl of molecular grade muscle glycogen (20 mg/ml) were added, and the entire mixture was kept at –20 ^{0}C for 30 min before centrifugiation at 4 ^{0}C for 30 min. The pellet was washed twice with 70% ethanol, dried in a Speed Vac and re-suspended in 20 µl of H_2O. pBluescript KS^+ was cut with the same enzymes, separated on agarose gel and purified as above. Ligation was done in a 20 µl reaction containing digested vector and fragments (1:6 molar ratio), 4 µl of 5X T4 ligase buffer (Gibco BRL) [250 mM Tris-HCl (pH7.6), 50 mM $MgCl_2$, 5 mM ATP, 5 mM dithiothreitol, 25 % (w/v) polyethylene glycol], 1 µl of T4 DNA ligase (1 unit/µl) (Gibco BRL). Ligation was left at room temperature for 1 hour and then kept at 4 ^{0}C overnight. The ligation reaction was brought to 100 µl with water, extracted with an equal volume of phenol/chloroform (50:50 v/v) and then with chloroform. One-tenth volume of 3 M sodium acetate, pH 5.2 and 2.5 volumes of ethanol were added to the aqueous phase, kept at –20^{0}C for 1 hour and centrifuged at 4 ^{0}C for 30 min. The pellet was washed two times with 70% ethanol, dried and dissolved in 5 µl H_2O for transformation.

Transformation

Fresh electrocompetent *E. coli* DH5α cells were prepared by inoculating 5 ml of YENP medium (0.75% Bact Yeast Extract, 0.8% Bacto Nutrient broth) with a single big colony of *E. coli* DH5α and grown overnight at 37 °C with shaking. One liter of YENP medium was inoculated with the 5 ml culture and grown at 37 °C with shaking to an $O.D_{600}$ = 0.4-0.5. Cells were chilled on ice, collected by centrifugation for 10 min at 4 ^{0}C, washed two times with 1/10 volume sterile distilled cold H_2O and one time with 1/50 volume of cold 10% glycerol. Then cells were re-suspended in a final volume of 3 ml of 10% glycerol, aliquoted into sterile microcentrifuge tube, and stored at – 80 ^{0}C. Cells were electroporated with 1.5 and 3.5 µl of ligated DNA at 200 volts, added to 1 ml of SOB (0.5% Bact Yeast Extract, 2% Bactotryptone, 10 mM NaCl, 2.5 mM KCl, 10 mM $MgCl_2$, and 10 mM $MgSO_4$) medium and grown for 1 hour at 37 ^{0}C with shaking. Aliquots of 10 and 100 µl were spread on LB ampicilin plates (one liter contains 10 g NaCl. 10 g tryptophane, 5 g yeast extract, 20 g agar, pH 7.0 and 80 µg/ml ampicilin, the antibiotic was added after autoclaving) that were previously spread with 40 µl X-Gal (20 mg/ml) and 34 µl IPTG (100 mM). White colonies were selected for plasmid DNA preparation.

Plasmid DNA isolation

White colonies were grown overnight in 3 ml LB medium containing 50 µg/ml ampicilin and the plasmid DNA was isolated using a Q1AGEN miniprep isolation kit according to the instructions provided by the manufacturer. The plasmid DNA was eluted in 50 µl H_2O for sequencing and further analysis.

B. Cloning of KCBP from Gymnosperms, spruce (*Picea abies*)

B-1. PCR amplification of KCBP motor domain from spruce cDNA library

KCBP motor domain of spruce was amplified from a cDNA library using PCR. Two degenerate primers, sense [5'-ATT/C/ATTT/CGCITAT/CGCICAA/GAG-3'] and antisense [5'-CIGCT/CTGT/CTCT/CTTCCAG/ATA-3'] corresponding to the conserved ATP-binding site and CBD, respectively in KCBP were used to amplify a C-terminal region of PaKCBP (~900 bp) from spruce cDNA library. Sense and antisense primers contained restriction sites for *EcoR*I and *BamH*I, respectively. The PCR reactions were performed in a final volume of 50 µl. The reaction mixtures were preheated at 94 °C for 4 min and cooled to 50 °C, and Taq polymerase was added to initiate the amplification reactions. Thirty-five cycles of amplification were performed in an Eppendorf Mastercycler Gradient followed by a final extension for 10 min at 72 °C. Each amplification cycle consisted of 1 min of denaturation at 94 °C, 1 min of annealing at 50 °C and 2 min of extension at 72 °C. PCR amplified products were separated on an agarose gel, purified with QIAGEN PCR purification kit (QIAGEN), cloned into pGEM-Teasy cloning vector following the instructions provided (Stratagene, La Jolla. CA), verified by sequencing and used as a probe for cDNA library screening.

B-2. Screening of spruce cDNA library

Approximately 5 x 10^5 recombinant plaques from amplified spruce cDNA library were screened for KCBP following the protocol described above (see section 1-1) with some modification. The probe was ^{32}P-labelled 900 bp PCR amplified fragment from the spruce cDNA library. After purification and confirmation of positive plaques, phage DNA from nine positive clones was digested with the cloning site *EcoRI,* and the clone with the biggest

insert was chosen for subcloning. The digested insert was purified and cloned into *EcoRI* site of pBluescript KS^+ for sequencing as described previously.

(C) Cloning of KCBP from green alga, *Stichococcus bacillaries*

C-1. PCR amplification of KCBP motor domain from *Stichococcus* DNA

KCBP motor domain of *Stichococcus* was amplified by PCR using genomic DNA as a template. Sense and antisense primers with restriction sites were similar to those used for spruce PCR amplification. The PCR conditions were similar to the previous conditions except that the extension time was three minutes for each cycle. The PCR product was purified, cloned into pBluescript, confirmed by sequencing and used as a probe for screening *Stichococcus* genomic library.

C-2. Extraction of high-molecular weight genomic DNA

Genomic DNA was isolated from frozen *Stichococcus* cells using a modified urea-phenol-containing buffer method (Golovkin and Reddy, 1996).

- About 0.5 g frozen cells were ground in liquid nitrogen and poured into 5 ml of lysis buffer {50 ml contains 215 g urea; 3.5 ml 5M NaCl; 2.5 ml 1M Tris-HCl, pH 8.0; 2 ml 0.5M EDTA; 2.5 ml of 20% sarkosyl; and 2.5 ml phenol (added freshly before use)}
- To the extract, 5 ml of phenol/chloroform/isoamyl alcohol (25:24:1 v/v/v), 0.5 ml of 10% SDS (w/v) was added and mixed gently but continuously for 30 min on a rocking platform
- The sample was spun for 15 min in a clinical centrifuge at 3000-4000 rpm for 15 min and the aqueous phase was collected and treated with 100 µg/ml RNase-free DNase for 1 hour at 37 ^{0}C

- The aqueous phase was extracted two more times with phenol/chloroform/isoamyl alcohol
- One-tenth volume of 3M sodium acetate pH 5.2, 2.5 volume of ethanol was added to the aqueous phase, and the DNA was spooled out with a fire-polished pasture pipette
- The spooled DNA was washed with 70% ethanol, dried and dissolved in 250 µl of TE.
- The DNA was precipitated by adding one volume of 5 M ammonium acetate, 2 volumes of ethanol and the DNA was spooled out as above.
- The DNA was washed two times with 70% ethanol, dried in a Speed Vac, dissolved in TE and the quality of the high molecular weight DNA was tested by running an 0.8% agarose gel.

C-3. Construction and screening of *Stichococcus* genomic library

For construction of a genomic library, genomic DNA was partially digested with *Sau*3A enzyme (Stratagene), and 9-20 kb fragments were collected and described as follows: 180 µg DNA were dispensed into 900 µl of 1X *Sau*3A reaction buffer and aliquoted into nine sterile microfuge tubes. The first tube contained 200 µl and the last tube was empty. To the first tube 1.5 µl (5 units/µl) of *Sau3*A was added and mixed well. Half of the first tube mixture was transferred to the second tube, mixed and this serial dilution was continued through the remaining tubes. The DNA in tubes 1 to 9 was incubated at 37 ^{0}C for 3, 10, 15, 30, 45, 60, 75, 90, and 120 min respectively. After incubation, the reaction was quickly stopped by adding diethylpyrocarbonate (DEPC) and EDTA to a final concentration of 0.1% and 10 mM, respectively. Samples were incubated at 65 ^{0}C for 5 min. Five µl from each tube were removed and run in 0.8% agarose gel to check the digestion (Fig 10). Digested DNA in all tubes was mixed, extracted once with phenol:chloroform (50:50 v/v) and once

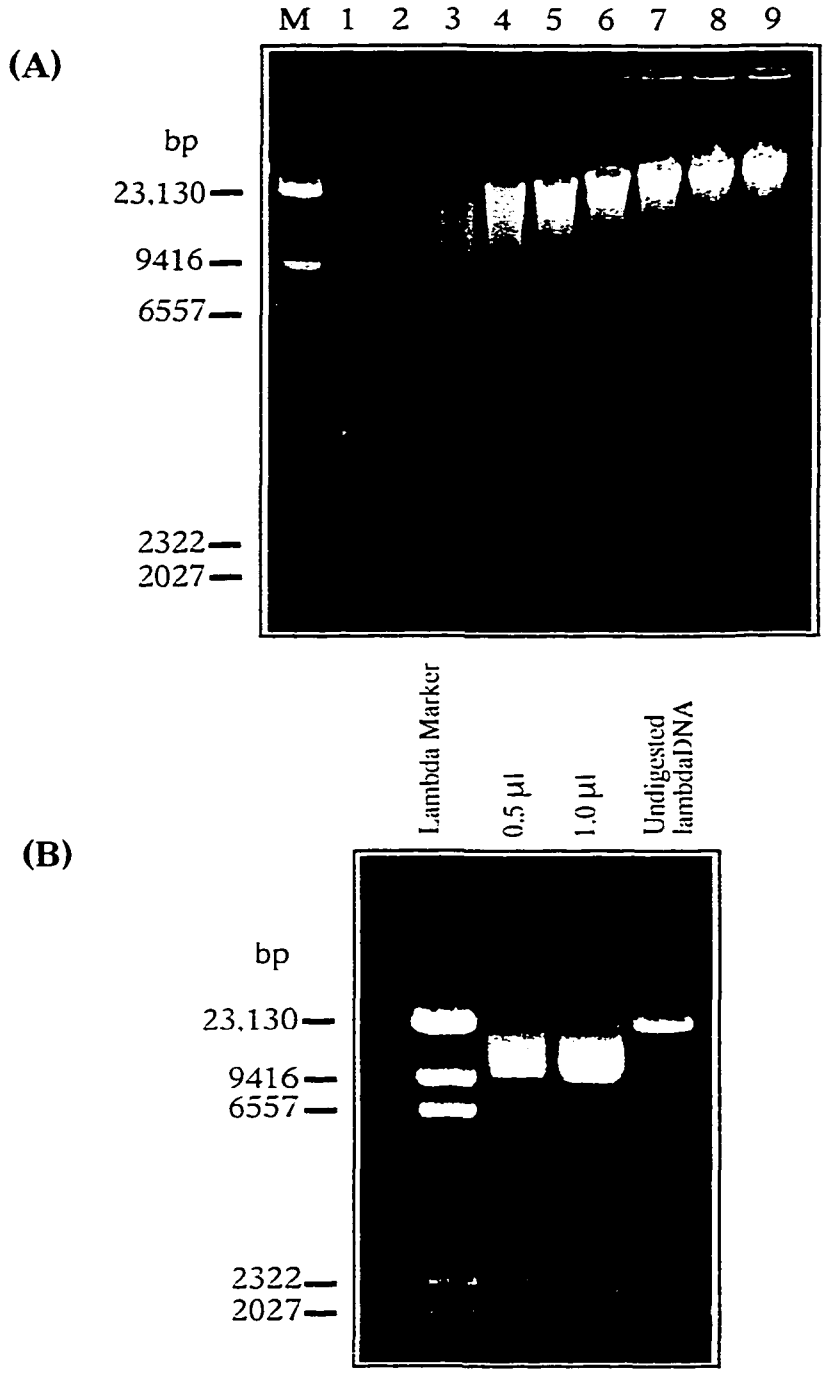

Fig. 10 **Partial digestion of genomic DNA.** (A) Genomic DNA was partialy digestes with *Sau3*A. (B) 9-20 kb genomic fragment used in preparing the library. The digested fractions were extracted with phenol:chloroform, and then with chloroform. Digested DNA was fractionated in 0.8% agarose gel and fragments, 9-20 kb were purified by low melting point agarose (LMPA) method. Purified fragments were run in 0.8% agarose gel along with digested and undigested Lambda DNA. DNA size maker is shown at the left in bp.

with chloroform, precipitated with ethanol in the presence of 1/10 volume sodium acetate (pH 5.2), washed with 70% ethanol and dissolved in 200 µl H_2O. DNA was size-fractionated on a 0.8% agarose gel at 20 V for 48 hour. Fragments of 9 to 20 kb were purified by the low melting point agarose method as previously described, dissolved in H_2O at 0.5 µg/µl concentration and ligated into Lambda DASH II replacement vector (Fig 11) that was predigested with *BamHI*, according to the instructions provided by Stratagene (La Jolla, CA). The ligated DNA was packaged using Gigapack III packaging extract (Startagene) and transformed into *Escherichia coli* XLI-blue MRA(P2). Approximately 2 X 10^5 pfu of an unamplified library were screened using ^{32}P-labelled PCR amplified product as described previously except, that XL1-Blue MRA (P2) *E. coli* cells were used as a host stain. Phage DNA from seven positive plaques was prepared using QIAGEN Lambda Midi preparation kit (QIAGEN), digested with *Not*I and the clone with the biggest insert was used for sequencing.

(D) Cloning of KCBP from Glaucophytes, *Cyanophora paradoxa*

D-1. PCR amplification of *Cyanophora paradoxa* KCBP motor domain

Motor domain of *Cyanophora* kinesin was amplified by PCR using cDNA library as a template. Two degenerate primers, sense [5'-ATT/C/ATTT/CGCITAT/CGCICA-A/GAG-3'] and antisense [5'-A/GAGIG/CA/TICCIGCIAG/AA/G-3'] corresponding to the conserved motifs in the motor domain of kinesin-like proteins (KLPs) were used to amplify a fragment (~450 bp) from *Cyanophora*. PCR reaction was carried out as described previously for the spruce cDNA library. PCR product was purified with QIAGEN PCR purification kit (QIAGEN), cloned into *EcoRI/BamHI* sites of pBluescript-KS$^+$ vector (Stratagene, La Jolla, CA) and verified by sequencing and used as a probe to screen genomic library.

(A)

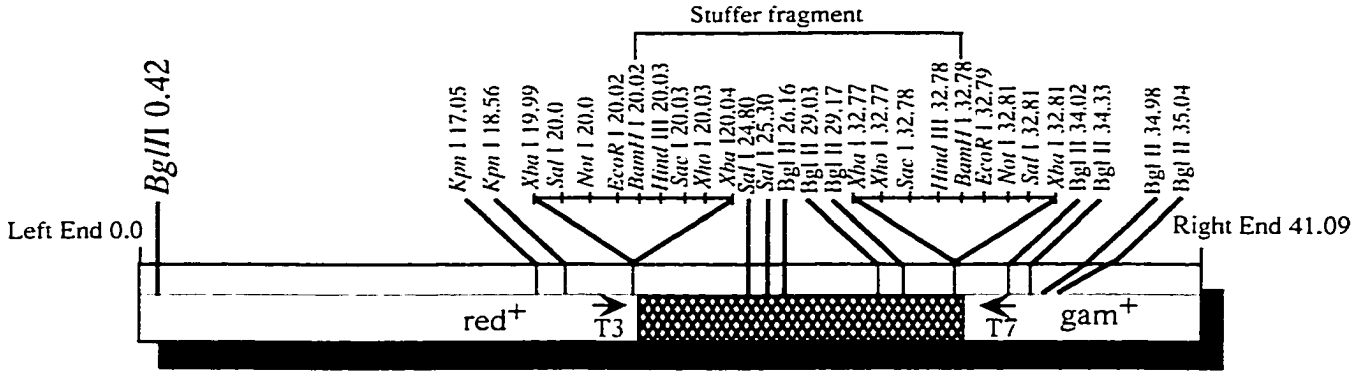

(B)

Xba I *Sal* I *Not* I T3 Promoter

5'-TCTAGAGAGCTGTCGACGCGGCCGCGGAATTAACCCTCACTAAAGGGAAC

EcoR I *BamH* I *Hind* III *Sac* I *Xho* I *Xba* I

GAATTCGGATTCAAGCCTGAGCTCCTCGAGAAATTCTCTAGA -3'

Xba I *Xho* I *Sac* I *Hind* III *BamH* I *EcoR* I

5'-TCTAGAGAATTTCTCGAGGAGCTCAAGCTTGGATCCGAATTC

T7 Promoter *Not* I *Sal* I *Xba* I

TTCGCCCTATAGTGAGTCGTATTACGCGGCCGCGTCGACAGCTCTCTAGA-3'

Fig. 11 **Map (A) and multiple cloning sites (B) of Lambda DASH II replacement vector.** Lambda dash phage (WT) contains active red+ and gam+ genes and so unable to grow on XL1-Blue MRA(P2). Lambda phages without these genes are able to grow on P2 lysogenic strains. The red and gam genes in the Lambda DASH II DNA are located on the stuffer fragment (shown in hatches), therefore after ligation only recombinant Lambda Dash II (red- gam-) can grow on P2 lysogen strain and the ones without insert can not grow. Target DNA cloned into BamH I sites can be removed by digestion with flanking unique enzymes such as *Not* I and *Sal*I. T3 and T7 primer regions can be used for sequencing.

D-2. Genomic library construction and screening

Genomic DNA was extracted from frozen *Cyanophora* cells as described previously. A genomic library was constructed and screened as described for *Stichococcus* except that the probe was a ^{32}P-labelled PCR amplified product from a *Cyanophora* cDNA library. Nine putative positive clones were analyzed by restriction digestion, and phage DNA from the biggest clone was prepared by QIAGEN kit, subcloned into pBluescript (KS+) and used for sequencing

III. DNA sequencing and sequence analysis

All the clones isolated in this study were sequenced by the dideoxynucleotide chain termination method using either double strand plasmid or phage DNA as a template (The Bioplymer Laboratory, University of Maryland). Universal primers, T3 and T7 were used for the first run and primer walking was used to obtain the complete sequences of the clones. Sequence analysis was performed using the Sequencher and Mac Vector sequence analysis software (International Biotechnologies, Inc). Searches for sequence similarity were performed with the BLAST network service provided by the National Library of Medicine (http://www.ncbi.nlm.nih.gov). Splicing sites were predicted using the Netplantgene, (http://genome.cbd.dtu.dk/htbin/nph-webface), a program that predicts the splice site in plant genes, and by comparing the deduced amino acid sequence with *Arabidopsis* KCBP. Alignment analyses were performed using MegAlign (DNASTAR). Protein domains were analyzed using the Simple Modular Architecture Research Tool (SMART) (V3.1) and PROSITE at http:Expasy tools.

IV. Phylogenetic analysis

To determine the phylogenetic relationship among different KCBPs cloned from phylogenetically *diverged* species and with other C-terminal KLPs, as well as some representative members of other KLP subfamilies retrieved from kinesin database (http://www.blocks.fhcrc.org/~kinesin/index.html), the conserved motor domains were used in phylogenetic analysis. Proteins were aligned by the Lasergene Megalign program using the Clustual method. The aligned sequences were used to build a phylogenetic tree using the PAUP (version 4.0b2) heuristic search method with tree bisection-reconnection branch swapping (Swofford, 1993). Bootstrap analysis with 100 random replicates was carried out using the heuristic method.

V. Southern Blotting

Genomic DNA from maize seedlings and from frozen *Cyanophora* cells was prepared as described previously for *Stichococcus* using modified urea-phenol-containing buffer (Golovkin and Reddy, 1996). Spruce genomic DNA was prepared from three-week old seedlings according to the procedure of Murray and Thompson, (1980) with modifications:

1. One g of tissue was ground in liquid nitrogen with a pestle and mortar. To the ground tissue 250 mg insoluble polyvinyl polypyrilidone (PVPP) was added and blended thoroughly
2. Ten ml extraction buffer { 2% (w/v) CTAB (cetrimethylammonium bromide) 100 mM Tris-HCl (pH 8.0), 1.4 M NaCl, 20 mM EDTA, and 0.4% β-mercaptoethanol} was added to the ground powder and incubated at 55-60 ^{0}C for 45 min with occasional shaking

3. After cooling the extract to room temperature, an equal volume of chloroform:isoamylalchol (24:1 v/v) was added, incubated for an additional 20 min with periodic mixing and centrifuged at 6,000 rpm in a table top centrifuge for 15 min at room temperature
4. The aqueous phase was transferred to a new tube, 1/10 volume of CTAB solution (10% CTAB and 0.7 M NaCl) was added, extracted with equal volume of chloroform: isoamyl alcohol as previously discussed, and centrifuged at 11,000 rpm (Sorvall SS34 rotor) at 20 ^{0}C for 10 min
5. The aqueous phase was split equally into two tubes, with one tube used for RNA extraction, as described later, and the second one used for DNA extraction
6. The DNA was precipitated by adding 2.5 volume of 95% cold ethanol and then kept overnight at –20 ^{0}C
7. The pellet was washed with 70% ethanol, dried, dissolved in TE, treated with RNase (100 µg/ml) at 37 ^{0}C for 1 hour, and extracted with phenol:chloroform (50:50 v/v) and then with chloroform
8. One-tenth volume of 3 M sodium acetate (pH 5.2), 2.5 volume cold ethanol was added and the pelleted DNA was collected by centrifugation at 12,000 rpm for 30 min at 4 ^{0}C
9. The pellet was washed twice with 70% ethanol, dried the and dissolved in TE.

Ten µg of genomic DNA was digested with different restriction enzymes, *Sph*I, *Sst*I, *Nco*I, *Kpn*I (for maize), *Bgl*II, *Eco*RI, *Kpn*I, *Xba*I (for spruce), *BamH*I, *Eco*RI, *Xho*I (for *Stichococcus*), and *Eco*RI, *Hind*III, *Kpn*I, *Pst*I, *Xho*I (for *Cyanophora*). Digested DNase were fractionated on a 0.8% agarose gel. In order to facilitate the transfer of the DNA from the gel to the membranes, the DNA was depurinated by treating the gels with 0.25 N HCl for

10 min. Gels were denatured in denaturing solution (1.5 M NaCl, 0.5 M NaOH) for one hour followed by neutralization in a neutralization solution (1.5 M NaCl, 0.5 M Tris-HCl, pH 8.0) for another hour. DNA was transferred to nylon membranes (Hybond N; Amersham) by the conventional capillary method using 10X SSC (1.5 M NaCl, 0.125 M $C_6H_5Na_3O_7.2H_2O$) (Ausubel *et al.*, 1987). The transferred DNA was fixed on membranes by exposing to UV light in a Stratalinker (Stratagene), followed by incubation in oven for 1 hour at 60 ^{0}C. Membranes were pre-hybridized (0.5 M sodium phosphate and 0.7% w/v SDS) for three hours at 60 ^{0}C and then hybridized [pre- hybridization solution with a ^{32}P-labelled probe] for 18 hours. The PCR amplified products that were used in library screening were used as probes. Radioactive probe was synthesized with an oligolabelling kit from Amersham using nanonucleotide random primers. Membranes were washed as described previously in the library screening procedure, except that there was a final wash with 0.1X SSC containing 1% SDS (w/v) at 68 ^{0}C for 10 min. Membranes were exposed and developed as before.

VI. Northern Blotting and Reverse Transcriptase (RT) PCR

A. RNA isolation by TRIAZOL method

Total RNA was isolated from 7-day-old maize seedling using TRIZOL (phenol and guanidine isothiocyanate) method (Life Technologies)

I. One gm of tissue was ground in liquid nitrogen,10 volumes of TRIZOL reagent were added to the powder, and incubated at room temperature for 5 minutes.

- Then 0.2 ml of chloroform per 1 ml of TRIZOL was added and the tubes were shaken vigorously by hand for 15 seconds and incubated at room temperature for 3 minutes.

- After centrifugation at 12,000g for 15 minutes at room temperature isopropyl alcohol (0.5 ml per 1 ml of TRIZOL reagent used for the initial homogenization) was added, incubated at room temperature for 15 minutes and centrifuged at 12,000g for 15 minutes at room temperature.
- The RNA pellet was washed with 75% ethanol, air-dried and dissolved in DEPC-treated H_2O for poly $(A)^+$ isolation.

Poly $(A)^+$ RNA was isolated from the total RNA using oligo (dT)-cellulose according to (Sambrook *et al.*, 1989). Total RNA was heated at 65 ^{0}C for 5 min and cooled to room temperature. An equal volume of loading buffer (1X = 50 mM Tris-HCl, pH 7.5, 0.4 M NaCl, 0.2% SDS) was added, applied onto oligo-(dT) cellulose column and washed extensively with loading buffer, followed by washing buffer (50 mM Tris-HCl, pH 7.5, 0.2% SDS, 0.1 M NaCl). Finally, poly $(A)^+$ RNA was eluted with pre-heated (50 °C) elution buffer containing 10 mM Tris-HCl, pH 7.5, 0.2% SDS, precipitated with 3 volumes ethanol, dried and dissolved in formamide

B. Isolation of RNA from spruce seedlings

Total RNA from three week-old spruce seedlings was prepared following the procedure used for genomic DNA extraction through the step 6 and then continued as follows:

- For RNA extraction, total nucleic acid was precipitated from aqueous phase by adding 2.5 volume of 95% ethanol and kept overnight at –20 ^{0}C.
- The pellet was washed with 70% ethanol, air dried and dissolved in DEPC-treated H_2O
- Four volumes of 4 M cold LiCl was added to the nucleic acid solution and kept on ice overnight.
- RNA was precipitated by centrifugation at 11,000 rpm for 10 min at 4 ^{0}C.

- The pellet was washed with cold 2 M LiCl, air dried and dissolved in DEPC-treated water.
- Total RNA was re-precipitated with 2.5 volume ethanol in the presence of 0.3 M sodium acetate.

Maize Poly $(A)^+$ RNA and spruce total RNA samples were electrophorosed on denaturing 1 % agarose gel containing 4 % formaldehyde. Gels were washed three times in DEPC-treated H_2O, 5 min each, followed by one wash in DEPC-treated 10 X SSC for 15 min. RNA was transferred overnight to a nylon membrane (Hybond N, Amersham) using DEPC-treated 10 X SSC buffer. Membranes were prehybridized in pre-hybridization solution {50% formamide, 5X SSPE, 5X Denhardt's solution, 0.1% SDS (w/v) and 100 μg/ml salmon sperm DNA} for 4 hours at 42 °C and then in hybridization solution (pre-hybridization solution plus ^{32}P-labelled probes) for 24 hours at the same temperature. PCR amplified products that were used for library screening and for Southern were used for Northern. Radioactive probes were synthesized with an oligolabelling kit as described previously. Following hybridization, the membranes were washed with 1X SSC buffer containing 0.1% w/v SDS at 65 °C for 15 minutes followed by a wash with 0.1X SSC buffer containing 0.1% w/v SDS at the same temperature and for the same time and then exposed to X-ray film.

C. Reverse transcription PCR (RT-PCR)

Total RNA from different maize tissues (roots, shoots, and whole seedlings) was isolated by TRIZOL Method (Life Technologies) as described previously. Total RNA was treated with deoxyribonuclease I, amplification grade, (Life Technologies) before being used as a template for RT-PCR. One microgram of DNase-treated total RNA was used to synthesize first strand DNA with an oligo (dT) primer and avian myeloblastasis virus (AMV)

reverse transcriptase in a 20 µl volume using Promega "Reverse Transcription System" (Madison, WI). Sense primer (5'-ATACCTTGCAATCTGAAC-G-3') and antisense primer (5'-CTAAAAAGTTCAGATG-TGTGG-3') were used to amplify 1014 bp sequence from cDNA. The PCR reactions were performed in a final volume of 50 µl using the "Expand™ long template PCR system" according to the instructions provided by the manufacturer, Roche Molecular Biochemicals. PCR parameters were similar to those used for previous PCR amplification (section 2-1). The amplified products were resolved by electrophoresis in 1 % agarose gel, blotted onto a nylon membrane (Hybond-N, Amersham) and probed with ^{32}P-labelled 6 kb fragment (*SalI/EcoR*I) of ZmKCBP, which contains the coding region for the motor and the coiled-coil domains. The nylon membrane was prehybridized and hybridized as described previously in Southern blotting.

VII. Western analysis and Expression of KCBP

A. Protein preparation

Crude proteins were prepared from maize seedlings and from frozen cells of *Cyanophora* as described earlier (Bowser and Reddy, 1997). Samples were ground in liquid nitrogen and extracted in 50 mM Tris-HCl, pH 7.4, 5mM DTT, 10 ng ml^{-1} N-a-P-tosyl-L-arginine methyl ester (TAME; Sigma), and complete protease inhibitor cocktail. After spinning at 100,000 g for 20 min, the supernatant was collected and used for SDS-PAGE. 20 µl of samples plus 10 µl of 3X sample loading buffer (0.1875 M Tris-HCl, pH 6.8, 6% SDS, 15% mercaptoethanol, 30% glycerol, and 0.0225% bromophenol blue) were run for 1 h at 200 V on an 8 % SDS-PAGE. Proteins were transblotted onto a nitrocellulose membrane (Life Science Products, Inc) using a BioRad transfer cell. KCBP was detected using affinity-purified antibody that was raised against CaM-binding domain (Bowser and Reddy, 1997).

B. Immunodetection with affinity-purified KCBP antibody

The nitrocellulose filters were blocked with 3% gelatin in TBS (20 mM Tris-HCl, pH 7.5, 0.5 M NaCl,) for 2 h at 30 °C with gentle shaking. After rinsing three times with TBST (TBS containing 0.05 % Tween-20), the membranes were incubated with affinity-purified KCBP antibody (1:400) (Bowser and Reddy, 1997) for 2 hrs at 30 °C in TBS containing 1 % gelatin. The membranes were then washed in TBST as before and incubated for 1 hr at 30 °C with alkaline phosphatase-conjugated goat anti-rabbit IgG (1:4000 dilution) in TBS containing 1 % gelatin. Immunoreactive bands were detected colorimetrically by immersing the filter in 10 ml of AP buffer (100 mM Tris-HCl, pH 9.5, 100 mM NaCl, 5 mM $MgCl_2$) containing 45 µl nitroblue tetrazolium chloride (NBT, 75 mg/ml) and 30 µl 5-bromo-4-chlorep-3-indolylphosphate p-toluidine salt (BCIP, 50 mg/ml).

C. Detection of KCBP with biotinylated CaM

Nitrocellulose membranes were blocked with 3% gelatin in TBS/Ca/Mg (50 mM Tris-HCl, pH 7.5, 50 mM $MgCl_2$, 200 mM NaCl, and 0.5 mM $CaCl_2$) for 2 hours at 30°C. After rinsing the membranes three times with TBST/Ca/Mg (TBS/Ca/Mg containing 0.05% Tween-20), they were incubated with 60 nM of biotinylated CaM in TBST/Ca/Mg containing 1% gelatin (Reddy *et al.*, 1996a). The blots were washed twice with TBST/Ca/Mg and incubated with Vectastain ABC.HRP (Vector Laboratories, Burlingame, CA) in TBST/Ca/Mg for 30 min. After washing three times with TBST/Ca/Mg, the CBDs were detected colorimetrically by immersing the filters in a substrate solution (0.8 mg/ml diaminobenzidine, 0.4 mg/ml $NiCl_2$ and 0.009% H_2O_2 in 100 mM Tris-HCl, pH 7.5). To determine the Ca^{2+} dependency of CaM binding, a duplicate blots was proceeded as above except that Ca^{2+} is replaced by 5 mM EGTA in all solutions (Fordham-Skelton *et al.*, 1994).

D. Expression of KCBP in *E.coli*

The C-terminal region of maize KCBP (ZmKCBP) and spruce KCBP (PaKCBP) were expressed in *E.coli* for further characterization. The C-terminal region of ZmKCBP (1329 bp fragment) containing the motor domain and the CBD was amplified from first strand cDNA by PCR using sense (5'-GCAGAATTCAATGCTGAGGTTGATAGC-TTGC-3') and antisense (5'-CCCAAGCTTAGTCATGCGATTGTCTGATCTC-3') primers with restriction sites for *EcoR*I and *Hind*III, respectively. The PCR reactions were performed in a final volume of 50 µl. The PCR parameters were denaturation for 1 min at 94 ^{0}C followed by 35 cycles of 30 sec denaturation at 94 ^{0}C, 1 min annealing at 60 ^{0}C, and 2 min extension at 72 ^{0}C, with a final extension for 10 min at 72 ^{0}C. The amplified product was digested with *EcoR*I and *Hind*III, run in 1% agarose gel, excised and purified by L.M.P. agarose method as described previously (section 1-3). Expression vectors, pET 32a and pET 28a (Novagen), were digested with the same enzymes, run in gel and purified as mentioned before. Ligation was performed in a 20 µl reaction containing the digested vector and fragments (1:3 and 1:6 molar ratios), 4 µl of 5X T4 ligase buffer (Gibco BRL), and 1 µl of T4 DNA ligase (Gibco BRL). Ligation was performed at room temperature for 1 hour and kept at 4 ^{0}C overnight and then used for transformation.

E. Transformation

Fresh heat shock competent *E. coli* BL21 (DE3) cells were prepared by inoculating 5 ml of SOB medium (0.5% Bact Yeast Extract, 2% Bactotryptone, 10 mM NaCl, 2.5 mM KCl, 10 mM $MgCl_2$, and 10 mM $MgSO_4$) with single big colony of *E. coli* BL21 (DE3) and grown overnight at 37 °C with shaking. One liter of SOB medium was inoculated with the 5 ml culture and grown at 37 °C with shaking to an $O.D_{600}$ = 0.3-0.4. Cells were chilled on ice,

collected by centrifugation at 1000g for 10 min at 4 °C and suspended in 1/3 volume of cold RF1 solution (100 ml contains 1.2 g RbCl, 0.99 g $MnCl_2.4\ H_2O$, 3 ml of 1 M potassium acetate, pH 7.5, 0.15 g $CaCl_2.2H_2O$, and 15 g glycerol). After 15 minutes on ice with gentle shaking, cells were centrifuged as before and re-suspended in 1/12.5 volume of RF2 (100 ml contains 2ml of 0.5 M MOPS, pH 6.8, 0.12 g RbCl, 0.11 g $CaCl_2.2H_2O$, and 15 g glycerol), aliquoted into microcentrifuge tubes, quick frozen and stored at –80 °C and thawed as needed. Five µl of ligation mixture was added to 75 µl of cells which were kept on ice for 5 minutes, heat shocked at 42 °C for 45 sec and then cooled on ice for 1 min. One ml of SOB medium was added and cells were incubated for 1 hour at 37 °C with shaking. Aliquots of 100 µl were spread on LB ampicilin (80 µg/ml) plates for pET32a and on Kan (30 µg/ml) plates for pET28a.

F. Protein induction

BL21 (DE3) cells transformed with either pET32a KCBP or pET28a KCBP (Fig 12), were cultured in 100 ml of LB medium with the appropriate antibiotic to an $O.D_{600}$ of about 0.6. Ten ml of culture was removed as the uninduced control. Expression of the protein was induced in the remaining 90 ml by adding 0.2 mM isopropyl β-D-thiogalactopyranoside (IPTG). Induced cells were grown for 8 hours at 30°C with shaking at 200 rpm. Cells were harvested, re-suspended in extraction buffer [50mM Tris-HCl, pH 7.5 and 150 mM NaCl supplemented with protease inhibitor cocktail (Roche Molecular Biochemicals) and 200 µg/ml lysozyme (Sigma)] and incubated on ice for 1 hr with shaking. Samples were

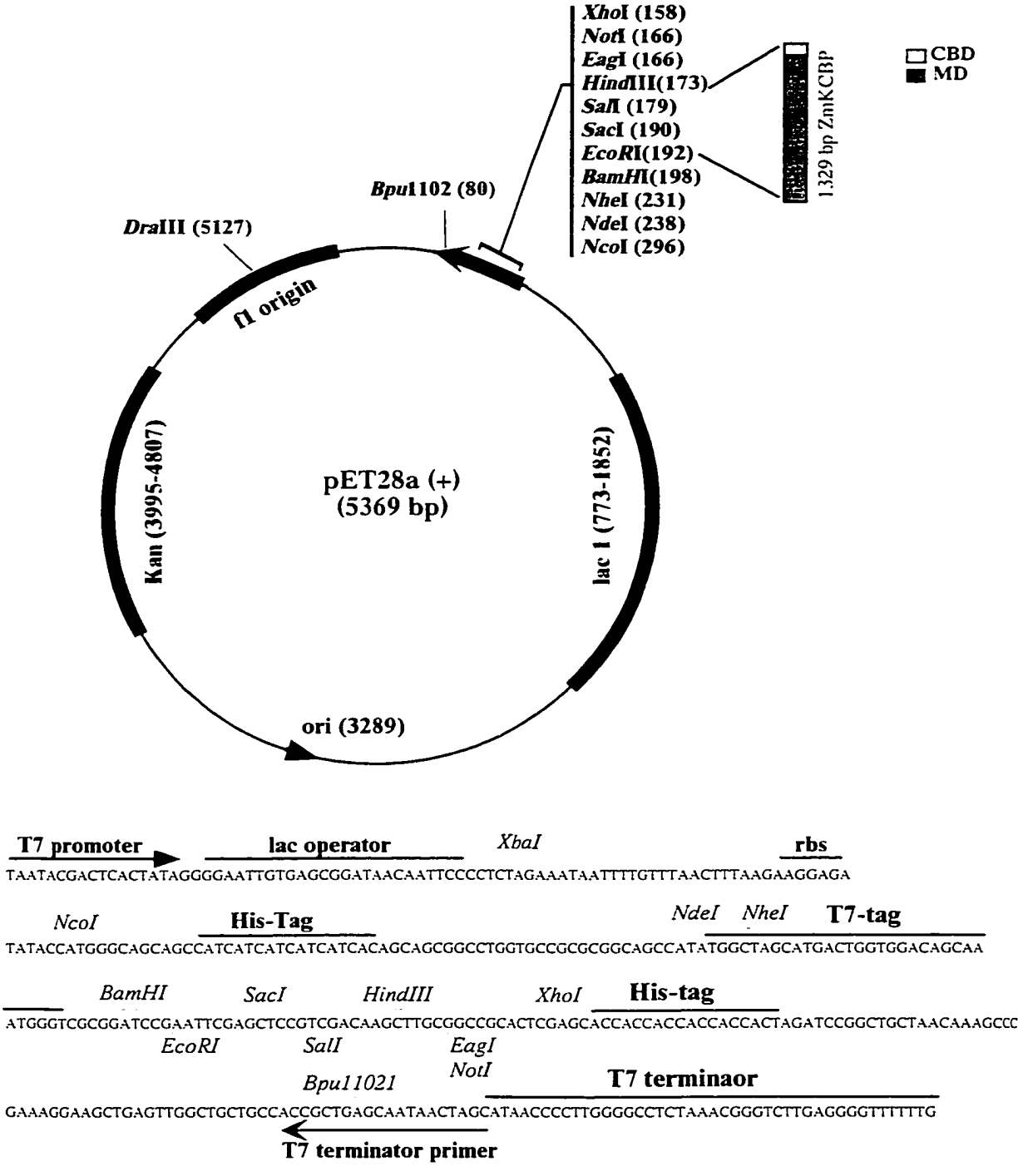

Fig. 12 **pET28a expression vector used to express ZmKCBP.** Motor domain and CBD of ZmKCBP was amplified by PCR using first strand cDNA as a template. 1329 bp fragment was directionaly cloned into pET 28a between *EcoR*I and *Hind*III clonning sites. The recombinant plasmid was transformed into BL21 (DE3) *E.coli* for fusion protein expression in the presence of IPTG. Figure modified from Novagen Catalog.

sonicated 5 times, 10 sec each, in an ice water bath and centrifuged at 12,000g for 15 minutes at 4 ^{0}C. The supernatant and pellet of the induced and uninduced cultures were analyzed using SDS-PAGE. Twenty µl of samples plus 10 µl of 3X sample loading buffer were run for 1 h at 200 V on a 10 % SDS-PAGE. Three gels were prepared, one gel was stained with Coomassie Blue staining (0.25% Coomassie blue R250, 7.5% acetic acid, and 42.5% methanol) and the others were blotted to a nitrocellulose membranes (Life Science Products, Inc) and detected with either KCBP-Ab or biotinylated CaM as described previously (sections VII-2 and VII-3).

G. Purification of KCBP by CaM Sepharose column

For purification of KCBP from *Cyanophora*, the crude extract was spun at 100,000 g, and the supernatant was adjusted to 2 mM $CaCl_2$ and loaded onto a CaM-Sepharose 4B column that was prepared and equilibrated according to the manufacturer's instructions (Pharmacia Biotechnology). After extensive washing with 10 volumes of washing buffer (50 mM Tris HCl, pH 7.5, 150 mM NaCl plus 2 mM $CaCl_2$), the bound protein was eluted with the elution buffer (50 mM Tris HCl, pH 7.5, 150 mM NaCl and 2 mM EGTA). Eluted fractions were electrophoresed either directly or after concentration using Biomax 0.5 Ultrafree filters (Millipore Corp., Bedford, MA). Proteins were transblotted onto nitrocellulose membranes as above and detected with either KCBP-Ab or biotinylated CaM as described previously (sections VII-2 and VII-3).

BL21 (DE3) cells transformed with pET28a ZmKCBP (Fig 12) construct showed the highest amount of induced protein in the soluble fraction, therefore these cells were used for further induction experiments. Cells were grown and the fusion protein was induced and extracted as described above with the following modifications. The sonicated extracts were

spun at 100,000 g for one hour to separate the soluble and insoluble protein fractions. The resulting supernatant was supplemented with 2 mM $CaCl_2$ (final concentration), loaded onto a CaM-Sepharose 4B column, washed and eluted as described previously (sections VII-7). The eluted fractions were run in 10% denaturing gel, blotted onto nitrocellulose membranes, and probed with KCBP antibody or biotinylated CaM in the presence of 1 mM $CaCl_2$ or 2 mM EGTA.

To express the C-terminal region of spruce KCBP, we transferred 1.6 kb fragment containing the coding region for motor domain and CaM-binding domain from pBluescript vector into pET 32a and pET 28a (Novagen) expression vectors. The recombinant plasmids were introduced into *E.coli* BL21 (DE3) strain for expression. Expression was monitored by probing protein blots of uninduced and induced cultures with either KCBP-antibody or biotinylated CaM (Fordham-Skelton *et al.*, 1994; Bowser and Reddy, 1997) as described for ZmKCBP protein. The soluble protein fraction from pET 28a was purified using CaM-Sepharose 4B column (Narasimhulu and Reddy, 1998). The eluted fractions were electrophoresed on SDS-PAGE, blotted and probed with KCBP-Ab (Bowser and Reddy, 1997) and ^{35}S CaM in the presence of 1 mM $CaCl_2$ or 2 mM EGTA (Saido *et al.*, 1992).

H. Immunodetection of KCBP in soluble and microsomal fractions

To detect the presence of KCBP in microsomal fractions, soluble and microsomal proteins from a twelve-day old *Arabidopsis* suspension culture were prepared as described previously with the following modifications. A 100 ml cell suspension culture was filtered to harvest the cells. Cells were ground in liquid nitrogen to a fine powder and extracted as above in extraction buffer supplemented with 250 mM sucrose. Homogenate was spun at 12,000 g for 20 min to remove the suspended particles. The clear supernatant was

centrifuged at 120,000 g for 1 hour to obtain the soluble and microsomal fractions. The pellet (microsomal fraction) was washed with the extraction buffer one time, centrifuged again, and the pellet was suspended in 1X SDS sample buffer. Proteins from the supernatant and pellets were run on a SDS-PAGE, transblotted onto nitrocellulose membranes and detected with KCBP antibodies as described previously.

CHAPTER 3

EXPERIMENTAL RESULTS

RESULTS

Cloning and characterization of KCBP from phylogenetically *diverged* photosynthetic eukaryotes

Part of this work has been published as "A Novel Calcium/Calmodulin-Regulated Kinesin-Like Protein is Highly Conserved Between Monocots and Dicots" Salah E. Abdel-Ghany and A.S.N. Reddy. DNA and Cell Biology, **19** (9): 567-578 (2000).

Kinesin-like CBP (KCBP), a novel Ca^{2+}/CaM-regulated microtubule (MT) motor protein, has been isolated and characterized recently from several dicot plants. Although it is highly conserved among dicots, it is not known if it is present in monocots, other seed plants (gymnosperms) and primitive photosynthetic eukaryotes. The main objective is to investigate the presence of KCBP homologs in a range of photosynthetic eukaryotes ranging from the most primitive unicellular protists to highly evolved monocots.

The cloning strategies used in my research are based on the fact that kinesin-like proteins (KLPs) in many organisms, ranging from primitive protists to highly evolved plants have a motor domain with a highly conserved ATP-binding site and putative MT-binding sites. In addition, KCBP from dicot plants has a characteristic CaM-binding domain (CBD), which does not have any sequence similarity to any protein in the database. Based on this information we designed degenerate primers that encode these conserved regions and performed PCR at different conditions using either genomic DNAs or cDNA libraries as templates to clone the KCBP motor domain from phylogenetically *diverged* species. PCR-amplified products were cloned into vectors and confirmed to be KLP motor domains by sequencing. These PCR-amplified products were then used as probes for screening either

cDNA or genomic libraries to obtain the full length KCBP genes. The motor domains along with the CBD of cloned KCBPs were cloned into expression vectors and the expressed proteins were characterized. The data presented here provide strong evidence for the presence of KCBP in all photosynthetic eukaryotes and conservation of important functional domains in KCBPs in the organisms studied. However, KCBP gene structure varies considerably between algae and angiosperms.

I. Cloning and characterization of KCBP from monocots: *Zea mays* KCBP (ZmKCBP)

In a protein-protein interaction-based screening of *Arabidopsis* expression library using biotinylated CaM as a probe, a novel Ca^{2+}/CaM regulated C-terminal motor (AtKCBP) has been cloned (Reddy *et al.*, 1996b). Homologs of KCBP have been cloned from two other dicot species (Reddy *et al.*, 1996a; Wang *et al.*, 1996). However, a homologue of KCBP had not been reported in monocots. To determine if KCBP is ubiquitous in all flowering plants, the degree of conservation and the phylogenetic relationship between those two groups of the angiosperms clade, we have screened a genomic library prepared from maize, a representative member of monocots. A partial cDNA that contained the coding region of the motor and CaM-binding domains of (CBD) *Arabidopsis* KCBP (Reddy *et al.*, 1996a) was used to screen the maize library. Fourteen positive clones were isolated after three rounds of screening at moderate stringency conditions (see methods section). Restriction digestion analysis of isolated clones indicated that all clones contained the overlapping regions of the same gene. Two genomic clones that contained the complete gene, as judged by Southern blotting with 5' and 3' regions of *Arabidopsis* KCBP cDNA, were selected to generate subclones for sequence analysis.

Nucleotide sequence of ZmKCBP

The nucleotide sequence of the genomic clone and the predicted amino acid sequence of the ZmKCBP gene are shown in Fig (13). This sequence is also available in the Gene Bank under the accession number AF223412. Analysis of the nucleotide sequence using NetPlantGene (http://genome.cbs.dtu.dk/htbin/nph-webface), a program that

```
ATTGATTGAT TAGTTGATGA ATTGTTTGAT TAACGATTAA TGATTGAATG ACAAATTGGT CAGTTTGTTG  70
ATGGGTTGAA CAAACAAACC TTTGAAACCA GCTGCTTTGT TTGTCAAACG GATCATTCGA CGAATTCGCC 140
CAAGTTGATG CTAAACAATC ACAAAAACAA ACAATCGAAC AATTGTGAGC AAACAATATC AGAAAATTGT 210
GGGTTGGTCG ATTGATTGAT TGTAGTATGG CCGTAATAAT TGGCGGATCT TGACTGAAGA TGAGTCGAGC 280
ATACTGCATG TGAATTCGAT CGATCACTTT TTTTTTTTTG AAATGAAAGA ATATCCAACA CTGGTTGATT 350
TGGAATTTTT TAACTTTAGC ATCGAGACAA ATGCATTATT CTTGTTTATG GTTTGCACGA AAGTCGAAAG 420
GTACCCCTAG TTGTCAGTTT GGTGGAAACA AAAACGAGGT AGGGTGTTAT GACCGGCCGC CACTACAGGC 490
GCCGGACAAC AGCAGAGGCG GCGGCCAATA ATAGGCATGC AGATTAGTTA GATAAGGATT AGAATATTAA 560
GGAGATAAGA TTTGTTAGAG AGAAAAGAGG AGATCTCAGA TTTGATCTCT TTAGATAAGG ACTAGAAGGG 630
AGTATAAATA CTTGTAAGCA CCACTCTATA TGAATTAAGC AGAAAACTAT TTAGTGTACT TCCTCCAAAG 700
GAAGCAGACG TGTTTTCTTC TGCCAAAGCC GTTGTCCAGC GTCCGCCGAA GAACAGCACG GCCACGGCGC 770
CCCTGCGCCA GCCCGCAACG CCTCATCCCT ACAATATGTG CAGTCTCTCT GATAGGAGCT CTAATCCTAT 840
CATAAGGAAA CTATACATCA CTATGTTACA ATTCAAATAG ACTGTAACAA GCATAATGTC GATTAGTCCT 910
ACATAATCTC TACATAATGT TCTTTAGATA TTGAGAGGTG AATGGAAAGT AAGAACAATC AGCACCACAT 980
                                                M  E  S  K  N  N  Q  H  H  I  10
TCAAgttaa gcgttacatt ctctttctaca tgcacaaaaa tacgaaaact gtaccctgta tactgcttacc 1050
  Q                                                                          11
attcaattgg ttaatttacc atcatttatc attgttactg gcattagaga caaggaaatt caattaggga 1120
ataccagcag ataccgtaag catcatgcag gctaaccaaa atgtccatta gggttctata aagtacagtt 1190
atcgaatttg atattgtaag aaatgctctg attcccactc tgataccagt gcttgaaaat aacagGTCGA 1260
                                                                     V  E  13
GGGTTTTCTC AAAGCAATGC AAAAGCAGAT TCATTCAGCT GGAAAACGTG GATTTTTTTC TAAAAAGTCT 1330
  G  F  L  K  A  M  Q  K  Q  I  H  S  A  G  K  R  G  F  F  S  K  K  S  36
GTTGGGCCAC AAACTCGCGA GAAGTTCACT TTGGAAGATA TGCTGTGCTT TCAAAAGgtg atgctctcaa 1400
 V  G  P  Q  T  R  E  K  F  T  L  E  D  M  L  C  F  Q  K                 55
atttcattcc atttgtgaag ttacgctgct gaagggcagg cttggtgcgg tggtgagagc tagcagcctc 1470
tccatatctg tgggaggaa ggcttgcctc ggtttatcct ttccctagac cccagtagtc cccgggcactg 1540
ggtctggctt gtgaagttac actgctgcac ttgtttcaac ttatctttct tctaaacttc tatggtaaag 1610
cttaaggtca atatctcaca ttaaatcaca tctatcattt tgttctgcta atttgttgat tctttttatc 1680
tcctgcagGA TTCTATTCCA ACTTCATTAC TAAAGATAAG CAATGACCTT GTAAGCCGCT CGATTAAGTT 1750
         D  S  I  P  T  S  L  L  K  I  S  N  D  L  V  S  R  S  I  K  L  76
GTTCCATGTC ATACTAAAGT ACATGGGCAT CGATTCACCA GCAATAATTA GTTTGGAGGA GAGAATAGAA 1820
  F  H  V  I  L  K  Y  M  G  I  D  S  P  A  I  I  S  L  E  E  R  I  E  99
TTTGTTGAGA AGCTCTACAA GCATACGTTA AAGCGTTCTG AACTTCGAGA TGAACTCTTT GCACAGATTT 1890
 F  V  E  K  L  Y  K  H  T  L  K  R  S  E  L  R  D  E  L  F  A  Q  I     122
CAAAACAAAC ACGTAACAAT CCTGATAGgt gagttgagct tctcatggat ggcaagcata tgtgtatacc 1960
S  K  Q  T  R  N  N  P  D  R                                              132
attgtaggaa ttatatttta ttgtacctgc agGGGTTGGT CAATAAGAGC TTGGGAGCTT ATGTACCTGT 2030
                                    G  W  S  I  R  A  W  E  L  M  Y  L    144
GTGCATCATC CATGCCACCA AGCAAAGATA TTGGGGCATA CTTGTCTGAG TATATTCACT TTGTTGCCCA 2100
C  A  S  S  M  P  P  S  K  D  I  G  A  Y  L  S  E  Y  I  H  F  V  A  H  168
TGGAGCCACA ACTGATGCTG ATGTTCGAGT TCTAGCACTG AACACACTAA ATGCATTAAA ACGATCAGTC 2170
  G  A  T  T  D  A  D  V  R  V  L  A  L  N  T  L  N  A  L  K  R  S  V  191
AAGGCGGGTC CTAGGATTAC AATTCCTGCA TGGGAGGAAA TAGAAGCTCT CTTAACAAGC CGGAAGCTTA 2240
 K  A  G  P  R  I  T  I  P  A  W  E  E  I  E  A  L  L  T  S  R  K  L  214
CAACAATTGT ATTTTTCTTG GATGAAACAT TTGAAGAGAT CACCTATGAC ATGGCAACAA CTGTTGCTGA 2310
T  T  I  V  F  F  L  D  E  T  F  E  E  I  T  Y  D  M  A  T  T  V  A  D  238
TGCTGTTGAG gtaaatgcat tttcccttag ctattagttt tagaattgat atatgctcaa taccttcaaa 2380
 A  V  E                                                                   241
```


Fig. 13

```
aatcttttag aagaatgtaa cattgttgtt ggaattcagc gataacatat ataatataag tggcttgtgt  2450
gaagtgcttc tgaatattgt gctattaatt aggacgtggt aagcaaaaaa tgctctattg ctctgtcata  2520
gaatgcaggc atatttatac tagcagatgc agtctaaaat ttaaactttc caaagatgtt gtaacttgta  2590
gcttgatgtt gtaaagatgc agtctaaaat ttaaactttc caaagatgtt gtaaagatgc agtcaagaag  2660
cataaaaact ctgacccttg gaaagttgag ttgacctcca tttagaatca ggttatatat atatatatct  2370
tagtgtgagc accttcttgg cttcaactca accttgcaaa gatgttgtaa cttgtagctt tatgccacaa  2800
tgccacatgg atggcgcgtt ttggttattg tccacttgct atttttttg ttgtttgaat tctagaacta  2870
atggaatttt gtgattgact gaaatattgt tttacttcca attctctgga gtagttttat ccctcctttt  2940
ctctgttggc aagtggcata tattcagccg cattacaaaa gttcagtgtt atgtgatgat atttatctgt  3010
tatattgttg tacttccctt aaacagttct gtcataagat ctgttgcaca attttttgtt ttttttctcg  3080
atcacgcagt agagctgcac atcattatat taagaaagga aaggtccaaa atagaccgaa atacaaagcc  3150
ctggagggca gaaaaacaaa cactggacct gactgcaatt tcttgtgaac tttgcaaatt tacaatatca  3220
tttgaaatta taatgtacta atgaaacaaa ataatcgatt taatgatagG AACTTGCTGG CATTATCAAA  3290
                                                E  L  A  G  I  I  K   248
CTTTCAGTGT ATTCTAGCTT CAGCCTATTT GAATGTCGGA AGGTTGTTAA TGGATCGAAG TCTTCAGAGA  3360
 L  S  V   Y  S  S  F   S  L  F   E  C  R   K  V  V  N   G  S  K   S  S  E   271
TTGGCAATGg taattaccaa tccatattgt ttttttcttt ctatttctta atttaattaa tgcatgtggt  3430
I  G  N                                                                      274
ttggatatca tggagcagga ggaaacatag gtgattttgt agaaaaattt caagtaaccg gtgcatttct  3500
ttatctctta tatgcagAGG AATACATTGG ATTAGATGAT AACAAATATA TTGGTGACTT GCTATCTGAA  3570
                  E   E  Y  I  G   L  D  D   N  K  Y   I  G  D  L   L  S  E   292
TTCAAATCAG CTAAGGATCG CAACAAAGGA GAAATTCTTC ATTGCAAACT GGTATTCAAG AAACGTCTCT  3640
 F  K  S   A  K  D  R   N  K  G   E  I  L   H  C  K  L   V  F  K   K  R  L   315
TCCGTGAGTC GGATGAGGCT GTGACTGATC CAATGTTTGT TCAGCTATCA TATGTCCAGg tactggttga  3710
F  R  E  S   D  E  A   V  T  D   P  M  F  V   Q  L  S   Y  V  Q              335
tagtattcat agctagctaa ctgaaggact gccagtttgt gtgttattgt tactcaagta atattgtttc  3780
cagaatagat ctaacaaata tcatttttct gcagTTGCAA CATGATTACA TTTTGGGAAA CTATCCTGTC  3850
                                    L  Q   H  D  Y   I  L  G  N   Y  P  V   347
GGCAGGGATG ATGCTTCACA ACTCTCTGCT CTTCAGATCT TGGTTGAGAT TGGATTCATT GATAATCCTG  3920
 G  R  D   D  A  S  Q   L  S  A   L  Q  I  L   V  E  I   G  F  I   D  N  P   370
AGTCCTGTGT gtaagtattt cttaaggtcc tacctgaatt cccatgccat ttttcagtgt agtatttctg  3990
E  S  C  V                                                                   374
gtggtaaata aaataatgtc ccccctgttt ttttgttctc accagTGAAT GGATATCACT TTTAGAGAGA  4060
                                                E  W  I  S  L   L  E  R   382
TTTCTTCCTA GACAAGTGGC GATTACCAGA GCAAAGCGAG ACTGGGAGCT TGACATCATT TCACGCTTTC  4130
 F  L  P   R  Q  V  A   I  T  R   A  K  R   D  W  E  L   D  I  I   S  R  F   405
AGTTAATGgt atttatctat ctcttgaact ctatatttat tagtctgtcg atatatttac aatttgcgtt  4200
Q  L  M                                                                      408
cacattggta aagcctcgtt agaactctag cttacctgag tactctgttt gattccagGA ACACTTATCA  4270
                                                            E   H  L  S   412
AAGGACGATG CACGGCAACA ATTTCTCAGA ATCTTAAGGA CTCTTCCATA TGGGAACTCT GTTTTCTTCA  4340
 K  D  D   A  R  Q  Q   F  L  R   I  L  R   T  L  P  Y   G  N  S   V  F  F   435
GTGTTCGGAA GATTGATGAT CCAATAGGAT TGCTACCTGG AAAAATTATT TTGGGGATCA ACAAACGAGG  4410
S  V  R  K   I  D  D   P  I  G   L  L  P  G   K  I  I   L  G  I   N  K  R  G  459
Ggtctgatct cgaccatgta atggaagctt catattcttt ctgctaagta aaactgacct tgaatttctg  4480
catgaatgca gGTTCACTTT TTCCGCCCGG TTCCCAAGGA ATATCTTCAT TCTGCAGAAC TAAGAGACAT  4550
             V  H  F   F  R  P   V  P  K  E   Y  L  H   S  A  E   L  R  D  I  479
CATGCAATTT GGTAGCAGCA ATACTGCTGT CTTCTTTAAA ATGCGGGTTG CTGGTGTTCT TCATATCTTT  4620
  M  Q  F   G  S  S   N  T  A  V   F  F  K   M  R  V   A  G  V  L   H  I  F   502
CAATTTGAAA CAAAGCAGgt attctaaagc ttcgaggcaa tagtttataa tacagccgat cctgttatat  4690
```


Fig. 13

```
 Q  F  E  T  K  Q                                                                                                  508
catccatagc tgttagaata acgatgactt tttagGGCGA GGAAATATGT GTAGCACTTC AAACACATAT  4760
                                     G  E  E  I  C  V  A  L  Q  T  H  I        520
AAATGATGTC ATGCTCCGCA GATATTCAAA AGCACGCTCT GGTAATAGTG TTACATCACA AAATGATGTT  4830
  N  D  V  M  L  R  R  Y  S  K  A  R  S  G  N  S  V  T  S  Q  N  D  V        543
AACCAAGCAT ATAAGCCACC AAATATCGAA ATGTTTGAAA AACGTGTCCA AGAACTGACA AAAACAGCCG  4900
 N  Q  A  Y  K  P  P  N  I  E  M  F  E  K  R  V  Q  E  L  T  K  T  A        566
AGGATTCTCA GAAGAAAGCA GATCAGgtaa gtacatttgc aacgaacaaa actggcaacc taatgtattt  4970
E  D  S  Q  K  K  A  D  Q                                                     575
gctagtgtaa cttgaaattt ctagactatt tctttgcatt tggatttcct gttgcagtgt tgcttcagtt  5040
aattgaatca aatatcgtcc tcctggccta ttaaaatata ctgttctgta gtggctaaaa attacagatc  5110
actttgtgtg tttgctcata atgacaaaat gacaattaac cgaaaagaaa cttgtacaga ttcatttgt   5180
cattccactt cttgttaata aataatgtgc ccgactagta gactaaaatt tccagaacac catatttagt  5250
caggtaggca ataattgata aatattggtt aatatggcta aacttcatga ttcatgaaca tctttattgtc 5320
ataaagaata tctttttagg tgttcgtaga gtacccaaat ccgtttacaa ttgccactta cactgtagtc  5390
atgtgagtgc ggccacagga catctttgaa cctatctttt gtctaatgca tagctaagaa aatggaaatg  5460
tctatcttat aaaagtgtac atttaataca tgtataacag tagacatctt gttgacgaaa taattgtgtt  5530
cctattatgt ttagTTGCGA GAAGATTTAC AGTTGAAGAC AAAACAAGAA ACAGAGATGC AAGAAGAGTT  5600
                 L  R  E  D  L  Q  L  K  T  K  Q  E  T  E  M  Q  E  E  L        595
GGAAGGGCTA AGAGATACCT TGCAATCTGA ACGACAAAGT TCCAAAGACA TAAAAAATGA GCTTGATAAG  5670
  E  G  L  R  D  T  L  Q  S  E  R  Q  S  S  K  D  I  K  N  E  L  D  K        617
CTAAAATCTC TATGTGATGA GAAAGAATCT GCTTTGCAGg taaggtgata ggttgcagat ttagttaaaa  5740
 L  K  S  L  C  D  E  K  E  S  A  L  Q                                       630
ttgtttggat catctgactt tccatttta gGCTGCCCTG ATGGAAAAAA GTAGACTTGA AACCAGATTA  5810
                                  A  A  L  M  E  K  S  R  L  E  T  R  L        643
ACTAGTGGCC AGGGCCGTGA GAGAGATACA TTGACAACTG TAGGCAGCAT CAATAATGAC ATTGAGgtat  5880
 T  S  G  Q  G  R  E  R  D  T  L  T  T  V  G  S  I  N  N  D  I  E            665
ctgtgacctg tttataactt ctttgtccac acttatttct gcaaagttgt tacaaacttc taatgcattt  5950
tactcttttg tgcctaaaag ATGCTTGCCA AGCTTGAGGA GGAGTTGAAA TCATACCAAA AAGAGCTTGA  6020
                      M  L  A  K  L  E  E  E  L  K  S  Y  Q  K  E  L  D        682
TGCATCAAAA GAGGTCTCAA AGAAGCTAAT GTTGGAAAAG AATATTCTTG ACCAGAAAGT TCAAAGGCTT  6090
  A  S  K  E  V  S  K  K  L  M  L  E  K  N  I  L  D  Q  K  V  Q  R  L        705
GAAAGAATGA AAAATGAAGA Ggttattctt attgttcctt ttttatgcta ttttttttctg ttctgatttc  6160
 E  R  M  K  N  E  E                                                          712
agagttaaaa gtttattcat ttcatatttc tgaaatatgg tttatatgat tatgcagAAA AGCGCAATGG  6230
                                                          K  S  A  M            714
AAAAGGTTTA TGCGGATGAA TGCTGTAAAC TGAAATCTCA GATTGCTGAA TTGGAGCAGA AATTGGAAGT  6300
E  K  V  Y  A  D  E  C  C  K  L  K  S  Q  I  A  E  L  E  Q  K  L  E  V        740
TGCTACACGA TCCTTAAATG TGGCTGAATC AAATCTTGCT GTAAGAAATG CTGAGGTTGA TAGCTTGCAA  6370
  A  T  R  S  L  N  V  A  E  S  N  L  A  V  R  N  A  E  V  D  S  L  Q        763
AATAGTCTGA AAGAACTTGA TGAGCTAAGA GAGTTCAAAG CGgtacgaga tgtacaatag ttgcatttgt  6440
 N  S  L  K  E  L  D  E  L  R  E  F  K  A                                    777
ttttatgtct ttcagaaagt aatacactct ttcattttgc attgtctcag GATGTTGACA GAAAGAATCA  6510
                                                  D  V  D  R  K  N  Q           784
ACAGACTGTT GAGATTCTTA AAAGGCAAGG AGCACAATTG GTGGAACTTG AGAATCTTTA TAAGCAAGAA  6580
  Q  T  V  E  I  L  K  R  Q  G  A  Q  L  V  E  L  E  N  L  Y  K  Q  E        807
CAGGTTCTAC GAAAGCGTTA CTATAATACA ATTGAAGgta aaccagaatt taatgtttgt gcttagtaat  6650
 Q  V  L  R  K  R  Y  Y  N  T  I  E                                          819
ggctatgatg ttttgtgatg aattgaccat gacttagttc caactcttta cagATATGAA AGGAAAAATA  6720
                                                  D  M  K  G  K  I              825
```


Fig. 13

```
AGAGTTTTTT GTCGCTTGCG CCCTCTAAGC GACAAGGAAC TTTCTTTTGA GGAGAAAAAT ATAGTTTGCA  6790
 R  V  F   C  R  L  R   P  L  S   D  K  E   L  S  F  E   E  K  N   I  V  C    848
GTCCTGATGA ATTTACAATT TCACATCCAT GGAAAGATGA AAAGTCAAAG CAACATATAT ATGATCGTGT  6860
S  P  D  E   F  T  I   S  H  P   W  K  D  E   K  S  K   Q  H  I   Y  D  R  V   872
TTTTGATGCA AACACAAGTC AAG AAGAAGT CTTTGAGGAT ACTAAGgtga atatttcaaa tgctatcttt  6930
  F  D  A   N  T  S   Q  E  E  V   F  E  D   T  K                              887
tgtgttgatg ccgtcggtaa tacaaatttt atttctaaga ttgttggctt catatgatct gttgaattta  7000
tgttcatttt gggtttcata tgatctgttg aatttatgtg atgcagTATC TGGTACAATC AGCTGTTGAT  7070
                          ATP-binding site          Y  L  V  Q  S   A  V  D   895
GGATATAATG TCTGTATATT TGCGTATGGC CAAACTGGTT CTGGAAAGAC TTTCACTATT TATGGTTCAG  7140
 G  Y  N   V  C  I  F   A  Y  G   Q  T  G   S  G  K  T   F  T  I   Y  G  S    918
AAAACAATCC TGGTCTTACT CCAAGGGCCA CATCTGAACT TTTTAGGGTG ATAAAGCGCG ATGGAAACAA  7210
E  N  N  P   G  L  T   P  R  A   T  S  E  L   F  R  V   I  K  R   D  G  N  K   942
ATATTCATTT TCTTTGAAGg taggaggaat atgtgtttgt catgttaggc atatgctctg ttcattcgta  7280
  Y  S  F   S  L  K                                                           948
tctgttaatc ttggctcatt aatttgtatt gttgacaagt actttgttct tgcattttacatg gtctgag  7350
aagcaaaaaa tgacttatat ttatatctga cactttcaca tattttaaca cgttctttag atccaagtat  7420
gccttctata ttatccttaa attctgtttt atacgcagGC ATATATGGTG GAGCTTTATC AAGATAATCT  7490
                                      A  Y  M  V   E  L  Y   Q  D  N  L   959
TGTGGACCTG TTATTGCCCA GAAATGCAAA GCAGCTGAAG TTAGAGATAA AAAAAGATTC CAAGgtataa  7560
  V  D  L   L  L  P   R  N  A  K   Q  L  K   L  E  I   K  K  D  S   K        980
gatttatttt cctaattcct atattcattt aatttatttg ttcttacagt gcactggata tgctacccta  7630
ccttttttct gcatatttga ttacttttct tatggacctt gttgtgcttt tcaggaacag tagcatccag  7700
atgtttgtgt ttcatactta gttagttgct aggacatgca gttaattcat ctcatttttt gacactaagg  7770
ctcctgtttg gaagcaaccc agtttttaag aaactggttt ttatcttttа gctaggagag ggcagcttct  7840
tggtttttaa gaaactggga atctaatttc tataaactga ggcataaaat gttatgtttg gaaccacctc  7910
aatttccata aaccagtttc ttagaaactg ggtgcttcca aacaagccct aaataacttg ctttagtact  7980
tttcggacag tttgtttctg catctccata ataattctgt tcaaattctg aaatatctat atctgctagt  8050
agtaattcaa acgaaccatc accttgatct gtgcagtttc cattgggaat tttacaagtg ttctttttta  8120
ccaatgtaca actttcatac tcacgggtta attaattact cgatactact ttttagGGTG TTGTTACCGT  8190
                                                        G  V  V  T  V   985
TGAAAATGTA ACAGTTGTGA GCATTTCAAG TATTGAGGAA CTGAGGGCTA TAATCTCAAG AGGTTCTGAG  8260
  E  N  V   T  V  V   S  I  S  S   I  E  E   L  R  A   I  I  S  R   G  S  E  1009
AGGAGGCACA CTGCTGGAAC GAATATGAAT GATGAGAGTT CAAGGTCTCA TTTAATTCTT TCAATCATTA  8330
 R  R  H   T  A  G  T   N  M  N   D  E  S   S  R  S  H   L  I  L   S  I  I   1031
TTGAAAGTAC AAATCTCCAA ACTCAATCAT ATGCAAGAGG CAAGgtatgt caggatgaag ctgtgaactt  8400
 I  E  S   T  N  L  Q   T  Q  S   Y  A  R   G  K                              1046
aaccccaatt tggtcgagtc tagtgacaat actttcatct ataacaatga aataaaaata ttgaatgttc  8470
tgtctccctg taaaaatatt ataagtactt tcatgcacat cgttgaactt ttgcatgctg tagaaaatac  8540
tatacctgtg atttgatgga ggctgttagc gaacattacc tggaaaacac acttcaacta gtcgtatttc  8610
aattgttcca taagattaaa caattatgtg ctttctgtag tatcttggcc tttgacagtc taaattattc  8680
atatgatgtt tgaatttcat tattattttt tcaatactat gcaatatgcg tctcagtgca tgttttaatt  8750
ttgtgtgtga tttaatatga agtacacagt ctgctagtgt gaagttcttt gtgttgttcc tcttagttga  8820
tatgattatt tcaaacagac aagctgcaga aaatattgtg tacctaacaa aagagactaa tatgctgcag  8890
acagttcttt gggaaagtag tgatttctca tatttctgct ggaactaaag tccttgagct gttgcaatta  8960
atgtccaagt ttgtttcata ttaaagggaa gaattgacag tgtttctctg tttgaacagC TAAGTTTTGT  9030
                                                        L  S  F  V   1050
GGACCTTGCT GGTTCTGAGA GGGTGAAAAA ATCAGGTTCA GCAGGAAAGC AATTGAAAGA AGCGCAAAGT  9100
 D  L  A   G  S  E   R  V  K  K   S  G  S   A  G  K   Q  L  K  E   A  Q  S   1073
ATAAATAAAT CTCTTTCTGC TTTGGCTGAT GTTATTGGTG CTTTATCTTC TGATGGACAA CATATACCTT  9170
```


Fig. 13

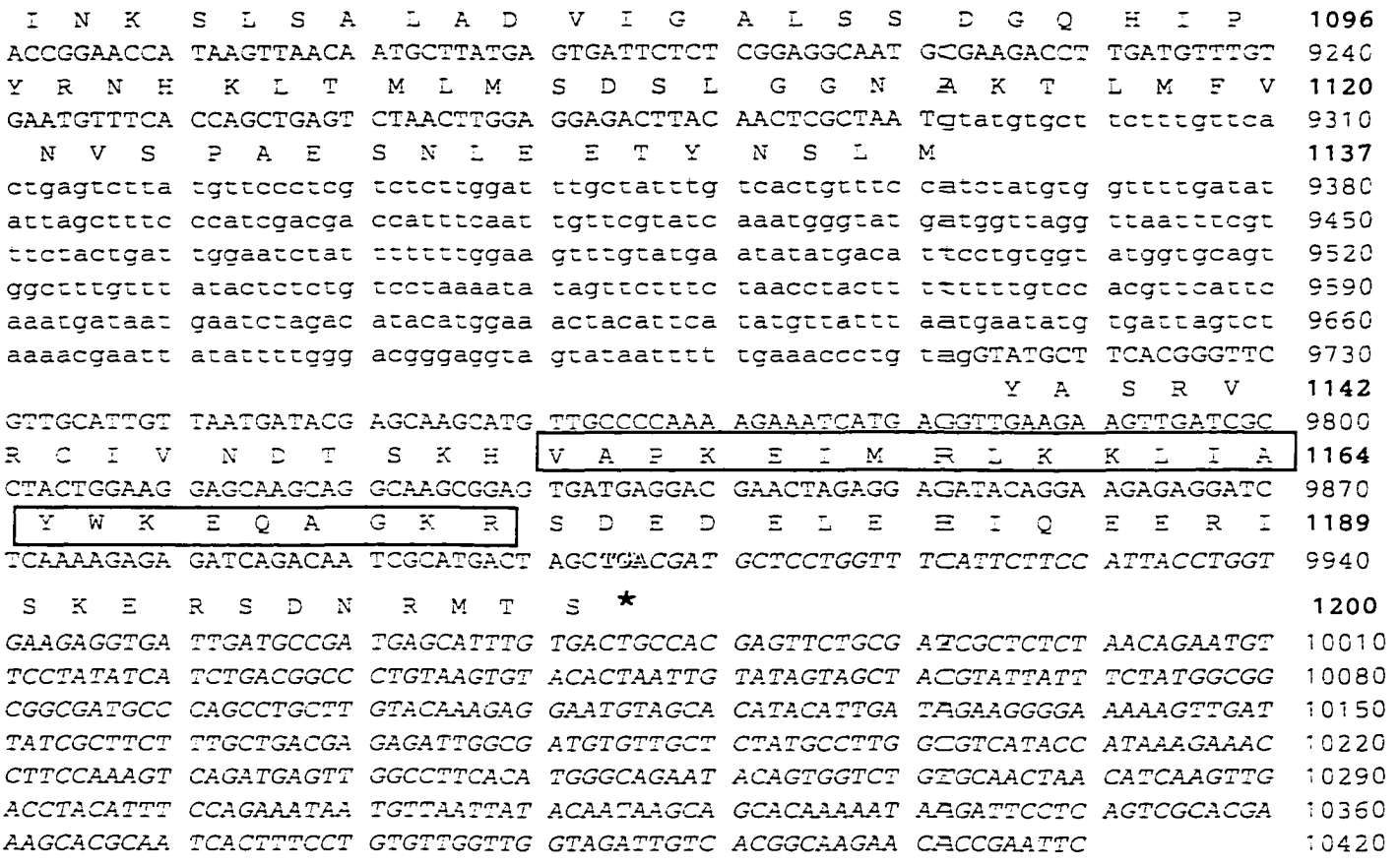

Fig. 13 Nucleotide and deduced amino acid sequence of Maize KCBP gene (ZmKCBP). Exons are shown in upper case and introns are presented in lower-case. Nucleot ide sequence preceding the translation initiation codon and following the translation termination codon are shown in upper case and italic. The predicted amino acid sequence is shown under the nucleotide sequence. The start codon is indicated with a shadow line and the stop codon is indicated with an asterisk. Numbers at right correspond to nucleotides and deduced amino acids (in bold). Amino acids sequences in bold denote putative PEST sequences as predicted by PESTfind program. The three hyperconservative sequences characteristic to all kinesins and KLPs as well as the amino acid residues (EDMKGKI) conserved in C-terminal KLPs and identical in KCBPs are shown in bold and underlined. The boxed region corresponds to the calmodulin-binding domain. The nucleotide sequence and the predicted amino acid sequence are available in the Genebank under the accession number AF223412.

predicts splice sites in plant genes, and comparison of the deduced amino acid sequence of the ZmKCBP with its homolog from *Arabidopsis* revealed the presence of twenty-two exons and twenty-one introns (Fig 13 and Table 4& 5). The predicted ZmKCBP consists of 1200 amino acids with a calculated molecular mass of 138 kDa compared to its dicot homolog from *Arabidopsis*, tobacco, and potato of 1261,1265, and 1265 amino acids respectively. Comparison of the exons in maize and *Arabidopsis* KCBP (Reddy *et al.*, 1998) showed that all exons except the first three exons have the same number of nucleotides/exon (Table 5). Three exons, which encode part of the tail region, are variable between maize and *Arabidopsis* KCBP gene. There is a deletion in the first exon of ZmKCBP and the third exon, which is the largest one in *Arabidopsis* KCBP (567bp), is interrupted by an intron in ZmKCBP gene (Table 4). The extra intron (# 2a) is 74 bp in length and it is most likely an intervening sequence because: i) all reading frames in this region have stop codons, ii) the predicted amino acid sequence in this region has no sequence similarity with other KCBPs from dicots; iii) this intron follows the GU-AG rule for 5' and 3' splicing sites that is maintained in all introns, and the percentage of prediction of splicing at the donor and acceptor sites using Netplant gene is 100 percent. Acquiring novel introns is a characteristic feature of some genes in monocots. Catalase gene one (*CAT1*) of *Oryza sativa* (rice, a monocot) acquired an intron in a novel position that is not present in its homologue from dicots (Frugoli *et al.*, 1998).

Although the length of KCBP exons is conserved between monocots and dicots, the introns are highly variable in length (62-949 nt) in ZmKCBP compared to AtKCBP (76-320 nt) (Table 4). Unlike AtKCBP introns where all introns are rich in A and T nucleotides (fourteen out of twenty introns contain 70% or more AT) (Reddy *et al.*, 1998), all introns of

Table (4) Comparison of intron's length and AT content of both *Arabidopsis* and maize KCBP genes and 5' and 3' splice site junctions of introns in maize KCBP gene.

No.	Length (bp)		AT Ratio (%)		5' Splice Site		3' Splice site	
					Maize KCBP splice junctions			
	Arab.	Maize	*Arab.*	Maize	Exon	Intron	Intron	Exon
1	108	271	65	64	CAA	GTTAAG	GAACAG	GTC
2	76	301	54	55	AAG	GTGATG	CTGCAG	GAT
2a	**	74	**	62	TAG	GTGAGT	CTGCAG	GGG
3	88	949	64	67	GAG	GTAAAT	TGATAG	GAA
4	83	148	65	70	ATG	GTAATT	ATGCAG	AGG
5	76	115	70	66	CAG	GTACTG	CTGCAG	TTG
6	112	105	68	63	TGT	GTAAGT	CACCAG	TGA
7	120	120	62	66	ATG	GTATTT	TTCCAG	GAA
8	109	80	74	61	GGG	GTCTGA	ATGCAG	GTT
9	85	87	72	66	CAG	GTATTC	TTTTAG	GGC
10	262	618	71	67	CAG	GTAAGT	GTTTAG	TTG
11	79	62	75	68	CAG	GTAAGG	TTTTAG	GCT
12	99	94	72	67	GAG	GTATCT	TAAAAG	ATG
13	85	106	73	76	GAG	GTTATT	ATGCAG	AAA
14	124	78	71	68	GCG	GTACGA	TCTCAG	GAT
15	80	86	76	66	AAG	GTAAAC	TTACAG	ATA
16	85	140	71	69	AAG	GTGAAT	ATGCAG	TAT
17	70	229	71	68	AAG	GTAGGA	ACGCAG	GCA
18	86	622	73	66	AAG	GTATAA	TTTTAG	GGT
19	320	645	70	67	AAG	GTATGT	GAACAG	CTA
20	98	422	73	67	AAT	GTATGT	CTGTAG	GTA

- Splice junctions were predicted with NetPlantGene (http://genome.cbs.dtu.dk/nph-webface) and by comparing the maize KCBP gene with the coding sequence of *Arabidopsis* KCBP gene.
- The consensus sequences at 5' and 3' splice junctions are AG/GTAAGT and TGY(A/C)AG/GT, respectively Goodall *et al.*, (1991). Nucleotides that are identical to consensus sequences are underlined.
- ** = Intron that is not present in the *Arabidopsis* KCBP gene.

Table (5): Comparison of exons length ant AT content of both *Arabidopsis* and maize KCBP genes.

No.	Length (bp)		AT Content (%)		Region coded by Exons
	Arab.	Maize	*Arab.*	Maize	
1	189	ND	51	ND	Tail region
2	211	132	48	59	Tail region
3	567	230	57	63	Tail region
3 a	**	328	**	57	Tail (MyTH4) region
4	97	100	65	60	Tail (Talin-like) region
5	182	182	67	62	Tail (Talin-like) region
6	116	116	54	58	Tail (Talin-like) region
7	103	103	55	58	Tail (Talin-like) region
8	153	153	56	59	Tail (Talin-like) region
9	147	147	58	59	Tail (Talin-like) region
10	201	201	63	61	Tail(Talin-like) region
11	165	165	61	63	Coiled-Coil region
12	105	105	57	55	Coiled-Coil region
13	138	138	68	63	Coiled-Coil region
14	195	195	66	61	Coiled-Coil region
15	127	127	65	64	Coiled-Coil region
16	203	203	64	66	Motor domain
17	183	183	61	62	Motor domain
18	96	96	66	63	Motor domain
19	198	198	59	62	Motor domain
20	272	272	58	60	Motor domain
21	365	ND	63	ND	CaM-Binding domain

- Splice site junctions were predicted with NetPlantGene Database (http://genome.cbs.dtu.dk/htbin/nph-webface) and by comparing the maize KCBP gene with the coding sequence of *Arabidopsis* KCBP gene.
- Exon that is not present in *Arabidopsis* KCBP gene.
- ND = not determined.

ZmKCBP except the fifth intron, have less than 70% AT content (Table 4). High AT content is a feature of plant introns (Goodall *et al.*, 1991). All the introns have the conserved GU and AG dinucleotides at their 5' and 3' ends, respectively (Table 4), thereby conforming to the GU-AG rule for 5' and 3' splice sites (White *et al.*, 1992; Brown *et al.*, 1996).

Functional domains in ZmKCBP

Secondary structure, probability of coiled-coil regions, and structural features of ZmKCBP based on its primary sequence are shown in Fig (14) and Table (5). Most kinesins have three distinct structural and functional domains: a globular tail, a coiled-coil region and a motor domain. Exons 1-10 contained the coding region for the tail region. The coiled-coil region is coded by exons 11-15 and the conserved motor domain is coded by the exons 16-21 (Table 5). The CaM-binding domain unique to KCBP and kinesin-C is coded by the last exon suggesting that KCBP may have evolved by fusion of an exon coding for a CaM-binding domain with a KLP gene. Domain fission and fusion have been recorded in both prokaryotics and eukaryotics. Multifunctional proteins in vertebrates that are composed of different domains correspond to separate gene products in *E.coli* (McCarthy *et al.*, 1983; Schweizer and Datta, 1989).

The deduced protein sequence of ZmKCBP were compared with both AtKCBP from a dicot and motor domain of kinesin-C from sea urchin. The motor domain of ZmKCBP (amino acids residues 823-1155) shares about 79% similarity with the motor domain of its homolog from dicot and about 51% with the motor domain of kinesin-C. This motor domain contained the conserved ATP-binding sequence (Yang *et al.*, 1989). Furthermore, ZmKCBP has the three hyperconserved motor sequences (Fig 13 shown in bold and underlined) found in all kinesin motor domains, and a fourth unique sequence (EDMKGKI) located in the

Fig. 14 **Predicted secondary structural features of maize (*Zea mays*) KCBP (ZmKCBP).** (A) The secondary structure of ZmKCBP as predicted by Robson-Garnier and Chau-Fasman methods. Regions predicted to be α-helices (Hlx), β-sheets (Sht) or β-turns (Trn) are indicated by solid boxes. (B) Probability of formation alpha-helical coiled-coil is determined using the coiled-coil program (Lupus *et al.*, 1991). The *y*-axis indicates the probability of coiled-coil formation; the *x*-axis designates the amino acid position along the length of the polypeptide starting from the amino terminus. (C) Schematic diagram of predicted domains of ZmKCBP. Color representation is as following: red = motor domain, blue = coiled-coil region, green = talin-like region, cyan = myosin-tail homology4 (MyTH4), black = calmodulin-binding domain. All figures are drawn to scale.

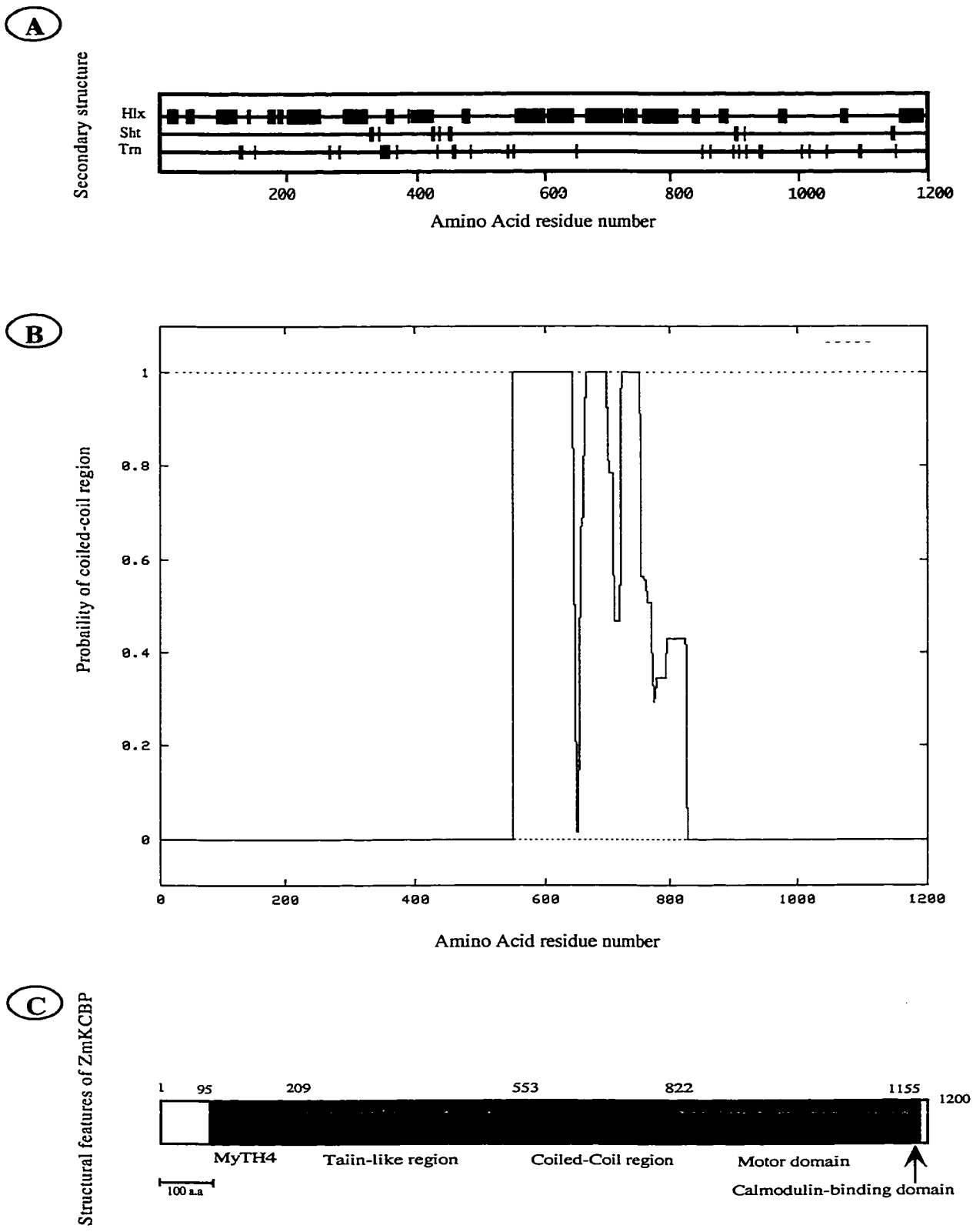

Fig. (14)

"neck" region upstream of the motor domain that is highly conserved among the carboxy-terminal kinesins and identical among the KCBPs (Saito *et al.*, 1997). The amino acid residues 553-822 of ZmKCBP predicted to forms the alpha-helical coiled-coil is shown in the secondary structure (Fig 14A) and as predicted by Lupus plot (Fig 14B) (Lupas *et al.*, 1991). This coiled-coil region is responsible for dimerization and is not highly conserved among KLPs. It shows about 43% sequence similarity to the AtKCBP coiled-coil region. This less conserved coiled-coil region spans about 22% of the KCBP, however in kinesin-C the coiled -coil region spans about 70% of the protein. Another domain that defines kinesin class specificity is the "neck" region, (ten to fourteen amino acids stretch) that connects the conserved catalytic core to the less conserved coiled-coil "stalk" domain (Vale. 1987; Endow and Waligora, 1998; Sablin *et al.*, 1998). The neck sequence of ZmKCBP is identical to that of both AtKCBP and kinesin-C. However, it displays a slight divergence from the neck of other C-terminal members (Saito *et al.*, 1997), suggesting that these KLPs form distinct class within the C-terminal subfamily. Sequence comparisons and mutagenesis studies have shown that "neck" regions are class conserved, responsible for directionality of the motor, and function as mechanical amplifiers that couple the ATP hydrolysis and energy into directional motion along the MT (Vale *et al.*, 2000).

The amino-terminal tail region (amino acid residues 95-533) of ZmKCBP showed significant similarities to the MyTH4 (~110 aa) and talin-like (~350 aa) regions present in myosin VIIa and X (29% identity and 49% similarity in the MyTH4 domain and 29% identity and 49% similarity in the talin-like region of *Homo sapiens* myosin VIIa). The MyTH4 domain and talin-like region are characteristic features of KCBP and have not been found in any other kinesin members of the kinesin superfamily. Kinesin C does not have

myosin and talin-like regions characteristic for KCBPs in plants. KCBP with its myosin and talin features is unique to plants and is highly conserved among angiosperms.

In many CaM target proteins, the CaM-binding domain has been shown to reside in a stretch of 18-20 amino acid residues that form a helix with the predominance of basic residues on one face and hydrophobic residues on the other. The previous characterized CBD (a 23 aa stretch) in *Arabidopsis* KCBP is highly conserved in maize KCBP (amino acid residues 1156-1179). CBD of ZmKCBP share 90% identity to CBD of AtKCBP and 35 % identity with the CBD of kinesin-C. This region, like CBD in AtKCBP, forms amphiphilic alpha helix with basic residues on one side and hydrophobic residues on the other side. CBD of ZmKCBP also has tryptophan residue which is characteristic for most of CBDs. The CBD is responsible for Ca^{2+}-dependent CaM-binding to these KLPs and the CBD confers Ca^{2+}/CaM regulation of KCBP activity (Reddy *et al.*, 1996a; Rogers *et al.*, 1999).

ZmKCBP is coded by a single gene and is expressed in all tissues

To determine the approximate copy number of ZmKCBP, genomic DNA was digested with four different restriction endonucleases (*Ssph*I, *Sst*I, *Nco*I, and *Kpn*I) and probed with 6 kb *SalI/EcoR*I fragment of ZmKCBP. With each restriction enzyme digestion, the expected number and size of bands were detected (Fig 15), suggesting that ZmKCBP is encoded by a single gene. The ZmKCBP homologue from *Arabidopsis* was shown to be a single gene (Reddy *et al.*, 1996b) and this was confirmed recently by the completion of the *Arabidopsis* genome sequence. Low stringency washes did not yield any additional bands, suggesting that the KCBP does not cross hybridize with other kinesin-like genes. Consistent with this finding, a Blastn search with ZmKCBP did not show any significant sequence similarity with other KLPs.

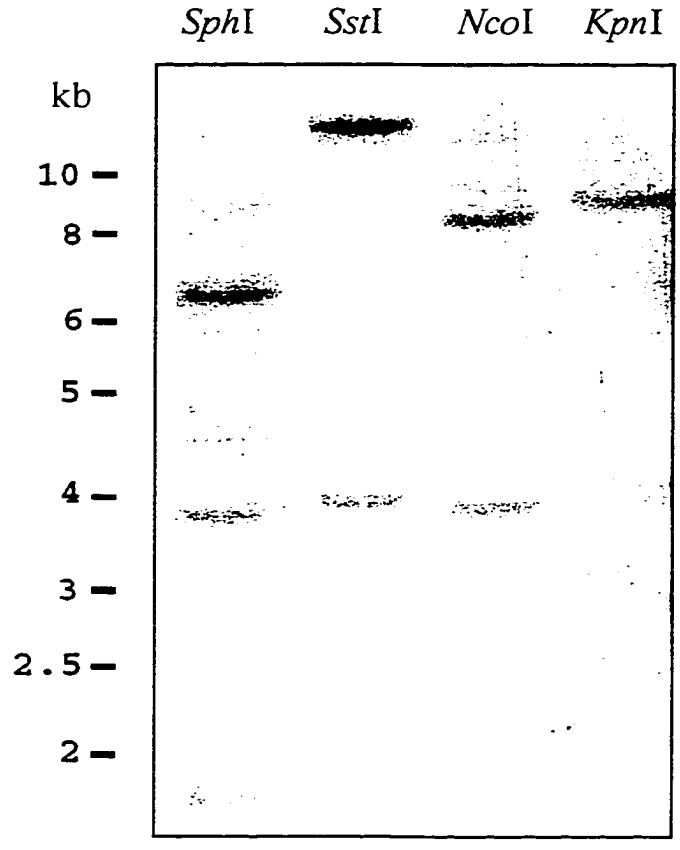

Fig. 15 Southern blot analysis of maize genomic DNA. Genomic DNA (10 μg) was digested with different restriction enzymes (*Kpn*I, *Nco*I, *Sst*I, *Sph*I). The digested DNA was electrophoresed in an 0.8% agarose gel, transferred onto a Hybond N-membrane, and probed with ^{32}P-labelled 6-kb *Sal*I/*Eco*RI genomic fragment which contains the motor domain, calmodulin-binding domain and part of the coiled-coil region. DNA size mass markers are shown on the left. kb = kilobase pairs.

In poly(A)$^+$ RNA blot analysis, a single transcript of about 5 kb hybridized with the ZmKCBP probe (Fig 16A). To examine the expression of ZmKCBP in different tissues, RT-PCR was performed with DNase treated RNA from root, shoot and whole seedling. Sense and anti-sense primers that correspond to exon 11 and exon 17 were used to amplify the cDNA. The expected size fragment (1014 bp) was amplified from all tissues (Fig 16B). These results, together with the RNA blot analysis of *Arabidopsis*, potato, and tobacco (Reddy *et al.*, 1996a; Reddy *et al.*, 1996b; Wang *et al.*, 1996) suggest that KCBP is expressed in all plant organs and that the mRNA levels vary with the highest expression in the actively dividing cells. Our RT-PCR data indicate that introns between exon 11 and exon 17 do not undergo alternative splicing.

Maize KCBP is detected by an affinity-purified antibody to *Arabidopsis* KCBP

CBD of ZmKCBP shares 90% identity with the CBD of *Arabidopsis*. The expression of ZmKCBP protein in maize tissue was examined by immuonoblot analysis using affinity-purified antibodies raised against the CBD of *Arabidopsis* KCBP (Bowser and Reddy, 1997). Two bands (~104 and 92 kDa) were detected in total protein extract of young maize seedlings (Fig 17). The molecular mass of the detected bands is smaller than the estimated molecular mass, which is about 138 kDa. It is likely that the smaller size of the protein is due to partial degradation of KCBP. Consistent with this finding, analysis of ZmKCBP with the PESTfind program, which predicts the PEST motifs, which are targets for proteolysis, identified five PEST sequences with significant scores (shown in bold, Fig 13). Moreover, it has been shown previously that KCBP as well kinesin C are highly susceptible to proteolytic degradation (Bowser and Reddy, 1997; Smirnova *et al.*, 1998; Rogers *et al.*, 1999). Extraction of KCBP in the absence of protease inhibitors or delay in preparing blots results in

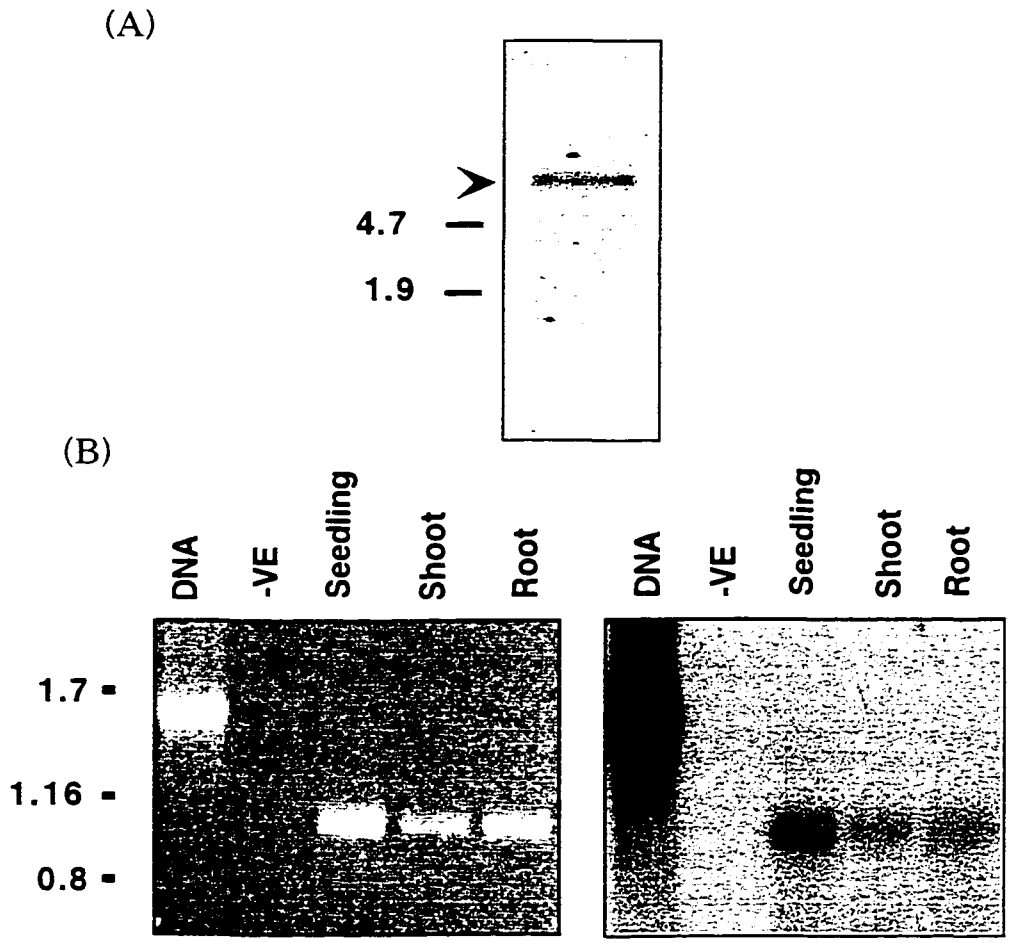

Fig. 16 **Expression of ZmKCBP in different tissues.** (A) Northern blot analysis. Poly $(A)^+$ RNA was isolated from maize seedlings, electrophoresed through formaldehyde-containing agarose gel, transferred onto a Hybond-N membrane, andprobed with ^{32}P-labelled 1.3 kb ZmKCBP cDNA that codes for the motor domain and calmodulin-binding domain. Numbers on the left indicate the size of 28S (4.7 kb) and 18S (1.9kb) ribosomal RNAs. Arrow indicates ZmKCBP transcripet. (B) Expression of ZmKCBP in different tissues. Total RNA from root, shoot and young seedling was used as a tmplate for RT-PCR. Amplified products were resolved by electrophoresis (left), blotted and probed with 6 kb genomic fragment (right). Maize DNA (DNA) and total RNA (-ve) were used as positive and negative controls rèspectively. Numbers indicated the length of size markers in (kb).

a smaller band (75 kDa) with increasing intensity (Bowser and Reddy, 1997; Smirnova *et al.*, 1998).

The C-terminal region of ZmKCBP contains a CBD

CaM binds and regulates the activity of many CBDs through Ca^{2+}. Analysis of the deduced amino acid sequence in the C-terminal region of the ZmKCBP showed a potential CaM binding site (1156-1179 amino acid residues). In addition, ZmKCBP is recognized by an antibody raised against the *Arabidopsis* CBD (Fig 17) suggesting that ZmKCBP is a CBD.

To determine if ZmKCBP interacts with CaM in a Ca^{2+}-dependent manner, a 1329 bp cDNA that contained the motor domain and the putative CaM-binding domain was expressed in *E. coli* using pET 28a and pET 32a expression system and tested the bacterially expressed protein for its ability to bind to CaM. Soluble and insoluble protein fractions from an induced culture showed the presence of a fusion protein, which bound to biotinylated CaM. Furthermore, the fusion protein was detected by the AtKCBP antibody also (Fig 18). The size of the fusion protein corresponds to the predicted size of the protein from the gene fusion. ZmKCBP fusion protein from soluble fraction was purified by CaM-Sepharose column. Fusion protein bound to CaM Sepharose column in the presence of Ca^{2+} (2 mM) was eluted from the column by adding 2 mM EGTTA. The eluted fractions were detected by KCBP-Ab and by biotinylated CaM (BioCaM) (Fig 19). Eluted fractions bound to BioCaM in the presence of Ca^{2+} and failed to bind in presence of EGTA (Fig 19). These results indicate that ZmKCBP is a CBD and the CaM-binding is a Ca^{2+}-dependent.

KCBP is present in both soluble and microsomal fractions

Our previous studies have shown that KCBP is present in the soluble fraction and is highly susceptible to proteolytic degradation (Bowser and Reddy, 1997; Smirnova *et al.*,

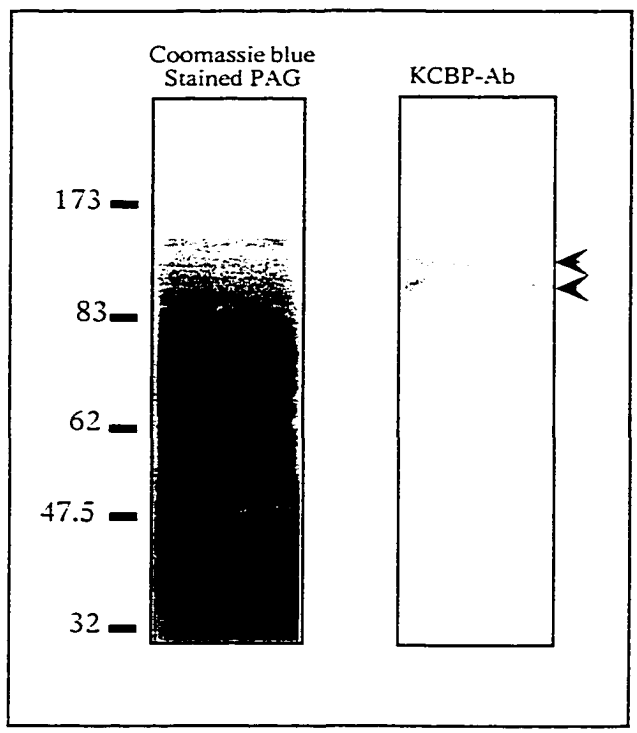

Fig. 17 **Western blot analysis of maize KCBP.** Immunodetection of KCBP using affinity-purified KCBP antibody raised againstthe calmdulin-binding domain of *Arabidopsis* KCBP (Bowser and Reddy, 1997). Proteins from maize seedling were fractionated on 8%SDS-containing polyacrylamide gel and either stained (left) or blotted and detected with KCBP antibody (right). Arrowheads represents two bands of molecular mass of about 104 and 92 kDa. Molecular mass markers are shown at the left in kDa.

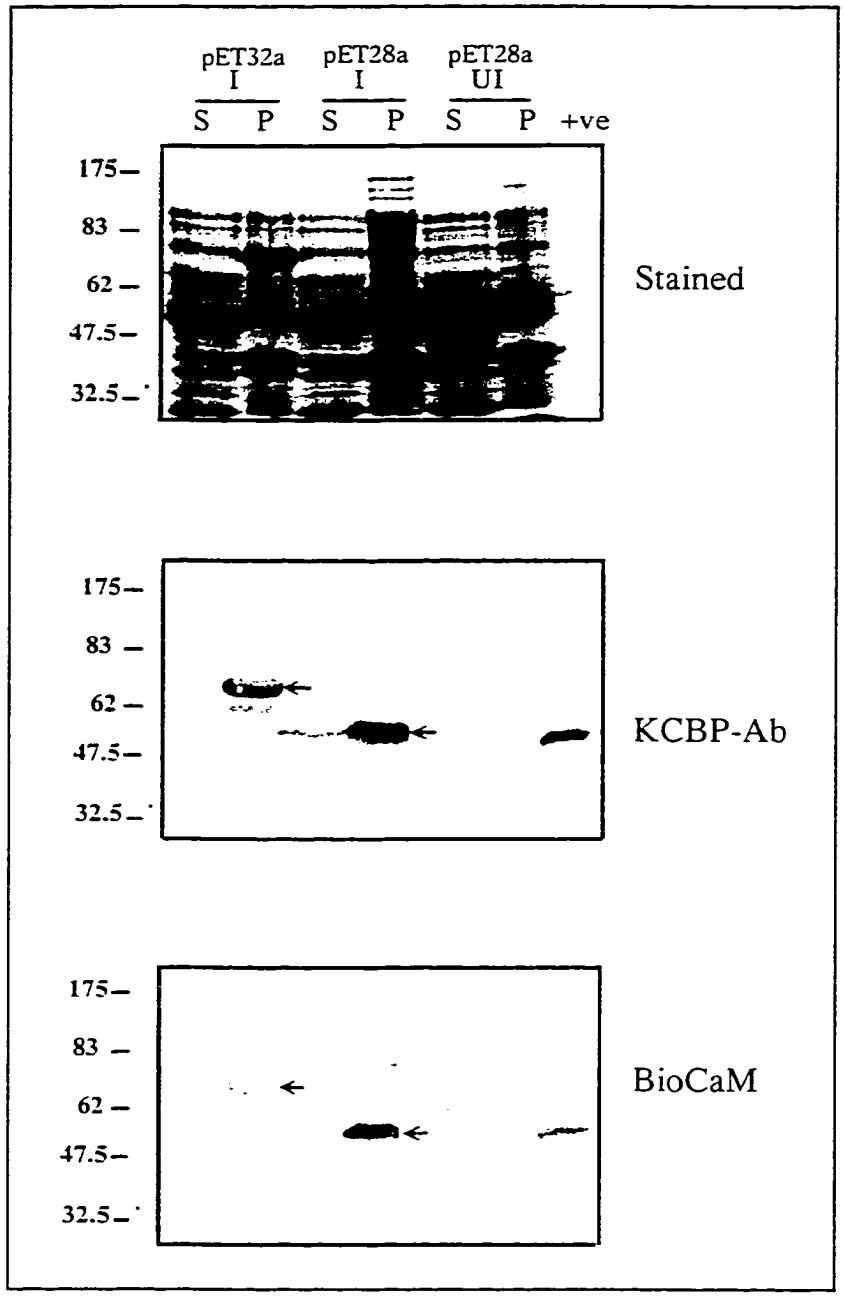

Fig. 18 **Expression of ZmKCBP in *E.coli*.** Partial ZmKCBP cDNA (1329 bp) containing the coding region for the motor and calmodulin-binding domains was amplified from first strand cDNA using PCR. The amplified fragment was cloned into expression vectors (pET 28a and pET 32a) and expressed in *E.coli*, BL21 (DE3). Fusion protein was expressed as described previously (Reddy et al., 1996b). Soluble (S) and pellet (P) fractions from induced (I) and uninduced (UI) cultures were separated by SDS-PAGE. Proteins were either stained with Coomassie blue (stained) or blotted and detected with affinity-purified KCBP-Ab (KCBP-Ab) or biotinylated calmodulin (BioCaM). The C-terminal region of *Arabidopsis* KCBP was used as a positive control (+ve). Molecular mass markers are shown at left in kDa. Location of fusion protein is indiated by arrows.

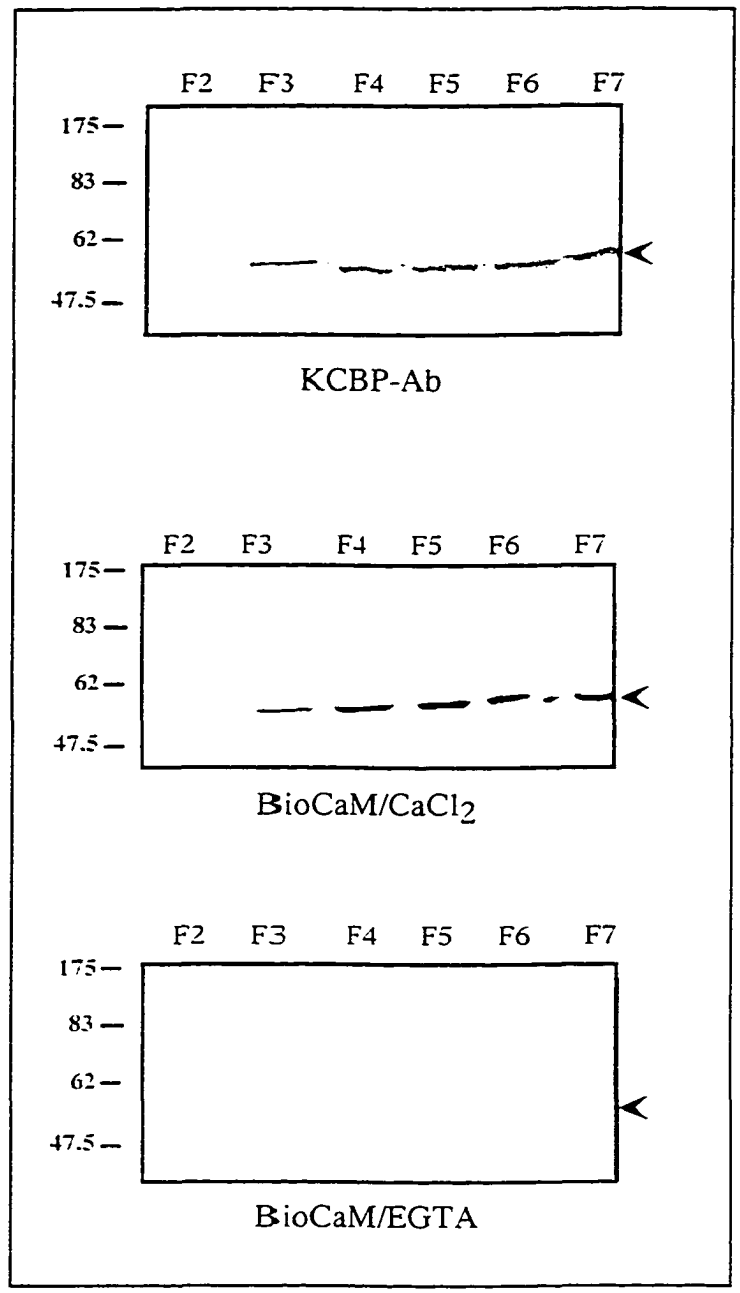

Fig. 19 **Purification of recombinant ZmKCBP by calmodulin-Sepharose column.** The cocentration of Ca^{2+} in soluble protein from induced culture of pET 28a was adjusted to 2 mM $CaCl_2$ and loaded onto CaM-Sepharose column. Column was washed with several volumes of binding buffer (see methods section) and the bound protein was eluted by replacing the $CaCl_2$ with 2 mM EGTA. Eluted fractions (F2-F7) were electrophoresed, trasferred onto nitrocellulose membranes, and probed with biotinylated calmodulin in the presence of 1 mM $CaCl_2$ (BioCaM/$CaCl_2$), 2 mM EGTA (BioCaM/EGTA), or with KCBP-Ab. Molecular mass markers are shown at left in kDa. Location of the right size of the fusion protein is indicated by arrow heads.

1998). Hence, in most cases, the size of the detected band is smaller than the calculated molecular weight of the protein. Because of punctuate staining of KCBP observed in some cases (Bowser and Reddy, 1997) it is of interest to test if KCBP is present in the microsomal fractions. To test this, soluble and microsomal protein fractions from *Arabidopsis* suspension culture were prepared and probed with KCBP antibody. As shown in Fig (20), a single band with a molecular size of about 140 kDa was detected in the microsomal fraction. This band corresponds to the size of the predicted protein. On the other hand, a band with a molecular size of about 101 kDa was detected in the soluble fraction. These results indicate that KCBP protein is present in both soluble and microsomal fractions and that KCBP in the microsomal fractions is protected from proteolytic degradation during the extraction process.

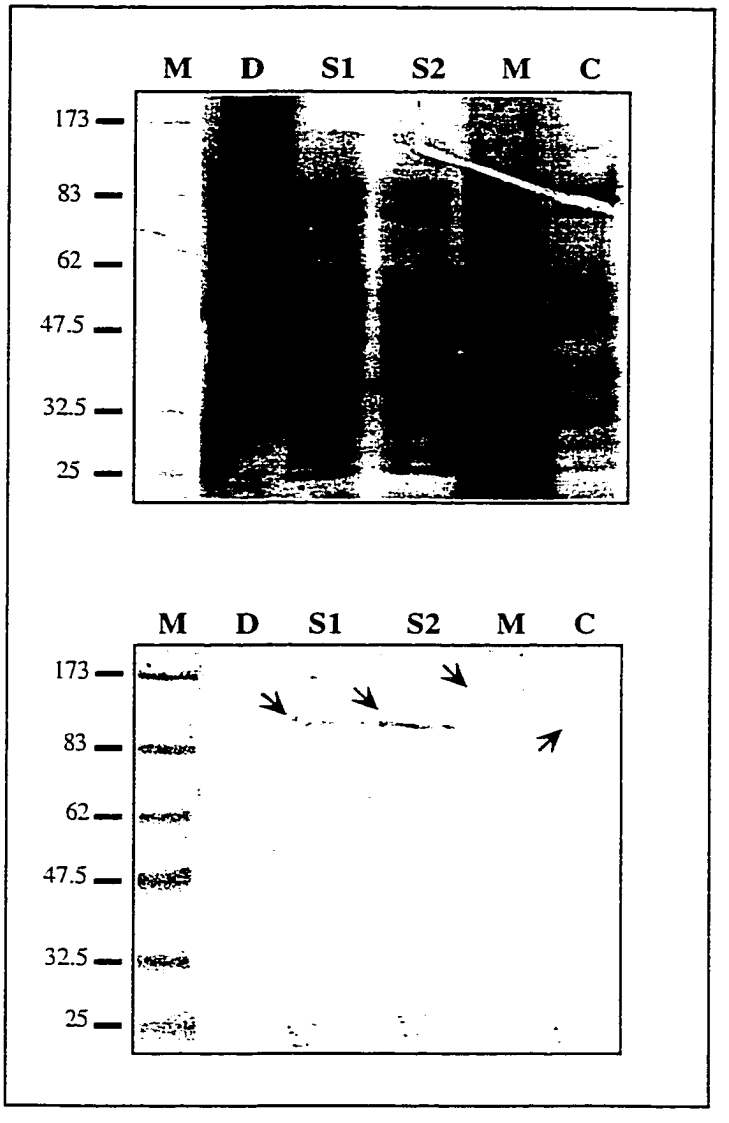

Fig. 20 **Detection of KCBP in soluble and microsomal fractions.** Crude protein extract from *Arabidopsis* suspension culture centifuged at 12,000g. to separate cell depris (D). The supernatant (S1) was collected and recentrifuged at 120,000g to separate the microsomal fraction (M) from the soluble one (S2). Soluble and microsomal fractions were separated on a SDS-PAGE and stained with Coomassie blue (upper) or blotted and probed with KCBP-Ab (lower). (C) represents the crude protein extract as a control. Molecular mass marker are shown at left in kDa. Arrows indicate the KCBP bands.

II. Cloning and characterization of KCBP from a gymnosperm,

Norway spruce, *Picea abies* (L.) Karst

Part of this work is included in a paper "Molecular evolution of a Ca^{2+}/CaM-regulated MT motor protein from phylogenetically *diverged* eukaryotes". Salah E. Abdel-Ghany, Paul Kugrens, and A.S.N. Reddy. Molecular Biology and Evolution. (In preparation)

Gymnosperms, an non-flowering seed plants, that evolved from ferns about 300 million years ago (MYA), and they gave rise to the angiosperm clade (Goremykin *et al.*, 1996; Samigullin *et al.*, 1999; Soltis *et al.*, 1999). They dominated the land flora throughout most of the Mesozoic era until about 100 MYA, just before the dominance of the flowering plants. There are four divisions of gymnosperms with living representatives: Cycadophyta (cycads), Ginkophyta (ginkgo), Coniferophyta (conifers), and Gentophyta (gentophytes). By far the most numerous, most widespread, and most ecologically important of the gymnosperms are the *Coniferophyta*. KCBP has been cloned from representative members of monocots and dicots and is highly conserved among angiosperm members. In order to examine the presence and the level of conservation of KCBP outside the angiosperms, we used PCR and cDNA library screening to clone KCBP from a conifer Norway spruce.

Isolation of a KCBP from spruce (PaKCBP)

The kinesin superfamily is defined by a motor domain that contains a highly conserved ATP-binding site. KCBPs from angiosperms have a characteristic CBD at the C-terminus with highly conserved stretch of amino acid residues (Fig 21). To isolate KCBP gene from spruce, two degenerate primers corresponding to these conserved regions were synthesized (Fig 21). Approximately 900 bp and 1 kb fragments were amplified from cDNA library (Fig 22). The amplified products were purified and cloned into pBluescript vector

(A)

ATP-binding site

AtKCBP	I	F	A	Y	G	Q	T	G	S	G	K	T
Kar3	I	F	A	Y	G	Q	T	G	S	G	K	T
Kata	I	F	A	Y	G	Q	T	G	S	G	K	T
DmNcd	I	F	A	Y	G	Q	T	G	S	G	K	T

(B)

CaM-bining region in KCBPs

R	L	K	K	L	V	A	Y	W	K	E	Q	A	G	K	K	**AtKCBP**
R	L	K	K	L	V	S	Y	W	K	E	Q	A	G	R	K	**StKCBP**
R	L	K	K	L	V	S	Y	W	K	E	Q	A	G	R	K	**NtKBP**
R	L	K	K	L	I	A	Y	W	K	E	Q	A	G	R	K	**ZmKCBP**

(C)

Sense primer

	BamHI	**I**	**F**	**A**	**Y**	**G**	**Q**	
5'-GCA	GGATCC	ATT	TTT	GCI	TAT	GCI	CAA	AC-3'
		C	C		C		G	
		A						

Antisense primer

	EcoRI		**A**	**Q**	**E**	**K**	**W**	**Y**	
5'-GCA	GAATTC	C	IGC	TTG	TTC	TTT	CCA	GTA	-3'
				C	C	C		A	

Fig. 21 (A) Alignment of the conserved ATP-binding site in different C-terminal KLPs. (B) Alignment of CBD in different KCBPs from angiosperms. AtKCBP (*Arabidopsis thaliana*), Kar3 (*Saccharomyces cerevisiae*), Kata (*Arabdopsis*), DmNcd (*Drodophila melanogaster),* StKCBP (Potato), NtKCBP (Tobacco). (C) Sequences of degenerate primers used to amplify spruce motor domain with calmodulin-binding domain. Inosine (I) is included in the sequence if the 3rd base in a codon has all four bases. Amino acids corresponding to thr nucleotide sequence shown over the nucleotide sequence in bold. Restriction sites are underlined.

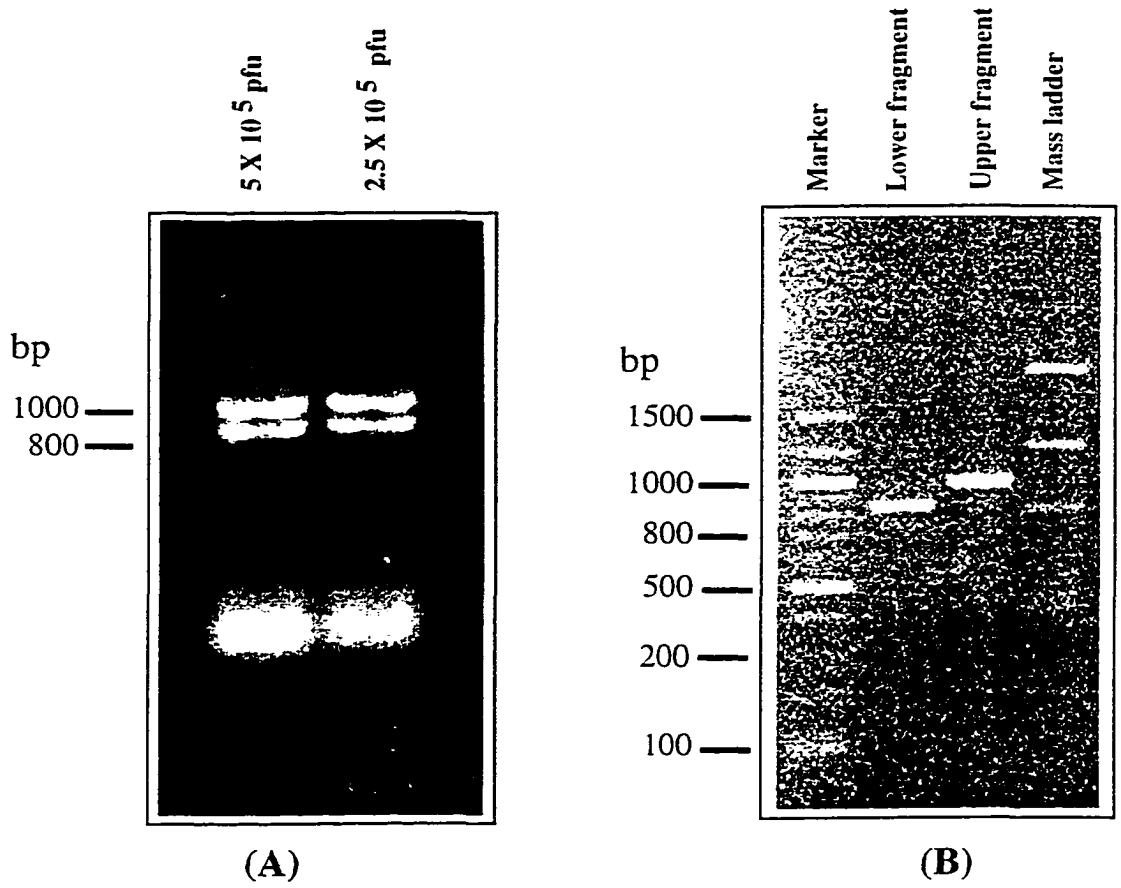

Fig. 22 Agarose gel electrophoresis of PCR-amplified product from spruce cDNA library using degenerate primers corresponding to ATP-binding site of different KLPs and calmodulin-binding sdomain (CBD) of KCBPs from dicots. 5 x 10^5 pfu were used for PCR reaction. (B) Agarose gel electrophoresis of purified PCR-product. Size markers are shown to left in bp.

and sequenced (Fig 22). Analysis of the deduced amino acid sequence of both clones using Blastp search showed that the sequence of the small fragment (900 bp) is highly similar to KCBP sequence from angiosperms (75 and 80.5% similarity to the KCBPs from maize and potato respectively). This PCR-amplified product was used as a probe to screen the cDNA library. Nine positive clones were obtained after three rounds of screening. DNA from these clones was digested with the cloning enzyme (*EcoR*1) and they fall into three groups with different inset lengths. Inserts from the longest clone (2.4 kb) were subcloned into pBluescript for sequencing.

Sequence analysis and domain organization of PaKCBP

The nucleotide and deduced amino acid sequence of PaKCBP was shown in Fig (23). Analysis of PaKCBP sequence using Blastp and comparing it with the KCBPs from angiosperms revealed that the isolated cDNA (2220 bp) encodes for amino acid residues that are similar to KCBPs from angiosperms with 64% similarity to the AtKCBP along the available sequence. Secondary structure, probability of coiled-coil formation and domain organization based on the primary sequence are shown in Fig (24). KCBPs from angiosperms have the three characteristic domains. In addition KCBP has unique domains (CBD, MyTH4 and talin-like region). PaKCBP has the same structural features. The CBD, amino acid 685-707, is located at the C-terminus region with percent identity of 60.9, 65.2, 78.3, and 78.3 to CBD of ZmKCBP, AtKCBP, NtKCBP, and StKCBP, respectively. The amino acid sequence of PaKCBP (352-684) showed about 75-80.5% sequence identity to the motor domains of KCBPs from angiosperms. On the other hand, the percent of identity of PaKCBP motor domain to the motor domain of other C-terminal KLPs ranged between 31-42 indicating that PaKCBP is a distinct KLP and is closer to KCBPs more than to other C-

terminal KLPs. This was supported by phylogenetic analysis, where PaKCBP was grouped as a member of KCBP subgroup in the C-terminal subfamily. The PaKCBP motor domain contained the conserved ATP-binding consensus sequence as well as four highly conserved peptide motifs of all KLPs motor domains that are implicated in MT-binding (Yang *et al.*, 1989). Another domain that defines kinesin class specificity is the "neck" region, a ~45 amino acid residue segment that emerges from the catalytic core of the motor domain (Vale and R.J., 1997). C-terminal kinesins as a group share a short conserved sequence (ELKGNI) in their neck region (Saito *et al.*, 1997). In all KCBPs including PaKCBP, this sequence display a slight divergence and they have their conserved sequence (EDMKGLIR) indicating that they form a distinct group within C-terminal subfamily.

In the region outside the motor domain (1-348), PaKCBP did not show any significant sequence similarity to other KLPs and poor similarity to the KCBPs from angiosperms and kinesin C (29.9-34.7% to KCBPs from angiosperms and 15.1% to kinesin C). Secondary structure and analysis of the predicted amino acid sequence has revealed that the region from amino acid 70 to 350 has extremely high probability to form coiled-coil structure (Lupas *et al.*, 1991) (Fig 24A & B). The presence of the coiled-coil region implies that PaKCBP may form a dimer. This less conserved coiled-coil region spans slightly less than the motor domain as in KCBP from angiosperms and is different from the coiled-coil region of kinesin C from sea urchin where it spans about 70% of the protein. Surprisingly, although the coiled-coil region is not conserved even among KCBPs, a phylogenetic tree of KCBPs including coiled-coil sequences is identical to a tree obtained using motor domains where PaKCBP is shown as the origin of angiosperms KCBPs and separated from kinesin C (Discussed later in section V). Outside the coiled-coil region, PaKCBP showed sequence

```
GCG GAT AAC AAT TTC ACA CAG GAA ACA GCT ATG ACC ATG ATT  42
 A   D   N   N   F   T   Q   E   T   A   M   T   M   I  14
ACG CCA AGC TCG AAA TTA ACC CTC ACT AAA GGG AAC AAA AGC  84
 T   P   S   S   K   L   T   L   T   K   G   N   K   S  28
TGG AGC TCC ACC GCG GTG GCG GCC GCT CTA GAA CTA GTG GAT 126
 W   S   S   T   A   V   A   A   A   L   E   L   V   D  42
CCC CCG GGC TGC AGG AAT TCG CGG CCG CTT GAA AAG CGT GTA 168
 P   P   G   C   R   N   S   R   P   L   E   K   R   V  56
CAA GAG ATG TCC AAA ATC ATA GAA GAA ACT CAA AGA AAG ACG 210
 Q   E   M   S   K   I   I   E   E   T   Q   R   K   T  70
GAT CAG CTT TCG GAA GAG CTT CAT GCA AGG GAA ATA AGG GAG 252
 D   Q   L   S   E   E   L   H   A   R   E   I   R   E  84
ACA GAA CTT GCA GAA GAA CTG GAA GGC CTG AAA GAC TCC TTG 294
 T   E   L   A   E   E   L   E   G   L   K   D   S   L  98
CAA GAA GAA CTG GAA GGC CTG AAA GAC TCC TTG CAA GCA GAG 336
 Q   E   E   L   E   G   L   K   D   S   L   Q   A   E 112
AGG CGT GCT TTA TCT GAA GTT GTT CAA GAT CGC GAC AAG TTC 378
 R   R   A   L   S   E   V   V   Q   D   R   D   K   F 126
CGT GCA TTG TTT GCT GAA AAA GAA TCT GCT TTT CAG ATG GCA 420
 R   A   L   F   A   E   K   E   S   A   Q   F   M   A 140
CTT TCA GAT AAG GGT TCT GCA GCA AGT CCG GCC AAT GAG CAC 462
 L   S   D   K   D   S   A   A   S   P   A   N   E   H 154
AAT GGA AAT TTA GAT TTG GAG AAC ACT CCT ACA AAA GCT TCC 504
 N   G   N   L   D   L   E   N   T   P   T   K   A   S 168
CTG GCG TCA TTA AGT AGA AGG GAT AGA GAT CTT CCA TTC ACA 546
 L   A   S   L   S   R   R   D   R   D   L   P   F   T 182
GAT AAA GGC AGA GTG TCA CAA AAT CAA AAC TTG AAT TCA CAG 588
 D   K   G   R   V   S   Q   N   Q   N   L   N   S   Q 196
GCA CAA ATT AAG GAA CTG AGG AAT GAA TTG AAG ACG CGG ACA 630
 A   Q   I   K   E   L   R   N   E   L   K   T   R   T 210
GAT GAT CTT CAT TCA GCA GAA GAA ATG TGC AAG AAA CTC TCC 672
 D   D   L   H   S   A   E   E   M   C   K   K   L   S 224
AAT GAA AAG CAA TTG CTT GAG CAG AAA GTT AGT CGC CTT GAG 710
 N   E   K   Q   L   L   E   Q   K   V   S   R   L   E 230
AAG AAG AAA ACA AAT GAG ACA CNG ACT TTG GAA AGG AAG TTT 756
 K   K   K   T   N   E   T   X   T   L   E   R   K   F 252
GAG CAA GAA CGT GAT GCG CTT AGA GTG CGA GTA GCT GAA TTG 798
 E   Q   E   R   D   A   L   R   V   R   V   A   E   L 266
GAG AAA AAG CTT ACT GAG AGG ACT CAA GAA TTG AGT GTT ACA 840
 E   K   K   L   T   E   R   T   Q   E   L   S   V   T 280
GAG TCT ACA TTA GCA GTT AGG ACT TCT GAA TTG GAT GCA GTT 882
 E   S   T   L   A   V   R   T   S   E   L   D   A   V 296
```


Fig. 23

```
CAA GGC AGC TTA AAG GAG CTG GAA GAG TTA CGA GAA ATG AAA  924
 Q   G   S   L   K   E   L   E   E   L   R   E   M   K  308
GAG GAC ATT GAT AGG AAG AAT GCA CAA ACA GCT TCA CTT TTG  966
 E   D   I   D   R   K   N   A   Q   T   A   S   L   L  322
AAG AAA CAA GCT GAA CAG TTA GCT GAG ATG GAA GTT CTT TAT 1008
 K   K   Q   A   E   Q   L   A   E   M   E   V   L   Y  336
AAG GAG GAG CAA GTC CTT AGA AAG CGA TAC TTC AAC ATG ATG 1050
 K   E   E   Q   V   L   R   K   R   Y   F   N   M   M  350
GAA GAT ATG AAA GGT AAG ATC AGA GTT TAT TGT CGC TGG CGA 1092
 E   D   M   K   G   K   I   R   V   Y   C   R   W   R  364
CCA CTT AGT GAG AAA GAG ACA TTT GAG AAA CAA AGG AGT GTT 1134
 P   L   S   E   K   E   T   F   E   K   Q   R   S   V  378
ATT ATC GCA CCA GAT GAA TTT ACA GTG GAG CAC CCC TGG AAG 1176
 I   I   A   P   D   E   F   T   V   E   H   P   W   K  392
GAT GAT AAG CCA AAG CAA CAT CAA TTT GAT CAT GTT TTT GAT 1218
 D   D   K   P   K   Q   H   Q   F   D   H   V   F   D  406
AGT AAT GCT ACC CAA GAC GAA GTT TTT GAG GAT ACA AGG TAT 1260
 S   N   A   T   Q   D   E   V   F   E   D   T   R   Y  420
CTG GTA CAG TCA GCA GTT GAT GGA TAT AAT GTT TGT ATA TTT 1302
 L   V   Q   S   A   V   D   G   Y   N   V   C   I   F  434
GCA TAT GGG CAA ACT GGC TCA GGC AAA ACA TTC ACT GTC TAT 1344
 A   Y   G   Q   T   G   S   G   K   T   F   T   V   Y  448
GGT TCA GAT AGA AAT CCA GGT CTA ACC CCA AGG GCT ATT GGG 1386
 G   S   D   R   N   P   G   L   T   P   R   A   I   G  462
GAG CTT TTT AAA ATT CTG AGC CGG GAC AGT AAC GAG TTC TCC 1428
 E   L   F   K   I   L   S   R   D   S   N   E   F   S  476
TTT CTG TTA AAG GTG TAT ATG GTG GAG TTA TAC CAG GAC TCA 1470
 F   L   L   K   V   Y   M   V   E   L   Y   Q   D   S  490
CTT GTA GAT TTG CTT CTG CCA AAG AAT GGA AAG CGA TTG AAA 1512
 L   V   D   L   L   L   P   K   N   G   K   R   L   K  504
CTT GAT ATT AAG AAA GAT GCA AAG GGA ATG GTT ATG GTG GAG 1554
 L   D   I   K   K   D   A   K   G   M   V   M   V   E  518
AAT GTT ACT CTT GTA ACT ATA TCT ACA TTT GAA GAG CTG GAA 1596
 N   V   T   L   V   T   I   S   T   F   E   E   L   E  532
GCT ATT GTT TGT AAA GGG ATA GAA AGG CGA CAC ACT TCT GGA 1638
 A   I   V   C   K   G   I   E   R   R   H   T   S   G  546
ACT CAG ATG AAT GCA GAA AGT TCA AGA TCA CAC TTA ATA CTT 1680
 T   Q   M   N   A   E   S   S   R   S   H   L   I   L  560
TCT ATA ATT ATA GAG AGC ACA AAT CTT CAA ACT CAG GTC CAA 1722
 S   I   I   I   E   S   T   N   L   Q   T   Q   V   Q  574
GTC AAG GGA AAG CTA AGC TTT GTC GAT CTT GCG GGA TCT GAG 1764
```


Fig. 23

```
 V   K   G   K   L   S   F   V   D   L   A   G   S   E   588
AGG GTG AAG AAA TCA GGA TCA ACA GGC AAT CAA TTG AAA GAG  1806
 R   V   K   K   S   G   S   T   G   N   Q   L   K   E   602
GCT CAA AGT ATC AAC CGG TCT CTT TCA GCC CTG GGT GAT GTT  1848
 A   Q   S   I   N   R   S   L   S   A   L   G   D   V   616
ATT AGT GCA CTG GCT TCT GAA GGG CAA CAT ATA CCC TAC AGA  1890
 I   S   A   L   A   S   E   G   Q   H   I   P   Y   R   630
AAT CAC AAG CTC ACG ATG CTC ATG AGT GAT TCA CTT GGT GGC  1932
 N   H   K   L   T   M   L   M   S   D   S   L   G   G   644
AAT GCC AAA ACC CTG ATG TTT GTT AAT ATA TCC CCA GCA GAA  1974
 N   A   K   T   L   M   F   V   N   I   S   P   A   E   658
TTT AAT TTG GAT GAG ACC CAT AAT TCC CTT TCA TAT GCT ACT  2016
 F   N   L   D   E   T   H   N   S   L   S   Y   A   T   672
CGA GTT CGC TCA ATT GTA AAT GAT GCA AGC AAA AAT GTG ACC  2058
 R   V   R   S   I   V   N   D   A   S   K   N   V   T   686
ACC AAG GAA GTT GCT AGG CTG AAG AGA ATG GTA GCT TAC TGG  2100
 T   K   E   V   A   R   L   K   R   M   V   A   Y   W   700
AAA GAG CAG GCA GGT AGA AAG GCA GAC GAA GAG GAA ATG GAA  2142
 K   E   Q   A   G   R   K   A   D   E   E   E   M   E   714
GAA ATC ACC GAG GAT CGA AAT ACC AGA GAC AAG AAC GAT GGA  2184
 E   I   T   E   D   R   N   T   R   D   K   N   D   G   728
CGC TCG TAG ACATGATTCTAAACTTGCAGAGGGAAA                 2220
 R   S   ♦                                              730
```

Fig. 23 **Nucleotide and deduced amino acid sequence of spruce (*Picea abies*) KCBP gene.** The predicted amino acid sequence is shown under the nucleotide sequence in bold. The stop codon is indicated with a diamond. The conserved regions in all kinesin-like proteins motor domain are shown in shadow format. The unique sequence (EDMKGKIRV) located in the "neck" region upstream of the motor domain that is highly conserved among the carboxy-terminal kinesins and identical among KCBPs (Saito *et al.*, 1997) is boxed. The calmodulin-binding region characteristic for KCBPs is underlined. Numbers at right correspond to nucleotides and deduced amino acids (in bold).

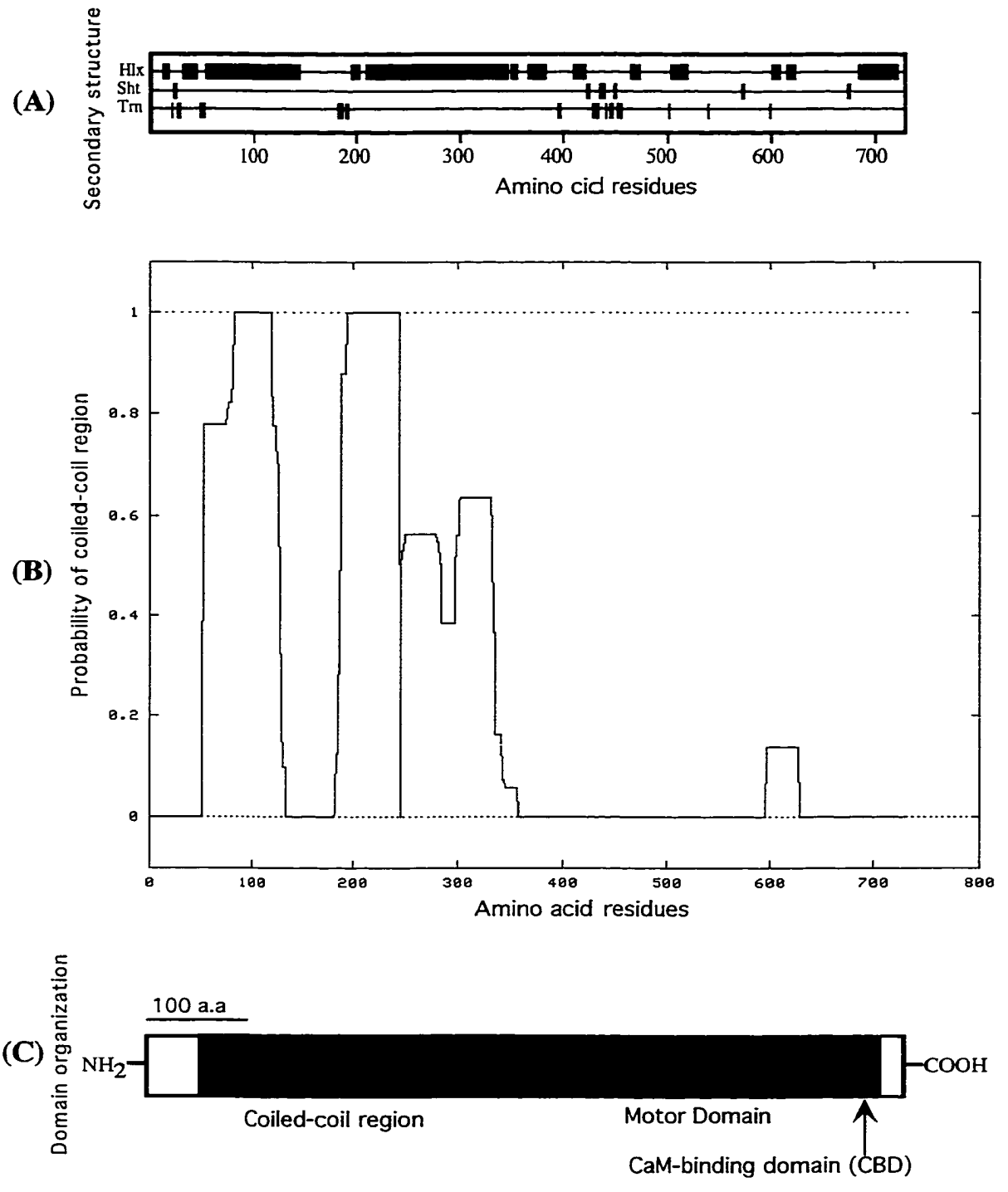

Fig. 24 **Predicted secondary structural features of spruce (*Picea abies*) KCBP (PaKCBP).** (A) The secondary structure of PaKCBP as predicted by Robson-Garnier and Chau-Fasman methods. Regions predicted to be α-helices (Hlx), β-sheets (Sht) or β-turns (Trn) are indicated by solid boxes. (B) Probability of formation alpha-helical coiled-coil is determined using the coiled-coil program (Lupus *et al.*, 1991). The *y*-axis indicates the probability of coiled-coil formation; the *x*-axis designates the amino acid position along the length of the polypeptide starting from the amino terminus. (C) Schematic diagram of predicted domains of PaKCBP. All figures are drawn to scale.

similarity to a talin-like region present in some myosins and characteristic for KCBPs. However, we do not have complete N-terminal sequence. Based on the conservation of other domains we predict that, mostly, the N-terminal region is conserved among all land plants and the evolution of KCBP proceeds the evolution of land plants.

PaKCBP transcript size is close to AtKCBP

To determine the size of the transcript and the expression of PaKCBP, RNA from three-week old spruce seedlings was probed with the two *EcoR*I fragments that correspond to CBD, motor domain and coiled-coil region of PaKCBP. A single transcript of about 4kb was found to hybridize with the cDNA (Fig 25). Hence, the isolated cDNA clone is partial. A single KCBP transcript of about 4 kb was detected in the RNA blot from *Arabidopsis* flowers, leaves, root, and suspension culture (Reddy *et al.*, 1996a). On the other hand, a single KCBP transcript of about 4.5 and 5 kb were obtained from RNA blots of tobacco and maize tissues respectively (Wang *et al.*, 1996; Abdel-Ghany and Reddy, 2000).

To determine the approximate copy number of PaKCBP, genomic DNA from spruce seedlings digested with different restriction enzymes (*Bgl*II, *EcoR*I, *Kpn*I, *and Xba*I) was probed with PaKCBP cDNA. Depending on the enzyme, three to four bands hybridized to PaKCBP clones Fig (26). From the restriction map of PaKCBP (Fig 26A), extra bands were obtained with all digestions. This is most likely due to the presence of introns with these restriction sites. So far, all studied KCBPs in different plants coded by a single gene and expressed in all tissues with high a level of expression in actively dividing cells.

The PaKCBP is a CaM-binding protein

CaM-binding domain of KCBPs from angiosperms were shown to be regulated by Ca^{2+}/CaM (Narasimhulu and Reddy, 1998; Abdel-Ghany and Reddy, 2000). To demonstrate

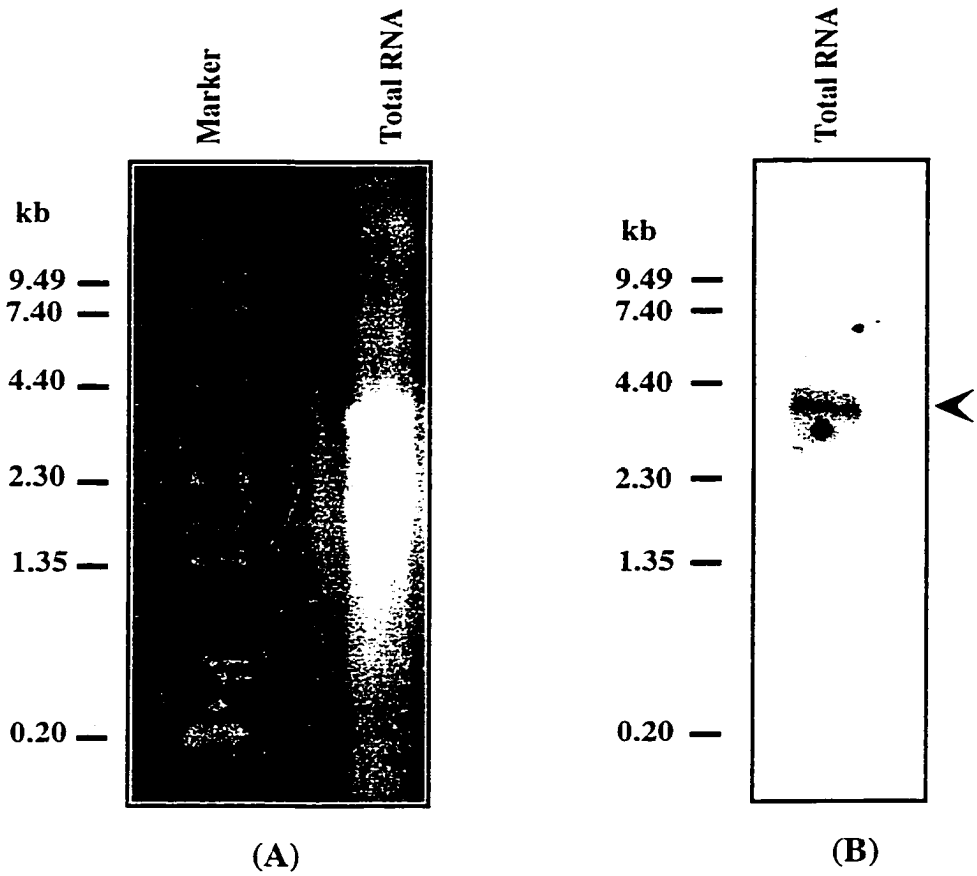

Fig. 25 **Northern blot analysis of spruce (*Picea abies*).** Total RNA was extracted from three-week old spruce seedlings and electrophoresed in 1% denaturing agarose gel and either stained (A) or blotted and probed with spruce 1.6 kb cDNA fragment (B). Arrow head indicates the size of the hybridized band. RNA size markers are shown at left in kb.

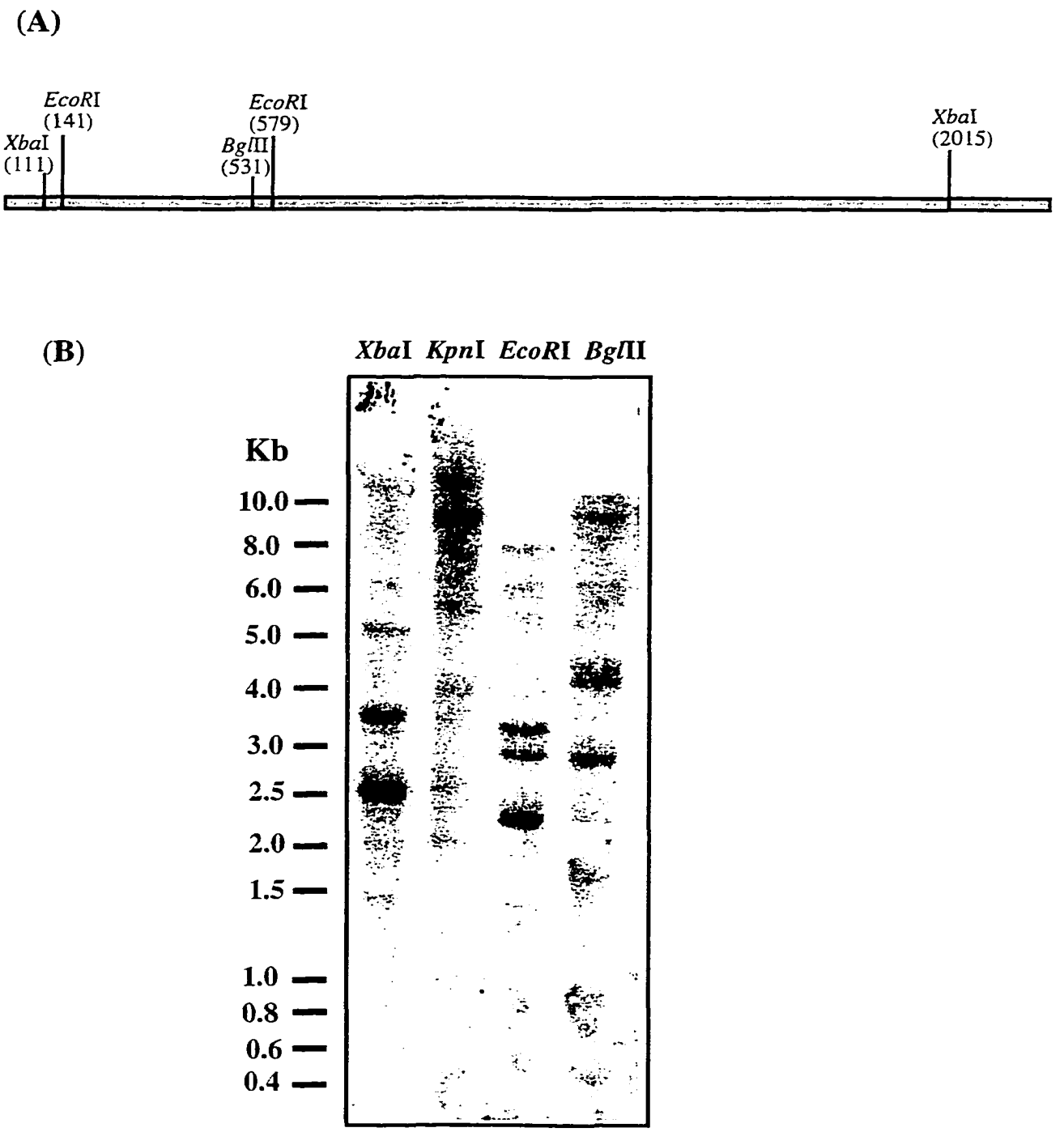

Fig. 26 **Restriction map and Southern blot analysis of spruce (*Picea abies*) genomic DNA.** (A) Restriction map of PaKCBP cDNA showing the position of the restriction enzymes used for digestion. (B) Southern blot analysis. Genomic DNA (10 μg) from three-weekold seedlings was digested with restriction endonucleases (*Xba*I, *Kpn*I, *Eco*RI, *Bgl*II), and probed with 1.6 kb cDNA fragment that encodes for motor domain and CBD. Size markers are shown at left in kb.

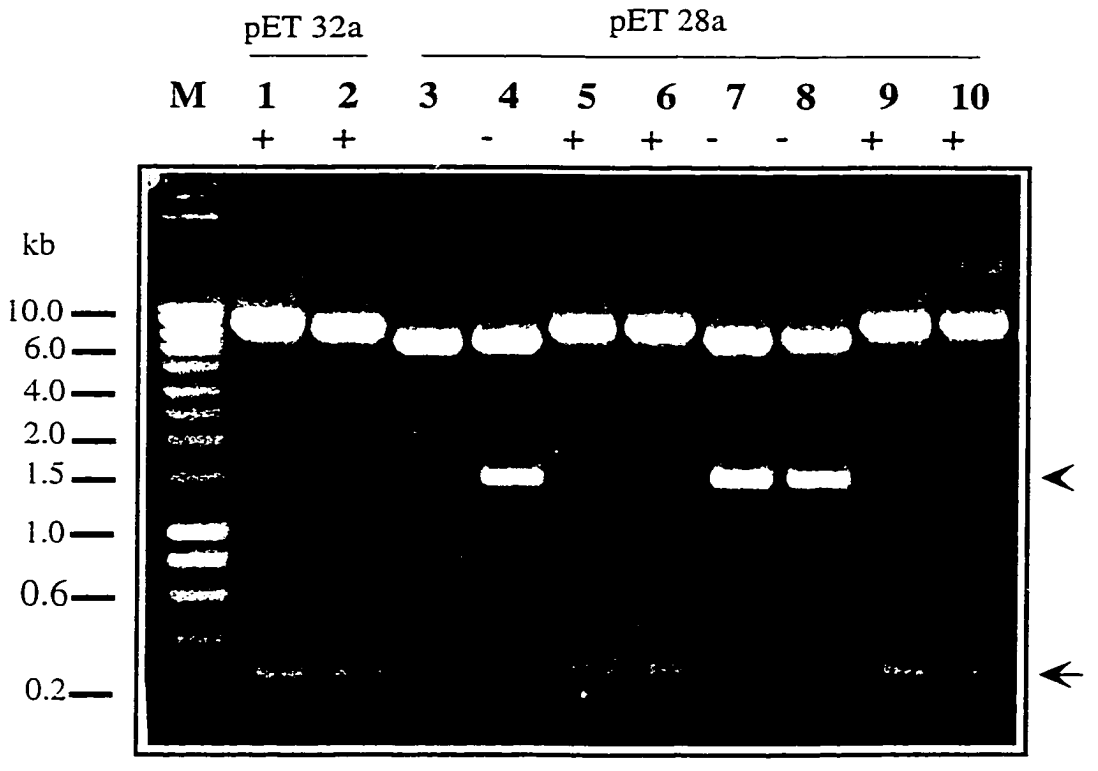

Fig. 27 **Confirmation of sense (+) and antisense (-) constructs of PaKCBP.** A cDNA fragment (1.6 kb) that encodes the motor domain and calmodulin-binding domain of PaKCBP was cloned into *EcoR*I site of pET 32a and pET 28a. Clones were digested with *Xho*I to relase 1450 bp fragment in antisense orientation (arrow head) and 250 bp fragment in the sense orientation (arrow). Clone number 3 is a nonrecombinant vector. Size markers are shown at left in kb.

Ca^{2+}/CaM-binding activities of PaKCBP, a 1.6 kb cDNA fragment that encodes the CBD and motor domains of PaKCBP was cloned into pET 28a and pET 32a expression vectors. Sense and antisense orientation of the clones was confirmed by restriction digestion with *Xho*I (Fig 27). Protein from soluble and pellet fractions of induced and uninduced cultures of both vectors were blotted and probed with affinity-purified KCBP-Ab that was raised against the CBD of AtKCBP (Bowser and Reddy, 1997). Specific bands were observed in both fractions of the induced cultures with a high proportion in the pellet fraction (Fig 28). The size of the fusion protein corresponded to the predicted size of the protein from gene fusion. A soluble protein fraction from pET 28a was bound to CaM-Sepharose column in the presence of 2 mM $CaCl_2$ and eluted in the presence of 2 mM EGTA. The eluted fractions were blotted and detected with 35S CaM as well as KCBP-Ab (Fig 29). The eluted fractions bound to ^{35}S CaM in the presence of Ca^{2+} but not in the presence of EGTA (Fig 29C&D). These results indicate that PaKCBP is a CBD and that the CaM binding is a Ca^{2+}-dependent.

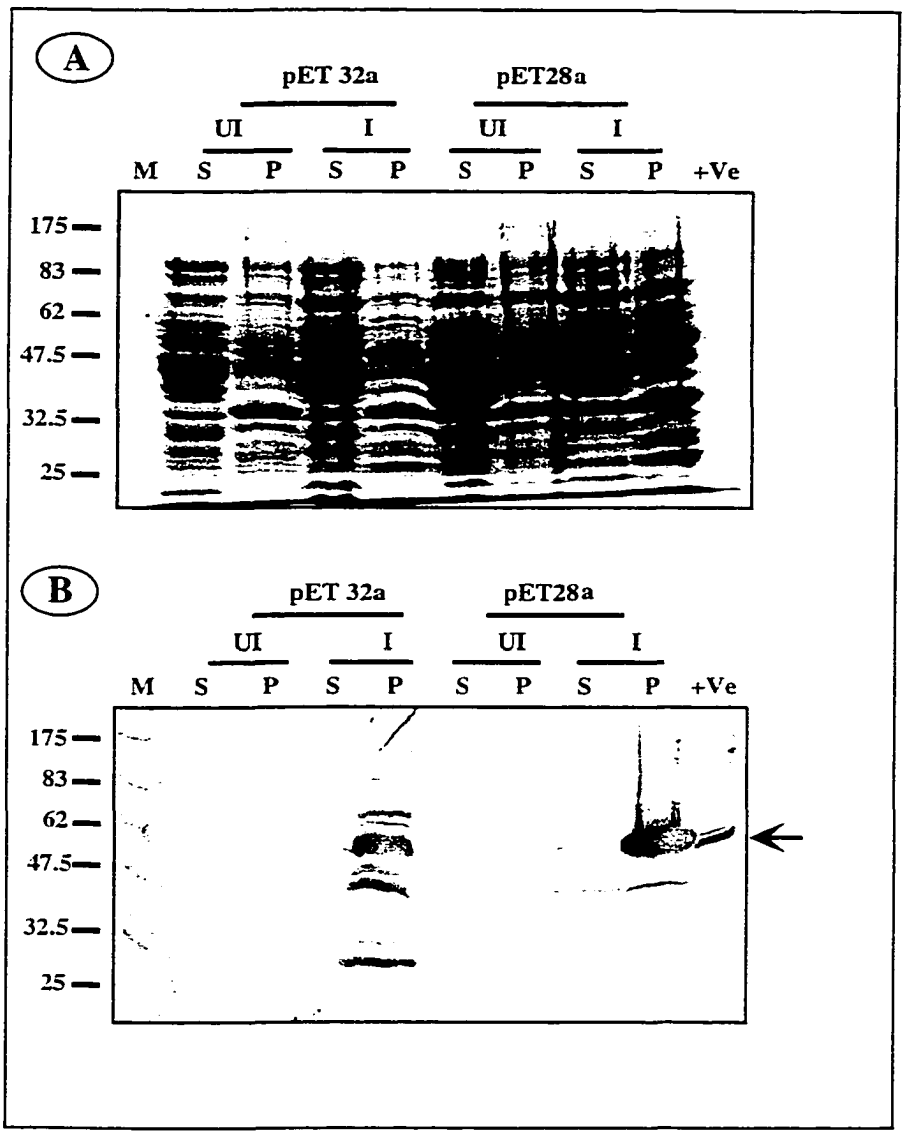

Fig. 28 **Expression of PaKCBP in *E.coli*.** Partial *Pa*KCBP cDNA (1600 bp) containing the coding region of the motor and calmodulin-binding domains was cloned into expression vectors (pET 28a and pET 32a) which transformed into BL21 (DE3) *E.coli*. Fusion protein was expressed as described previously (Reddy *et al.*, 1996b). Soluble (S) and pellet (P) fractions from induced (I) and uninduced (UI) cultures were separated by SDS-PAGE. Proteins were eitherstained with Coomassie blue (A) or blotted and detected with affinity-purified KCBP-Ab (B). The C-terminal region of *Arabidopsis* KCBP was used as a positive control (+ve). Arrow indicates the fusion protein. Molecular mass markers are shown at left in kDa.

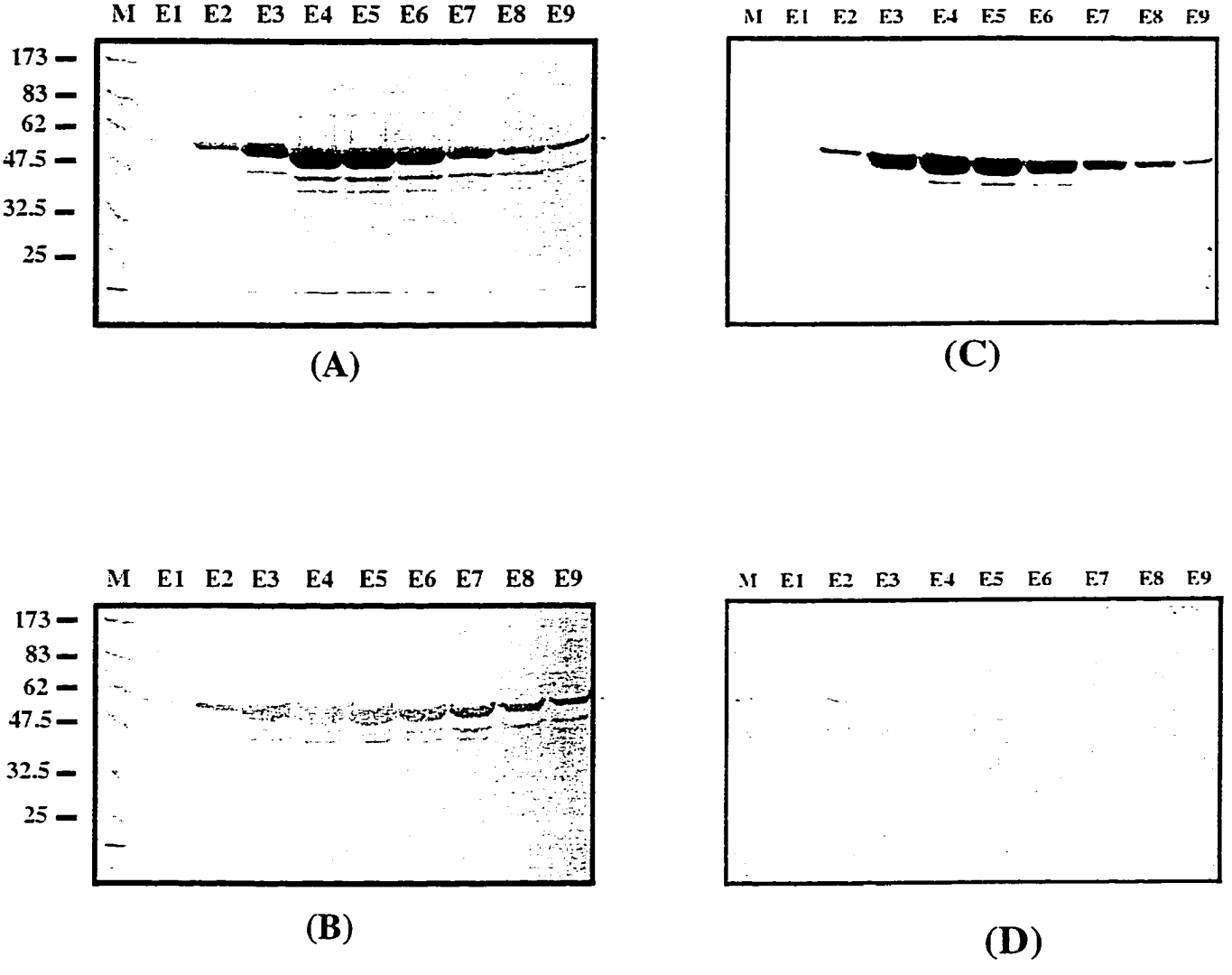

Fig. 29 **Purification of recombinant PaKCBP by calmodulin-Sepharose column.** Soluble protein from induced culture of pET 28a was adjusted to 2 mM $CaCl_2$ and loaded onto CaM-Sepharose column. Column was washed with several volumes of binding buffer (see methods section) and the bound protein was eluted by replacing the $CaCl_2$ with 2 mM EGTA in binding buffer. Eluted fractions (E1-E9) were electrophoresed, stained with Coomassie blue (A), trasferred onto nitrocellulose membranes, and probed with KCBP-Ab (B), or with ^{35}S-labelled calmodulin in the presence of 1 mM $CaCl_2$ (C), or in the presence of 2 mM EGTA (D). Molecular mass markers are shown at left in kDa.

III. Cloning and characterization of KCBP from *Stichococcus bacillaris*, a member of Charaphycean alga

Part of this work is included in a paper "Molecular evolution of a Ca^{2+}/CaM-regulated MT motor protein from phylogenetically *diverged* eukaryotes". Salah E. Abdel-Ghany, Paul Kugrens, and A.S.N. Reddy. Molecular Biology and Evolution. (In preparation)

KCBP homologues have been cloned and characterized from gymnosperms and angiosperms and found to be highly conserved. This result prompted us to search for KCBP homolog in a representative member of the land plants ancestor group, *Stichococcus bacillaries*.

Taxonomic position and evolutionary features of *Stichococcus*

Stichococcus is a unicellular charaphyte, but short filaments consisting of a few cells may sometimes be observed (Fig 30). This organism is commonly identified in collections made from terrestrial habitats and air (Prescott, 1951), inhabiting limestone walls or growing on bark or wood (Graham *et al.*, 1981), rooftops (Brook, 1968), or rock surfaces (Allen, 1971) and may occur as a phycobiont in lichens (Tschermak-Woess, 1988). *Stichococcus* is one of three genera of Order Klebsormidiales, Class Charaphyceae (Lee, 1999). Based on ultrastructural survies of cytokinesis, zoospores, meiospores, and gametes, the members of this order are regarded as more primitive than other the three orders of Charaphyceae, the Zygnematales, the Coleochaetales, and the Charales (Graham, 1993). Reproduction in the order occurs primarily asexually by filaments fragmentation into pieces, each developing into a new filament. Sexuality has not been found in the members of the group. Unlike other charaphytes, cell division in the Klebsormidiales occurs through formation of a cleavage furrow, but apparently neither a phragmoplast nor a cell plate is

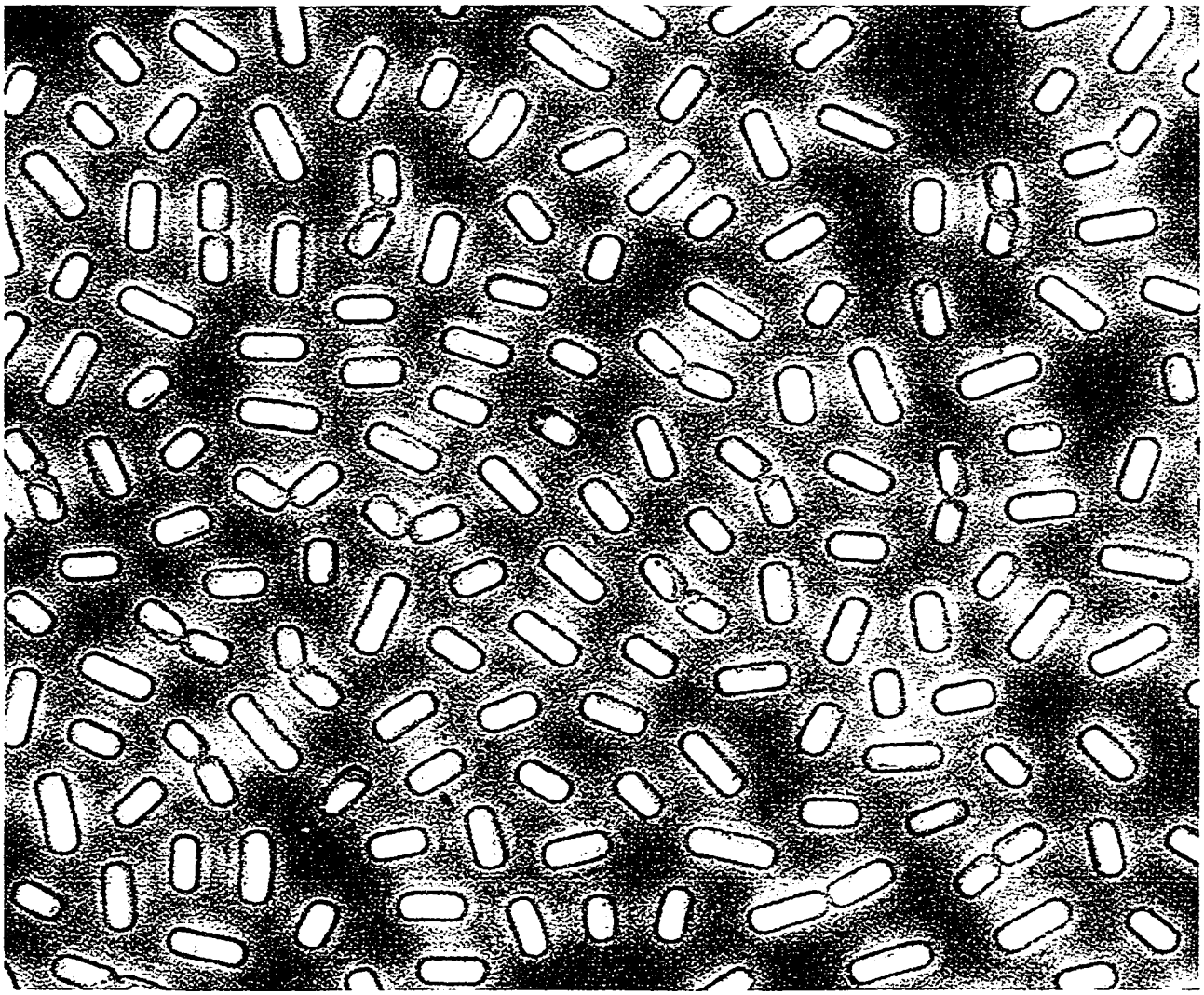

Fig. 30 Light microscopic picture of *Stichococcus*. The organism can be unicellular or the cylinderical cells jointed to form short or, less commonly, long unbranched filaments. Cells have partial chloroplasts. Reproduction is a sexual since sexuality has not been found in this organism. (Adopted from Canter-Lund and Lund, 1995).

formed. Still in many ways cytokinesis is similar to that in the zygnematales and for this reason a close relationship between the two orders has been suggested. Members of this order are also characterized by biflagellate zoospores that exhibit multilayered structures (MLSs) associated with their flagella, they produce the enzyme glycolate oxidase (Frederick *et al.*, 1973), they produce class I aldolase (Jacobshagen and Schnarrenberger, 1990), and they have open and persistent spindle during cytokinesis, (deJesus, 1989). All these characters are regarded as markers for relationship to land plants and also support the charaphyte origin of land plants.

Cloning of KCBP homolog from *Stichococcus bacillaries* (SbKCBP)

Two degenerate primers corresponding to conserved regions in the ATP-binding site of KLPs and CaM-binding domain of KCBPs were used to amplify KCBP motor domain and CBD from *Stichococcus* genomic DNA. A PCR amplified product of about 2kb was purified, cloned and sequenced. The sequence of the amplified product showed significant sequence similarity to KCBPs from angiosperms and gymnosperms, and it has all the conserved motifs characteristic for KCBP motor domain and CBD. To get the full-length KCBP, a genomic library prepared from *Stichococcus* in Lambda Dash II cloning vector was screened with the PCR amplified product. Seven putative positive clones, confirmed by Southern blots, were digested with restriction enzymes (*EcoR* I and *Bgl* II). To find out the clone that has the upstream sequence of the motor domain, two Southern blots were prepared with the isolated clones and probed with a 250 bp PCR-amplified genomic fragment, either from the N-terminal region or from the C-terminal region of the motor domain. The clone (# 4/1) that has the longest insert hybridizing with the N-terminal probe, but not with the C-terminal probe was used for subcloning and sequencing.

Nucleotide sequence of SbKCBP

The nucleotide sequence of StKCBP gene and the predicted amino acids are shown in Fig (31). Splice site predictions were made using the NetPlantGene program and by comparison of the deduced amino acid sequence of SbKCBP with its homolog from land plants. This analogy revealed the presence of twenty-eight exons and twenty-seven introns, compared to 20 exons and 19 introns in the corresponding region of its homolog from maize and 19 exons and 18 introns in its homolog from *Arabidopsis*. The higher number of exons and introns in StKCBP was compensated by a fewer number of nucleotides per exons and introns (Table 6), where the longest exon is 237 nt compared to 567 nt in AtKCBP and the longest intron is 225 nt compared to 949 nt in ZmKCBP. SbKCBP exons size are ranged between 29 nt to 237 nt and the introns size are ranged from 45 nt and 225 nt.

Unlike exons and introns of KCBP in flowering plants where all introns are rich in A and T nucleotides (most have 60% AT or more with the higher percent of 76 in AtKCBP introns and 68 in AtKCBP exons), the SbKCBP exons and introns are rich in G and C nucleotides. Twenty-one of twenty-eight exons contains less than 40% AT with the lowest percent of 29.3 (exon 21). Although the SbKCBP introns have low AT content, the AT content of introns is slightly higher than the exons with the lowest percent of 32 (intron 16) and the highest percent of 54.8 (intron 14) (Table 6). All the predicted introns have the conserved GU and AG dinucleotides at their 5' and 3' ends, respectively, thereby conforming to the consensus GU-AG rule for 5' and 3' splice sites (White *et al.*, 1992; Brown *et al.*, 1996).

```
ACAGGATGTGATCCCCACATCGACTGGTCAAGACTGGGGTCAGACAAGCTCAGG     54
CGCGCGCCGTCAAAAATGTTTAGGGNAGTGCAGAAGTACATGGGCATCGACGGA    108
TGGGGGCGGCGAGCAGCTGCCAGATGCCATGCTCGTGGAGGTGGCCGCGAAGCT    153
                                          E  V  A  A  K  L      6
CATGCATCAGGCCATCAAGCGGCCAGAGCTGCGGGATGAGCTGTACATGCAGgt    207
  M  H  Q  A  I  K  R  P  E  L  R  D  E  L  Y  M  Q         23
gatcgcctgactgcatgcattccacttttgagcagctgactgatgttgtggca     261
gcagaacctgcttcgtgtgagcgtctttgatcgactagcttcattgtcaatcgc    315
ggCTGCTGAAGCAGACGCGCGGCAGCACAGCGGGCCTACAGACAGTGCGCGCAT    369
   L  L  K  Q  T  R  G  S  T  A  G  L  Q  T  V  R  A      40
GGCAGCTGTTCTATTTGCTGGCGTGCCTTGCACCGCCGGGAAGGGCGTTCGTGG    423
W  Q  L  F  Y  L  L  A  C  L  A  P  P  G  R  A  F  V      58
CCCTGGTGTGCGAGTATGTGCACTCAGCGGGGGCAACAGGGGCAATGGGCGCCC    477
A  L  V  C  E  Y  V  H  S  A  G  A  T   G  A  M  G  A      78
CTGGCGAGGCGCGCGACTGGGCCGCCAAGACCTGGGCTGCGCTGAAGCGCTCAA    531
P  G  E  A  R  D  W  A  A  K  T  W  A  A  L  K  R  S      94
CAAAGTCTGGGCCGCGGCGCCAGgtgcgcagcgtggcaagcacagctgtgcagc    585
T  K  S  G  P  R  R  Q                                    102
gacaaccatctgccaaagtccattgtagctgtgcatgcttgctgcaagccatgg     639
cctggctgctggaccgccatgagacattgccactgtaacaccgtcacccattga    693
tcgtgcagCAACCCACAGCAGAGGAGATCGAGGCGCAGCTGAGCGGGCGGGCGC    747
         Q  P  T  A  E  E  I  E  A  Q  L  S  G  R  A      117
TGACAGCCGTGGTCTTCTTCCTGGACGAGACGTTCGAGGAGATTGCCTGGGACA    801
L  T  A  V  V  F  F  L  D  E  T  F  E  E  I  A  W  D      135
TGTCCACCACTGTGGTGGACGCCAACATGCAGCTGGCAGGCCTCATCAAGCTCA    855
M  S  T  T  V  V  D  A  N   M  Q  L  A  G  L  I  K  L    153
CCAACTACGAGACCTTCACCCTATTCGAATCCCGCAAGgtgagcgacgaagcca    909
T  N  Y  E  T  F  T  L  F  E  S  R   K                   166
gaccgtaaagctgtgaagcggtacacaaatcatcagacatcgctctgctgtgct     963
gccttagatacgctggcagtcgcgctgtgcagGTGCCGGGCAAGGGCGAGGACG   1017
                                       V  P  G  K  G  E  D   173
GGCAGCCGGCAGGGCTTGTGGAGGAGACAGTCCTGCTGGACGACCACAGgtgcc   1071
G  Q  P  A  G  L  V  E  E  T  V  L  L  D  D  H  R         190
atcagacgtagccatccctggctcaaggactcgcacatgctagctacacatgag   1125
ttgacacgtccattctcacgacgttaacgcttagcagtggccgctgaccaggag   1179
acatgcgtgcagGTACATTGCAGATGTGTTGGCAGAGGGCCGGGTGGCACGGGA   1233
               Y  I  A  D  V  L  A  E  G  R  V  A  R  E    204
GGCGGCTGGCGGCGATGCGGCCCGGCTGCTGTTCAAGAAGCGCATGTTCCGCGA   1287
  A  A  G  G  D  A  A  R  L  L  F  K  K  R  M  F  R  E    222
GACGGACGAGGCCATCAGCGAGCCCATCTTCATCAGCCTATCCTTCGTGCAGGC   1341
  T  D  E  A  I  S  E  P  I  F  I  S  L  S  F  V  Q  A    240
GCAGCACGACTACCTGGAGgtacatcctggtgcaactcgcacacatgctgcatc   1395
Q  H  D  Y  L  E                                          246
gcgcccatgtaaaagtctttgtgaacttcagctcatacaatgacacaccgtgga    1449
ctgtatgtactggcactgtagGGCAACTATCCGGTAGTCATGGAGGATGCTGCG   1503
                       G  N  Y  P  V  V  M  E  D  A  A     257
CAGATGGCGGCANTGCAGATCCACGCAGAGTTTGGGTCAACACTGCTGAACAAT   1557
 Q  M  A  A  X  Q  I  H  A  E  F  G  S  T  L  L  N  N     275
```


Fig. 31

```
GCAGAAGCAATGGAGGGTGCCATTGAGCGTTTTGTCACGAAGCAGgtgatgaag  1611
 A  E  A  M  E  G  A  I  E  R  F  V  T  K  Q             290
tgtggccggtanacggaaggctgcatgccggtgcanatgcttctagtgancagc  1665
gacacctgtcaaacnaatgtaccatgacactttgcatgcagGTGTTGATGTCCC  1719
                                          V  L  M  S     294
GGCCGAGAGAGGAATGGGTGCACAACATTGAGTCGCGCTATAAGGCACTAGAGA  1773
R  P  R  E  E  W  V  H  N  I  E  S  R  Y  K  A  L  E    312
ACTTCACACAGGAGGATGCTCGCCTTCAGTTCCTGCGCATTCTGCGTTCCCTGC  1827
N  F  T  Q  E  D  A  R  L  Q  F  L  R  I  L  R  S  L    330
CCTACGgtgtgcatgtacttgtgccggccaatngcatctggaacatnatacatg  1881
P  Y                                                     332
ctggaagttacccactgacatggcnaactatgctcaagtgcaagtgtacacttt  1935
cgcagGCAACTCTACATTCTTCTTCGTGAGGCGGATCGAGGACCCCATTGCACT  1989
      G  N  S  T  F  F  F  V  R  R  I  E  D  P  I  A  L   349
GCTGCCCAACAAGCTGATCCTGGGCATCAACAAGCGgtgcgcatgcctgcagag  2043
  L  P  N  K  L  I  L  G  I  N  K  R                    361
ggtgaacactggcagacgcagcagaagcaatcgtttctcgaaatagtgctctgc  2097
cggctgaaagtgcgtgcagcagtcagcaggtgtcattgtcatacagGGGCGTGC  2151
                                                G  V     363
ACTTCTTCCGGCCGGTGCCCAAAGAGTACCTGCACTCGGCGGAGCTGCGCGACA  2205
H  F  F  R  P  V  P  K  E  Y  L  H  S  A  E  L  R  D    381
TCATGCAGTTCGGTTCCAGCTCCTCTGCGGTCTTCTTCAAGATGCGCGTGGCTG  2259
I  M  Q  F  G  S  S  S  S  A  V  F  F  K  M  R  V  A    399
GCGTGCTGCACGTCTTCCAGTTCGACACACGCCAGgtgctgcaccaggttcaga  2313
G  V  L  H  V  F  Q  F  D  T  R  Q                      411
tgattggttactattaatgatagcggccccatgctgtctagcgttgatgacgtt  2367
tcatagcaaacagcacactgacaggatggccgcctgtgcagGGCGAGGACATCT  2421
                                          G  E  D  I     415
GCATGGCGCTGCAGACGCACATCAACGATATCATGATGAAGCGGCTGACGAAGG  2475
C  M  A  L  Q  T  H  I  N  D  I  M  M  K  R  L  T  K    433
CCAAGGCCGCAATGGTGGCCGATGGCGGCGCCGGTGCAACAGCGTCGCAGGGCG  2529
A  K  A  A  M  V  A  D  G  G  A  G  A  T  A  S  Q  G    451
CCCTGGCAGCTGGCGGCGACGGCGGCTATGGCCCGCGCTATGAGgcgcatatca  2583
A  L  A  A  G  G  D  G  G  Y  G  P  R  Y  E             466
gcgagatgcaggccaaactggacactgccaacaacaagtaagcacgctgccacg  2637
gctgtgcatagtgcagaaacatatgaacctaccatcgcttgagaccagcggggc  2691
attgtgccaaaangccgcagatcgtgaatgtctcaagctcccagaagGTGCACC  2745
                                          V  H           468
TTCAAACTGTCGTTTGCCTCTGCAGGGTGGAGCAGCTGCAGGCATCGCTGACGG  2799
L  Q  T  V  V  C  L  C  R  V  E  Q  L  Q  A  S  L  T    486
CGCAGGCAGCTAAGCAGGCCAGCCTCGAGGAGCAGCTTGCAGAGGCCCAGGAGC  2853
A  Q  A  A  K  Q  A  S  L  E  E  Q  L  A  E  A  Q  E    504
GGCTTGCCATGGAGGACGGCAACAAGgtacatggtccctcgcattacttgacaa  2907
R  L  A  M  E  D  G  N  K                               513
tatctgctgttcagctctgcacacatgtcccaaatgtgtggcgctgtcaccccc  2961
caaacttccaccctgcggatgatggcgtcctgaataacagGCATCAGACCTGGA  3015
                                          A  S  D  L  D  518
CCGGCTGGATCACTTGGCCAGCGACTGCGAGGCCCTGACCAAGGAGCTGATGGC  3069
```


Fig. 31

```
  R  L  D  H  L  A  S  D  C  E  A  L  T  K  E  L  M  A   536
AGCACgtaatcgccttgcgaagagcgagaaggacaagcatcaggtgtggagaac  3123
  A                                                      537
tcagatcagtgtctatttcctgcagcgggttgagggcaatatatgcccattgcg  3177
tgtcacacgtcactctgttgcatgctgatgtgcgatatgagCGCTTTTCTGCTG  3231
                                        A  L  F  C  W   542
GAATTCTGGGTGGCGCATGGTGTGCAGGCGGTCCAGATTGCAGTCACAGCAGCA  3285
  N  S  G  W  R  M  V  C  R  R  S  R  L  Q  S  Q  Q  Q   560
GTTGCAGAGGCTACGGCGCCGCCGCCGCCACCGCCAGAGCGCACCCGCGAGCTG  3339
L  Q  R  L  R  R  R  R  R  H  R  Q  S  A  P  A  S  W    578
GAGGACAAGATCgtggcgctgaccgcagagctcaaggctgccaatgacaagtgc  3393
R  T  R  S                                              582
ggttgaaggccacaacacgatgttttcgccatgtgcccaggagatggtccctga  3447
tcacgcattggcaaccatgtgacggcagctgctgctgcatataaagacaaaccg  3501
atgtaggtatcagatgacatcatgcctgatgtgttcattgcgtggtcaacagGC  3555
                                                     L  583
TGCGGGCACAGGAAGTGGCGGTGCGCGATGCCAAGCAGGAGGCGGAGCTGCTCC  3609
   R  A  Q  E  V  A  V  R  D  A  K  Q  E  A  E  L  L    600
AGAGCAAGCTCACTCGGCAGGCCGCAGCACGCGAGGCAGAGGTGGCCAATGCCA  3663
Q  S  K  L  T  R  Q  A  A  A  R  E  A  E  V  A  N  A    618
CCGCTGAGgtacattcaagcgtttgcgcatgttatttgagttgcacaccgagaa  3717
T  A  E                                                 621
atgttgatcgttgaattgagattctgtggcatgtgttgacacggcatgcatntg  3771
atgtgtgggaagcaatgccactagGTGTCCGCCATGCGGTCGGAGCTGAGGGAC  3825
                        V  S  A  M  R  S  E  L  R  D    631
CAGCTGACGGCCAAGGACGGCCAGATCAACGGGCTGGTGCAGGAGCAGGCCCCC  3879
 Q  L  T  A  K  D  G  Q  I  N  G  L  V  Q  E  Q  A  P   649
ATGCAGTCGCAGCTCAGCGAGGCACAGTCCCAGCTGCAGCAGgtgtgctctcat  3933
M  Q  S  Q  L  S  E  A  Q  S  Q  L  Q  Q               663
aacgcatagcatagtatgctcaaaccacgctgtgctgcctgtctctgcattgaa  3987
gcgctccatcatctggcagctcagcatgtccattaagtgcacgctcccattgtg  4041
tctcaccggtaacatgtcacagtaaccaacacaccagcaattaatctggcgtac  4095
tgcagTTCAAGGGTGACATCACGGAGCTGGAGGAGCTGCGGGAGCTGAAGGAGG  4149
      F  K  G  D  I  T  E  L  E  E  L  R  E  L  K  E    679
ACgtgacgcggcagcagcaggcgcaggcgacgctcatccagtcacagGCACGCG  4203
D                                                   A  R  681
GTGTCGGCGGCAATATGCAACACATTGCCAAAGAGTCCgtaaaatgcaaatcgt  4257
 G  V  G  G  N  M  Q  H  I  A  K  E  S                  694
tgtcaagacgtgcaaatcccagactgtagcaaatgcagcgctgaacatggtatg  4311
gtacattgtcgcagGCCAAGCGGCTGGATGAGCTGGACCGCCTGTATCGCGACG  4365
            A  K  R  L  D  E  L  D  R  L  Y  R  D       707
AGGCGCTCGCCCGCAAGAAAACCCACAATGCCATGGAGGATCTCAAGgtgggct  4419
E  A  L  A  R  K  K  T  H  N  A  M  E  D  L  K          723
gacaccagtgcgctgcgacacccgcccctggatcaacagtgtcaccagcctgct  4473
tcttgatcagcacttgcaacttccttgcggcccgagattgtgggtctttaagtg  4527
ggataggagcaccaaggctgccaactgaacaggtagtgctgattgctgcagGGT  4581
                                                    G    724
AAGATCAGGGTGTTCGCACGCATTCGGCCAATCATGGAGTTCGAGAAGGCCAAG  4635
```


Fig. 31

```
 K  I  R  V  F  A  R  I  R  P  I  M  E  F  E  K  A  K    742
GGGCAGACAGCAGTGCTGAACGTGCCGGATGAGCTCACGATCACGCACCTGTGG  4689
 G  Q  T  A  V  L  N  V  P  D  E  L  T  I  T  H  L  W    760
AAGGGCGCGCCCCGCGAGTACAGCTTTGACACCGTCTTCTCACCCGAGGCCTCC  4743
 K  G  A  P  R  E  Y  S  F  D  T  V  F  S  P  E  A  S    778
CAGGAGCAGgtgaaccgatgcttttcgggcaataatagcagcagatgctgcgag  4797
 Q  E  Q                                                  781
agagggtcgtatgaaagtatatgcctgtggctgtcagctgtatgatacctgctt  4851
tctcggactgcagGTGTTTGAGGACACAAAGCACCTGGTGCGCTCAGCGGTGGA  4905
                V  F  E  D  T  K  H  L  V  R  S  A  V  D  795
CGGCTACAATGTGTGCATCTTCGCGTACGGCCAGACCGGCTCAGgtgcgcactc  4959
   G  Y  N  V  C  I  F  A  Y  G  Q  T  G  S              809
tgccatacaagcaaacacggcagcaaagtcatgcatacgttgtaattggcagcc  5013
gggctaagacagtgtgccaagaccatgctgaagagtgccggtgcgcgcacagGC  5067
                                                  G      810
AAGACACACACGATGGCGGGCAACCCCACGGCGCCTGGCCTGGCACCCCGCGGC  5121
  K  T  H  T  M  A  G  N  P  T  A  P  G  L  A  P  R  G  828
GTAGAGGAGCTCTTCCGAGgtaacgacagcaaagacgtgctggtcatgagcatg  5175
 V  E  E  L  F  R                                        834
ccacccaactgtgtgccaaatgcatgtgatgtaactgtgttgctgagattcact  5229
gcgcagTCCTGAATGCGGACGCACGGAAGGCCAGCTTCTCGGTGTCAGCCTACA  5283
      V  L  N  A  D  A  R  K  A  S  F  S  V  S  A  Y    850
TGCTGGAGCTGTACCAGGATGACCTGTGCGACCTGCTGCGGCCCGCTGACACCT  5337
M  L  E  L  Y  Q  D  D  L  C  D  L  L  R  P  A  D  T    868
CCCGCAAGGGTGGCGAGgtgcgcaaaatgtgttagcagctgaatgttgagtagc  5391
S  R  K  G  G  E                                        874
tttggcagattgtgccatcgctgaaggtacgttgacatctatgtgggggttcga  5445
ggtctaccagcgtggccattcgacatgcagatcggcacattacatatgagacgc  5499
ctgctgcgtgatattccagaaagcgcaaagccctttgcatgtgacctttgctgc  5553
agccggtcaagccgccaaagctggagATCAAGAAGGACGCCAAGGGCATGGTCA  5607
                           I  K  K  D  A  K  G  M  V    883
CGGTGCCGGGCGCGACGGTGGTGGAGGTCACCTCCGGCAAGCAGCTGTGGGCTG  5661
T  V  P  G  A  T  V  V  E  V  T  S  G  K  Q  L  W  A  V  902
TCATCGAGGCTGGGCAGAAGAACCGCCATGTGGCGGCCACCCAggtacctgcgc  5715
  I  E  A  G  Q  K  N  R  H  V  A  A  T  Q              916
ctgcatgtagcggcttgtcctctactgacccgtgctctggtagggcccggctct  5769
ctgtggaagctcctttgtagtggatcggcttaacatcccgatttgatatgttgc  5823
agATGAACCGAGAGTCGAGCCGCAGCCACCTGATCGTGTCGATCATCGTCACGT  5877
   M  N  R  E  S  S  R  S  H  L  I  V  S  I  I  V  T    933
CCACAAACCTGCAGACACAGAATGTCACCCGCGGCAAGCTCAGCTTCGTGGATC  5931
S  T  N  L  Q  T  Q  N  V  T  R  G  K  L  S  F  V  D    951
TTGCAGGCTCTGAGCGgtaggcatttgcatatagtttccacagaatgatatgtg  5985
L  A  G  S  E  R                                        957
tgcaagacccaacagcactaaggcgtgctagtgtcttcctcggcgctaatcaca  6039
gatgagtgttccagtgcaacaaagacagctctctgctgttgcggcagGGTGAAG  6093
                                                V  K    959
AAGAGTGGCAGTGCGGGGGAGCAGCTGAAGGAGGCGCAGGCCATCAACAAGTCG  6147
 K  S  G  S  A  G  E  Q  L  K  E  A  Q  A  I  N  K  S    977
```


Fig. 31

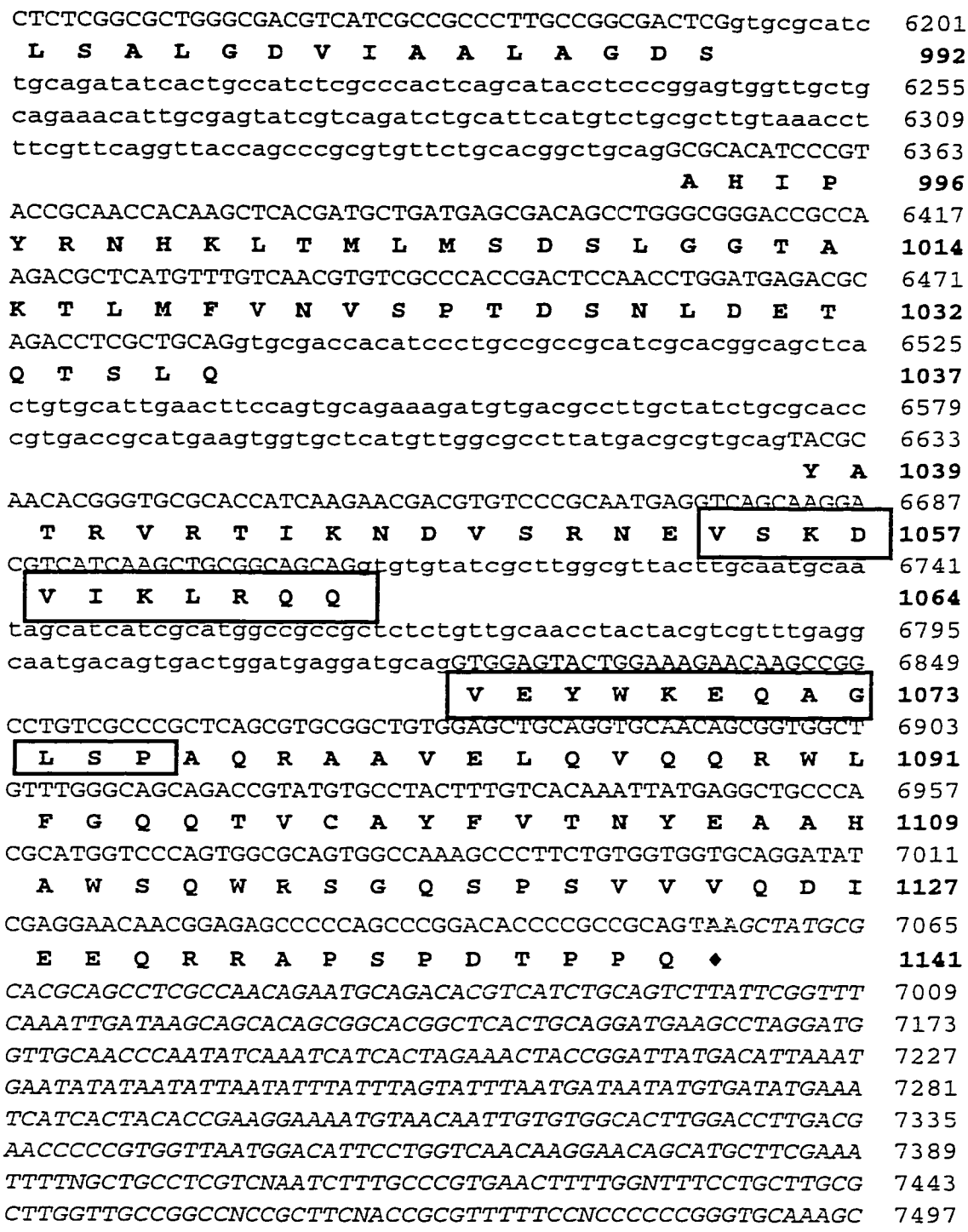

Fig. 31 Nucleotide and deduced amino acid sequence of *Stichococcus* KCBP gene (SbKCBP). Nucleotides sequence following the stop codon are shown in upper case letters and italic. Exons are shown in upper case and introns are presented in lower-case. The predicted amino acid sequence is shown under the nucleotide sequence in bold. The stop codon is indicated with a diamond. Numbers at right correspond to nucleotides and deduced amino acids (shown in bold). The three hyperconservative sequences characteristic to all kinesins like proteins as well as the amino acid residues (EDMKGKI) conserved in the neck region of KCBPs are underlined. The boxed region corresponds to the putative calmodulin-binding domain.

Table (6): Length and AT content of exons and introns and splice site junctions in *SbKCBP*.

No	Exons			Introns					
	Length (bp)	AT Ratio (%)	Coded Region by Exons	Length (bp)	AT Ratio (%)	Donor splice sites		Acceptor splice sites	
						Exon	Intron	Intron	Exon
1	ND	ND	Talin-like region	112	50	CAG	GTGATC	TCGCAG	CTG
2	237	31.2	Talin-like region	147	42.2	CAG	GTGCGC	GTGCAG	CAA
3	192	39.6	Talin-like region	102	44.1	AAG	GTGAGC	GTGCAG	GTG
4	71	29.6	MyTH4	125	44	CAG	GTGCCA	GTGCAG	GTA
5	169	35.5	MyTH4	110	51	GAG	GTACAT	CTGTAG	GGC
6	132	45.5	MyTH4	104	46.1	CAG	GTGATG	ATGCAG	GTG
7	127	44	MyTH4	107	50.5	ACG	GTGTGC	TCGCAG	GCA
8	85	44.7	MyTH4	118	45	GCG	GTGCGC	ATACAG	GGG
9	151	37.1	MyTH4	114	49.1	CAG	GTGCTG	GTGCAG	GGC
10	165	32.7	MyTH4	165	46.1	ATG	GTGGCC	CAGAAG	GTG
11	141	36.2	Coiled-coil	122	47.5	AAG	GTACAT	TAACAG	GCA
12	73	35.6	Coiled-coil	144	49.3	CAC	GTAATC	TATGAG	CGC
13	133	34.6	Coiled-coil	202	47	ATC	GTGGCG	CAACAG	GCT
14	118	30.5	Coiled-coil	124	54.8	GAG	GTACAT	CACTAG	GTG
15	126	31.7	Coiled-coil	179	49.5	CAG	GTGTGC	CTGCAG	TTC
16	51	39.2	Coiled-coil	45	32	GAC	GTGACG	TCACAG	GCA
17	45	42.2	Coiled-coil	84	54.7	TCC	GTAAAA	TCGCAG	GCC
18	29	37.9	Coiled-coil	166	42.7	AAG	GTGGGC	CTGCAG	GGT
19	174	38.5	Motor domain	112	50	CAG	GTGAAC	CTGCAG	GTG
20	85	40	Motor domain	116	44	CAG	GTGCGC	GCACAG	GCA
21	75	29.33	Motor domain	95	49.5	GAG	GTAACG	GCGCAG	TCC
22	119	35.3	Motor domain	225	47.5	GAG	GTGCGC	CTGGAG	ATC
23	126	33.3	Motor domain	120	44.2	CAG	GTACCT	TTGCAG	ATG
24	122	41.8	Motor domain	139	51.1	GCG	GTAGGC	CGGCAG	GGT
25	106	32.1	Motor domain	158	45.6	TCG	GTGCGC	CTGCAG	GCG
26	135	37.8	Motor domain	143	40.6	CAG	GTGCGA	GTGCAG	TAC
27	81	40.7	CBD	114	48	CAG	GTGTGT	ATGCAG	GTG
28	231	37.7	CBD	--	--	--	------	------	---

- Splice junctions were predicted with NetPlantGene (http://genome.cbs.dtu.dk/nph-webface) and by comparing the SbKCBP gene with the coding sequence of *Arabidopsis* KCBP gene.
- The consensus sequences at 5' and 3' splice junctions are AG/GTAAGT and TGY(A/C)AG/GT, respectively Goodall *et al.*, (1991). Nucleotides that are identical to consensus sequences are underlined.
- ND = not determined.

Functional domains in SbKCBP

Secondary structure, probability of coiled-coil formation and domain organization based on the primary amino acid sequence is shown in Fig (32). KCBPs, like most KLPs have three distinct structural and functional domains: a globular tail, a coiled coil region, and a motor domain. In addition, KCBPs from land plants have CBD at the C-terminal and the N-terminal region with MyTH4 and talin-like region present in myosin VIIa and X. Exons one, two, and three contained the available sequence of MyTH4 and exons 4 through 10 code for the talin-like region. Both MyTH4 and talin-like region are considered as tail domain of KCBP. The non-conserved coiled-coil region is encoded by exons 11 through 18, and the conserved motor domain is encoded by exons 19 through 25. The CBD characteristic for KCBPs and responsible for Ca^{2+}/CaM regulation is encoded by the last two exons. The CBD of SbKCBP is interrupted by an intron while in AtKCBP and ZmKCBP it is encoded by the last exon suggesting intron deletion through the evolution of KCBP. Motor domain of SbKCBP contained all of the conserved motifs that are implicated in ATP-and MT-binding. Another domain that defines kinesin class specificity is the "neck" region: (10-14 amino acid stretch) that connects the catalytic core with the coiled-coil domain (Sablin *et al.*, 1998). The neck sequence of SbKCBP (EDLKGKIR) is similar to that of KCBPs from land plants and to kinesin C from sea urchin and is slightly divergent from the neck of other C-terminal members (Saito *et al.*, 1997) suggesting the distinct phylogeny of KCBPs among C-terminals. The coiled coil region (aa 443-718) approximately spans the same length as in AtKCBP, ZmKCBP, and PaKCBP (about 20% of the protein) and is quite different from coiled-coil region of kinesin C where it cover 70% of the protein.

Fig. 32 **Predicted secondary structural features of *Stichococcus bacillaries* KCBP (SbKCBP).** (A) The secondary structure of ZmKCBP as predicted by Robson-Garnier and Chau-Fasman methods. Predicted α-helices (Hlx), β-sheets (Sht) or β-turns (Trn) are indicated by solid boxes. (B) Probability of formation alpha-helical coiled-coil (Lupus *et al.*, 1991). The y-axis indicates the probability of coiled-coil formation; the x-axis designates the amino acid position along the length of the polypeptide starting from the amino terminus. (C) Schematic diagram of predicted domains of SbKCBP. Color representation is as following: red = motor domain, blue = coiled-coil region, green = talin-like region, cyan = myosin-tail homology4 (MyTH4), black = calmodulin-binding domain. All figures are drawn to scale.

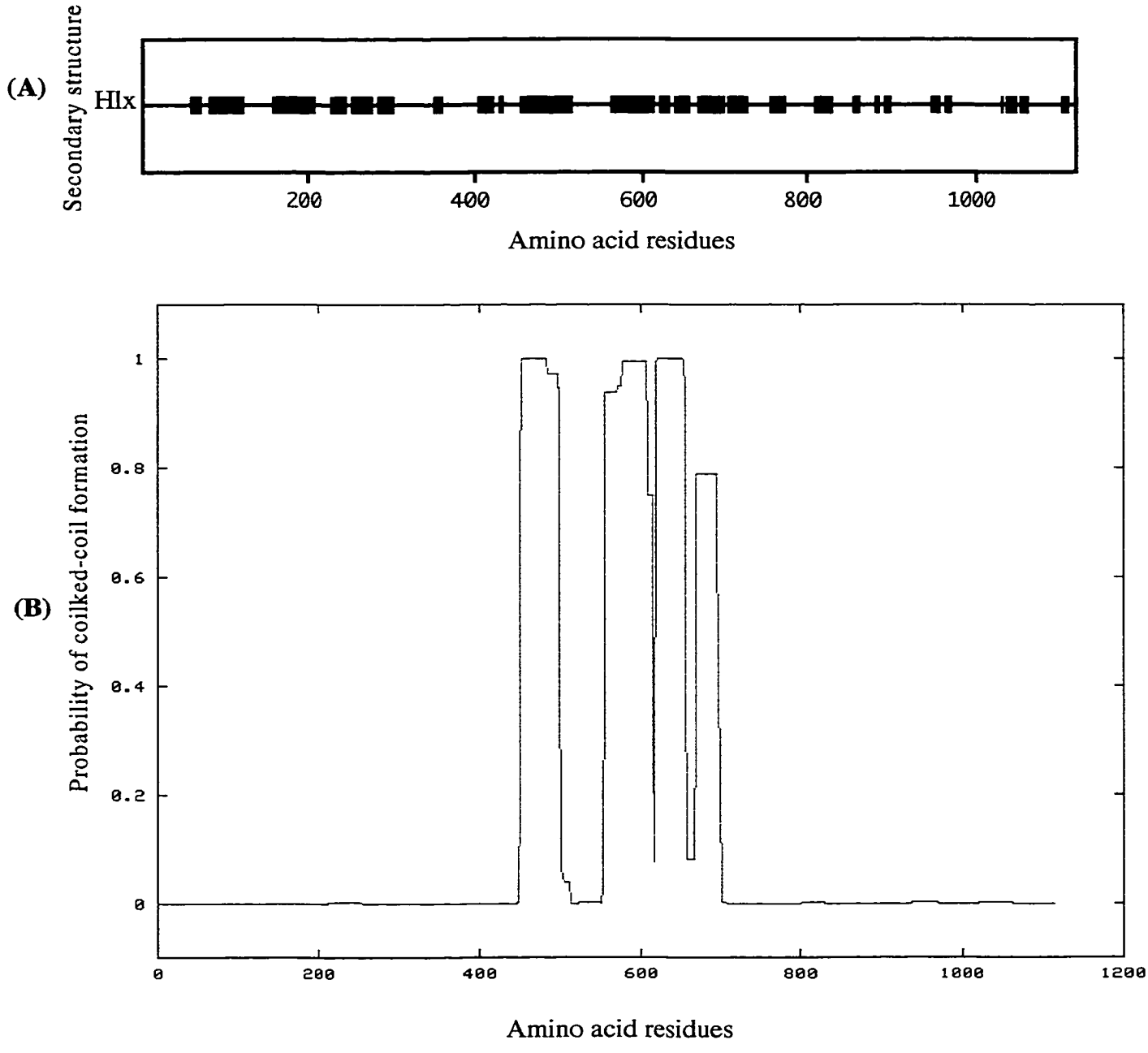

Southern blot analysis of StKCBP

To determine the approximate copy number of StKCBP, Southern blot analysis of *Stichococcus* genomic DNA was carried out (Fig 33) using a 2 kb PCR-amplified fragment corresponding to the motor domain and CBD of StKCBP as a probe. All the enzymes used in digestion have one hybridizing band with sizes ranging between 20 and 10 kb, indicating that StKCBP was coded by a single copy gene. Low-stringency washes did not yield any additional bands, suggesting that StKCBP does not cross-hybridize with other kinesin-like genes. Consistent with this, KCBP from other land plant species was found to be a single copy gene (Reddy *et al.*, 1996a; Wang *et al.*, 1996; Abdel-Ghany and Reddy, 2000).

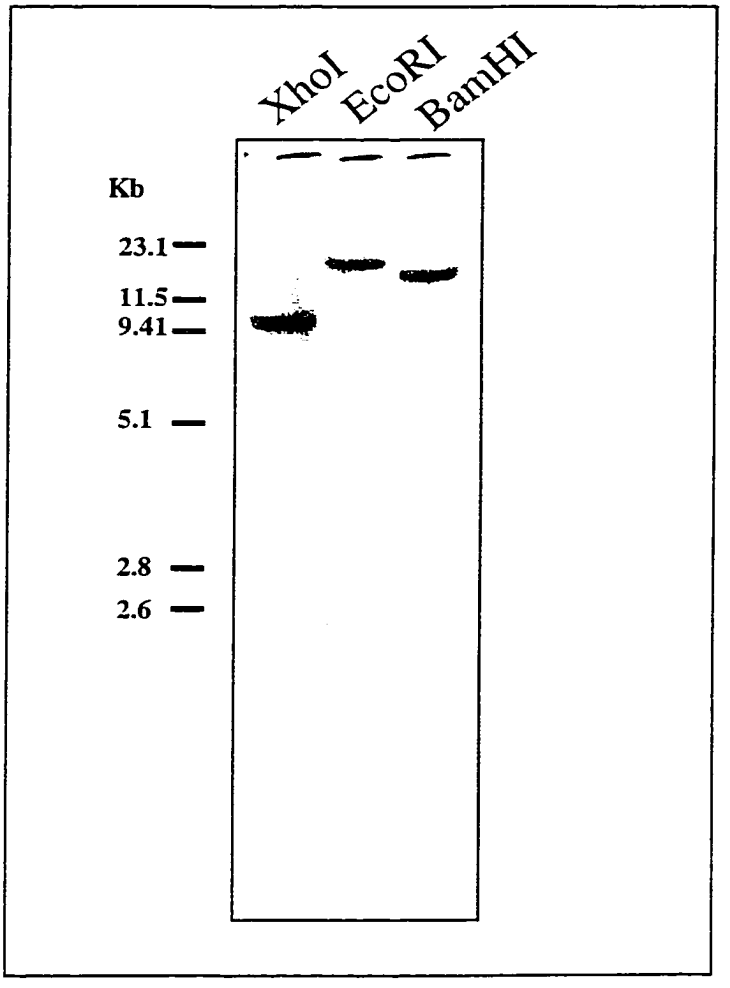

Fig. 33 **Southern blot analysis of *Stichococcus* genomic DNA**. Genomic DNA (10µg) was digested with restriction enzymes (*EcoR*I, *Hind*III, *Xho*I), separated in an 0.8% agarose gel, blotted and probed with 2 kb PCR-amplified genomic fragment that encodes motor and calmodulin-binding domains. Size markers are shown at left in kb.

IV. Cloning and characterization of KCBP from endosymbiont Glaucophyte, *Cyanophora paradoxa*

Part of this work has been published as "CpKLP1: A calmodulin-binding kinesin-like protein from *Cyanophora paradoxa* (Glaucophyta)". Salah E. Abdel-Ghany, Paul Kugrens, and A.S.N. Reddy. J. of Phycology, (**36**): 686-692 (2000).

Cyanophora paradoxa, an unusual protist belonging to the Division Glaucophyta, is a colorless freshwater microflagellate whose cells contain cyanobacterial endosymbionts called cyanelles (Fig 34) (Kugrens, 2001). Cyanelles have characteristics of both cyanobacteria and true chlorplasts and they have been considered to be an evolutionary intermediate between an endosymbiont and a chloroplast (Kies and Kremer, 1986). Usually, there are either one or two cyanelles per cell (Kies, 1979), although there may be up to eight cyanelles in some instances (Hall and Claus, 1963). The cyanelles have a concentric arrangement of unstacked thylakoids (Hall and Claus, 1963) (Fig 34), chlorophyll "a" and phycobilosomes. Cyanelles are surrounded by a cell wall remnant that contains peptidoglycan components (Aitken and Stanier, 1979). Another species of *Cyanophora*, *C. biloba*, has been characterized recently from Colorado (Kugrens *et al.*, 1999). There are some structural differences between the two species, both in the cyanelles and in the host cells (for review, see Kugrens *et al.*, (1999). For example the anterior fold of *C. paradoxa* is larger than that of *C. biloba*, both species have a ventral furrow, however, the ventral furrow of *C. paradoxa* is shallow compared to that of *C. biloba* which forms two lobes. Most of the time, the cyanelles of *C. biloba* have persistent deep constrictions that might represent incomplete cleavage furrow, while the constriction in cyanelles of *C. paradoxa* is a transient stage and observed during division (Meyer, 1997; Kugrens *et al.*, 1999). Sequence data from plastid

Fig. 34 **Scanning (A) and transmission electron micrograph (B&C) of *Cyanophora*.** (A) A cell showing anterior folds that are touching and covering the insertion points of the anterior and posterior flagella. (B) Higher magnification of a sectioned cyanelle showing phycobilisomes. (C) Frontal section through the dorsal portion of the cell showing two constricted cyanelles with dense cell bodies and concentric thylakoids (arrows directed to thylakoids), nucleus at the posterior end of the cyanelles, and the peripheral starch granules that located in the cortical cytoplasm. (AF) anterior flagellum, (PV) overlapping plate vesicles, (C) cyanelle, (S) starch granule, (N) nucleus, (NU), nucleolus. Scale bar = 1 μm. (Adopted from Kugrens *et al.*, 1999).

genes and retention of a bacterial cell wall by cyanelles support the hypothesis that glaucophytes represent the first branch of plastid evolution (Martin, 1998). Because of its unique position in evolution, *C. paradoxa* has been studied extensively, and considerable information regarding its structure, biochemistry, and molecular biology exists.

KCBP with its characteristic domains is believed to be a plant-specific KLP. To determine if KCBP is present in the most primitive photosynthetic eukaryotes, we used PCR and genomic library screening to clone and characterize a KCBP ortholog from *Cyanophora paradoxa*.

Isolation of a cDNA encoding a KLP from *C. paradoxa* (CpKLP1)

The kinesin superfamily is defined by a motor domain that contains blocks of highly conserved amino acids. To isolate kinesin-related gene sequences from *C. paradoxa*, degenerate primers corresponding to two regions of conserved amino acid sequence within the motor domain were synthesized (Fig 35). These sequences are highly conserved in most KLPs from distantly-related organisms. Approximately 500 bp fragment was amplified from *Cyanophora* cDNA library prepared in pBluescript vector (Fig 36). The amplified product was cloned into pBluescript vector and sequenced (Fig 37). The nucleotide sequence of the amplified fragment and the predicted amino acid sequence is shown in Fig (37). Analysis of the deduced amino acid sequence using the Blastp search showed a strong sequence similarity to the motor domains of KLPs with the highest sequence similarity to KCBPs. It also contains an ATP-binding site and two other motifs (SSRSH and VDLFAGTS) that are highly conserved in the motor domain of KLPs (Endow and Hatsumi, 1991; Reddy *et al.*, 1996a; Wang *et al.*, 1996; Rogers *et al.*, 1999) (Fig 37). Although there are stretches of amino acids that are highly conserved in all kinesin-like proteins, there are other amino acids

(A)

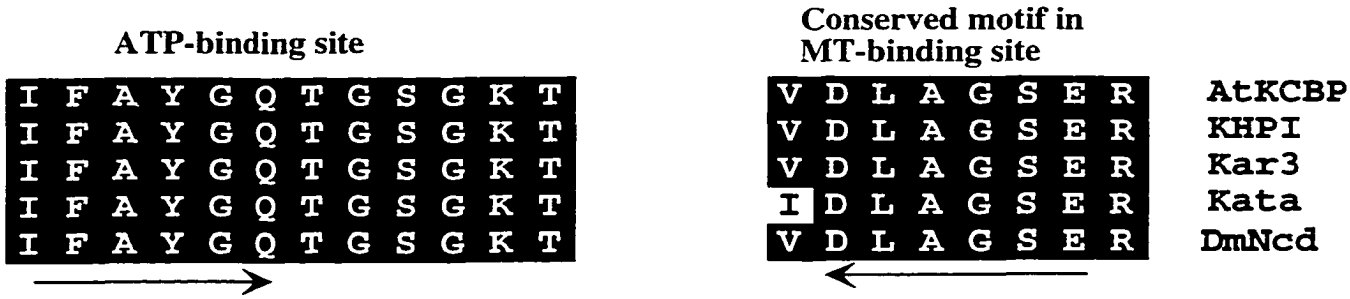

(B)

Sense primer

BamHI **I F A Y G Q**
5'-GCAGGATCC ATT TTT GCI TAT GCI CAA AC-3'
C C C G
A

Antisense primer

E S G A L D
EcoRI
5'-GCAGAATTC AAG IGA ICC IGC IAG ATC IA-3'
C CT A G

Fig. 35 (A) **Alignment of ATP- and putative microtubule-(MT) binding sites from different KLPs.** AtKCBP (*Arabidopsis thaliana*), KHP1(*Chlamydomonas*), Kar3 (*Saccharomyces cerevisiae*), Kata (*Arabdopsis*), DmNcd (*Drodophila melanogaster*). (B) Sequences of degenerate primers used to amplify CpKLP1motor domain. To reduce primer degenerecy, inosine (I) is used at some positions. Amino acids corresponding to nucleotide sequences are shown in bold. Restriction sites are shown underlined.

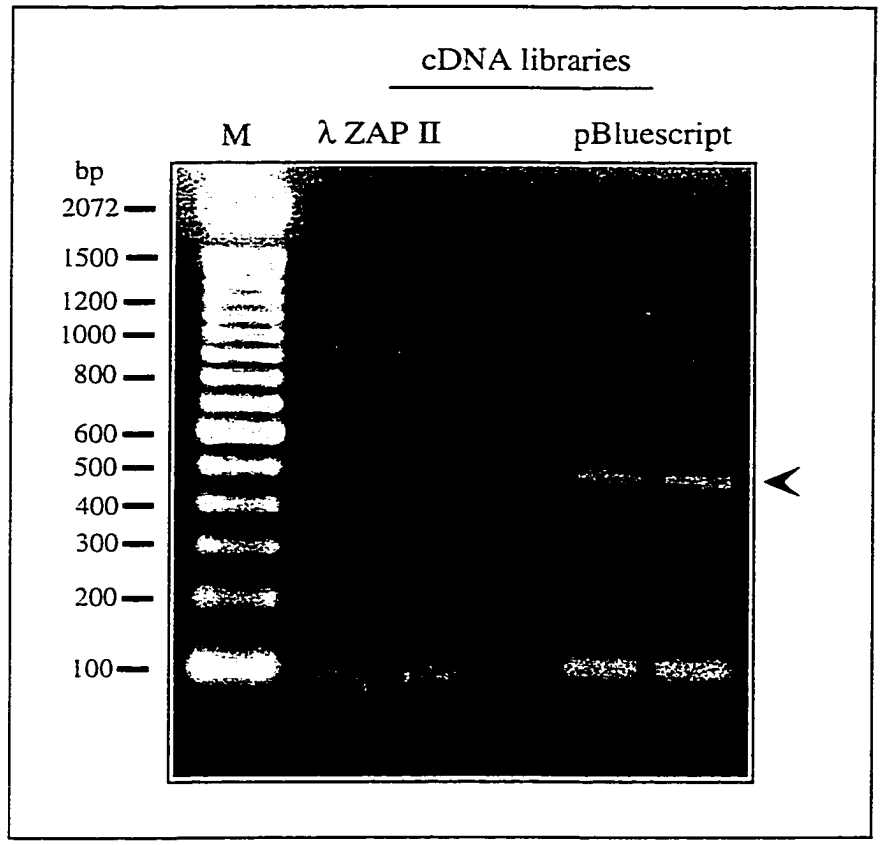

Fig. 36 Agarose gel electrophoresis of PCR-amplified product obtained with degenerate primers to conserved regions in the KLPs motor domain. 1 X 10^5 pfu of *Cyanophora* cDNA library prepared in Lambda ZAP II and pBluescript (about 1 ng DNA) was used as templats. A 500 bp fragment amplified from pBluescript library was cloned and sequenced. PCR products were separated on 1% agarose gel. Arrow head indicates the PCR products. Size markers are shown to the left.

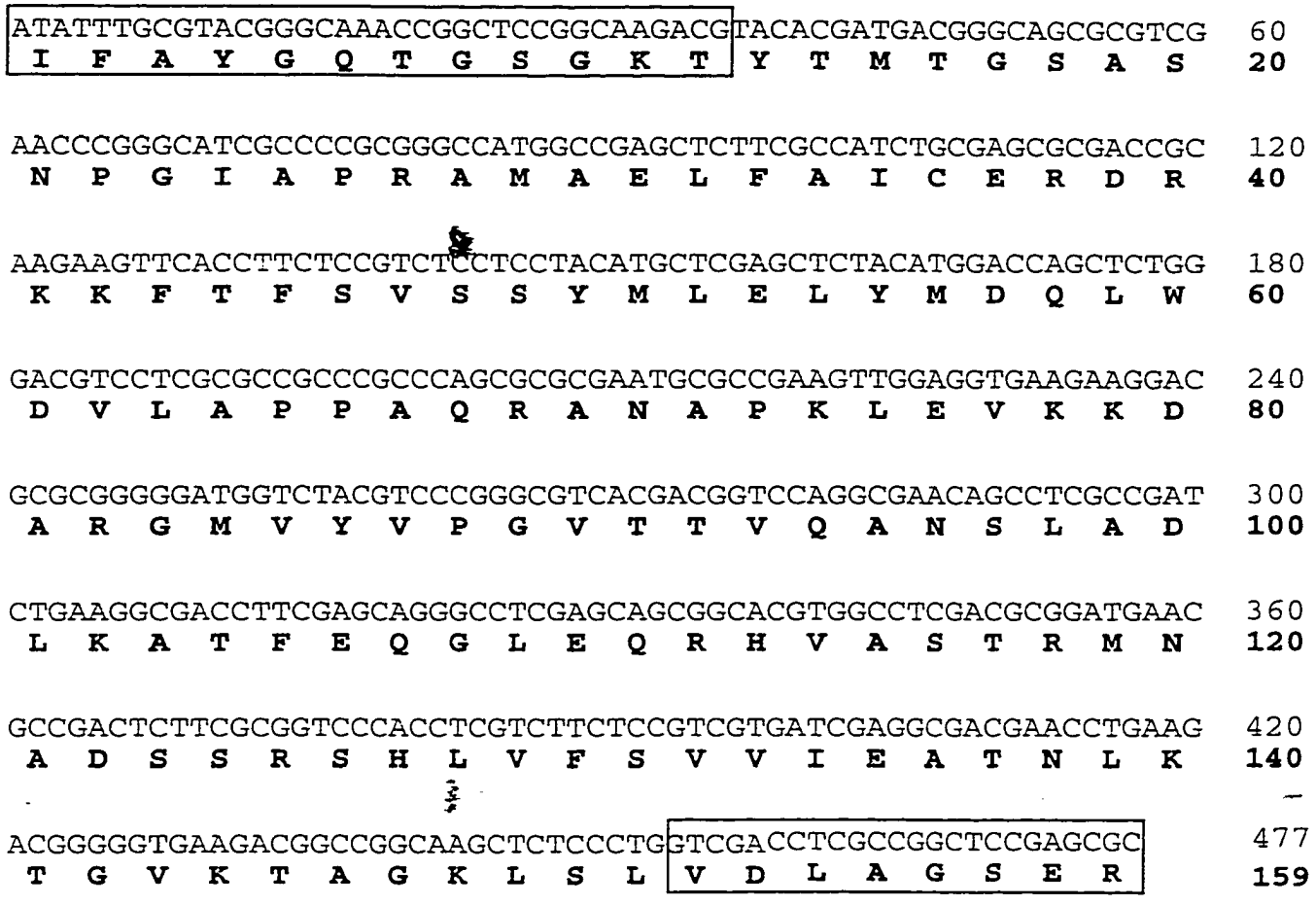

Fig. 37 **Nucleotide and deduced amino acid sequence of CpKLP1 PCR poduct**. The amino acid sequence is presented below the nucleotide sequense (in bold). Numbers at right correspond to nucleotides and deduced amino acids (in bold). Conserved regions in the motor domain of KLPs are boxed.

that are conserved only among KCBP and CpKLP1 (shown later in section V), suggesting that CpKLP1 is related to this group of KLPs. Overall, CpKLP1 shows higher sequence similarity to the motor domain of AtKCBP and kinesin-C from sea urchin (53.8 % and 48.7 % respectively) compared to other C-terminal KLPs from other organisms. These results indicate that CpKLP1 very likely belongs to the CaM-binding KLPs.

In phylogenetic analysis of CpKLP1 with the motor domain of all KLPs using the PAUP (data shown later in section V). CpKLP1 fell into the C-terminal subfamily indicating that it belongs to this subfamily of motors. It has been shown that the sequence characteristics of the motor region of C-terminal motors distinguish them from the N-terminal motors (Goodson *et al.*, 1994). Within the C-terminal subfamily, CpKLP1 fell into a distinct group of KLPs with a CaM-binding domain. This group of KLPs is characterized by a CaM-binding domain adjacent to the motor domain that is necessary for Ca^{2+}/CaM regulation (Narasimhulu *et al.*, 1997; Narasimhulu and Reddy, 1998). This analysis further confirms that the CpKLP1 belongs to CaM-binding kinesins.

KCBP –Ab cross-reacts with a specific protein in *C. paradoxa* crude extract

The available sequence does not allow us to conclude that CpKLP1 is an ortholog of KCBP. To test for the presence of KCBP in *Cyanophora*, a protein blot from *C. paradoxa* with affinity-purified KCBP antibody to CBD of AtKCBP (Bowser and Reddy, 1997) was probed. The antibody has been shown to detect KCBP in several angiosperms (Bowser and Reddy, 1997; Smirnova *et al.*, 1998; Vos *et al.*, 2000). Other CBDs as well as KLPs other than KCBPs do not interact with this antibody. The KCBP antibody detected a specific band in *Cyanophora* protein extract (Fig 38). The molecular mass of the immunodetected band is estimated to be about 133 kDa by comparing the mobility of the immunoreactive band

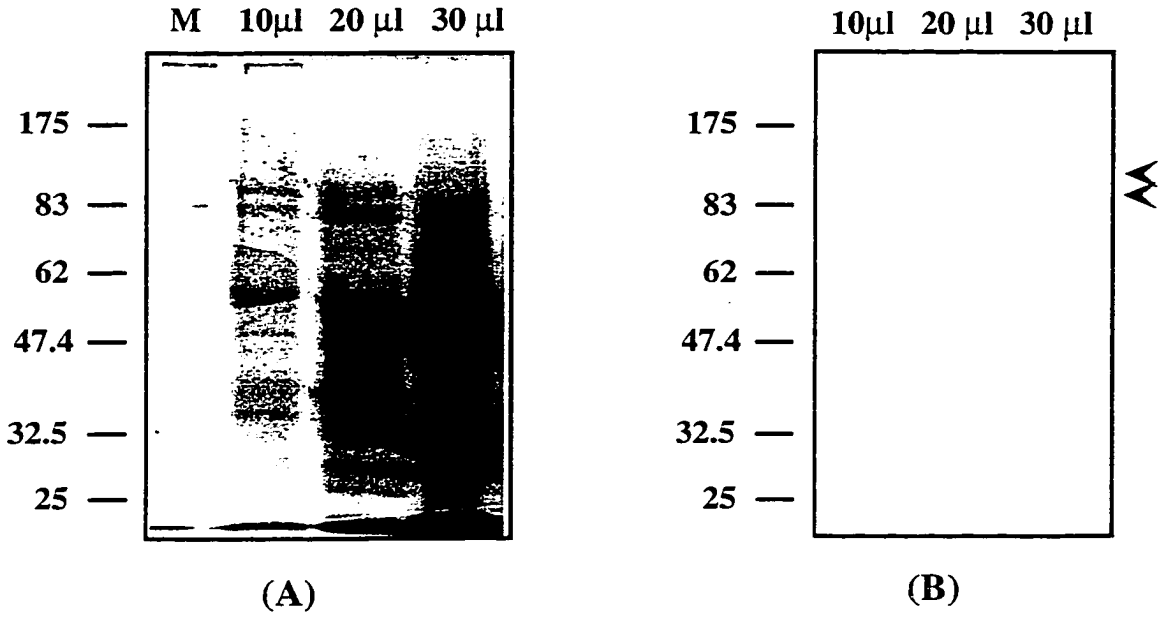

Fig. 38 **Immunodetection of KCBP in *Cyanophora paradoxa*.** Crude protein was fractionated on 8% SDS-containing polyacrylamide gels and either stained with Coomassie stain (A) or blotted onto a nitrocellulose membrane and detected with affinity-purified KCBP-Ab (B). Arrowheads represen the detected bands. Molecular mass markers are shown ot left in kDa.

with the *Arabidopsis* KCBP as well as known molecular mass markers. These results indicate that *Cyanophora* contains a polypeptide that cross-reacts with KCBP antibody. In maize, the estimated molecular mass of ZmKCBP is 137 kDa (Abdel-Ghany and Reddy, 2000) and the estimated molecular mass of CBD-containing KLP from sea urchin (kinesin-C) is 181 kDa (Rogers *et al.*, 1999). The KCBP antibody does not recognize other CBDs that are not related to KCBP (Bowser and Reddy, 1997). In *C. paradoxa* the size of the detected band (133 kDa) is close to the estimated molecular mass of KCBP from other plant systems.

Biotinylated CaM and KCBP antibody detect the same protein in protein fractions bound to CaM-Sepharose

It is known that KCBP interaction with MTs is Ca^{2+}/CaM-regulated (Narasimhulu and Reddy, 1998). KCBP binds CaM in presence of Ca^{2+} and is released in presence of Ca^{2+} chelators like EGTA. To determine binding of CpKLP1 to CaM, *Cyanophora* crude extract supplemented with protease inhibitor cocktail was passed through a CaM-Sepharose column in presence of 2 mM $CaCl_2$, and the protein bound to CaM was eluted with 2 mM EGTA. The eluted fractions were either probed with bio-CaM (Fig 39A) or concentrated with Biomax 0.5 Ultrafree centrifuge filters and then probed with KCBP antibody (Fig 39B). In both cases, a specific polypeptide with a molecular mass of about 133 kDa was detected. These results collectively suggest the presence of a CaM-binding kinesin-like protein in *C. paradoxa*.

Gene structure of CpKLP1

Repeated screening of cDNA libraries with CpKLP1 did not yield true positive signals. It is known that KCBP expression is cell cycle dependent (Bowser and Reddy, 1997; Vos *et al.*, 2000), hence it is likely that full-length CpKLP1 may be not represented in our

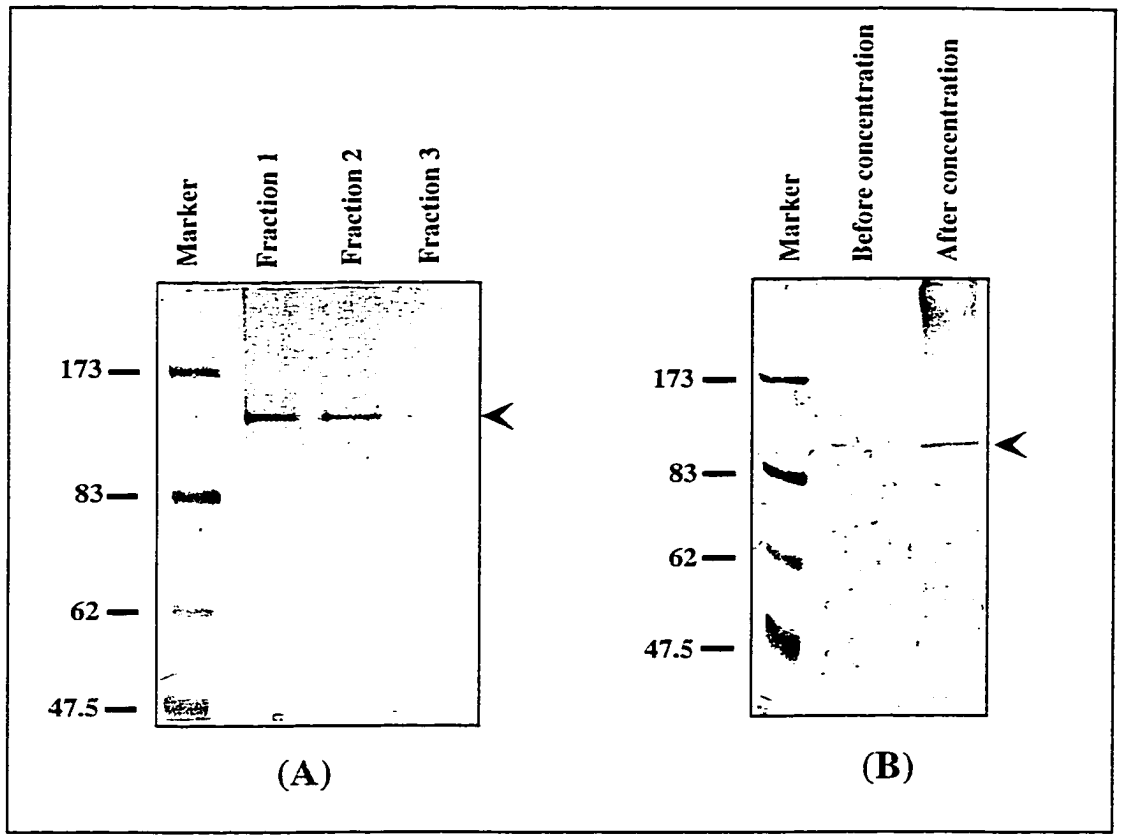

Fig. 38 **Purification of CpKLP1 with CaM-Sepharose column.** Protein from 10 day old cells was run through CaM-sepharose column in the presence of 2 mM $CaCl_2$. After washing with binding buffer, the bound protein was eluted in the presence of 2 mM EGTA. Eluted fractions were either probed with biotinylated calmodulin (A) or concentrated and probed with KCBP antibody (B). Arrow heads indicate the detected bands. Molecular mass marker are shown at left in kDa.

libraries. The other reason might be that CpKLP1 has a high GC content (shown later). Because of this high GC-content, we obtained false positives, even at high stringent conditions (e.g. genes encoding proline-rich proteins). For these reasons and our interest in studying the gene structure of *Cyanophora* KCBP, we constructed a genomic library from *C. paradoxa* in Lambda DASH II replacement vector. The genomic library was screened with PCR-amplified product,CpKLP1. Nine putative positive clones were purified by three rounds of screening and the phage DNA was prepared. Restriction digestion with *Not*I and Southern blotting confirmed that all seven clones contain the insert (Fig 40).

The size of the bands that hybridized with CpKLP1 range between 10 and 4.5 Kb. Restriction analysis digestion with single and double enzymes have indicated that the clone 3/1 has the longest hybridizing insert. Digestion of this clone with *EcoR*1 produced three bands of 6.0, 5.5, and 5.0 kb, of these the smallest one hybridized to CpKLP1 (Fig 41). These three fragments were cloned into pBluescript (Fig 42) and sequenced. The exons and introns sequence and the predicted amino acids of the motor domain and CBD are shown in Fig (43). Gene structure, including exons and introns length, percent of AT per exons and introns, and the splicing consensus sequences are shown in Table (7).

Analysis of the nucleotide sequence of the genomic clone with the nucleotide sequence of cDNA clone revealed the presence of 14 exons and 13 introns (Table 7) compared to 5 exons and 6 introns in the corresponding region of AtKCBP and ZmKCBP, respectively (Reddy *et al.*, 1998). CBD domain of CpKLP1 is interupted by the last intron although in AtKCBP is encoded by the last exon. Exons and introns vary greatly in their length, with the longest exon and intron being 117 and 240 nucleotides, respectively. In general most of the introns are shorter than their corresponding introns in AtKCBP. The

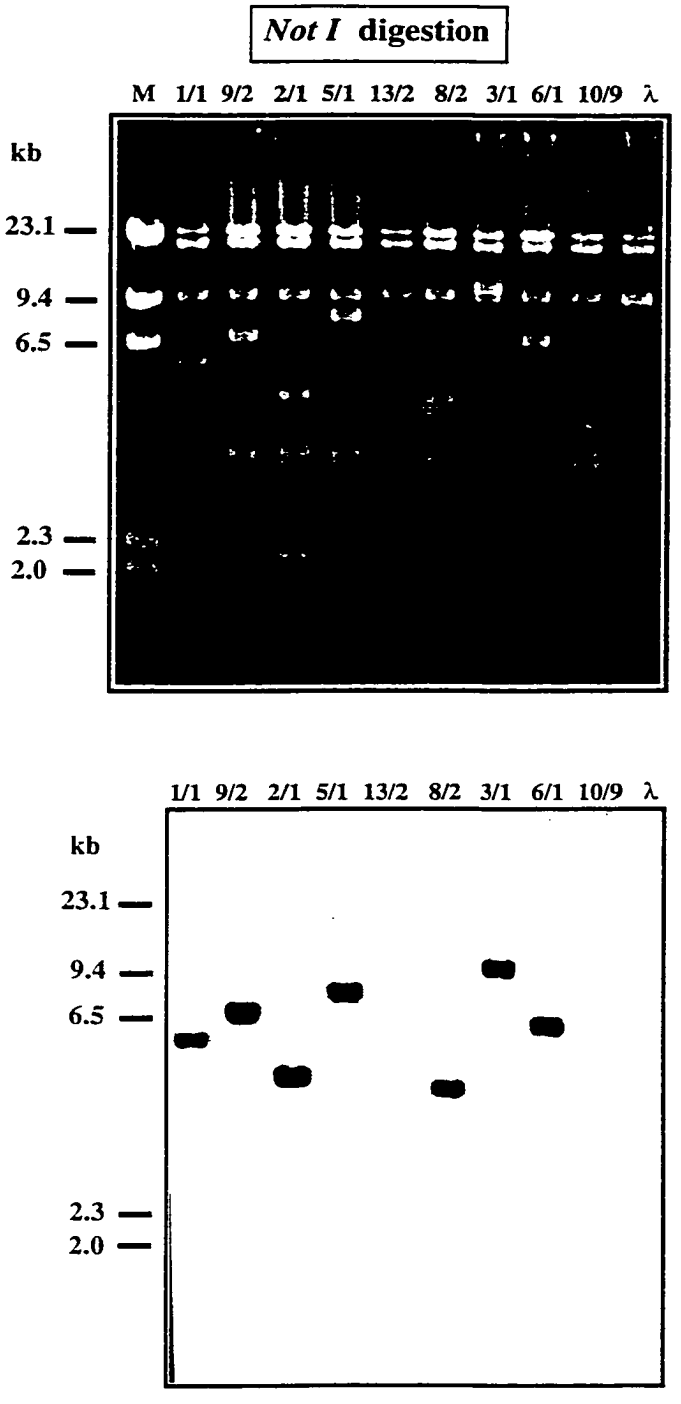

Fig. 40 **Restriction digestion and Southern blotting of *C. paradoxa* genomic clones.** Phage DNA was isolated from nine genomic clones, digested with *Not*I, separated on 0.8% agarose gel, blotted and probed with CpKLP1. Seven clones with different insert sizes showed hybridization. Size markers are shown at left in kp.

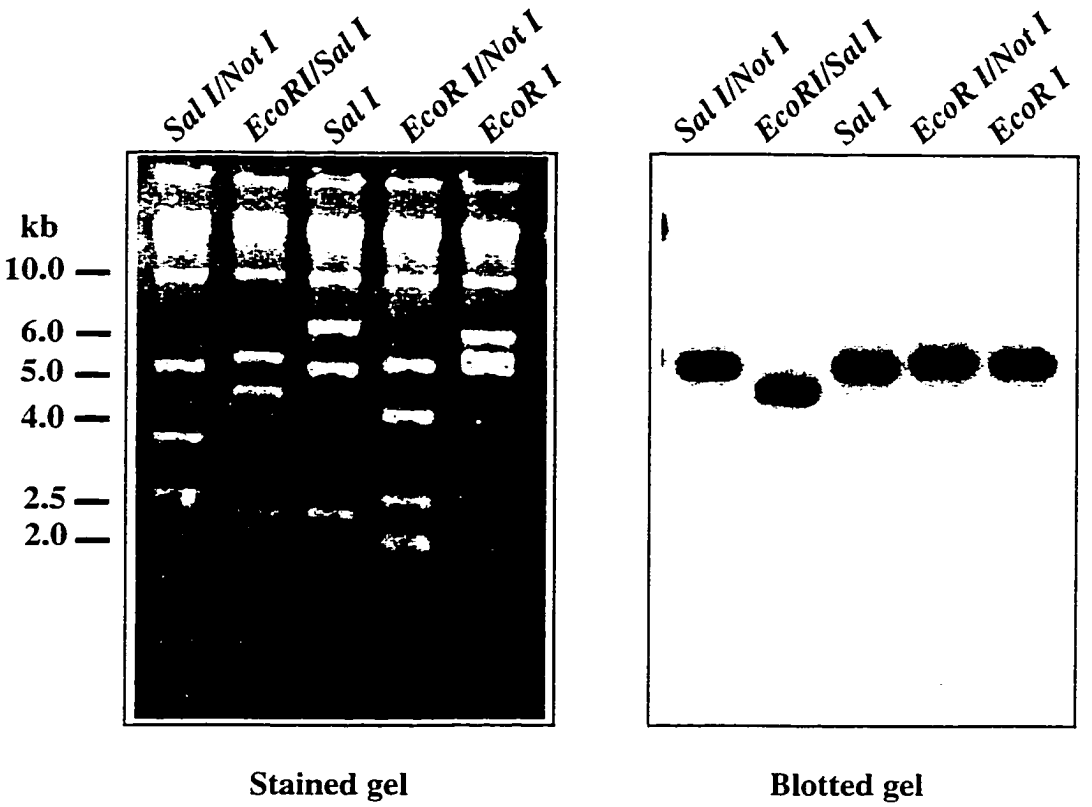

Fig. 41 **Restriction mapping and Southern blotting of genomic clone, 3/1.** DNA from genomic clone 3/1 was digested with different restriction enzymes, separated on 0.8% agarose gel, blotted and probed with CpKLP1. *EcoRI* digestion released three fragmens of about 6.0, 5.5, and 5.0 kb. The smallest fragment (5.0 kb) hybridized with the probe. DNA size markers are shown at left in kb.

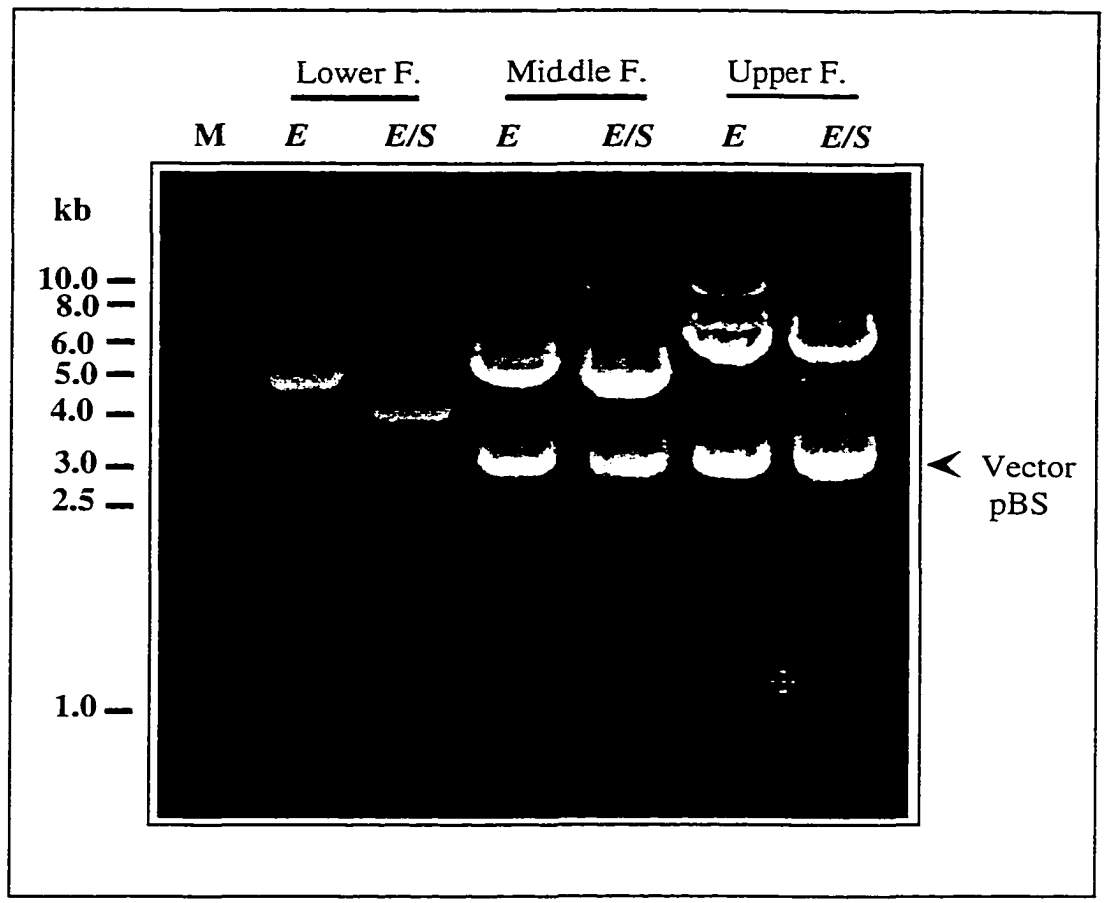

Fig. 42 **Confirmation of 3/1 subclones.** Three (lower, middle and upper) fagmens produced from *EcoR*I digestion were subcloned into *EcoR*I site of pBluescript vector for sequencing. *EcoR*I (*E*), *EcoRI/SalI* (*E/S*) are the enzymes used for confirmation. The smallest fragment, 5.0 kb has internal *Sal*I site which release about 400 bp. Arrow head represent the size of the linear pBS vetor. DNA size markers are shown at left in kb.

shortest exon (exon 7) encodes for 10 amino acid residues while the shortest intron is 67 bases in length. Comparison of the intron position in CpKLP1 with the corresponding region in AtKCBP showed that all introns are not conserved in their position, suggesting intron insertion and deletion through the course of evolution. Not only the position and number of introns is not conserved between AtKCBP and CpKLP1 but also the total length of introns per coding region is greatly different. The total length of introns in CpKLP1 motor domain plus CBD is 1358 bp compared to that in AtKCBP which is 700 bp.

The GC content of both exons and introns is very high, with the highest percentage of 82 and 89, respectively. All introns and 11 out of 13 exons have more than a 63 % GC ratio. Although we are in the era of genome sequencing we could not obtain the complete sequence of CpKLP1. In several trials, the signals dropped suddenly because of long stretches of GCs. All introns have the consensus AG at the 3' splice junction (acceptor site) and 10 of them have the consensus GT at the 5' splice junction (donor site) and the other three have GC instead of GT, so all the introns follows GU/GC-AG rule for 5' and 3' splicing sites.

The CpKLP1 contains a 23 amino acid CaM-binding domain at the C-terminus end (aa 314-337). The CBD of CpKLP1 shares 30%, 39% and 35% sequence identity with the CBDs of AtKCBP, ZmKCBP and Kinesin C from sea urchin. In spite of the low percentage of identity among these CBDs, all of them have conserved residues at conserved positions, and these residues are responsible for CaM interaction. The putative CaM-binding domain forms a basic amphiphilic structure where charged residues are segregated from hydrophobic residues. It will be interesting to get the sequence of the N-terminal region of CpKLP1 to determine whether it has myosin tail homology 4 and talin-like regions or not.

```
CCG TCT CCA TCC CCT CCA TCG ACT CCC NCC GCA GGG CAG ACG    42
                                        A   G   Q   T     4
AAG AGC TTC CAG TTC GAC GCG TGC TTC CCC GAG GAC ACC TCC    84
 K   S   F   Q   F   D   A   C   F   P   E   D   T   S    18
CAG GAG CGC GTC TTC GAG GAC ACC AAG GCG CGC CCG CGC CCC   126
 Q   E   R   V   F   E   D   T   K   A   R   P   R   P    32
GCT CCC CGC GCC CCA GCg ccc agc gcc cgc cct cct taa tag   168
 A   P   R   A   P   A                                    38
acg ccc acg cct gcg tct tta tag act tta gac ttt aaa ctt   210
cac aga cgc ccc cgc ccc cgc cca tct aag gac aca aag gcg   252
cgc ccc gcg ccc cgc gcc cag cgc cgc cgc cac cgc cgc ccg   294
ccg ccc ttt tga gGC TTG ACC CCG CGC GCC GCA CGC AGA ACC   336
                    L   D   P   A   R   R   T   Q   N    47
TGA TCC AGT CGG CGG TGG ACG GCT TCA ACG TCT GCA TCT TCG   378
L   I   Q   S   A   V   D   G   F   N   V   C   I   F    61
CGT ACG GGC AGA CCG GCT CCG GCA AGA Cgt gcg ccg ggg cca   420
A   Y   G   Q   T   G   S   G   K   T                    71
ggg cct cta gaa ccg cca ggg agc ggc tag agc ctc gcc ctg   462
cgc cgg cgc gtg gaa tcg gac taa ggt caa gcc gtc gct taa   404
tat cgg ccg gcg ctc aat atc ggc cag cgc cta gga tcg gct   546
att tct ttg gat cgc tga ggg gcg agc gag cgc ctc tag aat   588
ggg cta tat ctt cgg atc gct gag ggg cga acg ggc ggg cag   630
GTA CAC GAT GAC GGG CAG CGC GTC GAA CCC GGG CAT CGC CCC   672
  Y   T   M   T   G   S   A   S   N   P   G   I   A   P   85
GCG GGC CAT GGC CGA GCT CTT CGC CAT CTG CGA GCG CGA CCG   714
  R   A   M   A   E   L   F   A   I   C   E   R   D   R   99
CAA gtg cgc gca tcc tca ggc gca cgc gag aga gag aga aag   756
K                                                        100
ggg ccg ctt cta gaa cgg gag cac gcc tag ctt gcg cct ccg   798
cca cgc ccc gct cct agt ctg cga gcg cga ccg gaa gtg aga   840
gag aga ccc cgc ccc cgc ccc cgc ccc cgc ccc cgc ccc cgc   882
ccc cgc ccc cgc ccc cta gcc ttt tta gct cct agc tgg gga   924
cct aga tcc ctc gcc gtc tga gag cgc gtc cgc agG AAG TTC   966
                                            K   F       102
ACC TTC TCC GTC TCC TCC TAC ATG CTC GAG CTC TAC ATG GAC  1008
 T   F   S   V   S   S   Y   M   L   E   L   Y   M   D   116
CAG gcg cgc ctg ttg tcc cgc cgc ccc tcc ctc cgg ttc tta  1050
 Q                                                       117
agg cgc ctc taa cta act tcg ttc gca gCT CTG GGA CGT CCT  1092
                                    L   W   D   V   L    122
CGC GCC GCC CGC CCA GCG CGC Ggt ccg ttc gcc cca cct ttc  1134
  A   P   P   A   Q   R   A                              129
cac ccc acc cca ccc gct ccc ctt acc taa cct ggc ggt ccg  1176
gga aca gAA TGC GCC GAA GTT GGA GGT GAA GAA GGA CGC GCG  1218
          N   A   P   K   L   E   V   K   K   D   A   R   141
GGG GAT GGT CTA CGT CCC GGG CGT CAC GAC GGT CCA GGC GAA  1260
```


Fig. 43

```
  G   M   V   Y   V   P   G   V   T   T   V   Q   A   N   155
CAG CCT TGC CGA TCT GAA GGC GAC CTT CGA GCA GGg tac ccc   1302
  S   L   A   D   L   K   A   T   F   E   Q               166
cta ccc ccc ctc tcc ccc cct ctc cct ttt tct cct cac agc   1344
ttc tcg ggg acc ccg tca ctt acg ccg cgc cgc gcc gcc cgc   1386
agG CCT CGA GCA GCG GCA CGT GGC CTC GAC GCg tgc gcg cct   1428
  G   L   E   Q   R   H   V   A   S   T                 176
ttg att ccc gta ccc ctc ctt cat tcg ccc ccg ccc cgc cga   1470
ttt gcc ccc ccc ccc cag GGA TGA ACG CCG ACT CTT CGC GGT   1512
                        R   M   N   A   D   S   S   R     184
CCC ACC TCG TCT TCT CCG TCG TGA TCG AGG CGA CGg ttc gcg   1554
S   H   L   V   F   S   V   V   I   E   A   T           196
cgc ccg cgc gga ccg tgc cgc gcc gcg ccc gcg cgc ctg agg   1596
ggc tcc cgc ccg ctc gcc ccg ccc gcc gca gAA CCT GAA GAC   1638
                                        N   L   K   T   200
GGG GGT GAA GAC GGC CGG CAA GCT CTC CCT GGT CGA CCT CGC   1680
  G   V   K   T   A   G   K   L   S   L   V   D   L   A 214
CGG CTC CGA GCG CGT CGC CAA GTC CGA GGC CTC GGG CGC CAC   1722
  G   S   E   R   V   A   K   S   E   A   S   G   A   T 228
TCT CAA Ggc gcc tcc cct ctc tac ttc ttc tct ctt cct tct   1764
  L   K                                                 230
tct tct ggt ctg agg cgc ccg cgc ccg ccc gca gGA GGC CCA   1806
                                            E   A   Q   233
GTC GAT CAA CAA GTC CCT CTC CGC CCT CGG CGA TGT CAT CGC   1848
  S   I   N   K   S   L   S   A   L   G   D   V   I   A 247
CGC ACT gtg cgc cgt gat ggg atg gga gga ggc gca gcg cgc   1890
  A   L                                                 249
gag cgc tgg gcg gtg ttg ggc cgc gcg cgc ctc acg cgc ccc   1932
cgc ccc gcc ccg ccc cgc ccc gca gCT CGA GCG GCG CCG ACT   1974
                                S   S   G   A   D       254
TCA TCC CGT ACC GCA ACC ACA AGA TCA CGg tac ccg tgc cgc   2016
F   I   P   Y   R   N   H   K   I   T                   264
cgt cgc cgg tcc cgg acc tct cgc ccg gtg ccg acg ccg ggg   2058
ggc gta cgc gcg cag ATG CTG ATG CAG GAC TCG CTC GGC GGC   2100
                    M   L   M   Q   D   S   L   G   G   273
AAC GCG AAG ACC CTC ATG TTC GTC AAT GTC gtg cgt acc ctt   2142
 N   A   K   T   L   M   F   V   N   V                  283
ctc ctc ctc ccc ctc ccc gtc ctc ctc cgc ccc ccc tcc ccc   2184
atc tta cgc ccc gcc agT CGC CGA CGG ACT ACA ACG CGG ACG   2226
                        S   P   T   D   Y   N   A   D   291
AGT CGG CGA ACA GCC TGC AGT ACG CGG CCC GCG TGA AGA CCA   2268
E   S   A   N   S   L   Q   Y   A   A   R   V   K   T   305
TCA CGA ACA ACG CGA CCG TCG CCG TCG AGT CGA AGG AGA TCC   2310
I   T   N   N   A   T   V   A   V   E   S   K   E   I   319
AGC GCC TGg tac ccc ccc tcc tcc cct ccc ccc ccc ccc tag   2352
```


Fig. 43

Fig. 43 **Nucleotide and deduced amino acid sequence of the motor and calmodulin-binding domains of *Cyanophora paradoxa* kinesin-like protein (CpKLP1).** Exons are shown in upper-case letters and introns are presented in lower-case letters. The predicted amino acid sequence is shown under the nucleotide sequence. Stop codon is indicated with a diamond. The conserved regions in the motor domain of all KLPs are shown in bold. Amino acids corresponding to the CBD are underlined. Numbers at right correspond to nucleotides and deduced amino acids (in bold).

Table (7): Length, AT content and splice site junctions of exons and introns in the motor domain of CpKLP1

No.	Exons		Introns					
					5' splice site juntion		3' splice site junction	
	Length bp	AT Content %	Length bp	AT Content %	Exon	Intron	Intron	Exon
1	ND	ND	164	32	GC	GCCCAG	TTTGAG	GC
2	99	32	224	35	AC	GTGCGC	GGGCAG	GT
3	89	29	240	28	AA	GTGCGC	CCGCAG	GA
4	52	46	67	36	AG	GCGCGC	TCGCAG	CT
5	38	18	67	31	CG	GTCCGT	GAACAG	AA
6	112	36	93	29	GG	GTACCC	CCGCAG	GC
7	30	23	70	29	GC	GTGCGC	CCCCAG	GG
8	59	36	80	11	CG	GTTCGC	CCGCAG	AA
9	102	30	69	35	AG	GCGCCT	CCGCAG	GA
10	56	36	103	17	CT	GTGCGC	CCGCAG	CT
11	46	37	70	19	CG	GTACCC	GCGCAG	AT
12	57	42	71	27	TC	GTGCGT	CGCCAG	TC
13	117	34	68	24	TG	GTACCC	CAGAAG	GG
14	99	20	--	--		--	--	--

- The splice sites were predicted by using the Netplant gene, a program that predicts the splicing sites in plant genes and by comparing the cDNA sequence with the genomic DNA sequence.
- The consensus sequences at 5' and 3' splice junctions are AG/GTAAGT and TGY(A/C)AG/GT respectively. Nucleotides that are identical to consensus sequences are underlined Goodall *et al.*, (1991). Conserved nucleotides in the consensus sequences are underlined.
- ND = not determined.

CpKLP1 is a single-copy gene

To determine the approximate copy number of CpKLP1, Southern blot analysis of *C. paradoxa* genomic DNA was carried out. One hybridization band was detected with different restriction enzymes (*EcoR*1, *Hind*III, *Kpn*I, *Pst*I, *Xho*I) (Fig 44). Low stringency washes did not yield any additional bands, suggesting that the CpKLP1 does not cross hybridize with other genes especially KLPs. In *Arabidopsis*, tobacco, maize, and other systems, KCBP was shown to be a single-copy gene that is expressed in all tissues and that does not hybridize with other KLPs (Reddy *et al.*, 1996a; Wang *et al.*, 1996; Abdel-Ghany and Reddy, 2000).

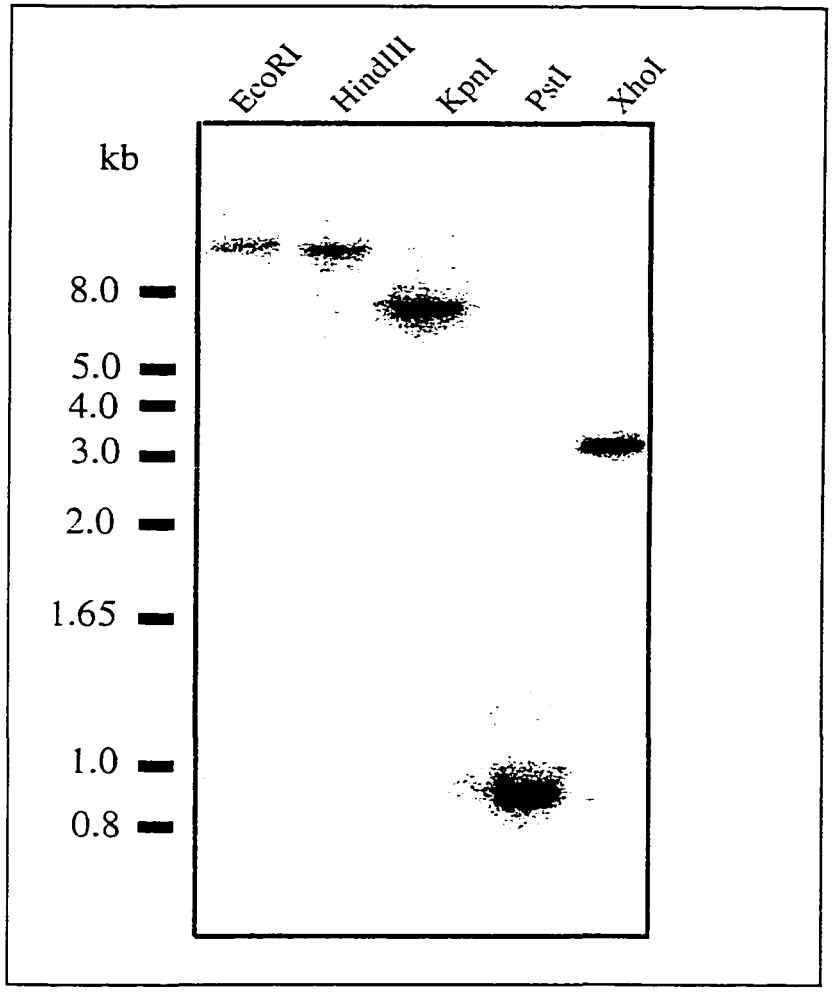

Fig. 44 **Southern blot analysis of *C. paradoxa* genomic DNA.** Genomic DNA (10 μg) was digested with restriction enzymes (*EcoR*I, *Hind*III, *Kpn*I, *Pst*I, and *Xho*I), separated in an 0.8% agarose gel, blotted and probed with PCR-amplified CpKLP1. DNA size markers are shown at left in kb.

V. Analysis of KCBPs

Part of this work is included in a paper "Molecular evolution of a Ca^{2+}/CaM-regulated MT motor protein from phylogenetically *diverged* eukaryotes". Salah E. Abdel-Ghany, Paul Kugrens, and A.S.N. Reddy. Molecular Biology and Evolution. (In preparation)

Evolutionary relationship among KCBPs and with other KLPs

So far seven KCBPs have been cloned and characterized from phylogenetically *diverged* photosynthetic eukaryotes. In addition, a CaM-binding KLP (kinesin C) was isolated from sea urchin. The amino acid sequence of the motor domains of KCBPs was analyzed using PAUP to determine the evolutionary relationships between KCBPs and other KLPs. Thirty-two C-terminal KLPs from different species and two representative members from each subfamily were used also with 8 CBD-containing KLPs (7 KCBPs plus kinesin C) in our analysis. The phylogenetic tree obtained is shown in Fig (45). KCBPs form a distinct group within the C-terminal subfamily including kinesin C from sea urchin, reflecting their distinct structural features among all C-terminal motors. The percents of similarity between the KCBPs' motor domains and the motor domains of all known C-terminal KLPs were calculated using the Clustal method (Table 8). The percent of similarity among KCBPs is significantly higher than the percent of similarity with other C-terminal motors, where the sequence similarity of C-terminal KLPs to KCBPs does not exceed 43.6%. On the other hand, the percent similarity among KCBPs was higher, reaching the highest value (95.1%) between members of the same family (tobacco and potato) while the lowest value (52.1%) was between kinesin C and KCBPs from photosynthetic organisms. The percent of similarity decreased gradually with the logic theme of evolution, where the percent of similarity between spruce KCBP and those from angiosperms ranged between 75.9 and 80.4,

Fig. 45 **Evolutionary relationship of KCBPs motor domain with the motor domain of all known C-terminal KLPs and with the motor domain of other subfamilies.** The phylogenetic tree obtained using PAUP (version 4.02b2) heuristic search method with tree bisection-reconnection (TBR) branch swapping. ScSMY1 (*Saccharomyces cerevisiae*), a highly divergent KLP, was used outgroup. Numbers represent the bootstrap values. Supporting values more than 50% are considered. Members of each subfamily are color-coded. CaM-binding KLPs form a distinct group within the C-terminal subfamily and are shown in red. At9C5.240 and ScKIP3 belong to KIP3 subfamily. HsKIF4 and MmKIF4 (KIF4 subfamily), AtMGL6.9 and MmKIF2 (KIF2 subfamily), HsCMKRP and MmKIFA (Un104/KIF1 subfamily), AnBimC and AtKRP125a (BimC subfamily), AtMAA21.110 and HsKHC (kinesin heavy chain, KHC, subfamily), HsMKLP1 and AtF28P10.150 (MKLP1 subfamily), SpKIN95 and Xlklp3 (KRP85/95 subfamily), Xlklp2 and HsCENPE (ungrouped KLPs). All other KLPs belong to C-terminal subfamily. Note that CrKLP1 belongs to C-terminal KLP subfamily, however it was grouped with the ungrouped KLP. Dash line represents the outgroup branch.

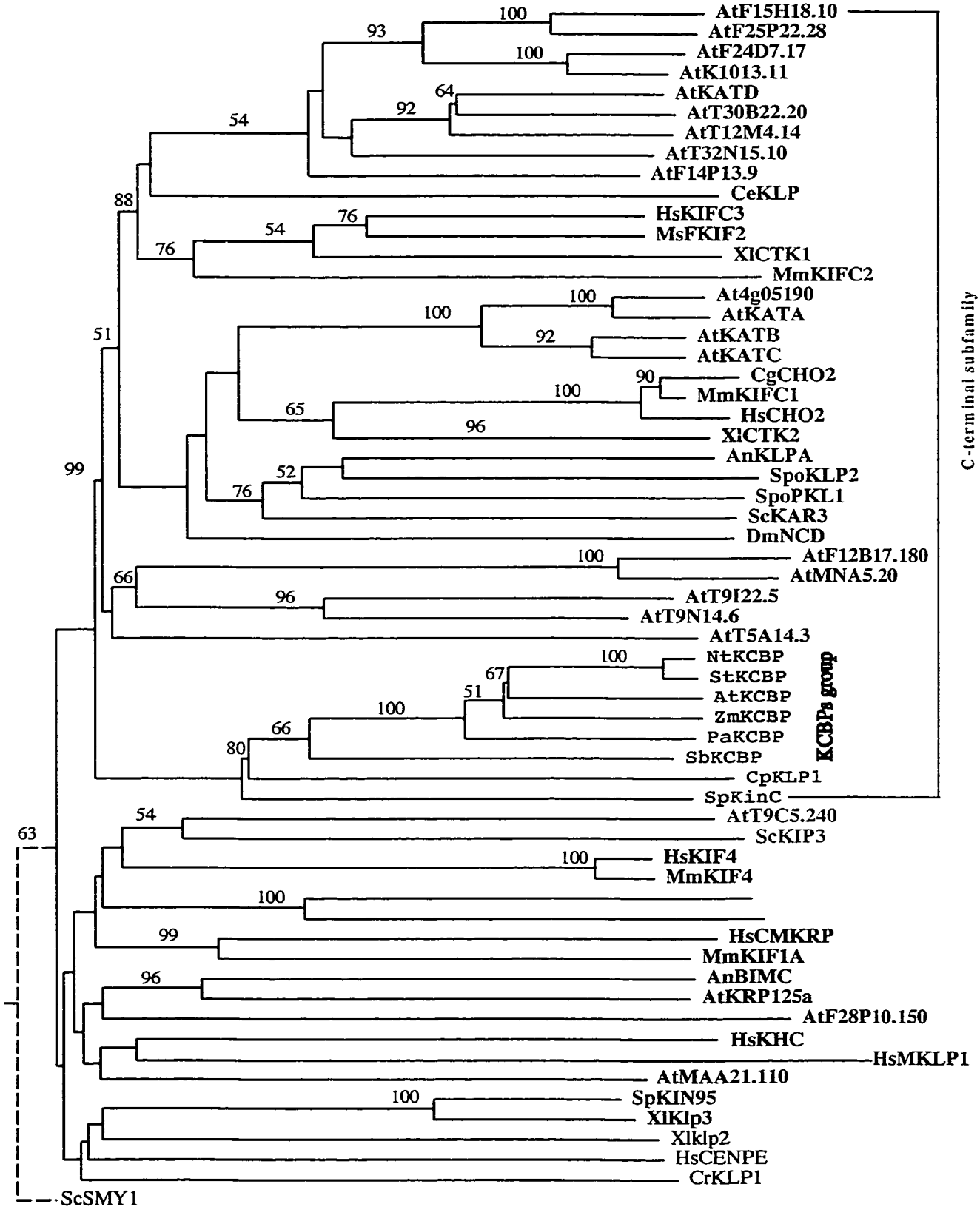

Fig. 45

Table (8): Percent of similarity in the motor domain of CaM-binding KLPs and other C-terminal KLPs using Clustal method.

	AtKCBP	NtKCBP	StKCBPP	ZmKCBP	PaKCBP	SbKCBP	CpKLP1	SpKinC
AnKLPA	37.3	37	36.7	35.1	38.6	39.3	35.5	36
At4g05190	36.7	38.2	37.7	36.6	39.2	40.2	37.1	37.2
AtF12B17.180	32.5	33.1	33.4	32.2	33.1	31.6	29.1	30.3
AtF14P13.9	40.3	39.7	40	36.7	40	42.3	38.3	40
AtF24D7.17	38.7	37.6	37.8	36.3	39	39.6	37.4	37.8
AtF25P22.28	37.7	37	37.7	35.7	38	40.5	37.7	3.5
AtK1013.11	38.9	38.6	38.6	37.4	39.6	41.1	36.1	38.9
AtKATA	36.4	37.6	37.3	36	38.6	41.1	36.7	38.7
AtKATB	38.6	39.1	39.5	38.4	39.8	42.3	37.7	38.1
AtKATC	38.6	39.1	39.2	37.2	40.1	41.1	37.1	38.7
AtKATD	39.8	41	40.4	38.7	41	42.3	38.7	41.4
AtMNA5.20	32.8	34.1	34.7	32.8	34.4	32.8	30.3	32.5
AtT12M4.14	40.5	38.8	38.8	37.5	39.2	42.4	35	38.5
AtT30B22.20	38.9	38.6	38.6	37.7	39.9	40.8	36.4	41.1
AtT32N15.10	39	37.7	38.7	36.4	37.7	42.2	35.8	39
AtT5A14.3	38.3	37.6	37.7	36.5	38.6	37.1	34.8	38.3
AtT9I22.5	36.7	36.7	37	37	38	40.9	32.5	36.7
AtT9N14.6	43.4	43.4	43.4	41.4	41.3	45	40.9	41.1
CeKLP	35.9	38.9	35.6	34.6	36.9	39.9	35	35
CgCHO2	36.4	34.9	36.4	36.9	36.1	33.5	32.9	34.5
DmNCD	35.5	35.5	35.8	33.6	34.9	35	29.1	35.1
HsCHO2	37	35.5	36.7	36.9	36.7	34.7	33.9	33.9
HsKIFC3	42	40.4	39.7	40.4	38.8	34.6	40.7	39.1
MmKIFC1	39.4	39.1	39.4	40.3	38.8	38.8	34.2	37.8
MmKIFC2	32.9	33.9	33.5	32.9	31.9	36.1	30.4	32.9
MsFKIF2	41.4	42.7	42.1	41.4	42.4	43.6	40.6	40.8
ScKAR3	33.7	34.9	37.3	34.8	36.1	32	32.3	34.5
SpoKLP2	34	35.5	33.7	34.8	33.1	36	31.3	34.8
SpoPKL1	37	36.1	35.8	36.6	36.1	34.7	34.2	37.5
XlCTK1	39.8	38.5	40.1	39	40.4	39.3	37.7	36.3
XlCTK2	38.9	38.5	38.6	37.8	37.3	38.7	37.1	35.4
AtKCBP		78.9	81.9	79.5	75.9	61.3	55.3	51.5
NtKCBP			95.1	78.3	78	61.2	53.4	521
StKCBPP				79.8	80.4	61.9	54.3	54.5
ZmKCBP					75	62.8	53.4	52.3
PaKCBP						61.9	53.4	56.3
SbKCBP							54.6	53.2
CpKLP1								52.1
SpKinC								

whereas the percent of similarity between green alga KCBP (SbKCBP) and land plants KCBPs ranged between 61.2 and 62.8. For the most primitive endosymbiotic *Cyanophora paradoxa* KCBP (CpKLP1), the percent of similarity ranged between 53.4 and 55.3. These results indicate that KCBP diverged from the motor protein ancestor that gave the C-terminal, N-terminal or internal KLPs, and it most likely does not evolve later from a C-terminal member by adding domains to its terminals.

To study the phylogeny and evolution of CaM-binding KLPs, phylogenetic trees using either the entire protein, the conserved motor domain or the non conserved coiled-coil region were constructed using PAUP (v. 4.0b2). Despite the significant differences in the level of conservation in these domains among KCBPs, similar phylogenetic trees were obtained in all cases (Fig 46). These results indicate that all KCBP domains are class specific. In these trees KCBPs from photosynthetic eukaryotes grouped in a separate clade from kinesin C. Grouping of kinesin C with KCBPs in a distinct group within the C-terminal subfamily and its separation in a distinct clade in the CBD-containing KLPs tree suggests the presence of a KCBPs ancestor protein before the divergence of plants and animals. In this clade KCBP from *Cyanophora paradoxa* (CpKLP1) is the ancestor protein and from it the algal KCBP (SbKCBP) diverged, which in turn evolved into land plants KCBPs. In land plants, spruce KCBP diverged into angiosperms KCBPs. In flowering plants KCBPs, StKCBP and NtKCBP are very close and they are closer to AtKCBP than to ZmKCBP.

Functional domains in KCBPs

The protein sequence of KCBPs from seven phylogenetically *diverged* species was aligned with the kinesin C using Meglign, and the residues that are similar in at least three proteins were shaded (Fig 47). Also the structural features based on the primary sequence

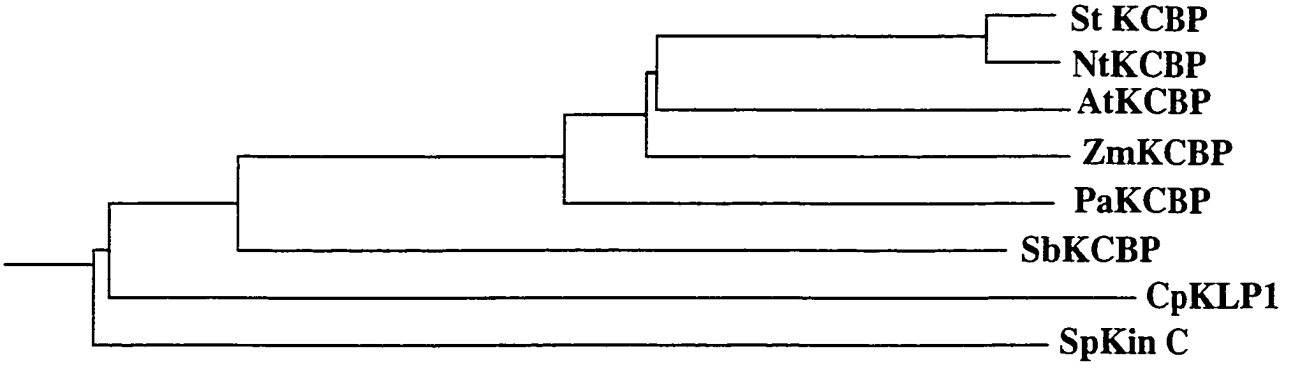

Fig. 46 **Phylogenetic tree of calmodulin-binding KLPs (KCBPs and kinesin C) using either the whole available protein, the motor domain, CBD, or the non-conserved coiled-coil region.** AtKCBP (*Arabidopsis thaliana*), StKCBP (*Solanum tuberosum*), NtKCBP (*Nicotiana tabacum*), ZmKCBP (*Zea mays*), PaKCBP (*Picea abies*), SbKCBP (*Stichococcus bacillaris*), SpKinC (*Strongylocentrotus purpuratus*) and CpKLP1 (*Cyanophora paradoxa*). In case of CpKLPI, we constructed tree using only the motor domain or the CBD. Similar trees were obtained in all cases. Proteins are aligned using the Clustal method.

were shown in Fig (48). Although the structural features of KCBPs are conserved, the level of conservation is variable with the highest level of conservation in the motor domain (Table 8). Motor domains of all characterized KCBPs are highly conserved and contain the conserved ATP-binding consensus sequence as well as four highly conserved motifs that are implicated in MT binding (Fig 47). The twenty-three amino acids CBD at the C-terminus of KCBPs are less conserved with the least conservation in CpKLP1. The percentage of similarity ranged from 18.2 to 39 with the CBD of KCBPs from green algae and land plants (Table 9). Although there is less conservation in the CBDs, all tested KCBPs were detected with affinity-purified antibody to the CBD of AtKCBP. All tested KCBPs were found to bind CaM in the presence of Ca^{2+} and failed to bind in the presence of EGTA indicating that they are Ca^{2+}/CaM-regulated. The coiled-coil region is the least conserved part (Table 10). In all KCBPs that have been characterized from photosynthetic organisms, the coiled-coil region spans about 20% of the protein size compared to kinesin C, where it spans about 70% of the protein and also is highly variable with the percent of similarity to coiled-coil of KCBPs ranging between 12.2 and 15.1.

Another domain that defines kinesin class specificity is the "neck" region, a approximately 45 amino acid residue segment that emerges from the catalytic core of the motor domain (Vale and Fletterick., 1997). C-terminal kinesins as a group share a short conserved sequence (ELKGNI) in their neck region (Saito *et al.*, 1997). In all KCBPs this sequence displays a slight divergence and they have their conserved sequence (EDMKGLIRV) confirming that they form a distinct group within C-terminal subfamily. The N-terminal region of all KCBPs for which sequences are available showed significant sequence similarity to MyTH4 and talin-like region present in myosin IIVa and X. These

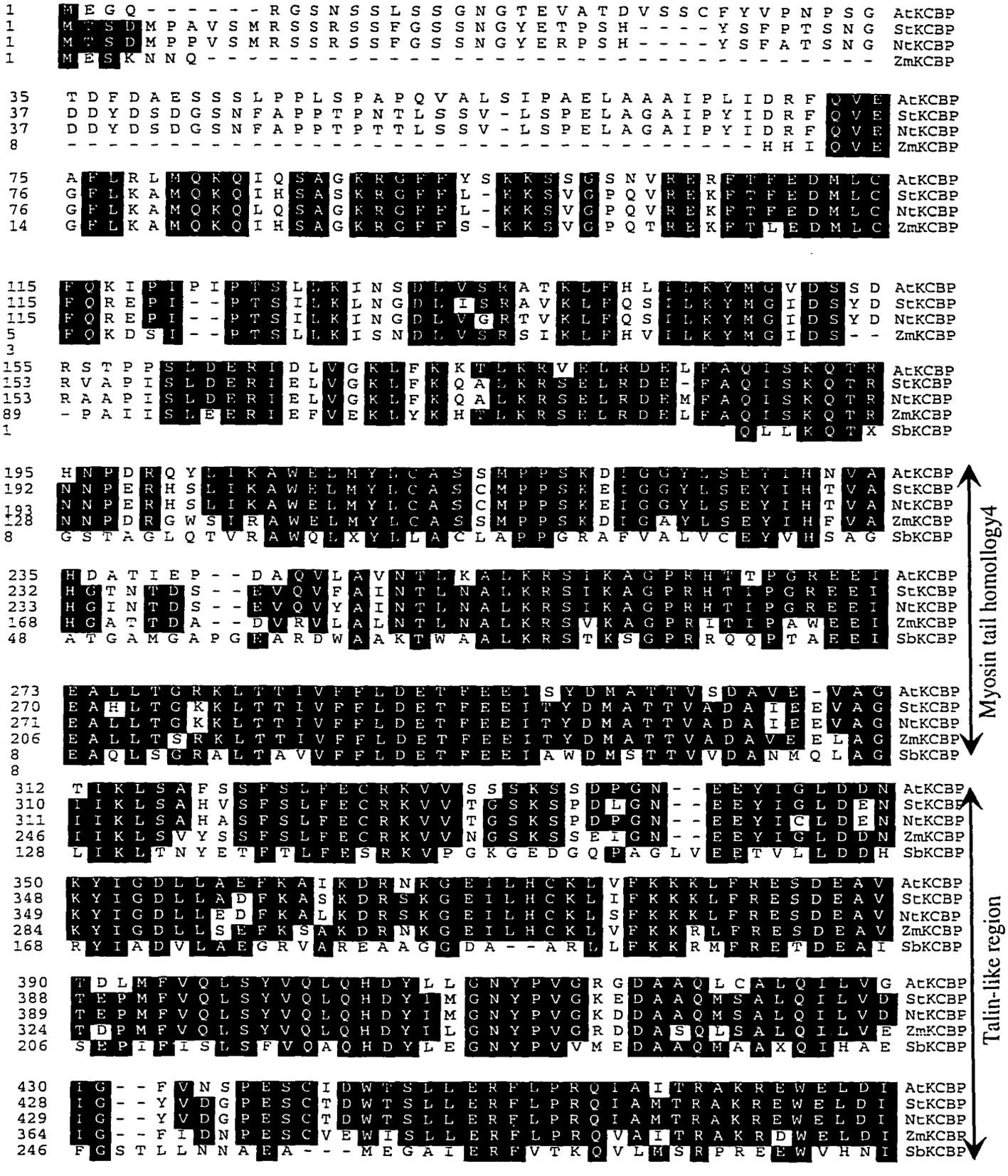

Fig. 47

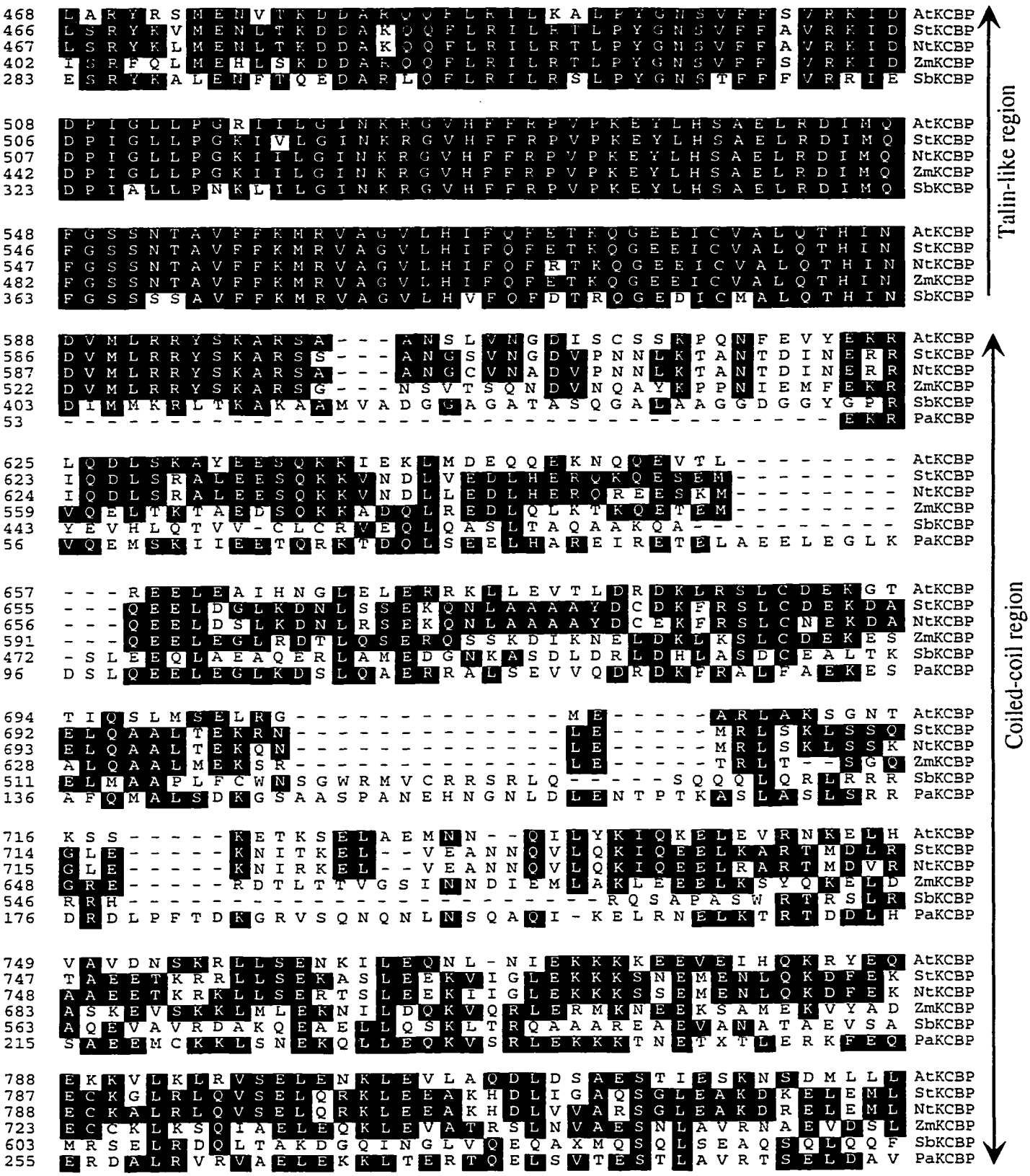

Fig. 47

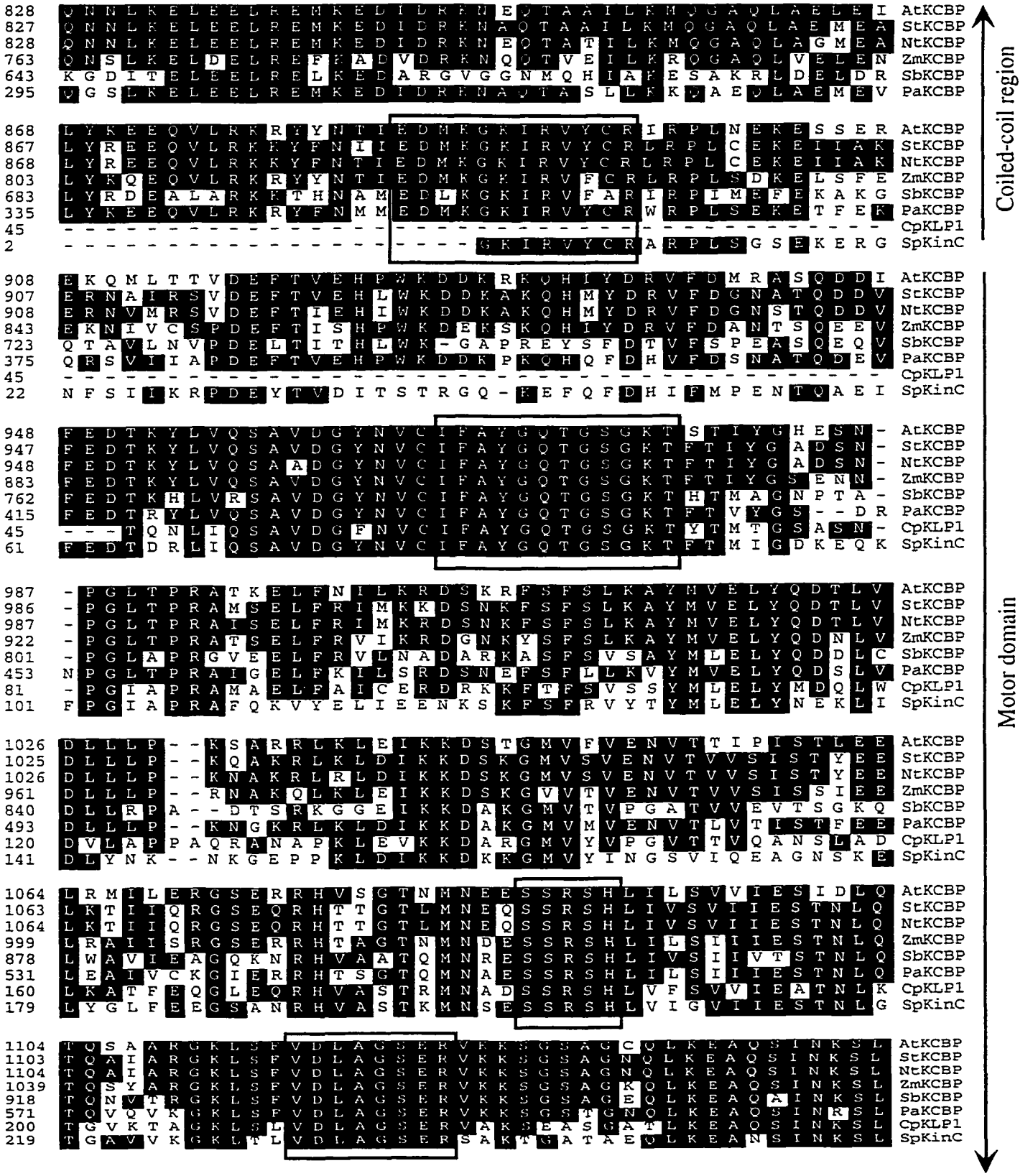

Fig. 47

Fig. 47 **Alignment of KCBP.** The available protein sequences of eight CaM-binding KLPs from phylogenetically divergent species were aligned using Megalign program. In the case of CpKLP1 and SpKin C, only the motor domain and the CBD are used in comparison. In the case of PaKCBP, the motor domain, the coiled-coil region and the CBD are used in comparison. Identical residues in more than three proteins were shaded. Gaps in the alignment are denoted by dashes. The four highly conserved regions in the motor domain of all KLPs and in the neck region of KCBPs are boxed. Numbers at left represent the amino acid residues. The names of the corresponding proteins were shown at the right: AtKCBP (*Arabidopsis thaliana*), StKCBP (*Solanum tuberosum*), NtKCBP (*Nicotiana tabacum*), ZmKCBP (*Zea mays*), PaKCBP (*Picea abies*), SbKCBP (*Stichococcus bacillaries*), CpKLP1 (*Cyanophora paradoxa*)and , SpKin C (*Strongylocentrotus puapuratus).*

Table (9): Percent of similarity in the calmodulin-binding domain (23 aa residues)of CaM-binding KLPs using Clustal method.

	AtKCBP	NtKCBP	StKCBPP	ZmKCBP	PaKCBP	SbKCBP	CpKLP1	SpKinC
AtKCBP		78.3	78.3	69.6	65.2	50	30.4	30.4
NtKCBP			95.7	65.2	78.3	54.5	34.8	30.4
StKCBPP				65.2	78.3	54.5	39.1	30.4
ZmKCBP					60.9	40.9	39.1	39.1
PaKCBP						50	30.4	34.8
SbKCBP							18.2	22.7
CpKLP1								35
SpKinC								

Table (10): Percent of similarity in the coiled-coil region of CaM-binding KLPs using Clustal method.

	AtKCBP	NtKCBP	StKCBPP	ZmKCBP	PaKCBP	SbKCBP	SpKinC
AtKCBP		66.8	66.2	55.5	29.8	32.8	12.7
NtKCBP			93	67.2	36.4	35.5	12.6
StKCBPP				66.7	33.2	35	12.2
ZmKCBP					34.7	33.4	12.4
PaKCBP						20.2	15.1
SbKCBP							13.2
SpKinC							

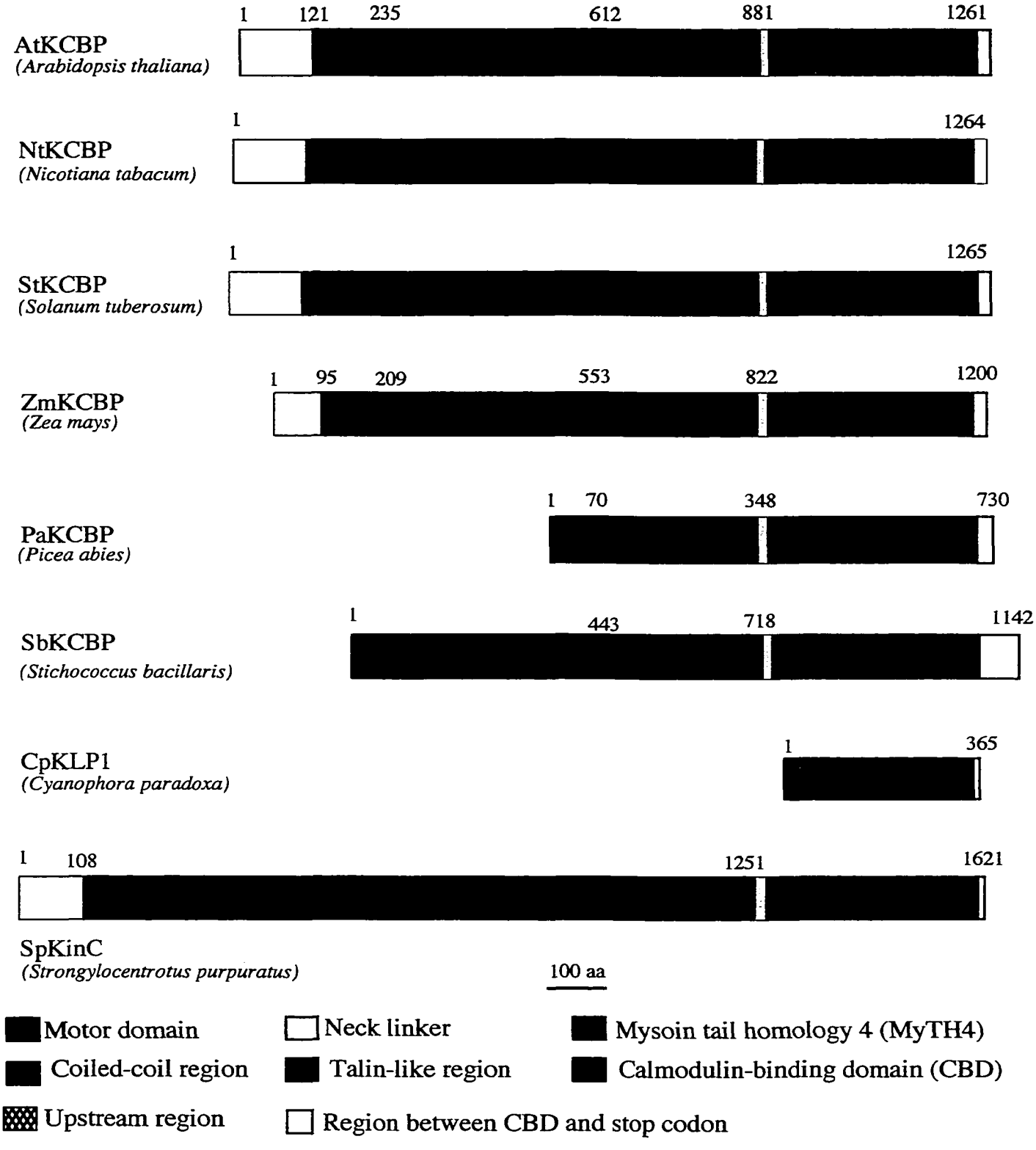

Fig. 48 **Domain organization of CaM-binding KLPs from eight phylogenetically divergent species.** Different domains are color-coded. Numbers represents the amino acid residues. PaKCBP, SbKCBP, and CpKLP1 are partial and lack the N-terminal region. All KLPs were aligned at the end of the CBD for domain length comparison.

domains have not been found in any other KLP including kinesin C, suggesting a functional significance of these regions (Reddy and Reddy, 1999). It will be interesting to see if CpKLP1 has these domains. However, based on the available sequence, it most likely contains these domains, and these domains might have co-evolved with the evolution of KCBP if they were not present in the KCBP ancestor.

KCBPs gene structure

To determine the conservation of the KCBP gene structure (number and length of exons and introns), the genomic sequence of four KCBPs from four phylogenetically *diverged* species was compared (Fig 49). KCBPs from lower organisms (*Cyanophora* and *Stichococcus*) are characterized by large number of shorter exons and introns per kb compared to angiosperm KCBPs. For example, the well defined motor domain of CpKLP1, SbKCBP, ZmKCBP, and AtKCBP has 13, 9, 5, and 5 introns respectively. The extra number of introns reflected the length of the genomic sequence, where about 1100 bp coding sequence of motor domain of AtKCBP and CpKLP1 is equivalent to 1800 and 2490 bp genomic sequence respectively. Also the GC content of exons and introns of KCBPs from lower eukaryotes is much higher than those in angiosperms KCBPs are (Discussed previously).

To study the conservation of intron position in KCBPs, the introns location in four KCBPs was determined (Fig 50). Although the intron position is highly conserved in the KCBP of flowering plants, it is highly divergent in the KCBPs of lower eukaryotes. No single intron position was found to be conserved in all KCBPs. Only the last intron in flowering plants and the one before the last one in *Stichococcus* are perfectly conserved,

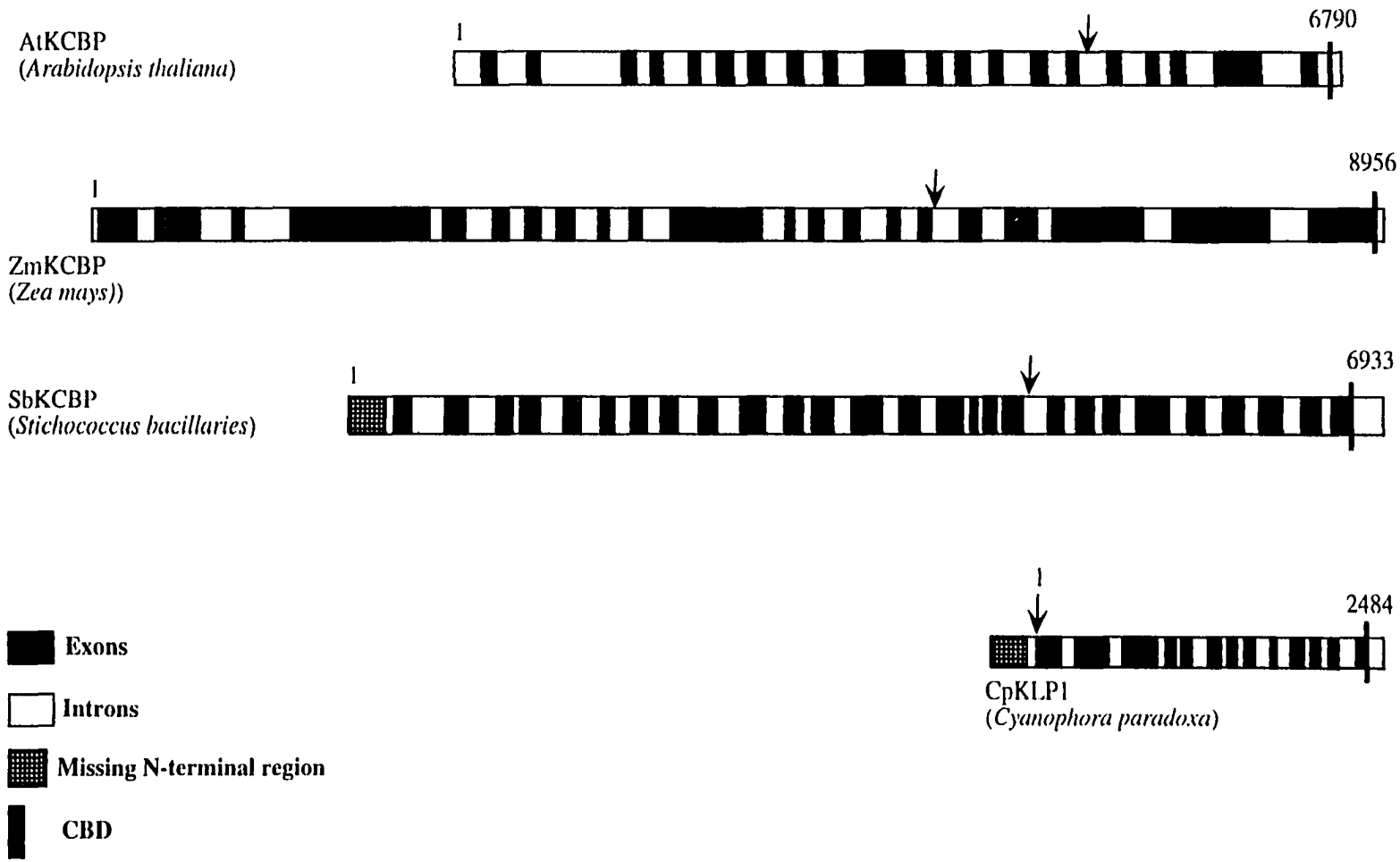

Fig. 49 **Structural organization og KCBPs gene from four phylogenetically divergent species**. Shaded boxes correspond to introns, and open boxes correspond to exons. Missing N-terminal region of unknown length is shown by hatches. Begining of the notor domains was shown by arrows. Numbers at the begining (left) correspond to the sequences at the start codon (in case of AtKCBP and ZmKCBP) or the begining of the available sequence (in case of SbKCBP and CpKLP1). Numbers at the end (right) indicate the location of the stop codon. All structural domains, except the missing sequences are drawn to scale.

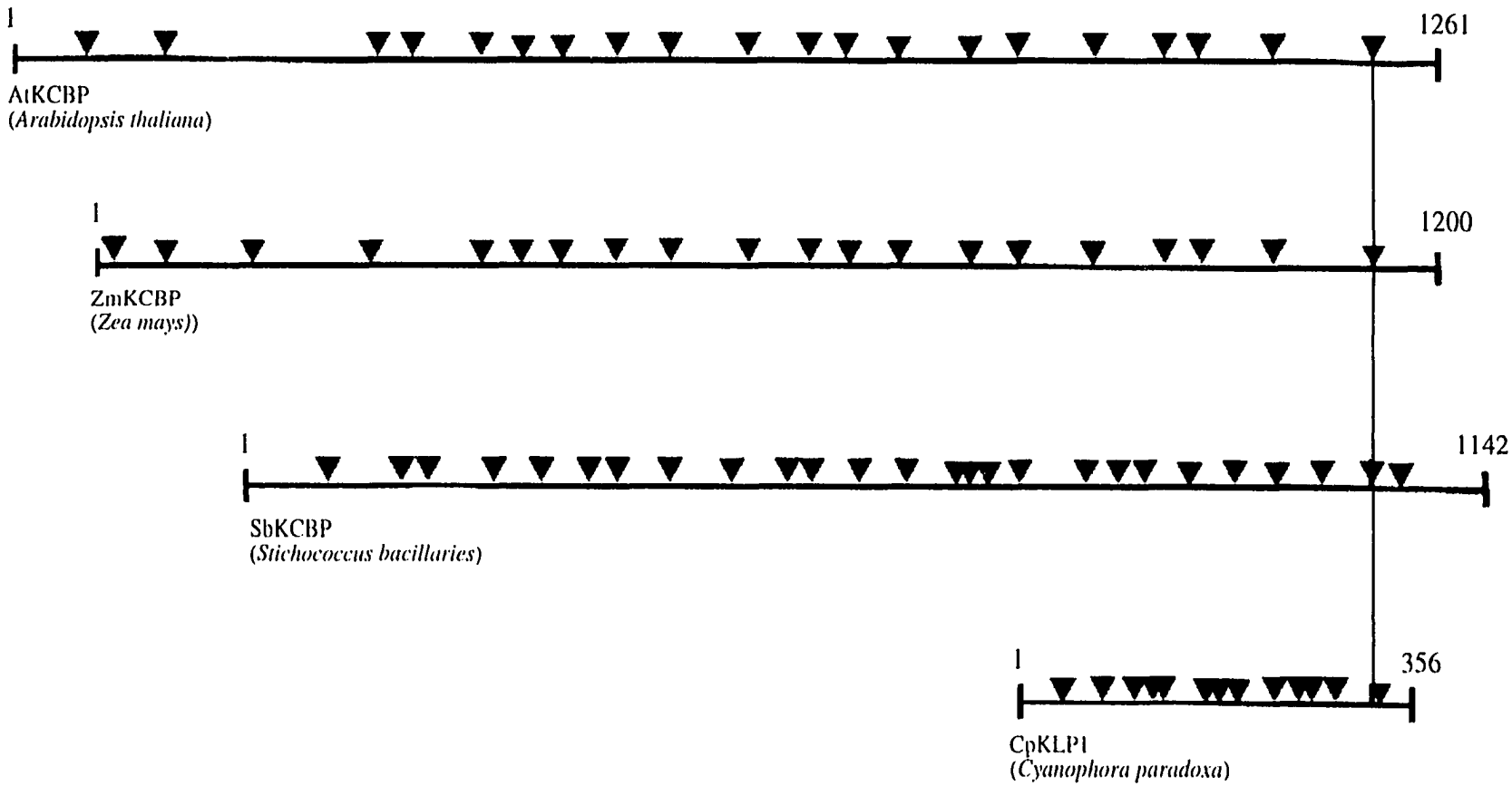

Fig. 50 **Schematic representation of the gene structure of KCBPs from phylogenetically divergent species.** The position of introns is shown by the triangles. The number at the begining (left) correspond to the starting amino acid (M) (in case of AtKCBP and ZmKCBP) or the begining of the available sequence (in case of SbKCBP and CpKLP1). The numbers at the end (right) correspond to the stop codon. The KCBPs were aligned, approximately at a conserved amino acid residue in the CBD (represented by vertical line). All rersidues are drawn to scal.

although it is not conserved in the *Cyanophora*, suggesting the continuous intron addition, deletion and rearrangement. CBD in flowering plants KCBPs is encoded by the last exon although it is interrupted by an intron in both *Stichococcus* and *Cyanophora* KCBPs.

CHAPTER 4

TRICHOME IN ARABIDOPSIS: THE ROLE OF CALCIUM AND CYTOSKELETON

INTRODUCTION

Unlike animal cells, plant cells are constrained within a rigid cell wall and are unable to change shape rapidly or migrate in response to environmental factors. Instead they respond by changing their direction of growth which is believed to be by the orientation of cellulose microfibrils in the cell wall (Kropf *et al.*, 1998). In plants, there are two different modes of cell expansion, namely diffuse growth and tip growth. The direction of diffuse growth is determined by the orientation of the cellulose microfibrils in the cell wall, which are aligned by MTs in the cell cortex. Tip growth, in contrast, is governed mainly by F-actin. Root hairs, pollen tube, and trichomes are three model systems that have been used extensively for the study of morphogenesis at the cellular level. Root hairs and pollen tubes grow predominantly at the tip into simple, tubular, and relatively uncomplicated structures. On the other hand, the trichomes in *Arabidopsis* progresses through a complex series of events before achieving their final stellate shape (Hulskamp and Schnittger, 1998).

Trichome morphogenesis

In *Arabidopsis*, trichomes are unicellular hairs that originate from epidermal cells, they up to 500 μm long and 50 μm wide at their base, and they contain sixteen times more DNA than diploid cells. Trichome development has been divided into a number of stages. These stages include the spatial selection and initiation of a trichome precursor cell (stages 1, 2), its growth into a tubular form (stage 3), followed by a fourth round of endoreduplication and splitting of the tube into a branched structure (stages 4, 5), extension of the branches and their proper orientation with regard to the proximodistal axis of the leaf blade (stage 6), and maturation of the trichome (stage 7) (Huelskamp *et al.*, 1999). It is therefore not surprising that at least 40 genes have been implicated in trichome morphogenesis (Huelskamp *et al.*,

1999). A large collection of *Arabidopsis* mutants affecting different aspects of trichome morphogenesis have been generated (Marks, 1977; Huelskamp *et al.*, 1994). These genes can be grouped into four classes on the basis of their phenotypes: (i) trichome differentiation mutants, which have a reduced size and not fully developed trichomes (Huelskamp *et al.*, 1994); (ii) endoreduplication mutants show a reduced or increased DNA content, and the mutant trichomes are smaller or larger and exhibit fewer or more branches, respectively (Huelskamp *et al.*, 1994; Oppenheimer, 1998; Perazza *et al.*, 1999); (iii) branching mutants which exhibit fewer or more trichome branches (Folkers *et al.*, 1997; Luo and Oppenheimer, 1999); (iv) the directionality of extension growth is impaired in mutants of the distorted (*dis*) group (Huelskamp *et al.*, 1994).

Trichome branching is a complex process and so far eighteen genes have been reported to be involved in trichome branching. In wild-type plants, the leaf trichome undergoes two consecutive branching events, primary and secondary branching. Primary branching produces two qualitatively different stems, a main stem and side stem with an angle of 119 degrees between them. The main stem is pointed toward the distal end of the leaf and undergoes secondary branching. Secondary branching is initiated in a plane perpendicular to the primary branch plane. Secondary branches exhibit an angle of about 83 degrees. Branching mutants can be distinguished into two classes. In one class of mutants, the number of endoreduplication cycles and consequently the DNA content, cell size and branching pattern are affected. This is suggested by two lines of evidence. First, trichome mutants with increased DNA levels such as *triptychon* (*try*), *kaktus* (*kak*), *rastafori* (*rfi*), *polychome* (*pym*) and *spindly* (*spy*) form up to eight branches, whereas trichomes with reduced DNA content such as *glabra3* (*gl3*) exhibit only one branch point and in some cases

no branching (Huelskamp *et al.*, 1994; Perazza *et al.*, 1999). A second line of evidence came from the tetraploid *Arabidopsis*, where trichomes have a DNA content of 64 C and up to eight branches. On the other hand, when DNA replication is inhibited by aphidicolin, the DNA levels in trichomes are drastically reduced and trichomes form fewer branches (Schwab *et al.*, 2000). In the second class of mutants, trichome branch number is altered, but endoreduplication is not changed. Twelve such mutants have been identified. One gene, *NOECK* (*NOK*) is a negative regulator and *nok* has up to seven branches (Folkers *et al.*, 1997). Eight genes, *STACHEL* (*STE*), *ANGUSTIFOLIA* (*AN*), *STHICHEL* (*STI*), *FURCA1* (*FRC1*), *FRC2*, *FRC3*, *FRC4*, and *ZWICHEL* (*ZWI*) are positive regulators of branching (Folkers *et al.*, 1997; Luo and Oppenheimer, 1999). Among the genes implicated in trichome morphogenesis, only three, *AN*, *FRC4* and *ZWI*, seem to be controlled by the negative branch regulator, *NOK*.

In *zwi* mutants, the branching pattern ranges from unbranched trichome (RLD *zwi* 9311-11) to trichomes with two stems of equal length (*zwi*). Genetic analysis shows that branching and growth defects in *zwi* mutants are not restricted to the main stem but also affect the side stem (Folkers *et al.*, 1997). This is suggested by *zwi try* and *zwi nok* double mutants. Whereas *try* and *nok* mutants frequently initiate additional secondary branch points on the side stem, no additional branch points are initiated on either stem in both double mutants. Instead the main stem was found to be twisted (Folkers *et al.*, 1997). Cloning of the *ZWICHEL* gene has revealed that it is a MT motor protein that was previously identified as a CaM-binding kinesin (KCBP) (Reddy *et al.*, 1996b; Oppenheimer *et al.*, 1997). It is, therefore, assumed that this motor protein is involved in either the transport of important

intracellular components and/or in the reorganization of MTs prior to branch initiation (Oppenheimer *et al.*, 1997).

Three suppressors of the *zwichel* (*zwi*) mutant named *suz1*, *suz2* and *suz3*, were identified that recovered the branching defect in *zwi-3* (Krishnakumar and Oppenheimer, 1999). While *suz1* and *suz2* display no obvious trichome phenotype in the absence of *zwi-3*, *suz2* exhibits more branches than wild-type. *Suz2* can also rescue *frc1*, providing a genetic evidence for a functional link between *ZWI* and *FRC1*. *zwi-3 suz1* double mutant, although single mutants of *zwi-3* and *suz1* are fertile, the double mutant exhibits a synthetic pollen tube growth phenotype suggesting a general and redundant role for *ZWI* in pollen tube growth (Krishnakumar and Oppenheimer, 1999).

Calcium and trichome morphogenesis

Cytoplasmic free Ca^{2+} ($[Ca^{2+}]_{cyt}$) plays a key role as a second messenger in many normal growth and developmental processes (Poovaiah and Reddy, 1987; Porter *et al.*, 1993; Reddy, 2001). In the resting state, the concentration of Ca^{2+} in the cytoplasm of plant cells is maintained low in the nanomolar range (100-200 nM), while Ca^{2+} concentration in the cell wall and in organelles is in the millimolar range (Reddy, 2001). In response to signals, $[Ca^{2+}]_{cyt}$ is elevated and this could be due to influx of Ca^{2+} from the apoplast and/or Ca^{2+} release from intracellular stores (ER, vacuoles, mitochondria, chloroplasts, and nucleus). Based on the type of signal or cell type internal and/or external Ca^{2+} stores could be involved in raising $[Ca^{2+}]_{cyt}$ through Ca^{2+} channels, Ca^{2+} ATPases or antiporters. Increase in $[Ca^{2+}]_{cyt}$ is transient and once Ca^{2+} is sensed by Ca^{2+} sensors, it returns to the resting level through efflux into the cell exterior and/or sequestration into cellular organelles. A large number of Ca^{2+} sensors (Ca^{2+}-binding proteins) have been characterized in plants (for review, see (Reddy, 2001).

Binding of Ca^{2+} to Ca^{2+}-sensor protein results in a conformational change in the Ca^{2+} sensor, which, in turn, modulates the activity of the sensor or its ability to interact with other target proteins to modulate their functions/activities.

CaM, a Ca^{2+}-binding protein with four Ca^{2+}-binding EF-hands, is considered to be the primary intracellular Ca^{2+} sensor in all eukaryotes (Poovaiah *et al.*, 1996). In most cases, the activated CaM (Ca^{2+}-bound CaM) interacts with its target proteins to turn the activity on (positive regulator) or off (negative regulator). However, in some cases CaM can interact with its target proteins in the absence of Ca^{2+} (Rhoads and Friedberg, 1997). Myosins, a superfamily of actin-based motors that perform a broad array of cellular functions, bind CaM in the absence of Ca^{2+} (Mermall *et al.*, 1998). In plants, Ca^{2+}/CaM is involved in stabilizing cortical MTs at low Ca^{2+} concentration and destabilizing the same at higher Ca^{2+} concentrations (Cyr, 1991; Fisher *et al.*, 1996). Two CBDs that show different sensitivities to Ca^{2+} are implicated in evoking these two opposing effects of CaM on cortical MTs. A pollen specific CBD from maize, MPCBP, has been cloned and shown to bind CaM in a Ca^{2+}-dependent manner (Safadi *et al.*, 2000). KCBP, a CaM-binding MT motor protein, has been cloned and characterized from various photosynthetic species (Reddy *et al.*, 1996a; Wang *et al.*, 1996; Abdel-Ghany *et al.*, 2000; Abdel-Ghany and Reddy, 2000). The activity of the KCBP is regulated by Ca^{2+}/CaM. Mutants of KCBP (*zwi*) have unbranched trichomes or trichomes with a primary branch point only (Oppenheimer *et al.*, 1997). Because the motor domain of KCBP, which is regulated by Ca^{2+}/CaM, is essential for trichome branching, it is likely that Ca^{2+} through CaM regulates trichome branching (Reddy, 2000). Ca^{2+}, through CaM, inhibits the KCBP motility, MT-dependent ATPase activity and dissociates KCBP/MT complexes. Based on genetic, *in vivo*, and *in vitro* studies with

KCBP, we speculate that artificial elevation in $[Ca^{2+}]_{cyt}$ level might inactivates KCBP and induce the *zwi* phenotype or other phenotypes in wild type trichomes.

To test our hypothesis, *Arabidopsis* seedlings were treated with a Ca^{2+}-gated ionophore (A23187) and ionomycin which are known to increase the $[Ca^{2+}]_{cyt}$ in plant and animal cells and followed the trichome morphogenesis (Bibikova *et al.*, 1999). Since KCBP is involved in MT organization, we also tested the role of MT cytoskeleton in cell morphogenesis by treating *Arabidopsis* seedlings with MT and actin-interfering drugs and studied trichome development.

MATERIAL AND METHODS

Plant materials and growth conditions

Arabidopsis thaliana (Columbia ecotype) was used in our study. Seeds of *zwi* mutants were provided by Dr. David Oppenheimer, University of Arizona, and Dr. Martim Hulskamp, Germany. Seeds were surface sterilized with 15% bleach and washed three times with sterile deionized water. After the final wash, the seeds were plated on MS medium (Murashige and F., 1962); GIBCOBRL, life Technologies) supplemented with 3% sucrose and 0.7% phytoagar (GIBCOBRL, Life Technologies). Plates were incubated at 4 ^{0}C for 2 days and then placed in a tissue culture room at 22-25 ^{0}C, under 16-hour light/8-hour dark conditions.

Ionophores and CaM antagonists treatment

Twenty-five seedlings (4- to 6-days old) with the first pair of developing leaves were selected for treatments. Ca^{2+}-gated ionophore (A23187) and ionomycin (Sigma) were diluted from a 10 mM stock in DMSO. Trifluoperazine (TFP, Sigma) and chlorpromazine (CP,

Sigma) were diluted from 100 mM stock in DMSO. Naphthalenesulfonamide derivatives (W-5 and W-7, Sigma) were prepared from 10 mM stock in H_2O. Thapsigargin (Calbiochem) was prepared from 500 μM stock in DMSO. A 2-μl drop of either ionophore or ionomycein (10 μM in 0.1 % DMSO supplemented with 5 mM $CaCl_2$), TFP or CP (40 μM in 0.1% DMSO), W-5 or W-7 (150 μM in H_2O), 1μM thapsigargin in (0.1% DMSO) were placed on the adaxial surface of the developing first leaves pair while watching under a dissecting scope. Plates were kept in the growth chamber for 96 hours at 100% humidity. For each treatment, one half of the seedlings was randomly chosen for counting the trichome number and branch points and the second half was used for scanning electron microscopy, when needed. All experiments were repeated at least three times. As controls, seedlings were treated with 0.1 % DMSO the same way. Also as a positive control for CaM antagonists, we tested the effect of these antagonists on auxin-induced elongation of *Zea mays* coleoptiles.

Effect of CaM antagonists on auxin-induced elongation of corn coleoptile

Corn seeds were sown in plastic trays containing few layers of Whatman filter paper and kept in the dark for about 5 days. One cm segments of dark grown coleoptiles, excluding 3-mm tip, were excised under a dim green light and transferred to a beaker containing distilled water for 1 hour prior to the treatment. Sets of 10 presoaked coleoptile were transferred to Petri dishes (5 cm diameter) containing 10 ml of incubation medium consisting of 10 mM KH_2PO_4 (pH 6.3), 1.5 % w/v sucrose, 10 mM sodium citrate, 10 μM NAA, and 0.1 % v/v DMSO. Three different concentrations of CaM antagonists, 1X, 2X, 3X, (1X= the concentration used for the *Arabidopsis* seedlings treatment) were used. All dilutions of the CaM antagonists were made using the same buffer. Coleoptiles were kept in the dark for 18

h and the length was measured using a millimeter graph paper. As a control, set of coleoptiles was kept in NAA-containing buffer without any treatment for the same period of time.

Treatment with cytoskeleton-interfering agents

Twenty seedlings (4-to 6- day old) with a first pair of leaves were placed on a 1 cm sterilized Whatman filter paper strip in a 5 cm plastic Petri dish containing 2 ml of liquid MS medium. Actin depolymerizing agents, cytochalasin D (1, 5 and 10 μM, Sigma), Latrunculin A, (1, 5 and 10 μM, Calbiochem), and MT depolymerizing, Oryzaline, (1 and 5 μM, Dow Flanko), propyzamide, (1 and 5 μM, Chem Service), and Paclitaxol, (1, 5, and 10 μM. Sigma) were used. Actin or MT-interacting drugs were added directly to the liquid MS medium. We used the minimum concentrations that produced a visible effect in a four-day period. Plates were kept in a tissue culture room. As controls, seedlings were placed in liquid MS medium containing 1, 5, and 10 μl of DMSO or ethanol, solvents used in preparing the drugs.

Microscopy and Image processing

Leaves of treated and control plants were fixed in 1 % osmium tetroxide prepared in distilled H_2O using a method of (Parducz, 1967). After one hour fixation at 4 ^{0}C, samples were rinsed two times in H_2O and dehydrated in an ethanol series, starting from 50 up to 100% at 10% increments, 30 min each. Samples were dried in a Polaron critical point dryer for 1 h, gold-sputter-coated to 17 nm thickness with a Hummer VII sputer coater and viewed in a Philips 505 scanning electron microscope. Images were stored as TIF files and processed using the Adobe Photoshop 5.0 program (Adobe System Inc. Mountain View, CA).

RESULTS

Scanning electron microscopy of wild-type and *zwichel* trichomes

To compare wild type (WT) and *zwi* trichomes, SEM pictures for both WT and *zwi* trichomes were taken (Fig 51). The total number of trichomes per leaf and the number of branches were counted using a dissecting microscope (Table 11). Wild-type trichome development has been divided into seven discrete stages based on specific morphological landmarks (Huelskamp *et al.*, 1999). These stages include initiation, elongation, primary branching, secondary branching, extension and maturation to achieve the final stellate shape with precise directions and angles between the branches. Mature WT trichomes of Columbia ecotype have a long stalk (the distance between the primary branch point and the leaf surface) surrounded by 8 socket cells, three branches (two branch points) and in very few cases four branches (three branch points) with pointed ends (Fig 51A).

In *zwi* mutants, the trichomes initiate normally, but the stalk is very short and the primary branch point produces two short blunt-ended branches 180 degrees apart (Fig 51B). In the same mutant, about 46 % of the trichomes have lack with only a primary branch containing a fine tip and a small swelling at the base (Table 11 and Fig 51B). Large numbers of *zwi* mutants have been generated using T-DNA insertion, EMS, or fast neutron. These mutants vary in their trichome phenotype depending on the severity of the mutation. The trichome phenotypes of two mutants have been shown in Fig (51C & D). RLD *zwi* w2 mutants, generated by EMS mutation have two branches, a short stalk and the length of the main branch is varied (Fig 51C). About 4% of the trichomes are unbranched (Table 11). In this mutant the coding sequence of the amino acid seventy-two was changed from CAG (glutamine) to TAG (stop codon) (Oppenheimer, unpublished data), hence, should produce

Fig. 51 **Scanning electron micrograph of wild-type and different *Arabidopsis zwi* mutants.** (A) Wild-type arabidopsis leaf showing wild-type trichome with three branches (two branch points). (B) *zwi* mutant is the first identified *zwi* mutant. It is not characterized at the molecular level. Note that about 46 % of the trichomes are unbranched with swollen base and about 54% of them have one branch point (two branches) with 180 degrees apart. Stalk length is reduced compared to the wild-type. **(C)** RLD *zwi* w2 mutant is generated by EMS mutation. Most of the trichomes (about 97 %) have two branches but the length of the main stem is varied (white arrows). **(D)** RLD 9311-11 mutant, generated by fast neutron bombardment, shows a severe phenotype. Most of the trichomes are unbranched and appear as a spikes with some deformation. Right panel represents magnification of trichomes from the leaves (left panel). Scale bar is shown for each picture.

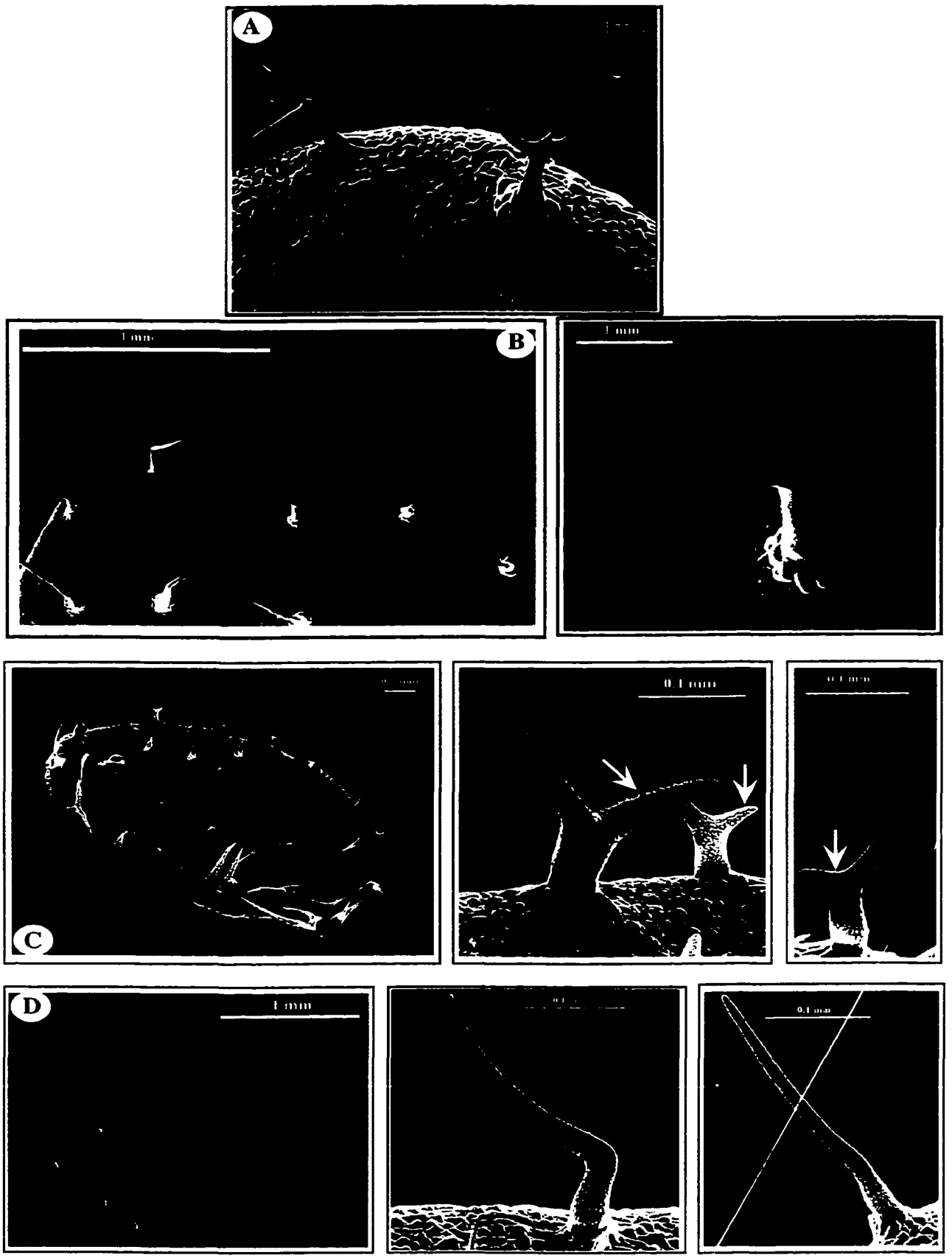

a protein of only 72 aa lacking all functional domains. Based on this we would expect a severe phenotype. However, trichome phenotype is a lot less severe than in other mutants. Hence, it is possible that another methionine down stream, with a newly generated codon, may function and produce a protein lacking only a small region at the N-terminus. In animals, internal ribosomal entry sites are found in proteins involved in cell cycle regulation and apoptosis (Holcik *et al.*, 2000). Also, multiple internal ribosomal entry sites are suggested in human genes to regulate the transcription of specific classes of genes (van der Velden and Thomas, 1999). RLD *zwi* 9311-11 mutant, generated by fast neutron, has a severe phenotype (Fig 51D). About 70% of the trichomes are unbranched with some deformation, and the other trichomes (30%) have two branches with a phenotype that is similar to the *zwi* phenotype (Table 11 and Fig 51D). There is no significant difference in the number of trichomes per leaf in WT and *zwi* mutants suggesting that *ZWI* is either not necessary for trichome initiation or these alleles do not affect trichome initiation.

Changes in cytosolic calcium concentrations alter trichome morphogenesis

In vitro analysis revealed that ZWI/KCBP is negatively regulated by Ca^{2+}/CaM. Also from *zwi* mutants analysis it is assumed that ZWI/KCPBP is partially working in *zwi* mutants, and therefore there are different phenotypes depending on the severity of the mutation. To further confirm the role of ZWI/KCBP in trichome morphogenesis and to determine if there are other Ca^{2+}-regulated processes that regulate trichome morphogenesis, we treated *Arabidopsis* WT seedlings with Ca^{2+} ionophore (A23187), ionomycin and CaM antagonists. Ionophores are known to increase the cytosolic Ca^{2+} concentration (Bibikova *et al.*, 1999). Treatment of *Arabidopsis* seedlings with this agent affects trichome number, and branching, as well as morphology (Table 11 and Fig 52A-H). The effect is variable

depending on the stage of trichome development. The number of trichomes has been reduced significantly (about 37% reduction) compared to the WT. In terms of branching, about 15% of the trichomes are unbranched and appear as spikes with blunt ends. These unbranched trichomes are not straight and mostly resemble those observed in the severe phenotype of *zwi* (RLD *zwi* 9311-11). About 15% of the trichomes have two branches (one branch point). In addition to the severe *zwi* phenotype, which represented by unbranched trichomes and trichomes with one branch point, other phenotypes also were observed. Some of the trichomes are aborted, represented by small bulge with two little extensions (Fig 52E). In other cases trichome precursors did not initiate trichomes suggesting that Ca^{2+} through ZWI or through some other means affect trichome initiation (Fig 52A). Some trichomes have very short and swollen stalks with two branches that resemble trichomes of *distorted 1* (*dis1*) mutants (Fig 52G). Trichomes did not elongate straight but they are short and twisted with blunt ends (Fig 52H). These trichomes have little bulges, which may represent branch initiation but no extension (Fig 52B & H)) suggesting that *zwi* or other processes are affected by Ca^{2+} concentration participate in branch extension. High cytosolic Ca^{2+} may affect cytoskeletal elements or cytoskeleton-associated motor proteins. Trichomes, which are developed later after ionophore treatment, show different phenotypes. Trichomes are twisted and irregular in their growth and some of them are larger in size than WT (Fig 52F & H). However, their stalks are short and thick, compared to control ones. In a few cases new secondary branch points were developed that produced extra branches. Trichomes that are larger in size have extra branches confirming the relationship between cell size/growth and secondary branch point formation. Distance between primary branch point and secondary branch point is longer than in the control. These phenotypes collectively suggest that Ca^{2+}

Table (11): Average number of trichomes on fully expanded first leaf pair of wild type, *zwi* mutant alleles and in wild-type leaves treated with various chemicals. Trichomes from twenty-five leaves were counted for each line or treatment.

Genotype	number of branch points (%)			Number of trichomes /leaf
	0	1	2	
Wild type	0.0	0.0	100	32.2 ± 1.8
zwi mutant	46.3	53.7	0.0	30.2± 1.4
RLD zwi w2	3.7	96.3	0.0	28.0 ± 1.2
RLD zwi 9311-11	69.8	30.2	0.0	31.1 ± 0.9
Ionophore (10 μM)	15.4	15.4	69.2	20.3 ± 1.0
W7 (400 μM)	0.0	0.0	100	34.0 ± 1.6
CP (500 μM)	0.0	0.0	100	32.2 ± 1.3
TFP (500 μM)	0.0	0.0	100	30.7 ±1.8
Thapsigargin (500 nM)	0.0	0.0	100	32.5 ± 0.7

Fig. 52. **Effect of Ca^{2+}-gated ionophore (A23187) on *Arabidopsis* trichome development.** 4-6 day-old *Arabidopsis* seedlings were treated with 2 μl drop of 10 μM ionophore (A23187) supplemented with 5 μM $CaCl_2$. **(A-H)** Scanning electron micrograph showing different phenotypes associated with ionophore treatment. **(A)** SEM picture for a seedling showing the first and second pair of leaves after 4 days of treatment. The first pair was subjected for treatment and so showed severe phenotypes, while the second pair was developed after treatment and therefore showed less effect. **(B)** Magnified SEM picture of one leaf of the second pair showing different phenotypes. **(C)** Higher magnification of a part of the leaf showing three different types of phenotypes. **(D, E)** Two areas in figure **C** (shown in squares) are magnified showing bulges with little extension (**E**, arrowheads) and branch initials that did not extend (**D**, white arrows). **(F)** Magnified trichomes showing new secondary branch points, deformation in the width and length of the stalks. **(G)** SEM for part of a leaf showing the distorted phenotype. Trichomes have very short and swollen stalk with two short branches. **(H)** SEM of unbranched, twisted trichome with blunt end and aborted branch points (white arrows). Scale bar is shown.

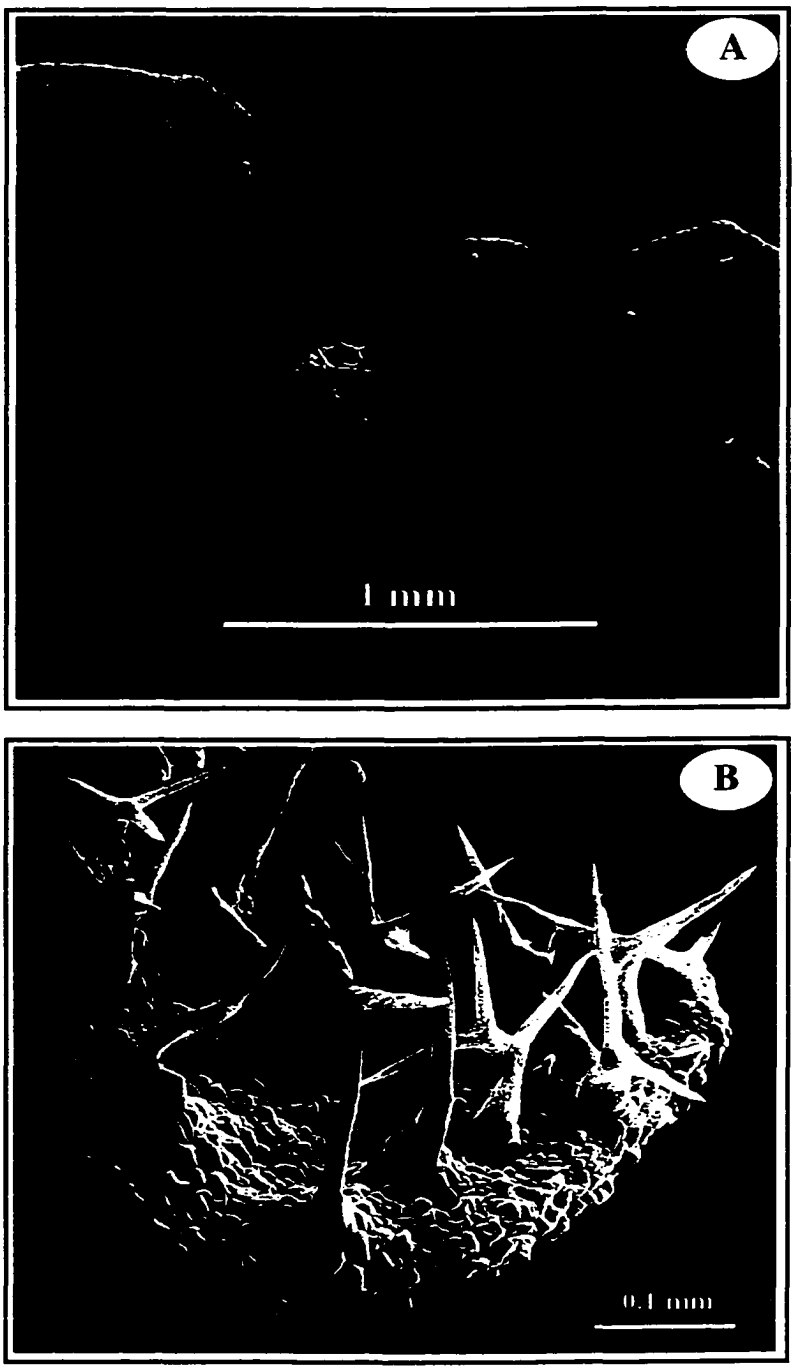

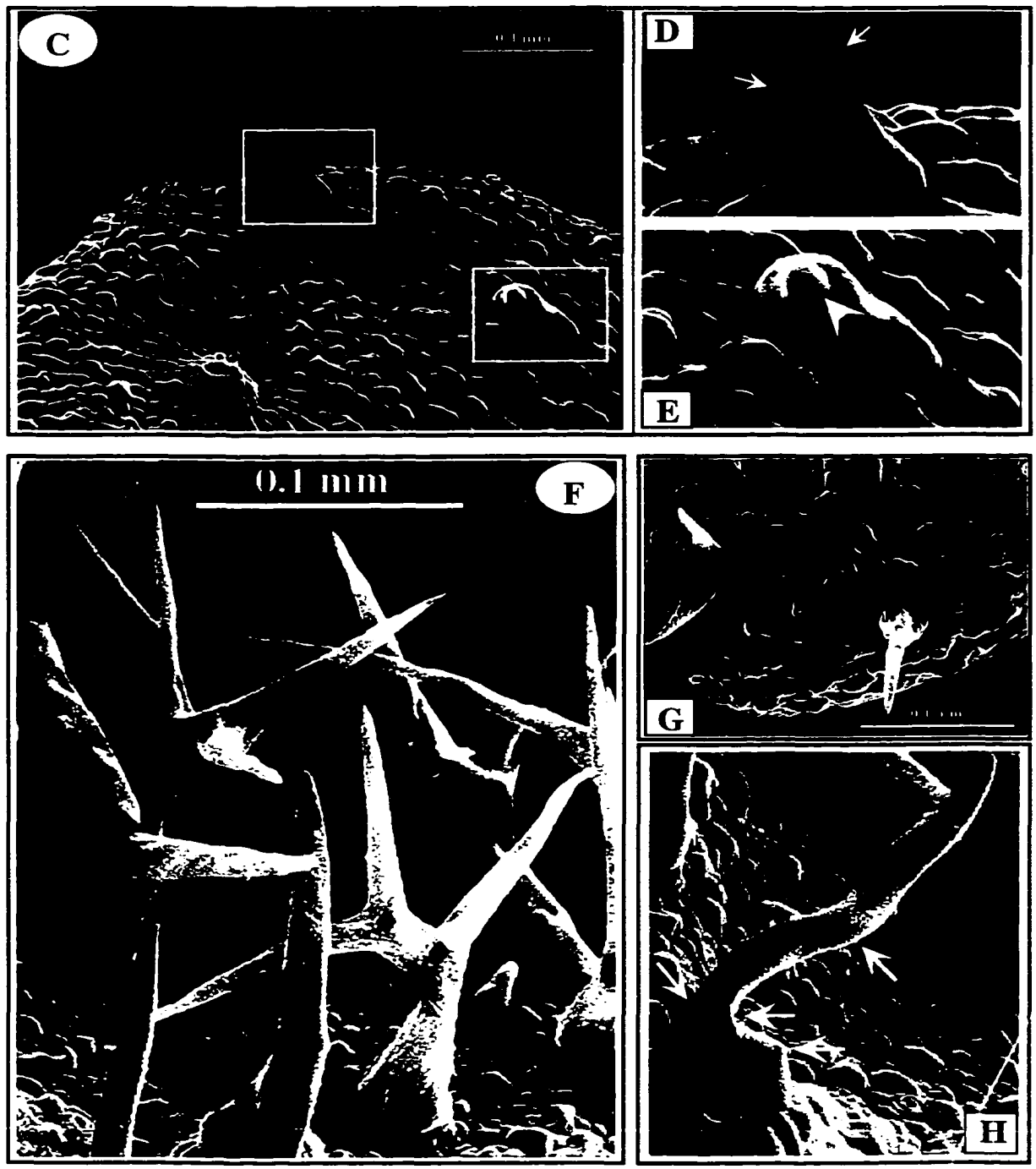

concentration through KCBP or through some other mechanisms affect different stages of trichome morphogenesis and the effect is dose dependent because the newly developed leaves after treatments showed less severe phenotypes. In case of ionomycin treatments similar phenotypes were observed, including trichomes with two branches as well as aborted trichomes, but the phenotypes are less severe than that in ionophore treatments (Fig 53). Increasing the ionomycin concentrations more than 10 μM affected the plant growth. On the other hand, all CaM antagonists that were used did not affect trichome morphology or trichome number (Table 11). These agents were applied at 10 times of their Ic_{50} concentration. As a positive control, we tested the effect of these CaM antagonists on the auxin-induced elongation of corn coleoptile (Fig 54). It has been shown that CaM-antagonists inhibit auxin-induced elongation in maize coleoptile (Raghothama *et al.*, 1985). The addition of increasing concentrations of CaM antagonists to the incubation medium progressively decreased auxin-induced elongation in corn coleoptiles confirming that these agents are effective.

Importance of MT dynamics in trichome morphogenesis

It is proposed that ZWI/KCBP has a role(s) in MT organization during cell division and trichome morphogenesis (Reddy and Day, 2000). To confirm the role of MT cytoskeleton in trichome morphogenesis we treated *Arabidopsis* seedlings with MT stabilizing (taxol) and MT depolymerizing (oryzaline and propyzemide) drugs (Fig 55, 56 & 57). All treatments led to loss of polar growth and to the formation of balloon-like structures depending on the developing stage of trichomes. Trichomes at the distal part of the leaf have branches with little deformation. Trichome cells that are affected at an early stage of development merely formed distended bulges, while trichome cells at later stages of

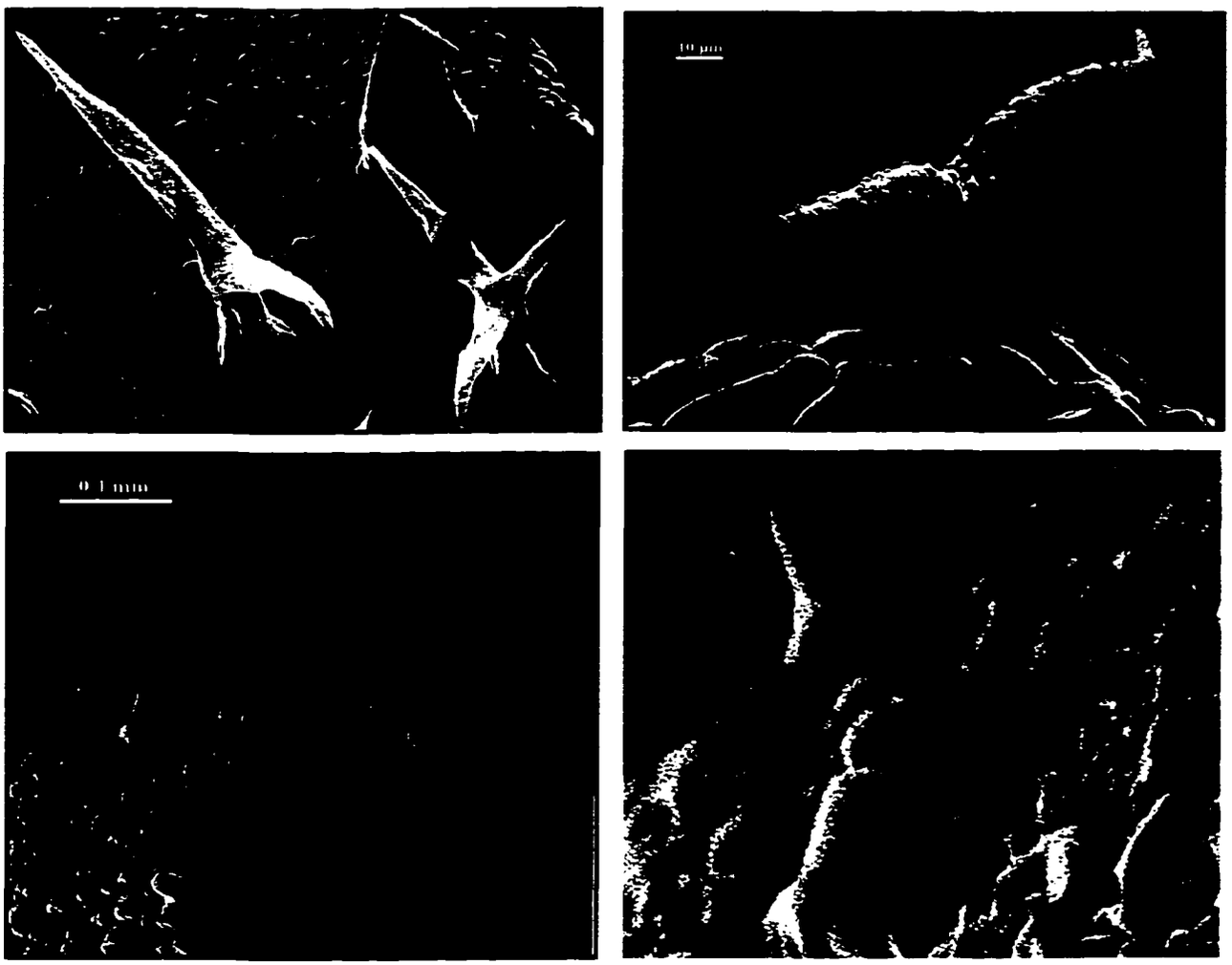

Fig. 53 **Effect of ionophore on *Arabidopsis* trichome morphogenesis.** 4 to 6 days-old *Arabidopsis* seedlings were treated with 2 µl drop of 10 µM ionomucein supplemented with 5 mM $CaCl_2$. After 4 days of incubation in growth chamber, leaves were used for Scanning electron microscopy (see methods section). Left panel represents magnified trichomes. Scale bars are shown.

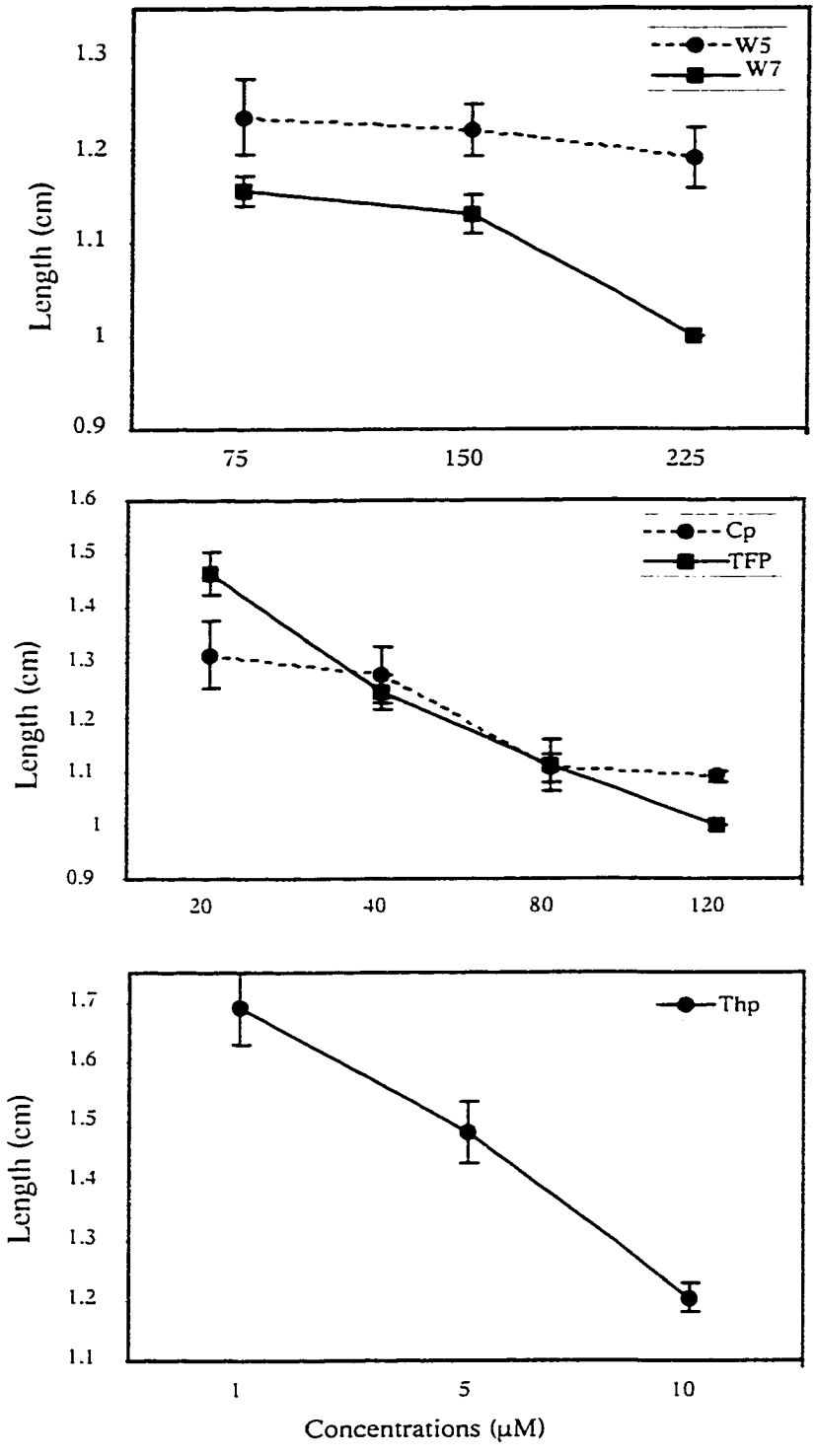

Fig. 54 Efect of CaM antagonists on NAA-induced oat coleoptile elongation. 1 cm long coleoptile segments were incubated in the dark or 18 h at room temperature. The CaM antagonists were added to the incubation medium at the begining of the incubation (see mathods section). The values represents the average elongation of 20 coleoptile segments. Cp (chloropromazine), TFP (Trifluoperazine), Thp (Thapsigargin). The vertical bars represent SE

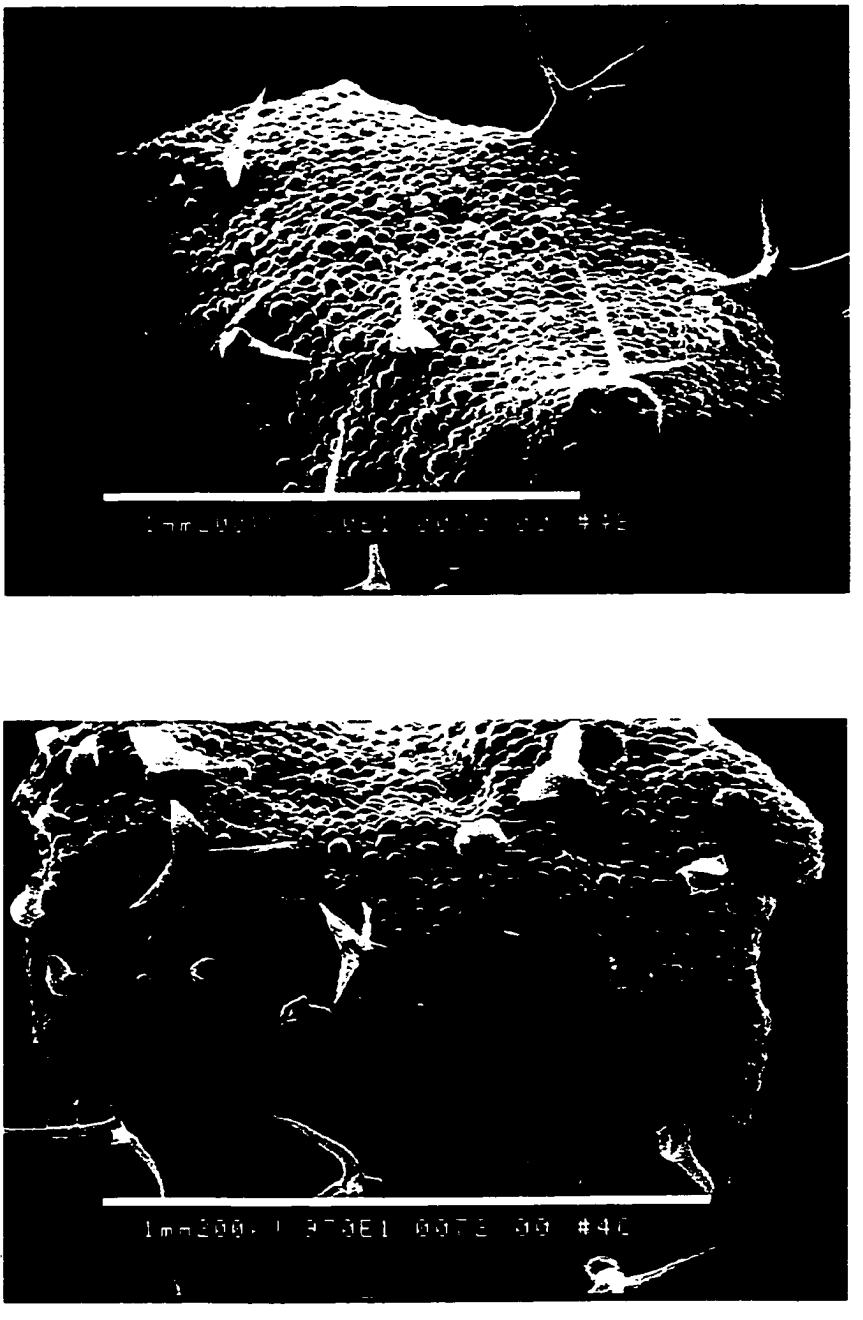

Fig. 55 Effect of microtubule stabilizing drog (taxol) on *Arabidopsis* trichome morphogenesis. *Arabidopsis* seedlings (4 to 6 day-old) were treated with 5 and 10 μM taxol for 4 days and then used for scanning electron microscopy. Scale bars are shown

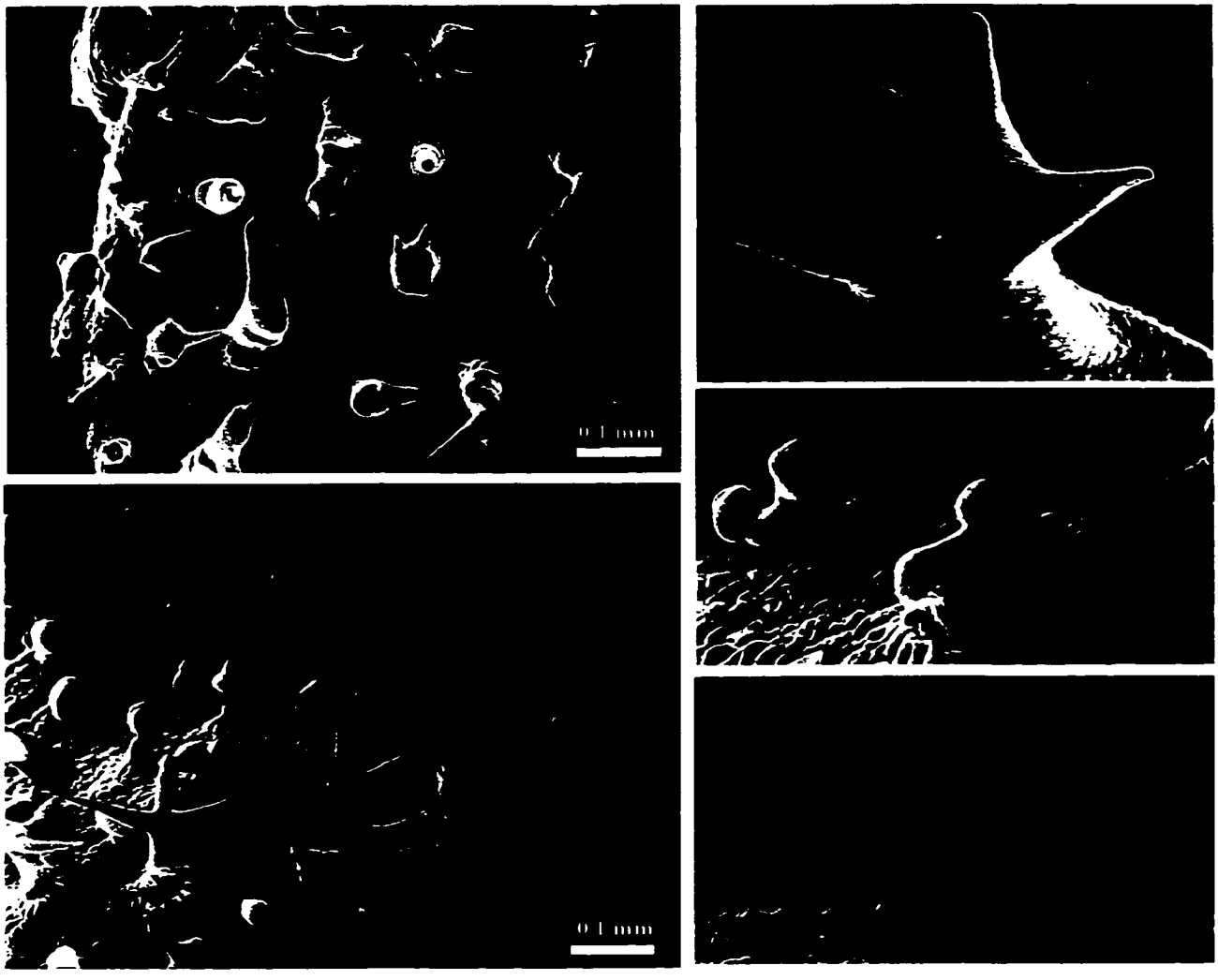

Fig. 56 **Effect of microtubule destabilizing drug (Propyzamide) on *Arabidopsis* trichome morphogenesis**. *Arabidopsis* seedlings (4 to 6 day-old) were treated with 5 μM propyzemide for 4 days and then used for scanning electron microscopy. Note that the branch formation was inhibited and balloon-like structures have been formed. Right panel shows magnified trichomes from the left panel pictures. Scale bar is shown for each picture.

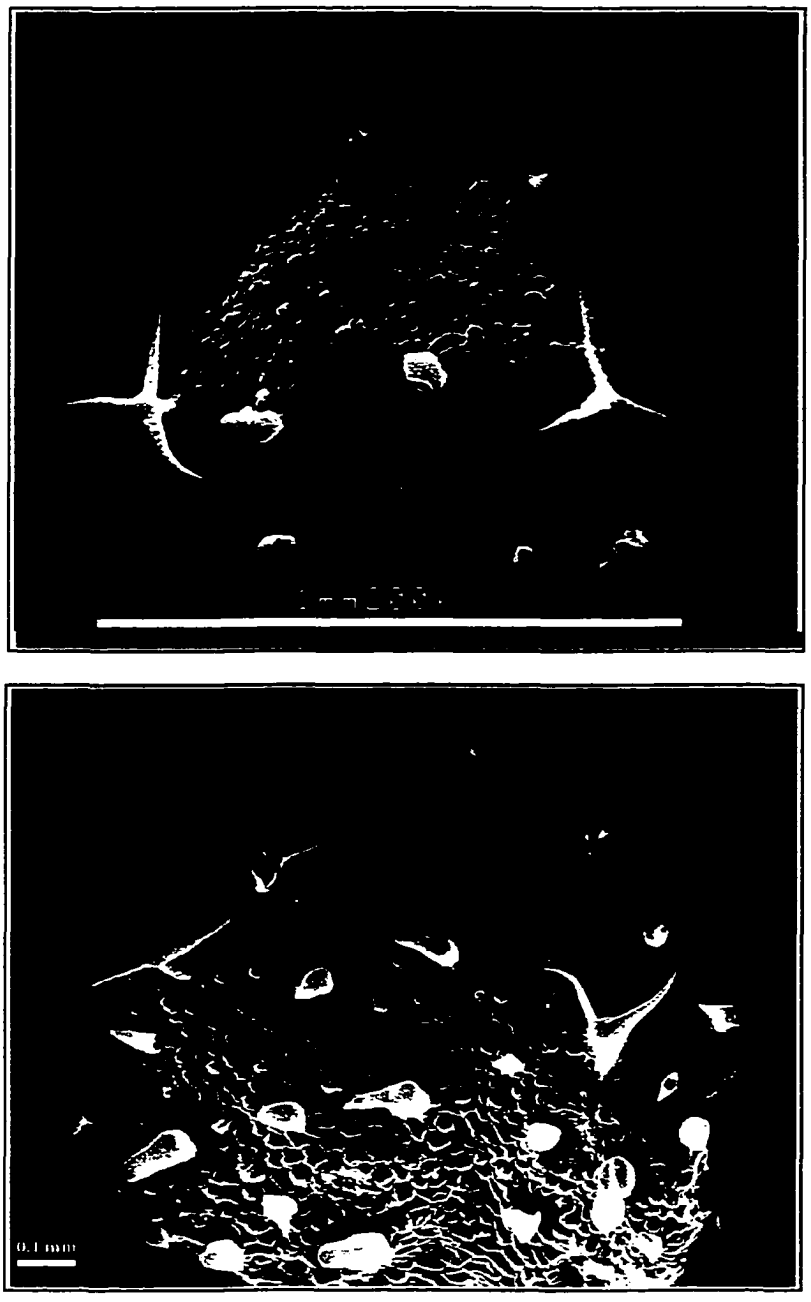

Fig. 57 **Effect of microtubule destabilizing drug (Oryzalin) on *Arabidopsis* trichome morphogenesis.** *Arabidopsis* seedlings (4 to 6 day-old) were treated with 5 μM oryzalin for 4 days and then used for scanning electron microscopy. Note that the trichomes show different abnormal phenotypes depending on their developmental stages. Scale bar is shown.

development characteristically produced a subapical or mid-line bulges. The trichomes that are formed at the leaf base are more severely affected, lost their normal shape completely and could be distinguished from other epidermal cells only by their enlarged size and a roughly triangular appearance. In all cases branching of the trichomes was severely impaired. These results indicate that the MT dynamics determines the basic architecture of trichome by controlling both stalk formation and branch initiation. The *fass* mutant, which is defective in MT organization, has unbranched trichomes similar to phenotypes observed in *zwi* and *sti*, suggesting that MT organization is important for normal trichome development.

Treatment with actin interfering drugs distorts trichomes

Two well-characterized actin interfering drugs, cytochalasin-D (CD) and Latrunculin-A (Lat-A), were used to treat seedlings of *Arabidopsis* (Fig 58A & B). These drugs showed little/ no effect on the initial outgrowth of the trichomes, but severely affected the later stages of trichome morphogenesis and caused formation of aberrant trichomes with distorted phenotypes, even on the same leaf. These distorted phenotypes ranged from a completely ballooned cell with no distinct branching point, to trichomes in which one primary branch extends unidirectionally and disproportionately at the expense of the other. These distorted phenotypes closely resemble those formed in mutants of "distorted class". Actin organization has been studied in six trichome distorted mutants (Mathur *et al.*, 1999). These mutants were found to have a defect in actin organization compared to WT trichomes. These findings indicate that the functional actin cytoskeleton is essential for the later stages of trichome morphogenesis and for branch elongation.

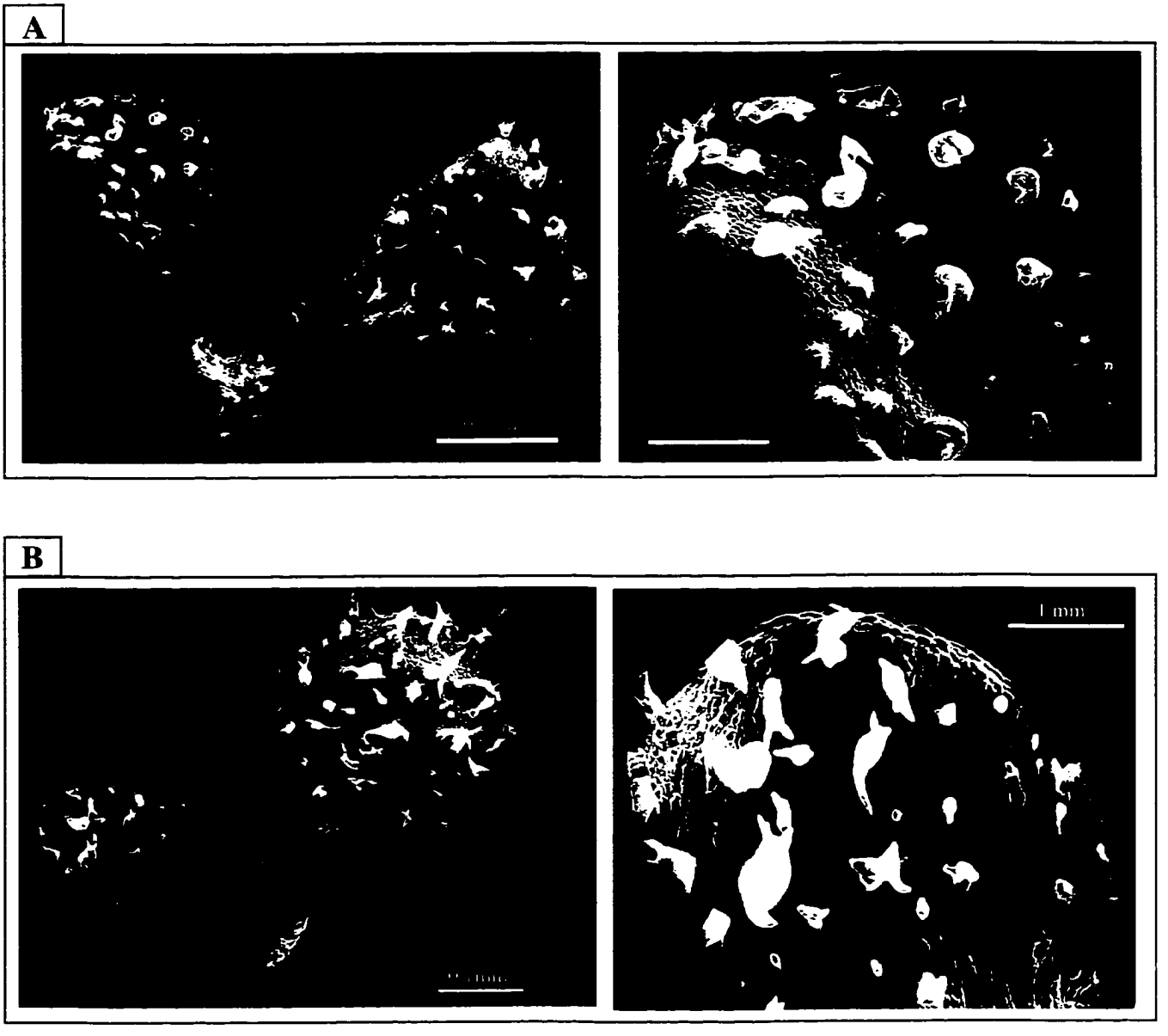

Fig. 58 **Effect of actin-interacting drugs on *Arabidpsis* trichome morphogenesis.** *Arabidopsis* seedlings (4 to 6 day-old) were incubated in MS medium supplemented with actin-interferring drugs, cytochalasin D (CD) or Latrunculuin A (Lat A) for 4 days. **(A)** Scanning electron micrographs of 5 μM CD-treated seedlings **(B)** Scanning electron micrographs of 5 μM Lat A-treated seedlings. Note the distorted trichome phenotype in both treatments. Scale bars are shown.

DISCUSSION

Increase in cytosolic Ca^{2+} affects trichome morphogenesis

Genetic and biochemical studies with *zwi* imply a role of KCBP/ZWI in trichome morphogenesis. To investigate the involvement of Ca^{2+} in trichome morphogenesis, *Arabidopsis* seedlings were treated locally with the Ca^{2+}-ionophore (A23187) and ionomycin. These chemicals, especially, the ionophore have been used widely to artificially increase the cytosolic Ca^{2+} concentration. In root hair and pollen tube Br-A23187 was used to generate a $[Ca^{2+}]_{cyt}$ gradient (Bibikova *et al.*, 1999). Ionophore treatment has resulted in changes in trichome number and trichome morphology (Table 11 and Fig 52). Different levels of *zwi* phenotypes have been observed ranging from unbranched trichomes to trichomes with one branch point. In addition, other phenotypes that have not been observed with *zwi* mutations have been observed in our treatment. These phenotypes range from uninitiated trichomes, aborted trichomes represented by a bulge with little extension, distorted trichomes with very short and swollen stalk, twisted trichomes, to trichomes with larger size and more branch points than the untreated ones. These phenotypes closely resemble phenotypes produced by mutants other than *zwi*. High $[Ca^{2+}]_{cyt}$ might affect trichome morphogenesis either by affecting KCBP function(s) or through other Ca^{2+}-regulated events such as cyclin-dependent protein kinases (cDPKs), other CBDs or myosins.

ZWI/KCBP is involved in different aspects of trichome development and a minimum threshold of its function is necessary to produce the wild-type trichomes. (Krishnakumar and Oppenheimer, 1999). All *zwi3* suppressors are only partial suppressors (the branch number defect is suppressed, but the short stalk defect is not) suggesting, that ZWI regulates branch position and branch number in two separate processes or these two stages requires two

different functional domains of ZWI/KCBP. Krishnakumar and Oppenheimer. (1999) hypothesized that control of branch position may require ZWI/KCBP motor function, which is lacking in *zw3* mutants, but branch initiation does not require motor function and a functional tail domain is enough to rescue the branch initiation defect. Therefore it is reasonable to predict that blocking of ZWI/KCBP completely will produce other phenotypes. *ZWI* function has been shown to be controlled by the negative branch regulator NOECK (Hulskamp, 2000) and spatial trichome morphology depending on the balance of their activities

ZWI encodes a kinesin-like protein containing a CaM-binding domain at the C-terminal region and myosin-tail homology 4 (MyTH4) and talin-like region at the N-terminal region (Reddy *et al.*, 1996b). KCBP is a minus-end directed motor protein, contains two MT-binding sites, and shows in vitro MT bundling in the presence of either Ca^{2+} or CaM (Reddy *et al.*, 1996b; Kao *et al.*, 2000). The characteristic features of ZWI/KCBP strongly suggests that the reduced growth and branching competence in *zwi* mutants are a result of impaired directional transport of cellular factors to spatially defined regions or improper organization of MTs (Oppenheimer *et al.*, 1997; Reddy and Day, 2000).

Six mutants belonging to the distorted class have been studied, and all of them show a defect in actin organization (Mathur *et al.*, 1999). The fact that ZWI/KCBP has myosin tail homology 4 (MyTH4) and talin-like region characteristic of some myosins suggests that this protein may, in some way, interact with actin filaments to cross-bridge these cytoskeletal elements or to facilitate cargo exchange between MT and actin-based motor proteins (Reddy and Reddy, 1999). Therefore distorted phenotypes observed in our experiment might relate to distorted actin organization by non-functional ZWI. Another possibility is that increased

Ca^{2+} might affect trichome morphogenesis by inhibiting the actin-based motor protein or affect actin organization. A number of reports have been shown that the cytoplasmic streaming and movement of organelles along actin cables in pollen tubes, trichomes, leaf cell and stamen hair cells are inhibited by Ca^{2+} (Doree and Picard, 1980; Kikuyama and Tazawa, 1982; Woods *et al.*, 1984; Hepler and Callaham, 1987; Shimmen and Yokota, 1994; Yokota *et al.*, 1999). In an *in vitro* motility assay, Ca^{2+} has been shown to inhibit the motility and actin-dependent ATPase activity of myosin I and causes dissociation of the bound CaMs leading to inhibition of movement (Collins *et al.*, 1990; Wolenski *et al.*, 1993). Recently, an 18-kD polypeptide, which is likely to be CaM was isolated from lily pollen tubes (Yokota *et al.*, 1999). The polypeptide can bind myosin heavy chains at low Ca^{2+} level and induces motility. However, at high Ca^{2+} concentration it dissociates and irreversibly inhibits the motile activity of myosin (Yokota *et al.*, 1999). Further experiments using the similar kinds of treatments on transgenic *Arabidopsis* having GFP-tubulin, GFP-actin and GFP-ZWI/KCBP should provide clear insights into the role of ZWI/KCBP in trichome morphogenesis.

MTs and microfilaments have distinct roles in trichome morphogenesis

Studies with MT or actin interfering drugs indicated that MTs play an important role during early stages of trichome development and actin microfilaments are required for later stages of development. Treatment with MT drugs has clear effect of the initial stages of trichome development. Trichome cells appear as swellings with little polarized growth following oryzaline, propyzemide and taxol treatment (Fig 55,56&57). It appears that the *Arabidopsis* trichome initial grows in a polar fashion by diffuse growth in a manner similar to that described for cotton trichomes (Hulskamp and Schnittger, 1998). The direction of

diffuse growth is determined by the orientation of cellulose microfibrils in the cell wall, which in turn are guided and aligned by cortical MTs (Kropf *et al.*, 1998). Treatment with MT depolymerizing agents causes depolymerization of this cortical MT arrays resulting in the isotropic expansion of trichome initials and the appearance of swollen forms. It is likely that during the formation of branch points on the tubular trichome initials, the MTs reorganize to direct the growth. MT reorientation can be accomplished by either depolymerization or repolymerization of the exciting MTs or movement of the existing MTs (Reddy and Day, 2000). In both cases MT stabilizing or depolymerizing drugs will interfere with such reorganization resulting in unbranched or sparsely branched trichomes. Other molecular and genetic studies also indicate the role of MTs in trichome morphogenesis has been reported. *fass (fs)* mutant with defective MT organization during cell division produce unbranched trichomes similar to those found in *sti* and *zwi* mutants (Jurgens *et al.*, 1994; Torres-Ruiz and Jurgens, 1994; Huelskamp *et al.*, 1999). Using *Arabidopsis* plants expressing GFP fused to a MT-associated protein 4 (MAP4), it has been reported that during trichome branching, MTs reorient with respect to the longitudinal growth axis (Mathur and Chua, 2000). ZWI/KCBP is a minus-end directed kinesin like protein, has two MT-binding sites, and shows *in vitro* MT bundling (Kao *et al.*, 2000). Therefore, it is possible that ZWI/KCBP participates in MT reorganization and stabilization *in vivo*. Transient treatment of reduced-branching mutant, *zwi*, and branchless *sti* mutant with taxol initiates new branches (Mathur *et al.*, 1999). However, long term treatment with taxol reduces branching supporting the hypothesis that depolymerization and reorientation of MTs is important for trichome morphogenesis.

Once trichome initials are formed, they extend by tip growth, which is governed by F-actin (Kropf *et al.*, 1998). Longitudinal cables of actin filaments are involved in vesicle transport to the apical dome of pollen tube, fungal hypha and trichome tips and these vesicles disappear in the presence of actin-interfering drugs (Miller *et al.*, 1996; Szymanski *et al.*, 1999). Immunolocalization studies and visualization of actin cytoskleton in live cells with GFP-tagged actin-binding protein indicate that actin filaments are necessary for later stages of trichome development (Mathur *et al.*, 1999; Szymanski *et al.*, 1999). Finally we conclude that both MTs and actin filaments are necessary for trichome morphogenesis either directly to direct the polar growth or indirectly by supporting the motor proteins.

CHAPTER 5

GENERAL DISCUSSION

DISCUSSION

KCBP is present in most primitive photosynthetic eukaryotes

The kinesin-like calmodulin (CaM) binding protein (KCBP), a minus end-directed MT motor protein was previously cloned and characterized from dicot species (Reddy *et al.*, 1996a; Reddy *et al.*, 1996b; Wang *et al.*, 1996). Like other members of the kinesin superfamily, KCBP has three (tail, stalk, and motor) structural domains. In addition, KCBP has two structural features: a CBD, with significant sequence similarity to MyTH4, that is responsible for regulation by Ca^{2+}/CaM and a talin-like region that is also present in some myosins (Chan *et al.*, 1996; Reddy and Reddy, 1999). These features in KCBP are highly conserved among the characterized KCBPs in dicots. Immunolocalization and microinjection studies with KCBP-specific antibody have demonstrated that KCBP is involved in cell division, especially the organization and formation of plant-specific MT arrays and trichome morphogenesis (Bowser and Reddy, 1997; Oppenheimer *et al.*, 1997; Smirnova *et al.*, 1998; Vos *et al.*, 2000). A KCBP ortholog has not been found in the completely sequenced genome of *D. melanogaster*, *C. elegans*, and *S. cerevisiae*. The involvement of KCBP in plant specific-functions and its absence in animals suggest that KCBP may have evolved only in the plant lineage. However, it is not known if KCBP is present in primitive photosynthetic organisms that gave rise to land plants and in the highly evolved monocots. During the course of my research, I investigated the presence of KCBP orthologs in several photosynthetic organisms. I have cloned and characterized KCBP orthologs from phylogenetically divergent species including maize, a highly evolved flowering plant, spruce (*Picea abies*), a representative member of gymnosperms,

Stichococcus, a member of charaphyte algae, the group from which land plants are thought to have arisen, and *Cyanophora paradoxa* (Glaucophyta) the most primitive living photosynthetic eukaryote.

Most phylogenetic analyses of plastid localized or plastid derived genes (Bhattacharya and Medlin, 1995; Nelissen *et al.*, 1995; Zhou and Ragan, 1995), comparison of gene organization (Reith and Munholland, 1993), and nuclear genes (Moreira *et al.*, 2000) support the monophyletic origin of plastids from cyanobacteria about 1.2 billion years ago, with the glaucophytes (e.g. *Cyanophora*) representing the first branch of plastid evolution (Martin, 1998; Cavalier-Smith, 2000; Palmer, 2000). In this phylogenetic clade the charaphycean lineage (green algae) is the closest relative to land plants (Graham, 1993; Kranz *et al.*, 1995). However, which members of the charaphycean algae are the immediate sister group of the land plants is less certain. Based on these phylogenetic studies I chose four organisms, which represent major groups in the evolution of photosynthetic eukaryotes, to study the evolution of KCBP. *Cyanophora* represents a primary stage of plastid evolution, *Stichococcus* represents a transition state between life in the water and on the land and also represents the beginning of phragmoplast formation (Graham, 1993). KCBP has been shown to be essential in the MT arrays in flowering plants. Spruce from gymnosperms represents an intermediate stage between vascular seedless plants and angiosperms.

Molecular cloning and analysis of KCBP from these organisms show that, although photosynthetic eukaryotes evolved about 1.2 billion years ago (Palmer, 2000), the predicted amino acid sequence of KCBP and unique features are highly conserved in all studied species. The highest degree of conservation was observed in the motor domain (Fig 47). The coiled-coil region showed the least conservation, while the class specific neck linker is

mostly identical in all characterized KCBPs. Although the CBD is less conserved, an affinity purified KCBP antibody raised against CBD of *Arabidopsis* KCBP detected a specific expected size band in all tested species including the most primitive *Cyanophora*. The MyTH4 and talin-like region are also present in all KCBPs (Fig 48). These observations suggest that KCBP, with its characteristic domains, may have evolved early along with plant evolution from a single common ancestor to perform plant-specific functions or was present in the host organism before the evolution of plastids. Although the protein is conserved, gene structure (position, length and number of the intervening sequences) is conserved only in the flowering plants but not in the lower organisms. The motor domain of KCBP (CpKLP1) and *Stichocooccus* has 13 and 9 introns compared to 5 introns in the corresponding region of KCBP from monocots and dicots (Fig 49). However, the coding sequence length is about the same in these organisms. In general there is a tendency for reduction of the number of the introns and increase in their length from primitive to most recent organisms. In a survey of intron and exon lengths in different organisms, (Hawkins, 1988) showed that higher organisms including higher plants have mostly larger introns than lower organisms (Hawkins, 1988). For example, in higher plants only one third of the tested introns (219 introns) has 100 nt or less and the mean length is 249 nt with some exceptions (Hawkins, 1988). However, in lower organisms, the average length of introns is 86 nt. Conservation of introns number and location in KCBP of angiosperms suggests that these introns have been acquired during angiosperm evolution and conserved in most of the angiosperms. However, the length of introns is variable (Table 4 & Fig 49). Cloning KCBP genomic sequences from gymnosperms, vascular seedless plants (pteridophytes) and non vascular plants (bryophytes) should define the level of conservation of intron position in land

plants. Conservation of intron position was observed in many genes in the flowering plants and in vertebrates (Kusakabe *et al.*, 1999). Members of the actin gene family and catalase gene family have conserved introns in novel positions as well as some lost introns (Shah *et al.*, 1983; Frugoli *et al.*, 1998). The location of one intron was found to be conserved in the motor domain of KCBP from *Stichococcus* and flowering plants, suggesting the origin of this intron before the evolution of land plants. This result is supported by the existence of two conserved introns in actin-coding region and one conserved intron in the 5'-untranslated region of the actin gene of the green alga, *Mesostigma viride* and the embryophytes (Bhattacharya *et al.*, 1998). Also, three conserved introns have been found in the actin genes of *Cosmarium, Selaginella*, and many members of the tracheophytes (An *et al.*, 1999).

Reduction in the number of introns in KCBP and the lack of conservation in their position is obvious throughout the course of the evolution. This observation raises many questions: (1) Can introns be gained or lost? (2) What are the factors that regulate intron loss and/or gain? (3) What does intron distribution tell us about the evolutionary relationship between organisms? (4) What is the relation between introns and the surrounding coding sequences?. Most of these questions should be answered in the near future as many orthologs from various organisms are characterized and with the availability of sophisticated Bioinformatic tools. However, some assumptions based on limited comparison of genes that explain the origin and distribution of introns, and some of them can explain the evolution of KCBP. It is proposed that introns are inserted randomly in the ancestors, but selection against introns that interrupt domain-encoding regions is active at the level of RNA or protein (Craik *et al.*, 1983; Hickey and Benkel, 1986). Daniels *et al.*, (1985) concluded that "introns that occur between potentially useful domains will add survival value and will

predominate over those that split genes at random locations". In a study of the diversity of intron positions, (Stoltzfus *et al.*, 1997) showed that if all different intron positions published so far for actin genes are packed into hypothetical ancestral gene, they would break up the gene into exons with a median length of only 14 bp, with many minuscule exons (about 26% would be 1-6 bp in length) (Stoltzfus *et al.*, 1997). The author suggested the intron sliding has contributed to the diversity of intron positions (Stoltzfus *et al.*, 1997). In a similar statistical analysis of the exon-intron structure of higher and lower eukaryotic genes, (Kriventseva and Gelfand, 1999) concluded that there is a universal preference for exons with the total length divisible by 3 and introns positioned between codons are preferred, whereas those positioned between the first and the second position in codon are avoided. In case of KCBP from angiosperms, this correlation is clear since about 70% of the introns are inserted between codons compared to 48% and 46% of the KCBP introns of *Stichococcus* and *Cyanophora* KCBPs are inserted between codons. Furthermore, other studies have showed a correlation between the genome size and the total intron length per gene (Deutsch and Long, 1999), and there is a minimum intron size requirement (about 50 nts) for intron splicing. In all cloned KCBP genes, there is no single intron less than 50 nts (Tables 4, 6, 7). In a recent study, a correlation between the length of introns and the codon usage of the coding sequences of the corresponding genes was shown (Vinogradov, 2001), which in some cases can be related to the level of gene expression. This correlation is positive in the case of unicellular eukaryotes and inverted in multicellular organisms (Vinogradov, 2001). GC content in exons and introns of a KCBP gene from lower organisms is significantly higher than the GC content of KCBP in flowering plants (Tables 4, 6 and 7). For example, the GC content of KCBP exons and introns from *Stichococcus* and *Cyanophora* ranged between 50

and 89% with most of them about 70%. However, the GC content of KCBP exons and introns from angiosperms ranged between 24 to 52% with most of them about 40%. Analysis of eight nuclear genes in the insect lineage has shown that the common ancestor has an elevated GC content, and there is preferential replacement involving amino acids encoded by low-GC-content codons (Rodriguez-Trelles *et al.*, 2000).

KCBP, a nuclear-coded single gene, is a good candidate to study the phylogenetic relations among plants

Most phylogenetic studies that support the monophyletic origin of glaucophytes, rhodophytes and green plants are based on plastid-localized or plastid-derived genes. On the other hand, the issue of how these organisms are related has not been well resolved by nuclear gene phylogeny although this interrelationship must be established independently using several nuclear genes. Comparison of actin sequences from different organisms support a monophyletic origin (Bhattacharya and Weber, 1997). On the other hand, nuclear genes encoding small-subunit ribosomal RNA (SSU rDNA) (Fan *et al.*, 1995; Kumar and Rzhetsky, 1996) and the largest subunit of RNA polymerase II (RPB1) (Sidow and Thomas, 1994; Stiller and Hall, 1997) provide strong statistical support for an emergence of the rhodophyta before the common ancestor of animals, fungi and green plants. Therefore, additional nuclear markers clearly are needed to resolve the relationship between the host components of these symbiotic associations. KCBP is a single-copy gene in all broadly studied organisms and it also has conserved domains with highly conserved sequences. These sequences can be used to design PCR primers to analyze KCBP sequences from widely diverged photosynthetic eukaryotes and the nucleotides and protein sequences obtained from such analyses can be used for reconstructing the photosynthetic eukaryotes

relationships. Actin genes are the most extensively used genes in such studies (Moniz de Sa and Drouin, 1996; Bhattacharya and Weber, 1997; Bhattacharya *et al.*, 1998; An *et al.*, 1999). However, in multicellular eukaryotes the actin genes are not single copy genes but they form gene family produced by gene duplication. In the phylogenetic analysis of DNA sequence data, it is important that homologs regions are compared because errors can result from comparison of paralogous sequences which result from gene duplication and subsequent divergence (Li and Grauer, 1991). For this reason, single copy regions are preferred. However, not many single genes that are highly conserved have been used in phylogenetic analysis. More accurately, when a phylogeny is constructed from one gene sequence like KCBP, the resulting tree really represents the history and evolution of that gene, not necessarily the organisms (Li and Grauer, 1991). So other single-copy genes in addition to KCBP gene are also needed for determining the phylogeny of plants.

KCBP and a CaM-binding kinesin from sea urchin (kinesin C) may have evolved by convergent evolution

KCBPs from all studied photosynthetic eukaryotes and kinesin C from sea urchin have a CBD at the C-terminus that responsible for regulating the interaction of the motor domain with MTs in a Ca^{2+}-dependent manner (Song *et al.*, 1997; Deavours *et al.*, 1998b; Narasimhulu and Reddy, 1998; Rogers *et al.*, 1999; Kao *et al.*, 2000). Over 250 KLPs have been characterized from various eukaryotes. However, kinesin heavy chains other than KCBP and kinesin C are not known to bind CaM (Matthies *et al.*, 1993; Reddy *et al.*, 1996b; Rogers *et al.*, 1999). In the phylogenetic tree, kinesin-C groups with KCBPs from photosynthetic eukaryotes in a distinct group within the C-terminal subfamily. Outside the motor domain, there is no sequence similarity between KCBPs and kinesin-C whereas KCBP

tail is highly conserved among organisms. Two evolutionary propositions may explain the relationship between KCBPs and kinesin-C. First, KCBP and kinesin-C are not related and the CBD was added to both of them independently (convergent evolution) during the course of evolution [e.g. as a result of gene transfer (Smith *et al.*, 1992), domain swaps (Doolittle and Bork, 1993), to confer specific Ca^{2+}/CaM-regulation. The arguments in support of this proposition are: the conserved MyTH4 and talin-like regions present in the N-terminal region of all characterized KCBPs are not present in kinesin C (Fig 48); the coiled-coil region spans about 70% of the protein in kinesin C and only about 20% of the protein in KCBPs (Fig 48). KCBP homologs are not found in the completely sequenced genomes of *D. melanogaster*, *C. elegans* and *S. cerevisiae*. Also fusion of the CaM-binding domain from *Arabidopsis* to the motor domain of C-terminal (Ncd) and N-terminal kinesin (DK) of *Drosophila* confers CaM-binding property to these motifs (Kao *et al.*, 2000). The second proposition is that the KCBPs and kinesin-C are related KLPs through divergent evolution from a KLP ancestor before the divergence of plants and animals from a common ancestor, which is believed to have occurred about 1.5 billion years ago (Wang *et al.*, 1999). This could be accomplished by domain insertion or deletion at the amino-terminal region of the motor to carry out specific cargoes or to confer plant-specific functions. The arguments that support the divergent evolution are: the percent of similarity in the motor domain of kinesin C and KCBP is significantly higher than the percent of similarity between the motor domain of KCBP and all other C-terminal KLPs (approximately the same percent of similarity between *Cyanophora* KCBP to other KCBPs) (Table 8). Also the class-specific coiled-coil linker, a short motif that links the catalytic core of the motor domain to the coiled-coil region, is mostly identical in kinesin C and KCBPs and is diverged from other C-terminal KLPs (Fig

47). The class-specific cluster of residues in the kinesin motor domain is found in the neck linker and not within the catalytic core (Case *et al.*, 2000). Sequence analysis of the conserved neck regions generates a phylogenetic tree that reveals a clear clustering of related motors (Case *et al.*, 2000). Neck linker and neck region, not the location of the motor domain, are responsible for directional determination (Woehlke and Schliwa, 2000). Also kinesin C is grouped with KCBPs in a phylogenetic tree using the motor domain of all known kinesins in the analysis (Reddy, 2001). We can not exclude either of these possibilities based on our phylogenetic analysis and sequence similarity. However, we favor the second proposition and this is mainly because of very high sequence similarity between the motor domain of kinesin C and KCBP and the presence of CBD in both. Further functional characterization of kinesin C from organisms like sea urchin and KCBPs from lower photosynthetic eukaryotes like *Cyanophora* should help understand the evolution of these CaM -binding KLPs. Consistent with our hypothesis that many KLP subfamilies contain representatives in plants, fungi and animals and the members of the same subfamily have significant sequence similarity in the motor domain and perform similar functions, suggesting they may have evolved prior to divergence of plants, animal and fungi (Reddy, 2001). Furthermore, all KLP subfamilies (either C-terminal, N-terminal or internal) may have evolved from common ancestor KLP and diverged during the course of evolution to perform specific functions in different organisms. Kull *et al.*, (1998), used several criteria to evaluate the evolutionary relationships between motor proteins and concluded that the motor domain of kinesins and myosins may have evolved from an ancestral proto-motor by divergent evolution (Kull *et al.*, 1996; Kull *et al.*, 1998).

KCBP is unique to photosynthetic eukaryotes

Photosynthetic eukaryotic lineage has plastids and mitochondria but fungi and animal lineages have only mitochondria. FtsZ, found in nearly all prokaryotes, plays critical roles in cell divisions and usually accumulated at the furrow between dividing cells (Beech *et al.*, 2000). Although FtsZ does not share sequence similarity with tubulin, it is structurally related to tubulin (Beech *et al.*, 2000). In the chloroplasts of many phylogenetically diverged organisms, homologs of the bacterial FtsZ are essential components of organelle division (Osteryoung and Pyke, 1998; Strepp *et al.*, 1998). A homolog of bacterial FtsZ was cloned from the chromophyte alga *Mallomonas splendens* (MsFtsZ-mt) using FtsZ from bacteria as a probe. MsFtsZ-mt has a mitochondrial targeting signal and localizes to the middle and the edges of the dividing mitochondria as indicated by a specific antibody as well as GFP-fusion protein (Beech *et al.*, 2000). No potential mitochondrial FtsZ has been identified in the complete genomes of *C. elegans or S. cerevisiae* (Beech *et al.*, 2000). However, the distribution of MsFtsZ-mt is strikingly similar to that shown by Dnm1, a dynamin-related guanosine triphosphatase that regulates mitochondrial division in yeast and *C. elegans* (Bleazard *et al.*, 1999; Sesaki and Jensen, 1999). It is proposed that the FtsZ homologs are not present in the fungal and animal lineage and a dynamin-like protein has taken the role of FtsZ in mitochondrial division in those organisms (Beech *et al.*, 2000; Osteryoung, 2000). Similarly, KCBP may be present and evolved only in plants to perform a plant-specific function. Differences in cytoskeletal organization, especially MT arrays organization, between plants and animals should require specific motors and supports the uniqueness of KCBP to plants.

Structural features of KCBP suggest an interaction between MT and actin cytoskeleton

The N-terminal region of all KCBPs cloned from phylogenetically diverged photosynthetic eukaryotes shows significant similarities to the MyTH4 and talin-like regions present in myosin VIIa and X. These two regions have not been found in any other known members of the kinesin superfamily, suggesting that KCBP is a molecular hybrid consisting of a motor domain from MT-based motors and a tail region of actin-based motors (Reddy and Reddy, 1999). The existence of a talin-like region and a MyTH4 domain in KCBPs and actin-based motors (myosin VIIa and X) is interesting and suggest that these domains may have functional significance through interaction with the actin cytoskeleton or proteins that interact with myosins. KCBP and myosin could interact with some unknown protein(s) through their tail homology regions either to cross-bridge MT and actin filaments or to facilitate cargo exchange between these types of molecular motors (Reddy, 2001). Direct interactions of MT- and actin-based transport motors have been reported (Lillie and Brown, 1994; Brown, 1999; Huang *et al.*, 1999). The MT network is responsible for long-range transport of cellular components whereas the actin network is proposed to be used for local delivery (Sangfroid, 1995). For example, in sea urchins long-range Ca^{2+}-regulated transport of exocytotic vesicles requires a MT-based motor, whereas an actin-based motor is used for short-term transport (Bi *et al.*, 1997). Ponting, (1995) has noted that Af-6, a protein of unknown function, has a domain homologus to the tail of a monomeric kinesin, and a domain resembling the globular tail of class V myosin. The significance of this finding in not known (Longford and Molyneaux, 1998). It may simply reflect the common evolutionary origin of myosins and kinesins (Kull *et al.*, 1996) or indicate protein interaction between kinesin and

myosins. Although, the possibility that KCBP and myosins (VIIa and X) may interact with a common protein(s) is attractive, it seems unlikely because the lack of any myosins with MyTH4 and/or talin-like regions in the *Arabidopsis* genome (Reddy and Day, 2001). On the other hand, the talin-like region in KCBPs may be involved in anchoring the MT filaments to plasma membrane and talin has been shown to bind membranes (Girault *et al.*, 1998).

In plant cells there is some direct and indirect evidence indicates that there is cooperation between MTs and actin filaments during cell division and morphogenesis. In root hairs and pollen tubes, longitudinal cables of MTs and actin filaments extend along the length of the cell and are distributed throughout the cortex and endoplasm (Lancelle *et al.*, 1987; Cai *et al.*, 1997). Immunolocalization studies have shown that MTs are scarce in the apical dome of the angiosperms pollen tube (Huang *et al.*, 1993). However, in spruce pollen tube and protonema of ferns, MTs are enriched at elongating tips, where they form an array beneath the plasma membrane that is perpendicular to the direction of tube growth (Lazzaro, 1999). Treatment with cytoskeleton destabilizing agents showed that intact MTs and actin filaments are necessary for proper growth and positioning of cell contents in both pollen tubes and root hairs (Lazzaro, 1999). Analysis of the cytoskeleton of the *tangled1* (*tan1*) of maize, a mutant with a defect in the proper orientation of plain of cell division during cytokinesis, showed that both actin and MTs of the phragmoplast are essential for proper joining of the cell plate at the position predetermined by the proprophase band (Cleary and Smith, 1998). Furthermore, in guard cells, an interplay between Ca^{2+}, MTs and stomatal function was hypothesized (Marcus *et al.*, 2001) suggesting the involvement of a motor protein like KCBP in stomatal opening and closing. The Interaction between MTs and actins was observed also in phycoplasts forming organisms. *Chlamydomonas reinhardtii*, which

divides by an actin-myosin based cleavage furrow, has four rootlet MTs that emanate from the MT organizing center in a cross-shaped or cruciate pattern (Gaffel and S., 1990). During cytokinesis, the phycoplats originates from the four-membered rootlet MTs and forms perpendicularly to the spindle axis (Johnson and Porter, 1968; Gaffel and S., 1990; Schibler and Hunag, 1991). The cleavage furrow is positioned along the phycoplast and is correlated with the position of distal ends of the four membered rootlet MTs (Holmes and Dutcher, 1989). Disruption of rootlet and phycoplast MTs by MT destabilizing agents, oryzaline and vinblastin, caused abnormal distribution of actin and the failure of cytokinesis (Ehler and Dutcher, 1998). In untreated *Chlamydomonas* cells, actin and myosins were localized along the rootlet MTs and form a ring or half ring around the spindle in metaphase (Ehler *et al.*, 1995) and along the rootlets of the cleavage furrow during cytokinesis (Ehler and Dutcher, 1998). KCBP with MyTH4, talin like region and two MT-binding sites is an example of a molecular motor that can provide interaction between myosins and MTs. Further characterization of the N-terminal region of KCBP by different approaches as double immunolocalization with N-terminal specific antibody and actin antibodies, visualization of KCBP in live cells using green fluorescent protein, (GFP) and the yeast-two hybrid screen with the N-terminal tail should help understanding the possible roles of these specific domains and the functional significance of this highly conserved N-terminal tail in photosynthetic organisms. Preliminary results have showed the binding of KCBP to actin filaments (Kao *et al.*, 2000).

KCBP is important for cell morphogenesis

Genetic screening of *Arabidopsis* plants that have altered trichomes indicates a role for KCBP in trichome morphogenesis (Oppenheimer *et al.*, 1997). Mutation in the

AtKCBP/ZWI cause a failure of the *Arabidopsis* trichomes to branch properly resulting in a two-branched trichome with a greatly shorted stalk (Huelskamp *et al.*, 1994; Folkers *et al.*, 1997; Oppenheimer *et al.*, 1997). How does KCBP/ZWI influence trichome branching? Trichome branching requires localized cell wall expansion, and in plant cells cortical MT arrays are implicated in cell expansion by controlling the orientation of newly synthesized cellulose microfibrils (Giddings and Staehelin, 1991; Lloyd, 1994; Nicol and Hofte, 1998; Kost *et al.*, 1999). MT reorientation can be accomplished by either depolymerization or polymerization of MTs or movement of exciting MTs (Reddy and Day, 2000). Since KCBP/ZWI is a MT motor and required for branching , it might be involved in reorientation of MTs, thereby directing the deposition of cellulose microfibrils. The two MT-binding sites on KCBP/ZWI, its ability to bundle MTs, and its minus-end motor activity support the idea that it is likely to participate in MT reorganization and directing the transport of secretary vesicles to regions of localized growth (Narasimhulu and Reddy, 1998; Kao *et al.*, 2000; Reddy and Day, 2000). Another possibility for the role of KCBP in trichome branching is that the two MT-binding sites of KCBP and/or KCBP-interacting protein(s) are responsible for stabilization of the MTs (Mathur and Chua, 2000). The supporting evidence is that using paclitaxol, a known MT stabilizer, *zwi* mutants can be induced to form growth points indicative of branch formation (Mathur and Chua, 2000). Visualization of KCBP and MT organization in wild-type and *zwi* mutants during different stages of trichome development using GFP should help us understand the role of KCBP in trichome morphogenesis. All of the *zwi* mutants grow normally with only the defect in trichome morphogenesis observed (Oppenheimer *et al.*, 1997; Krishnakumar and Oppenheimer, 1999). Trichomes are well characterized in angiosperms including monocots and dicots and there are reports about their

existence in some ferns like *Dennstaedtia cicutaris,* but of course, they are not present in lower eukaryotes like green algae or *Cyanophora.* This raises the question: Does KCBP has functions other than trichome morphogenesis? If yes, what are the other functions and if no, why KCBP is highly conserved even the in lower photosynthetic eukaryotes and is not present in fungi and animals. Most likely, KCBP function is redundant in other cells whereas in trichomes the other kinesins with functional overlap with KCBP might not be expressed or they might not substitute for KCBP function in trichomes. Several reports indicate that the function of many kinesins in-non plant systems are redundant (Reddy, 2001).

KCBP function in cell division

Cytokinesis in animal cells, unlike in plant cells, involves furrowing of the plasma membrane between daughter nuclei (Smith, 1999). Based on the processes associated with cytokinesis, whether the nuclear envelope breaks down or not, cell division in plants is divided into two major types. The first has a "closed, fenestrated" spindle (i.e., the nuclear envelope remains intact throughout mitosis, except for polar holes or fenestrations through which MTs enter the prophase nucleus) and a "phycoplast", an array of MTs, whose distinguishing feature is that the MTs are oriented in the plane of cytokinesis (Pickett-Heaps, 1976). Rhodophyta, Chlorophyta and some members of Ulvophyta have this kind of cell division (Stewart and Mattox, 1984). The second kind of cell division is characterized by open spindles (the nuclear envelope disperses during mitosis) with spindle MTs persisting perpendicular to the plane of cytokinesis. This arrays of MTs, called the phragmoplast, is important in laying the new cell wall between daughter cells. The Charaphyta and land plants have this second type of cell division. In Glaucophyta (e.g. *Cyanophora*) a MT array was observed in late telophase between daughter nuclei, and it is not clear whether these MTs

form a phycoplast or a phragmoplast (Pickett-Heaps, 1976). Most likely this MT array is a phycoplast based on the fact that red algae and some green algae have phycoplasts.

Immunolocalization and microinjection studies with KCBP antibodies have showed that KCBP is localized to the preprophase band, the phragmoplast, the mitotic spindle, and the cell plate (Bowser and Reddy, 1997; Smirnova *et al.*, 1998; Vos *et al.*, 2000). Furthermore, the expression is regulated in a cell-cycle-dependent manner with the highest levels in the M-phase (Bowser and Reddy, 1997). KCBP is a minus-end directed motor protein with two MT-binding sites, so it can cross-link MTs and moves towards the minus ends, thereby focusing the ends into poles and providing the MT focusing activity required for pole formation in plant cells that lack centrosomes. Spindle convergence is a characteristic feature of other C-terminal KLPs such as XCTK2 and Ncd (Matthies *et al.*, 1996). (Walczak *et al.*, 1998) showed that XICTK2 plays a role in focusing the spindle poles. A similar function has been proposed for Ncd in *Drosophila* oocytes (Matthies *et al.*, 1996, Moore, 1996). Although KCBP, a minus-end motor, shows prominent association with the phragmoplast, it is not likely to be involved in transporting vesicles to the cell plate since the MT in the phragmoplast are oriented with their plus ends facing cell plate. However, a possible function of KCBP is recycling of the Golgi vesicles membranes from the expanding cell plate, a process which requires a minus-end directed motor protein (Reddy, 2001). Furthermore, KCBP may also be involved in forming the phragmoplast by cross-linking MTs, a property associated with C-terminal motors in yeast and animals (McDonald and Goldstein, 1990; Chandra *et al.*, 1993; Endow *et al.*, 1994a). A few other members of the kinesin family have been localized to the phragmoplasts: a plus-end-directed MT motor, TKRP125 (Asada and Shibaoka, 1994; Asada *et al.*, 1997), and minus-end-

directed MT motor, KATA (Liu *et al.*, 1996). AtPAKRP1, an amino terminal KLP, localized to the phragmoplast MT array near the future cell plate during cytokinesis (Lee and Liu, 2000). Recently, another plus-end motor, DcKRP120-2, belong to Bim-C subfamily was cloned from carrot cells and strongly decorates the phragmoplast mid-line where the plus-end of MTs overlap (Barroso *et al.*, 2000). None of these proteins were localized to the vesicles suggesting other motors are involved in vesicle motility. What is the difference between the role of KCBP and other C-terminal KLPs in cell division? KCBP is possibly function in cell division through Ca^{2+} amplitude signals via CaM. Presence of CBD and the regulation of KCBP affinity by Ca^{2+}/CaM support this hypothesis. There is considerable indirect data pointing to a regulatory role for Ca^{2+} in cell division (Lambert and Vantard, 1986; Zhang *et al.*, 1990). It has been shown that a rise in cytosolic Ca^{2+} follows anaphase onset in stamen hair cells and correlates directly with the velocity of chromosomes separation during anaphase (Hepler and Callaham, 1987; Zhang *et al.*, 1990). Also injection of Ca^{2+} under conditions that stimulate modest amount of kinetochore MT depolymerization can accelerate chromosome motion during anaphase by two fold (Zhang *et al.*, 1992). On the other hand, injection of BAPTA buffers, which can reduce local Ca^{2+} gradient, markedly slow cell plate expansion. Application of caffeine, an alkaloid thought to modulate Ca^{2+} levels, also affects cytokinesis by blocking late stages of phragmoplast expansion, leading to inhibition of cell plate formation (Valster and Hepler, 1997). These studies indicate that Ca^{2+} gradients play a central regulatory role in cell division and some of these effects are likely mediated by CaM through CBDs like KCBP (Reddy and Day, 2001). In support of this, microinjection of Ca^{2+}-saturated CaM causes the disruption of mitosis in dividing cells and injection of CAPP1-CaM, a competitive antagonist of CaM, leads to mitotic inhibition (Keith, 1987).

Visualization of the cytoskeleton along with MT and actin disruption studies has suggested a variety of roles for cytoskeletal filaments in the formation and positioning of new cell wall. Phragmoplast MTs and actin filaments are both essential for cytokinesis but appear to play different roles. The data available suggest a role for MTs in guiding vesicle movement to the cell plate, and for F-actin in stabilization and consolidation of cell plate as well guidance of phragmoplasts to established cortical division sites. Identification and functional analysis of molecules interacting with cytoskeletal filaments in dividing cells could substantially advance our understanding of their functions in cytokinesis. For example, identification of motor protein on the surface of cell plate vesicles could clarify the contributions of MTs and actin filaments to vesicle transport (Smith, 1999).

In summary, using molecular approaches I cloned and characterized KCBP homologs from phylogenetically diverged photosynthetic eukaryotes. Analyses of structural organization of KCBP genes have shown that KCBP with its characteristic domains is conserved among all studied organisms, suggesting its origin along with or prior to the evolution of plastids. KCBPs from all studied organisms were detected by affinity-purified KCBP antibody to the CBD, suggesting the topology conservation of their CBDs. Although the coding sequences are highly conserved, the intervening sequences are highly diverged. KCBP from different organism has been cloned into bacterial expression vectors and the expressed protein was shown to bind CaM in a Ca^{2+}-dependent manner. Cloning of KCBP homologs from other representative organisms and their further characterization especially the amino terminal region is needed to understand the plant-specific roles of KCBP. From the result presented here, together with what is known about KCBP, I conclude that KCBP with its unique domains present in all photosynthetic eukaryotes. Its presence in algae and

glaucophyta strongly support roles in processes other than trichome morphogenesis. Based on immnuolocalization and microinjection studies in flowering plants, it is likely that KCBP has one or more roles in cell division in all photosynthetic eukaryotes. These role, most likely, involve Ca^{2+} and CaM regulation as well as interaction with actin or actin-interacting proteins.

REFERENCES

Abdel-Ghany, S., Kugrens, P., and Reddy, A.S.N. (2000). CpKLP1: A calmodulin-binding kinesin-like protein from *Cyanophora paradoxa* (Glaucophyta). J Phycol. **36,** 686-692.

Abdel-Ghany, S., and Reddy, A.S.N. (2000). A novel calcium/calmodulin-regulated microtubule motor protein is highly conserved between monocots and dicots. DNA and Cell Biology. **19,** 567-578.

Adam, D. (2000). Now for the hard ones. Nature. **408,** 792-793.

Aitken, A., and Stanier, R.Y. (1979). Characterization of peptidoglycan from the cyanelles of *Cyanophora paradoxa.* J. Gen. Microbiol. **112,** 218-223.

Allen, T. (1971). Multivariate approaches to the ecology of algae on terrestrial rock surface in North Vales. J. Ecol. **59,** 803-826.

An, S.S., Mopps, B., Weber, K., and Bhattacharya, D. (1999). The origin and evolution of green algal and plant actins. Mol. Biol. Evol. **16,** 275-85.

Asada, T., and Collings, D. (1997). Molecular motors in higher plants. Trends Plant Sci. **2,** 29-37.

Asada, T., Kuriyama, R., and Shibaoka, H. (1997). TKRP125, a kinesin-related protein involved in the centrosome-independent organization of the cytokinetic apparatus in tobacco BY-2 cells. J. Cell Sci. **110,** 179-189.

Asada, T., and Shibaoka, H. (1994). Isolation of polypeptides with microtubule-translocating activity from phragmoplasts of tobacco BY-2 cells. J. Cell Sci. **107,** 2249-2257.

Asada, T., Sonobe, S., and Shibaoka, H. (1991). Microtubule translocation in the cytokinetic apparatus of cultured tobacco cells. Nature. **350,** 238-241.

Ausubel, F., Brent, R., Kingston, R., Moore, D., Seidman, J., Smith, J., and Struhl, K. (Ed.). (1987). Current Protocols in Molecular Biology. (New York: John Wiley and Sons).

Bagavathi, S., and Malathi, R. (1996). Introns and protein revolution-an analysis of the exon/intron organisation of actin genes. FEBS Lett. **392,** 63-65.

Barkman, T.J., Chenery, G., McNeal, J.R., Lyons-Weiler, J., Ellisens, W.J., Moore, G., Wolfe, A.D., and dePamphilis, C.W. (2000). From the cover: independent and combined

analyses of sequences from all three genomic compartments converge on the root of flowering plant phylogeny. Proc. Natl. Acad. Sci. U S A. **97,** 13166-13171.

Barroso, C., Chan, J., Allan, V., Doonan, J., Hussey, P., and Lloyd, C. (2000). Two kinesin-related proteins associated with the cold-stable cytoskeleton of carrot cells: characterization of a novel kinesin, DcKRP120-2. Plant J. **24,** 859-868.

Barton, N.R., and Goldstein, L.S.B. (1996). Going mobile: Microtubule motors and chromosome segregation. Proc. Natl. Acad. Sci. USA. **93,** 1735-1742.

Baskin, T.I., and Cande, W.Z. (1990). The structure and function of the mitotic spindle in flowering plants. Annu. Rev. Plant Physiol. Plant Mol. Biol. **41,** 277-315.

Beech, P.L., Nheu, T., Schultz, T., Herbert, S., Lithgow, T., Gilson, P.R., and McFadden, G.I. (2000). Mitochondrial FtsZ in a chromophyte alga. Science. **287,** 1276-1279.

Bhattacharya, D., and Medlin, L. (1995). The phylogeny of plastids: a review based on comparison of small-subunit ribosomal RNA coding regions. J. Phycol. **31,** 489-498.

Bhattacharya, D., and Medlin, L. (1998). Algal phylogeny and the origin of land plants. Plant Physiol. **116,** 1-7.

Bhattacharya, D., and Weber, K. (1997). The actin gene of the glaucocystophyte *Cyanophora paradoxa*: analysis of the coding region and introns, and an actin phylogeny of eukaryotes. Curr. Genet. **31,** 439-446.

Bhattacharya, D., Weber, K., An, S.S., and Berning-Koch, W. (1998). Actin phylogeny identifies *Mesostigma viride* as a flagellate ancestor of the land plants. J Mol. Evol. **47,** 544-550.

Bi, G.Q., Morris, R.L., Liao, G., Alderton, J.M., Scholey, J.M., and Steinhardt, R.A. (1997). Kinesin- and myosin-driven steps of vesicle recruitment for Ca^{2+}-regulated exocytosis. J Cell Biol. **138,** 999-1008.

Bibikova, T.N., Blancaflor, E.B., and Gilroy, S. (1999). Microtubules regulate tip growth and orientation in root hairs of *Arabidopsis* thaliana. Plant J. **17,** 657-665.

Bleazard, W., McCaffery, J.M., King, E.J., Bale, S., Mozdy, A., Tieu, Q., Nunnari, J., and Shaw, J.M. (1999). The dynamin-related GTPase Dnm1 regulates mitochondrial fission in yeast. Nat. Cell Biol. **1,** 298-304.

Bloom, G.S., and Endow, S.A. (1994). Motor proteins 1: Kinesins. Protein profile. **1,** 1059-1116.

Bloom, G.S., Wagner, M.C., Pfister, K.K., and Brady, S.T. (1988). Native structure and physical properties of bovine brain kinesin and identification of the ATP-binding subunit polypeptide. Biochemistry. **27,** 3409-4316.

Bowser, J., and Reddy, A.S.N. (1997). Localization of a kinesin-like calmodulin-binding protein in dividing cells of *Arabidopsis* and tobacco. Plant J. **12,** 1429-1438.

Brady, S.T. (1985). A novel brain ATPase with properties expected for the fast axonal transport motor. Nature. **317,** 73-75.

Brady, S.T. (1995). A kinesin medley: Biochemical and functional heterogeneity. Trends Cell Biol. **5,** 159-164.

Brook, A. (1968). The discoloration of roofs in the United State and Canada by algae. J. Phycol. **4,** 250-263.

Brown, J.W.S., Smith, P., and Simpson, C.G. (1996). *Arabidopsis* consensus intron sequences. Plant Mol. Biol. **32,** 531-535.

Brown, S.S. (1999). Cooperation between microtubule- and actin-based motor proteins. Ann. Rev. Cell Dev. Biol. **15,** 63-80.

Cai, G., Bartalesi, A., Del Casino, C., Moscatelli, A., Tiezzi, A., and Cresti, M. (1993). The kinesin-immunoreactive homologue from *Nicotiana tabacum* pollen tubes: Biochemical properties and subcellular localization. Planta. **191,** 496-506.

Cai, G., Moscatelli, A., and Cresti, M. (1997). Cytoskeletal organization and pollen tube growth. Trends Plant Sci. **2,** 86-91.

Cai, G., Romagnoli, S., Moscatelli, A., Ovidi, E., Gambellini, G., Tiezzi, A., and Cresti, M. (2000). Identification and characterization of a novel microtubule-based motor associated with membranous organelles in tobacco pollen tubes. Plant Cell. **12,** 1719-1736.

Case, R.B., Pierce, D.W., Hom-Booher, N., Hart, C.L., and Vale, R.D. (1997). The directional preference of kinesin motors is specified by an element outside of the motor catalytic domain. Cell. **90,** 959-966.

Case, R.B., Rice, S., Hart, C.L., Ly, B., and Vale, R.D. (2000). Role of the kinesin neck linker and catalytic core in microtubule-based motility. Curr. Biol. **10,** 157-160.

Cavalier-Smith, T. (1982). The origin of plastids. Biol. J. LINN. Soc. **17,** 289-306.

Cavalier-Smith, T. (1987). The simultaneous symbiotic origin of mitochondria, chloroplasts, and microbodies. Ann N Y Acad. Sci. **503,** 55-71.

Cavalier-Smith, T. (1995). Zooflagellate phylogeny and classification. Tsitologiia. **37,** 1010-1029.

Cavalier-Smith, T. (2000). Membrane heredity and early chloroplast evolution. Trends Plant Sci. **5,** 174-182.

Chan, J., Rutten, T., and Lloyd, C. (1996). Isolation of microtubule-associated proteins from carrot cytoskeletons: a 120 kDa map decorates all four microtubule arrays and the nucleus. Plant J. **10,** 251-259.

Chandra, R., and Endow, S.A. (1993). Expression of microtubule motor proteins in bacteria for charcteriztion in *in vitro* motility assays. In Methods in Cell Biol., L. Wilson & P. Matsudaira., Eds., (Academic Press, Inc : New York), pp. 115-128.

Chandra, R., Salmon, E.D., Erickson, H.P., Lockhart, A., and Endow, S.A. (1993). Structural and functional domains of the *Drosophila* ncd microtubule motor protein. J. Biol. Chem. **268,** 9005-9013.

Chen, Z.-Y., Hasson, T., Kelley, P.M., Schwender, B.J., Schwartz, M.F., Ramakrishnan, M., Kimberling, W.J., Mooseker, M.S., and Corey, D.P. (1996). Molecular cloning and domain structure of human myosin-VIIa, the gene product defective in usher syndrome 1B. Genomics. **36,** 440-448.

Chisholm, D. (1989). A convenient moderate-scale procedure for obtaining DNA from bacteriophage Lambda. BioTechniques. **7,** 21-23.

Cleary, A.L., and Smith, L.G. (1998). The Tangled1 gene is required for spatial control of cytoskeletal arrays associated with cell division during maize leaf development. Plant Cell. **10,** 1875-1888.

Collins, K., Sellers, J.R., and Matsudaira, P.T. (1990). Calmodulin dissociation regulates brush border myosin-I (110K-calmodulin) activity in vitro. J. Cell Biol. **110,** 1137-1147.

Consortium, T.C.S. (1998). Genome sequence of the nematode C. elegans: a platform for investigating biology. The *C. elegans* sequencing consortium. Science. **282,** 2012-2018.

Craik, C.S., Rutter, W.J., and Fletterick, R. (1983). Splice junctions: association with variation in protein structure. Science. **220,** 1125-1129.

Cyr, R.J. (1991). Calcium/calmodulin affects microtubule stability in lysed protoplasts. J. Cell Sci. **100,** 311-317.

Daniels, C.J., Gupta, R., and Doolittle, W.F. (1985). Transcription and excision of a large intron in the tRNATrp gene of an archaebacterium, *Halobacterium volcanii*. J Biol. Chem. **260,** 3132-3134.

Day, I.S., Miller, C., Golovkin, M., and Reddy, A.S.N. (2000). Interaction of a kinesin-like calmodulin-binding protein with a protein kinase. J. Biol. Chem. **275,** 13737-13745.

Deavours, B.E., Reddy, A.S., and Walker, R.A. (1998a). Ca^{2+}/calmodulin regulation of the *Arabidopsis* kinesin-like calmodulin- binding protein. Cell Motil. Cytoskeleton. **40,** 408-416.

Deavours, B.E., Reddy, A.S.N., and Walker, R.A. (1998b). Ca^{2+}/calmodulin regulation of the *Arabidopsis* kinesin-like calmodulin- binding protein. Cell Motil. Cytoskeleton. **40,** 408-416.

deJesus, M. (1989). Taxonomic distribution of copper-zinc superoxide dismutase in green algae and its phylogenetic importance. J. Phycol. **25,** 767-772.

Desai, A., Verma, S., Mitchison, T.J., and Walczak, C.E. (1999). Kin I kinesins are microtubule-destabilizing enzymes. Cell. **96,** 69-78.

Deutsch, M., and Long, M. (1999). Intron-exon structures of eukaryotic model organisms. Nucleic Acids Res. **27,** 3219-3228.

Donoghue, M.J., and Doyle, J.A. (2000). Seed plant phylogeny: Demise of the anthophyte hypothesis? Curr. Biol. **10,** R106-9.

Doolittle, R.F., and Bork, P. (1993). Evolutionary mobile modules in proteins. Sci. Amer. **269,** 50-56.

Doree, M., and Picard, A. (1980). Release of Ca^{2+} from intracellular pools stops cytoplasmic streaming in Tradescantia stamen hair cells. Experienta. **36,** 1291-1292.

Doyle, J.A. (1998). Molecules, morphology, fossils, and the relationship of angiosperms and Gnetales. Mol. Phylogenet Evol. **9,** 448-462.

Ehler, L.L., and Dutcher, S.K. (1998). Pharmacological and genetic evidence for a role of rootlet and phycoplast microtubules in the positioning and assembly of cleavage furrows in *Chlamydomonas reinhardtii*. Cell Motil. Cytoskeleton. **40,** 193-207.

Ehler, L.L., Holmes, J.A., and Dutcher, S.K. (1995). Loss of spatial control of the mitotic spindle apparatus in a *Chlamydomonas reinhardtii* mutant strain lacking basal bodies. Genetics. **141,** 945-960.

Endow, S.A. (1999). Determinants of molecular motor directionality. Nature Cell Biol. **1,** E163-E167.

Endow, S.A., Chandra, R., Komma, D.J., Yamamota, A.H., and Salmon, E.D. (1994a). Mutants of the *Drosophila* ncd microtubule motor protein cause centrosomal and spindle pole defects in mitosis. J. Cell Sci. **107,** 859-867.

Endow, S.A., and Hatsumi, M. (1991). A multimember kinesin gene family in *Drosophila.* Proc. Nat. Acad. Sci. USA. **88,** 4424-4427.

Endow, S.A., Henikoff, S., and Soler-Niedziela, L. (1990). Mediation of meiotic and early mitotic chromosome segregation in *Drosophila* by a protein related to kinesin. Nature. **345,** 81-83.

Endow, S.A., and Higuchi, H. (2000). A mutant of the motor protein kinesin that moves in both directions on microtubules. Nature. **406,** 913-6.

Endow, S.A., Kang, S.J., Satterwhite, L.L., Rose, M.D., Skeen, V.P., and Salmon, E.D. (1994b). Yeast Kar3 is a minus-end microtubule motor protein that destabilizes microtubules preferentially at the minus ends. EMBO J. **13,** 2708-2713.

Endow, S.A., and Komma, D.J. (1996). Centrosome and spindle function of the *Drosophila* Ncd microtubule motor visualized in live embryos using Ncd-GFP fusion proteins. J. Cell Sci. **109,** 2429-2442.

Endow, S.A., and Waligora, K.W. (1998). Determinants of kinesin motor polarity. Science. **281,** 1200-1202.

Euteneur, U., Jackson, W.T., and McIntosh, J.R. (1982). Polarity of spindle microtubules in *Haemanthus* endosperm. J. Cell Biol. **94,** 644-653.

Falson, P. (1992). Improved phenol-based method for the isolation of DNA fragments from low melting temperature agarose gels. BioFeedback. **13,** 120-121.

Fan, J., Griffiths, A.D., Lockhart, A., Cross, R.A., and Amos, L.A. (1996). Microtubule minus ends can be labelled with a phage display antibody specific to alpha-tubulin. J. Mol. Biol. **259,** 325-330.

Fan, M., Chen, L.C., Ragan, M.A., Gutell, R.R., Warner, J.R., Currie, B.P., and Casadevall, A. (1995). The 5S rRNA and the rRNA intergenic spacer of the two varieties of *Cryptococcus neoformans.* J Med. Vet. Mycol. **33,** 215-221.

Fey, J., and Marechal-Drouard, L. (1999). Compilation and analysis of plant mitochondrial promoter sequences: An illustration of a divergent evolution between monocot and dicot mitochondria. Biochem. Biophys. Res. Commun. **256,** 409-414.

Fisher, D.D., Gilroy, S., and Cyr, R.J. (1996). Evidence for opposing effects of calmodulin on cortical microtubules. Plant Physiol. **112,** 1079-1087.

Folkers, U., Berger, J., and Hulskamp, M. (1997). Cell morphogenesis of trichomes in *Arabidopsis*: differential control of primary and secondary branching by branch initiation regulators and cell growth. Development. **124,** 3779-3786.

Fordham-Skelton, A.P., Safadi, F., Golovkin, M., and Reddy, A.S.N. (1994). A non-radioactive method for isolating complementary DNAs encoding calmodulin-binding proteins. Plant Mol. Biol. Reptr. **12,** 355-363.

Fowler, J.E., and Quatrano, R.S. (1997). Plant cell morphogenesis: plasma membrane interactions with the cytoskeleton and cell wall. Annu. Rev. Cell. Dev. Biol. **13,** 697-743.

Franklin, A.E., and Cande, W.Z. (1999). Nuclear organization and chromosome segregation. Plant Cell. **11,** 523-534.

Frederick, S., Gruber, P., and Tolbert, N. (1973). The occurrence of glycolate dehydrogenase and glycolate oxidase in green plants. Plant Physiol. **52,** 318-323.

Frugoli, J.A., McPeek, M.A., Thomas, T.L., and McClung, C.R. (1998). Intron loss and gain during evolution of the catalase gene family in angiosperms. Genetics. **149,** 355-365.

Fuchs, E., and Cleveland, D.W. (1998). A structural scaffolding of intermediate filaments in health and disease. Science. **279,** 514-519.

Gaffel, G.P., and S., E.-G. (1990). Elucidation of the engima of the "metaphase band" of *Chlamydomans reinhardtii*. Protoplasma. **156,** 139-148.

Gauger, A.K., and Goldstein, L.S. (1993). The *Drosophila* kinesin light chain. Primary structure and interaction with kinesin heavy chain. J. Biol. Chem. **268,** 13657-13666.

Giddings, T.H., and Staehelin, L.A. (1991). Microtubule-mediated control of microfibril deposition: A reexamination of the hypothesis. In The Cytoskeletal Basis of Plant Growth and Form, C. W. Lloyd., Eds., (Academic Press : New York), pp. 85-89.

Gilson, P.R., and McFadden, G.I. (1996). The miniaturized nuclear genome of eukaryotic endosymbiont contains genes that overlap, genes that are cotranscribed, and the smallest known spliceosomal introns. Proc. Natl. Acad. Sci. USA. **93,** 7737-7742.

Girault, J.A., Labesse, G., Mornon, J.P., and Callebaut, I. (1998). Janus kinases and focal adhesion kinases play in the 4.1 band: A superfamily of band 4.1 domains important for cell structure and signal transduction. Mol. Med. **4,** 751-769.

Goddard, R.H., Wick, S.M., Silflow, C.D., and Snustad, D.P. (1994). Microtubule components of the plant cell cytoskeleton. Plant Physiol. **104,** 1-6.

Goffeau, A., Barrell, B.G., Bussey, H., Davis, R.W., Dujon, B., Feldmann, H., Galibert, F., Hoheisel, J.D., Jacq, C., Johnston, M., Louis, E.J., Mewes, H.W., Murakami, Y., Philippsen, P., Tettelin, H., and Oliver, S.G. (1996). Life with 6000 genes. Science. **274,** 546, 563-567.

Goldstein, L.S.B. (1993). With apologies to Scheherazade: Tails of 1001 kinesin motors. Annu. Rev. Genet. **27,** 319-351.

Goldstein, L.S.B., and Philip, A.V. (1999). The road less traveled: Emerging principles of kinesin motor utilization. Annu. Rev. Cell Dev. Biol. **15,** 141-183.

Golovkin, M., and Reddy, A.S.N. (1996). Structure and expression of a plant U1 snRNP 70K gene: Alternative splicing of U1 snRNP 70K pre-mRNAs produces two different transcripts. Plant Cell. **8,** 1421-1435.

Goodall, G.J., Kiss, T., and Filipowicz, W. (1991). Nuclear RNA splicing and small nuclear RNAs and their genes in higher plants. Oxford Surv. of Plant Mol. & Cell Biol. **7,** 255-296.

Goodson, H.V., Kang, S.J., and Endow, S.A. (1994). Molecular phylogeny of the kinesin family of microtubule motor proteins. J. Cell Sci. **107,** 1875-1884.

Goremykin, V., Bobrova, V., Pahnke, J., Troitsky, A., Antonov, A., and Martin, W. (1996). Noncoding sequences from the slowly evolving chloroplast inverted repeat in addition to rbcL data do not support gnetalean affinities of angiosperms. Mol. Biol. Evol. **13,** 383-396.

Graham, L. (1993). Origin of land plants (John Wiely and Sons,. New York).

Graham, L., Macentee, F., and Bold, H. (1981). An investigation of some subaerial green algae. Texas J. Sci. **33,** 13-16.

Graham, S.W., and Olmstead, R.G. (2000). Utility of 17 chloroplast genes for inferring the phylogeny of the basal angiosperms. Am. J. Bot. **87,** 1712-1730.

Granger, C.L., and Cyr, R.J. (2001). Use of abnormal preprophase bands to decipher division plane determination. J. Cell Sci. **114,** 599-607.

Gunning, B.E., and Wick, S.M. (1985). Preprophase bands, phragmoplasts, and spatial control of cytokinesis. J. Cell Sci. Suppl. **2,** 157-179.

Gunning, B.E.S. (1982). The cytokinetic apparatus: Its development and spatial regulation. In The Cytoskeleton in Plant Growth and Development, C. W. Lloyd., Eds., (Academic Press: London), pp. 229-292.

Hall, W., and Claus, G. (1963). Ultrastructural studies on the blue-green algal symbiont in *Cyanophora paradoxa* Korschikoff. J. Cell Biol. **18,** 551-563.

Hasson, T., and Mooseker, M.S. (1995). Molecular motor, membrane movements and physiology: emerging roles for myosins. Curr. Opin. Cell Biol. **7,** 587-594.

Hatsumi, M., and Endow, S.A. (1992). Mutants of the microtubule motor protein, nonclaret disjunctional, affect spindle structure and chromosome movement in meiosis and mitosis. J Cell Sci. **101,** 547-559.

Hawkins, J.D. (1988). A survey on intron and exon lengths. Nucleic Acids Res. **16,** 9893-908.

Henningsen, U., and Schliwa, M. (1997). Reversal in the direction of movement of a molecular motor. Nature. **389,** 93-95.

Hepler, P.K., and Callaham, D.A. (1987). Free calcium increases during anaphase in stamen hair cells of *Tradescantia*. J. Cell Biol. **105,** 2137-2143.

Hepler, P.K., and Jackson, W.K. (1968). Microtubules and early stages of cell-plate formation in the endosperm of *Haemanthus katherinae* Baker. J. Cell Biol. **38,** 437-446.

Hickey, D.A., and Benkel, B. (1986). Introns as relict retrotransposons: implications for the evolutionary origin of eukaryotic mRNA splicing mechanisms. J. Theor. Biol. **121,** 283-291.

Hirokawa, N. (1998). Kinesin and dynein superfamily proteins and the mechanism of organelle transport. Science. **279,** 519-526.

Hirokawa, N., Pfister, K., Yorifuji, H., Wagner, M., Brady, S., and Bloom, G. (1989). Submolecular domains of bovine brain kinesin identified by electron microscopy and monoclonal antibody decoration. Cell. **56,** 867-878.

Holcik, M., Sonenberg, N., and Korneluk, R.G. (2000). Internal ribosome initiation of translation and the control of cell death. Trends Genet. **16,** 469-473.

Holmes, J.A., and Dutcher, S.K. (1989). Cellular asymmetry in *Chlamydomonas reinhardtii*. J Cell Sci. **94,** 273-285.

Huang, B.Q., Pierson, E.S., Russell, S.D., Tiezzi, A., and Cresti, M. (1993). Cytoskeletal organisation and modification during pollen tube arrival, gamete delivery and fertilisation in *Plumbago zeylanica*. Zygote. **1,** 143-154.

Huang, J.D., Brady, S.T., Richards, B.W., Stenolen, D., Resau, J.H., Copeland, N.G., and Jenkins, N.A. (1999). Direct interaction of microtubule- and actin-based transport motors. Nature. **397,** 267-270.

Huelskamp, M., Misra, S., and Jurgens, G. (1994). Genetic dissection of trichome cell development in *Arabidopsis*. Cell. **76,** 555-566.

Huelskamp, M., Schnittger, A., and Folkers, U. (1999). Pattern formation and cell differentiation: Trichomes in *Arabidopsis* as a genetic model system. Int. Rev. Cytol. **186,** 147-178.

Hulskamp, M. (2000). How plants split hairs. Curr. Biol. **10,** R308-310.

Hulskamp, M., and Schnittger, A. (1998). Spatial regulation of trichome formation in *Arabidopsis thaliana*. Semin. Cell. Dev. Biol. **9,** 213-220.

Jacobshagen, S., and Schnarrenberger, C. (1990). Two class I aldolases in *KLebsomidium flaccidum* (Charaphyceae): an evolutionary link from chlorophytes to higher plants. J. Phycol. **26,** 312-317.

James, P., Vorherr, T., and Carafoli, E. (1995). Calmodulin-binding domains: Just two faced or multifaceted. Trends Biochem. Sci. **20,** 38-42.

Johnson, H.B. (1975). Plant pubescence: An ecological perspective. Bot. Rev. **41,** 233-258.

Johnson, U.G., and Porter, K.R. (1968). Fine structure of cell division in *Chlamydomonas reinhardtii*. J. Cell Biology. **38,** 403-425.

Jurgens, M., Hepler, L.H., Rivers, B.A., and Hepler, P.K. (1994). BAPTA-calcium buffers modulate cell plate formation in stamen hairs of Tradescantia: evidence for calcium gradients. Protoplasma. **183,** 86-99.

Kao, Y.-L., Deavours, B.E., Phelps, K.K., Walker, R., and Reddy, A.S.N. (2000). Bundling of microtubules by motor and tail domains of a kinesin-like calmodulin-binding protein from *Arabidopsis*: Regulation by Ca^{2+}/calmodulin. Biochem. Biophys. Res. Commun. **267,** 201-207.

Keeling, P.J., Deane, J.A., Hink-Schauer, C., Douglas, S.E., Maier, U.G., and McFadden, G.I. (1999). The secondary endosymbiont of the cryptomonad *Guillardia theta* contains alpha-, beta-, and gamma-tubulin genes. Mol. Biol. Evol. **16,** 1308-1313.

Keith, C.H. (1987). Effect of microinjected calcium-calmodulin on mitosis in PtK_2 cells. Cell Motil. **7,** 1-9.

Kenrick, P., and Crane, P. (1997). The origin and early evolution of plants on land. Nature. **389,** 33-39.

Kies, L. (1979). Zur systematischen Einordnung von *Cyanophora paradox*, *Gleochaete wittrockiana* und *Glaucocystis nostochinearum*. Ber. Dtsch. Bot. Ges. **92,** 445-454.

Kies, L., and Kremer, B. (1986). Typification of the Glaucocystophyta. Taxon. **35,** 128-133.

Kikuyama, M., and Tazawa, M. (1982). Ca^{2+} ion reversibly inhibits the cytoplasmic streaming of *Nitella*. Protoplasma. **113,** 241-243.

Kim, A.J., and Endow, S.A. (2000). A kinesin family tree. J. Cell Sci. **113,** 3681-3682.

King, S.M. (2000). The dynein microtubule motor. Biochim. Biophys. Acta. **1496,** 60-75.

Kirschner, M., and Mitchison, T. (1986). Beyond self-assembly: from microtubules to morphogenesis. Cell. **45,** 329-342.

Kohler, S., Delwiche, C.F., Denny, P.W., Tilney, L.G., Webster, P., Wilson, R.J., Palmer, J.D., and Roos, D.S. (1997). A plastid of probable green algal origin in *Apicomplexan parasites*. Science. **275,** 1485-9.

Kost, B., Mathur, J., and Chua, N.-H. (1999). Cytoskeleton in plant development. Curr. Opin. Plant Biol. **2,** 462-470.

Kost, B., Spielhofer, P., and Chua, N.H. (1998). A GFP-mouse talin fusion protein labels plant actin filaments in vivo and visualizes the actin cytoskeleton in growing pollen tubes. Plant J. **16,** 393-401.

Kozielski, F., Sack, S., Marx, A., Thormahlen, M., Schonbrunn, E., Biou, V., Thompson, A., Mandelkow, E.M., and Mandelkow, E. (1997). The crystal structure of dimeric kinesin and implications for microtubule-dependent motility. Cell. **91,** 985-94.

Kranz, H.D., Miks, D., Siegler, M.L., Capesius, I., Sensen, C.W., and Huss, V.A. (1995). The origin of land plants: phylogenetic relationships among charophytes, bryophytes, and vascular plants inferred from complete small-subunit ribosomal RNA gene sequences. J. Mol. Evol. **41,** 74-84.

Krishnakumar, S., and Oppenheimer, D.G. (1999). Extragenic suppressors of the *Arabidopsis* zwi-3 mutation identify new genes that function in trichome branch formation and pollen tube growth. Development. **126,** 3079-3088.

Kriventseva, E.V., and Gelfand, M.S. (1999). Statistical analysis of the exon-intron structure of higher and lower eukaryote genes. J. Biomol. Struct. Dyn. **17,** 281-288.

Kropf, D.L., Bisgrove, S.R., and Hable, W.E. (1998). Cytoskeletal control of polar growth in plant cells. Curr. Opin. Cell Biol. **10,** 117-122.

Kugrens, P. (2001). Structure and phylogeny of *Cyanophora species*. In Symbiosis, J. e. Seckbach., Ed., (Kluwer Academic Publishers : Dordrecht, Netherlands), pp. (In press).

Kugrens, P., Clay, B., and Meyer, C. (1999). Ultrastructure and description of *Cyanophora biloba*, sp. nov., with additional observations on *C. paradoxa* (Glaucophyta). JH. Phycol. **35,** 844-854.

Kull, F.J., Sablin, E.P., Lau, R., Fletterick, R.J., and Vale, R.D. (1996). Crystal structure of the kinesin motor domain reveals a structural similarity to myosin. Nature. **380,** 550-555.

Kull, F.J., Vale, R.D., and Fletterick, R.J. (1998). The case for a common ancestor: kinesin and myosin motor proteins and G proteins. J. Muscle Res. Cell Motil. **19,** 877-886.

Kumar, S., and Rzhetsky, A. (1996). Evolutionary relationships of eukaryotic kingdoms. J. Mol. Evol. **42,** 183-193.

Kuriyama, R., Kofron, M., Essner, R., Kato, T., Dragas-Granoic, S., Omoto, C.K., and Khodjakov, A. (1995). Characterization of a minus end-directed kinesin-like motor protein from cultured mammalian cells. J. Cell Biol. **129,** 1049-1059.

Kusakabe, R., Satoh, N., Holland, L.Z., and Kusakabe, T. (1999). Genomic organization and evolution of actin genes in the *amphioxus Branchiostoma* belcheri and Branchiostoma floridae. Gene. **227,** 1-10.

Kuznetsov, S.A., Vaisberg, E.A., Shanina, N.A., Magretova, N.N., Chernyak, V.Y., and Gelfand, V.I. (1988). The quaternary structure of bovine brain kinesin. EMBO J. **7,** 353-356.

Lambert, A.M., and Vantard, M. (1986). Calcium and calmodulin as regulators of chromosome movements during mitosis in higher plants. In Molecular and Cellular Aspects of Calcium in Plant Development, A. J. Trewavas., Eds., (Plenum: New York), pp. 175-183.

Lancelle, S.A., Cresti, M., and Hepler, P.K. (1987). Ultrastructure of the cytoskeleton in freeze-substituted pollen tubes of *Nicotiana alata*. Protoplasma. **140,** 141-150.

Langford, G.M. (1995). Actin- and microtubule-dependent organelle motors: interrelationships between the two motility systems. Curr. Opin. Cell. Biol. **7,** 82-88.

Lazzaro, M.D. (1999). Microtubule organization in germinated pollen of the conifer Picea abies (*Norway spruce*, Pinaceae). Am. J. Bot. **86,** 759.763.

Lee, R.E. (1999). Phycology (Cambridge, University press, Cambridge).

Lee, Y.-R.J., and Liu, B. (2000). Identification of a phragmoplast-associated kinesin-related protein in higher plants. Curr. Biol. **10,** 797-800.

Leopold, P.L., McDowall, A.W., Pfister, K.K., Bloom, G.S., and Brady, S.T. (1992). Association of kinesin with characterized membrane-bounded organelles. Cell Motil. Cytoskeleton. **23,** 19-33.

Li, W., and Grauer, D. (1991). Fundamentals of molecular evolution. (Sinauer, Sunderland, Mass.).

Lillie, S.H., and Brown, S.S. (1994). Immunofluorescence localization of the unconventional myosin, Myo2p, and the putative kinesin-related protein, Smy1p, to the same regions of polarized growth in *Saccharomyces cerevisiae*. J. Cell Biol. **125,** 825–842.

Liu, B., Cyr, R.J., and Palevitz, B.A. (1996). A kinesin-like protein, KatAp, in the cells of *Arabidopsis* and other plants. Plant Cell. **8,** 119-132.

Liu, G.-Q., Cai, G., Del Casino, C., Tiezzi, A., and Cresti, M. (1994). Kinesin-related polypeptide is associated with vesicles from *Corylus avellana* pollen. Cell Motil. Cytoskel. **29,** 155-166.

Lloyd, C. (1994). Why should stationary plant cells have such dynamic microtubules? Mol. Biol. Cell. **5,** 1277-80.

Longford, G.M., and Molyneaux, B. (1998). Myosin V in the brain: mutation lead to neurological defects. Brain Res. Rev. **28,** 1-8.

Luo, D., and Oppenheimer, D.G. (1999). Genetic control of trichome branch number in *Arabidopsis*: the roles of FURCA loci. Development. **126,** 5547-5557.

Lupas, A., Van Dyke, M., and Stock, J. (1991). Predicting coiled coils from protein sequences. Science. **252,** 1162-1164.

Marcus, A.I., Moore, R.C., and Cyr, R.J. (2001). The Role of Microtubules in Guard Cell Function. Plant Physiol. **125,** 387-395.

Marks, D.M. (1977). Molecular genetic analysis of trichome developement in *Arabidopsis*. Ann. Rev. Plant Physiol. Plant Mol. Biol. **48,** 137-163.

Martin, W. (1998). Gene transfer to the nucleus and the evolution of chloroplasts. Nature. **393,** 162-165.

Martin, W., Gierl, A., and Saedler, H. (1989). Molecular evidence for pre-Cretaceous angiosperm origins. Nature. **339,** 46-48.

Martin, W., and Herrmann, R. (1999). Gene transfer from organelles to the nucleus: how much, what happen and why? Plant Physiol. **118,** 9-17.

Mathews, S., and Donoghue, M.J. (1999). The root of angiosperm phylogeny inferred from duplicate phytochrome genes. Science. **286,** 947-50.

Mathur, J., and Chua, N.H. (2000). Microtubule stabilization leads to growth reorientation in *Arabidopsis* trichomes. Plant Cell. **12,** 465-477.

Mathur, J., Spielhofer, P., Kost, B., and Chua, N. (1999). The actin cytoskeleton is required to elaborate and maintain spatial patterning during trichome cell morphogenesis in *Arabidopsis thaliana*. Development. **126,** 5559-5568.

Matthies, H.J.G., McDonald, H.B., Goldstein, L.S.B., and Theurkauf, W.E. (1996). Anastral meiotic spindle morphogenesis: role of the nonclaret disjunctional kinesin-like protein. J. Cell Biol. **134,** 455-464.

Matthies, H.J.G., Miller, R.J., and Palfrey, H.C. (1993). Calmodulin binding to and cAMP-dependent phosphorylation of kinesin light chains modulate kinesin ATPase activity. J. Biol. Chem. **268,** 11176-11187.

McCarthy, A.D., Goldring, J.P., and Hardie, D.G. (1983). Evidence that the multifunctional polypeptides of vertebrate and fungal fatty acid synthases have arisen by independent gene fusion events. FEBS Lett. **162,** 300-4.

McDonald, H.B., and Goldstein, L.S.B. (1990). Identification and characterization of a gene encoding a kinesin-like protein in *Drosophila*. Cell. **61,** 991-1000.

Meluh, P.B., and Rose, M.D. (1990). *KAR3*, a kinesin-related gene required for yeast nuclear fusion. Cell. **60,** 1029-1041.

Mereschkowsky, C. (1910). Theorie der zwei Plasmaarten als Grundlage der Symbiogenesis, einer neuen Lehre von der Entstehung der Organismen. Biologisches Centralblatt. **30,** 278-303, 321-347, 353-367.

Mermall, V., Post, P.L., and Mooseker, M.S. (1998). Unconventional myosins in cell movement, membrane traffic, and signal transduction. Science. **279,** 527-533.

Meyer, C. (1997) The ultrastructure of *Cyanophora Biloba* sp. nov. (Glaucophyta) from an alpine pond in Colorado and new details on *Cyanophora paradoxa*. M.Sc, Colorado State University.

Miller, D.D., Lancelle, S.A., and Hepler, P.K. (1996). Actin microfilament do not form a dense meshwork in Lilium longiflorum pollen tube tips. Protoplasma. **195,** 123-132.

Mishler, B.D. (1994). Cladistic analysis of molecular and morphological data. Am. J. Phys. Anthropol. **94,** 143-156.

Mitchison, T., and Kirschner, M. (1984). Dynamic instability of microtubule growth. Nature. **312,** 237-42.

Mitchison, T.J. (1993). Localization of an exchangeable GTP binding site at the plus end of microtubules. Science. **261,** 1044-1047.

Mitsui, H., Nakatani, K., Yamaguchi-Shinozaki, K., Shinozaki, K., Nishikawa, K., and Takahashi, H. (1994). Sequencing and characterization of the kinesin-related genes *katB* and *katC* of *Arabidopsis thaliana*. Plant Mol. Biol. **25,** 865-876.

Mitsui, H., Yamaguchi-Shinozaki, K., Shinozaki, K., Nishikawa, K., and Takahashi, H. (1993). Identification of a gene family (*kat*) encoding kinesin-like proteins in *Arabidopsis thaliana* and the characterization of secondary structure of KatA. Mol. Gen. Genet. **238,** 362-368.

Moniz de Sa, M., and Drouin, G. (1996). Phylogeny and substitution rates of angiosperm actin genes. Mol. Biol. Evol. **13,** 1198-1212.

Moore, J.D., and Endow, S.A. (1996). Kinesin proteins: a phylum of motors for microtubule-based motility. BioEssays. **18,** 207-219.

Mooseker, M.S., and Cheney, R.E. (1995). Unconventional myosins. Annu. Rev. Cell Dev. Biol. **11,** 633-675.

Moreira, D., Le Guyader, H., and Phillippe, H. (2000). The origin of red algae and the evolution of chloroplasts. Nature. **405,** 69-72.

Mountain, V., and Compton, D.A. (2000). Dissecting the role of molecular motors in the mitotic spindle. Anat. Rec. **261,** 14-24.

Murashige, T., and F., S. (1962). Revised medium for rapid growth and bioassays with tobacco tissue culture. Physiol. Plant. **15,** 473-497.

Murray, M.G., and Thompson, W.F. (1980). Rapid isolation of high molecular weight plant DNA. Nucleic Acids Res. **8,** 4321-5.

Narasimhulu, S.B., Kao, Y.-L., and Reddy, A.S.N. (1997). Interaction of *Arabidopsis* kinesin-like calmodulin-binding protein with tubulin subunits: Modulation by Ca^{2+}-calmodulin. Plant J. **12,** 1139-1149.

Narasimhulu, S.B., and Reddy, A.S.N. (1998). Characterization of microtubule binding domains in the *Arabidopsis* kinesin-like calmodulin-binding protein. Plant Cell. **10,** 957-965.

Navone, F., Niclas, J., Hom-Booher, N., Sparks, L., Bernstein, H.D., McCaffrey, G., and Vale, R.D. (1992). Cloning and expression of a human kinesin heavy chain gene: Interaction

of the COOH-terminal domain with cytoplasmic microtubules in transfected CV-1 cells. J. Cell Biol. **117,** 1263-1275.

Nelissen, B., Van de Peer, Y., Wilmotte, A., and De Wachter, R. (1995). An early origin of plastids within the cyanobacterial divergence is suggested by evolutionary trees based on complete 16S rRNA sequences. Mol. Biol. Evol. **12,** 1166-1173.

Nicol, F., and Hofte, H. (1998). Plant cell expansion: scaling the wall. Curr. Opin. Plant Biol. **1,** 12-17.

Oppenheimer, D.G. (1998). Genetics of plant cell shape. Curr. Opin. Plant. Biol. **1,** 520-524.

Oppenheimer, D.G., Pollock, M.A., Vacik, J., Szymanski, D.B., Ericson, B., Feldmann, K., and Marks, D. (1997). Essential role of a kinesin-like protein in *Arabidopsis* trichome morphogenesis. Proc. Natl. Acad. Sci. USA. **94,** 6261-6266.

Osteryoung, K. (2000). Organell fission. Crossing the evolutionary divide. Plant Physiol. **123,** 1213-1216.

Osteryoung, K.W., and Pyke, K.A. (1998). Plastid division: evidence for a prokaryotically derived mechanism. Curr. Opin. Plant. Biol. **1,** 475-479.

Palmer, J.D. (2000). A single birth of all plastids? Nature. **405,** 32-33.

Parducz, B. (1967). Ciliary movement and coordination in ciliates. Int. Rev. Cytol. **21,** 91-128.

Paterson, A., Lan, T., Reischmann, K., Chang, C., Lin, Y., Liu, S., Burow, M., Kowalski, S., Katsar, C., DelMonte, T., Feldmann, K., Schertz, K., and Wendel, J. (1996). Toward a unified genetic map of higher plants, transcending the monocot-dicot divergence. Nature genetics. **14,** 380-382.

Perazza, D., Herzog, M., Hulskamp, M., Brown, S., Dorne, A.M., and Bonneville, J.M. (1999). Trichome cell growth in *Arabidopsis thaliana* can be derepressed by mutations in at least five genes. Genetics. **152,** 461-76.

Pickett-Heaps, J. (1976). Cell division in eukaryotic algae. BioScience. **26,** 445-450.

Pidoux, A.L., and Cande, W.Z. (1993). pk11: a kinesin-like protein from *Schizosaccharomyces pombe*, which localises to the mitotic spindle. Mol. Biol. Cell. **4,** 243a.

Ponting, C.P. (1995). AF-6/cno: neither a kinesin nor a myosin, but a bit of both. Trends. Biochem. Sci. **20,** 265-266.

Poovaiah, B.W., McFadden, J.J., and Reddy, A.S.N. (1987). The role of calcium ions in gravity signal perception and transduction. Physiol. Plant. **71,** 401.

Poovaiah, B.W., and Reddy, A.S.N. (1987). Calcium messenger system in plants. CRC Cri. Rev. Plant Sci. **6,** 47-103.

Poovaiah, B.W., and Reddy, A.S.N. (1993). Calcium and signal transduction in plants. CRC Cri. Rev. Plant Sci. **12,** 185-211.

Poovaiah, B.W., Takezawa, D., An, G., and Han, T.J. (1996). Regulated expression of a calmodulin isoform alters growth and development in potato. J. Plant Physiol. **149,** 553-558.

Porter, J.A., Yu, M., Doberstein, S.K., Pollard, T.D., and Montell, C. (1993). Dependence of calmodulin localization in the retina on the NINAC unconventional myosin. Science. **262,** 1038-1042.

Prescott, G. (1951). Algae of the Western Great lakes area. (Bloomfield Hills, MIch.).

Raghothama, K.G., Mizrahi, Y., and Poovaiah, B.W. (1985). Effect of calmodulin antagonists on auxin-induced elongation. Plant Physiol. **79,** 28-33.

Rahman, A., Friedman, D.S., and Goldstein, L.S. (1998). Two kinesin light chain genes in mice. Identification and characterization of the encoded proteins. J. Biol. Chem. **273,** 15395-15403.

Reddy, A.S.N. (2001). Calcium: silver bullet in signaling. Plant Sci. **160**, 381-404

Reddy, A.S.N. (2001). Molecular motors and their functions in plants. Intl. Rev. Cytol. & Cell Biol. **204**, 97-178

Reddy, A.S.N., and Day, I. (2001). Analysis of kinesins in the *Arabidopsis thaliana* genome. Plant Physiol. Submitted.

Reddy, A.S.N., and Day, I.S. (2000). The role of the cytoskeleton and a molecular motor in trichome morphogenesis. Trends Plant Sci. **5,** 503-505.

Reddy, A.S.N., Narasimhulu, S.B., and Day, I.S. (1998). Structural organization of a gene encoding a novel calmodulin-binding kinesin-like protein from *Arabidopsis*. Gene. **204,** 195-200.

Reddy, A.S.N., Narasimhulu, S.B., Safadi, F., and Golovkin, M. (1996a). A plant kinesin heavy chain-like protein is a calmodulin-binding protein. Plant J. **10,** 9-21.

Reddy, A.S.N., Safadi, F., Narasimhulu, S.B., Golovkin, M., and Hu, X. (1996b). A novel plant calmodulin-binding protein with a kinesin heavy chain motor domain. J. Biol. Chem. **271,** 7052-7060.

Reddy, V., and Reddy, A.S.N. (1999). A plant calmodulin-binding motor is part kinesin and part myosin. Bioinformatics. **15,** 1055-1057.

Reddy, V.S., Safadi, F., Zielinski, R.E., and Reddy, A.S.N. (1999). Interaction of a kinesin-like protein with calmodulin isoforms from *Arabidopsis*. J Biol Chem. **274,** 31727-31733.

Reith, M., and Munholland, J. (1993). The ribosomal RNA repeats are non-identical and directly oriented in the chloroplast genome of the red alga *Porphyra purpurea*. Curr. Genet. **24,** 443-450.

Rhoads, A.R., and Friedberg, F. (1997). Sequence motifs for calmodulin recognition. FASEB J. **11,** 331-340.

Robb, D.L., Heasman, J., Raats, J., and Wylie, C. (1996). A kinesin-like protein is required for germplasm aggregation in *Xenopus*. Cell. **87,** 823-831.

Rodriguez-Trelles, F., Tarrio, R., and Ayala, F.J. (2000). Evidence for a high ancestral GC content in *Drosophila*. Mol. Biol. Evol. **17,** 1710-1717.

Rogers, G.C., Hart, C.L., Wedman, K.P., and Scholey, J.M. (1999). Identification of kinesin-C, a calmodulin-binding carboxy-terminal kinesin in animal (*Strongylocentrotus purpuratus*) cells. J. Mol. Biol. **294,** 1-8.

Sablin, E.P. (2000). Kinesins and microtubules: their structures and motor mechanisms. Curr. Opin. Cell Biol. **12,** 35-41.

Sablin, E.P., Case, R.B., Dai, S.C., Hart, C.L., Ruby, A., Vale, R.D., and Fletterick, R.J. (1998). Direction determination in the minus-end-directed kinesin motor ncd. Nature. **395,** 813-816.

Sack, S., Kull, F.J., and Mandelkow, E. (1999). Motor proteins of the kinesin family. Structures, variations, and nucleotide binding sites. Eur. J. Biochem. **262,** 1-11.

Sack, S., Muller, J., Marx, A., Thormahlen, M., Mandelkow, E.M., Brady, S.T., and Mandelkow, E. (1997). X-ray structure of motor and neck domains from rat brain kinesin. Biochemistry. **36,** 16155-16165.

Safadi, F., Reddy, V., and Reddy, A.S.N. (2000). A pollen-specific novel calmodulin-binding protein with tetratricopeptide repeats. J. Biol. Chem. **275,** 35457-35470.

Saido, T.C., Shibata, M., Takenawa, T., Murofushi, H., and Suzuki, K. (1992). Positive regulation of μ-calpain action by polyphosphoinositides. J. Biol. Chem. **267,** 24585-24590.

Saito, N., Okada, Y., Noda, Y., Kinoshita, Y., Kondo, S., and Hirokawa, N. (1997). KIFC2 is a novel neuron-specific C-terminal type kinesin superfamily motor for dendritic transport of multivesicular body-like organelles. Neuron. **18,** 425-438.

Sambrook, J., Fritsch, F.F., and Maniatis, T. (1989). Molecular cloning-A laboratory manual (Cold Spring Harbor Laboratory, New York).

Samigullin, T.K., Martin, W.F., Troitsky, A.V., and Antonov, A.S. (1999). Molecular data from the chloroplast rpoC1 gene suggest a deep and distinct dichotomy of contemporary spermatophytes into two monophyla: gymnosperms (including Gnetales) and angiosperms. J. Mol. Evol. **49,** 310-315.

Saunders, W., Hornack, D., Lengyel, V., and Deng, C. (1997). The *Saccharomyces cerevisiae* kinesin-related motor Kar3p acts at preanaphase spindle poles to limit the number and length of cytoplasmic microtubules. J. Cell. Biol. **137,** 417-431.

Sawin, K.E., and Endow, S.A. (1993). Meiosis, mitosis and microtubule motors. BioEssays. **15,** 399-407.

Schibler, M.J., and Hunag, B. (1991). The col ^{R}4 and col ^{R}15 β-tubulin mutations in *Chlamydomonas reinhardtii* confer sensitivity to microtubule inhibitors and herbicides by enhancing microtubule stability. J. Cell Biology. **113,** 605-614.

Schwab, B., Folkers, U., Ilgenfritz, H., and Hulskamp, M. (2000). Trichome morphogenesis in *Arabidopsis*. Philos. Trans. R. Soc. Lond. B. Biol. Sci. **355,** 879-883.

Schweizer, H.P., and Datta, P. (1989). Identification and DNA sequence of tdcR, a positive regulatory gene of the tdc operon of *Escherichia coli*. Mol. Gen. Genet. **218,** 516-522.

Seiler, S., Kirchner, J., Horn, C., Kallipolitou, A., Woehlke, G., and Schliwa, M. (2000). Cargo binding and regulatory sites in the tail of fungal conventional kinesin. Nat. Cell Biol. **2,** 333-338.

Sesaki, H., and Jensen, R.E. (1999). Division versus fusion: Dnm1p and Fzo1p antagonistically regulate mitochondrial shape. J Cell Biol. **147,** 699-706.

Shah, D.M., Hightower, R.C., and Meagher, R.B. (1983). Genes encoding actin in higher plants: intron positions are highly conserved but the coding sequences are not. J. Mol. Appl. Genet. **2,** 111-26.

Shimmen, T., and Yokota, E. (1994). Physiological and biochemical aspects of cytoplasmic streaming. Int. Rev. Cytol. **155,** 97-140.

Sidow, A., and Thomas, W.K. (1994). A molecular evolutionary framework for eukaryotic model organisms. Curr Biol. **4,** 596-603.

Smirnova, E., Reddy, A.S.N., Bowser, J., and Bajer, A.S. (1998). A minus end-directed kinesin-like motor protein, KCBP, localizes to anaphase spindle poles in Haemanthus endosperm. Cell Motil. Cytoskeleton. **41,** 271-280.

Smirnova, E.A., and Bajer, A.S. (1994). Microtubule converging centers and reorganization of the interphase cytoskeleton and the mitotic spindle in higher plant Haemanthus. Cell Motil Cytoskeleton. **27,** 219-33.

Smith, L.G. (1999). Divide and Conquer: cytokinesis in plant cells. Curr. Opi. Plant Biol. **2,** 447-453.

Smith, M.W., Freng, D.F., and Doolittle, R.F. (1992). Evolution by acquisition: the case for horizontal gene transfer. Trends Biochem. Sci. **17,** 489-493.

Snedden, W.A., and Fromm, H. (1998). Calmodulin, calmodulin-related proteins and plant responses to the environment. Trends Plant Sci. **3,** 299-304.

Soltis, D.E., Mort, M.E., Soltis, P.S., Hibsch-Jetter, C., Zimmer, E.A., and Morgan, D. (1999). Phylogenetic relationships of the enigmatic angiosperm family podostemaceae inferred from 18S rDNA and rbcL sequence data. Mol. Phylogenet. Evol. **11,** 261-272.

Song, H., Golovkin, M., Reddy, A.S.N., and Endow, S.A. (1997). *In vitro* motility of AtKCBP, a calmodulin-binding kinesin-like protein of *Arabidopsis*. Proc. Natl. Acad. Sci. USA. **94,** 322-327.

Staehelin, L.A., and Hepler, P.K. (1996). Cytokinesis in higher plants. Cell. **84,** 821-824.

Stewart, K.D., and Mattox, K.R. (1984). The case for a polyphyletic origin of mitochondria: morphological and molecular comparisons. J. Mol. Evol. **21,** 54-57.

Stewart, R.J., Thaler, J.P., and Goldstein, L.S.B. (1993). Direction of microtubule movement is an intrinsic property of the motor domains of kinesin heavy chain and *Drosophila* ncd protein. Proc. Nat. Acad. Sci. USA. **90,** 5209-5213.

Stiller, J.W., and Hall, B.D. (1997). The origin of red algae: implications for plastid evolution. Proc. Natl. Acad. Sci. USA. **94,** 4520-4525.

Stoltzfus, A., Logsdon, J.M., Palmer, J.D., and Doolittle, W.F. (1997). Intron & quot; sliding& quot; and the diversity of intron positions. Proc. Natl. Acad. Sci. USA. **94,** 10739-10744.

Strepp, R., Scholz, S., Kruse, S., Speth, V., and Reski, R. (1998). Plant nuclear gene knockout reveals a role in plastid division for the homolog of the bacterial cell division protein FtsZ, an ancestral tubulin. Proc. Natl. Acad. Sci. USA. **95,** 4368-4373.

Swofford, D.L. (1993). PAUP: Phylogenetic Analysis Using Parsimony 3.1.1. Computer program distributed by the Illinois Natural History Survey, Champaign, Illinois

Sylvester, A.W. (2000). Division decisions and the spatial regulation of cytokinesis. Curr. Opin. Plant Biol. **3,** 58-66.

Szymanski, D.B., Lloyd, A.M., and Marks, D.M. (2000). Progress in the molecular genetic analysis of the trichome initiation and morphogenesis in *Arabidopsis*. Trends Plant Sci. **5,** 214-219.

Szymanski, D.B., Marks, D.M., and Wick, S.M. (1999). Organized F-actin is essential for normal trichome morphogenesis in *Arabidopsis*. Plant Cell. **11,** 2331-2348.

Tamura, K., Nakatani, K., Mitsui, H., Ohashi, Y., and Takahashi, H. (1999). Characterization of katD, a kinesin-like protein gene specifically expressed in floral tissues of *Arabidopsis thaliana*. Gene. **230,** 23-32.

Tandre, K., Albert, V.A., Sundas, A., and Engstrom, P. (1995). Conifer homologues to genes that control floral development in angiosperms. Plant Mol. Biol. **27,** 69-78.

Thomas, T.R. (2001) Interaction of a kinesin-like calmodulin-binding protein with a novel EF-hand-containing putative calcium-binding protein. M.Sc. Colorado State University.

Tiezzi, A., Moscatelli, A., Cai, G., Bartalesi, A., and Cresti, M. (1992). An immunoreactive homolog of mammalian kinesin in *Nicotiana tabacum* pollen tubes. Cell Motil. Cytoskel. **21,** 132-137.

Torres-Ruiz, R.A., and Jurgens, G. (1994). Mutations in the FASS gene uncouple pattern formation and morphogenesis in *Arabidopsis* development. Development. **120,** 2967-2978.

Traas, J., Bellini, C., Nacty, P., Kornenberger, J., Bouchez, D., and Caboche, M. (1995). Normal differentiation patterns in plants lacking microtubular preprophase bands. Nature. **375,** 676-677.

Tschermak-Woess, E. (1988). Handbook of Lichenology (CRC Press, Boca Raton, Fla).
Vale, R.D. (1987). Intracellular transport using microtubule-based motors. Ann. Rev. Cell Biol. **3,** 347-378.

Vale, R.D. (1996). Switches, latches and amplifiers: Common themes of G proteins and molecular motors. J. Cell Biol. **135,** 291-302.

Vale, R.D., Case, R., Sablin, E., Hart, C., and Fletterick, R. (2000). Searching for kinesin's mechanical amplifier. Philos. Trans. R. Soc. Lond. B. Biol. Sci. **355,** 449-457.

Vale, R.D., and Fletterick. R, J. (1997). The design plan of kinesin motors. Annu. Rev. Cell Dev. Biol. **13,** 745–777.

Vale, R.D., and Goldstein, L.S.B. (1990). One motor, many tails: An expanding repertoire of force-generating enzymes. Cell. **60,** 883-885.

Vale, R.D., and R.J., F. (1997). The design plan of kinesin motors. Annu. Rev. Cell Dev. Biol. **13,** 745–77.

Vale, R.D., Reese, T.S., and Sheetz, M.P. (1985). Identification of a novel force-generating protein, kinesin, involved in microtubule-based motility. Cell. **42,** 39-50.

Valster, A.H., and Hepler, P.K. (1997). Caffeine inhibition of cytokinesis: Effect on the phragmoplast cytoskeleton in living *Tradescantia* stamen hair cells. Protoplasma. **201,** 158-171.

van der Velden, A.W., and Thomas, A.A. (1999). The role of the 5' untranslated region of an mRNA in translation regulation during development. Int. J. Biochem. Cell Biol. **31,** 87-106.

Vinogradov, A.E. (2001). Intron Length and Codon Usage. J. Mol. Evol. **52,** 2-5.

Vos, J.W., Safadi, F., Reddy, A.S., and Hepler, P.K. (2000). The Kinesin-like calmodulin binding protein is differentially involved in cell division. Plant Cell. **12,** 979-990.

Walczak, C.E., Vernos, I., Mitchison, T.J., Karsenti, E., and Heald, R. (1998). A model for the proposed roles of different microtubule-based motor proteins in establishing spindle bipolarity. Curr. Biol. **8,** 903-913.

Walker, M.L., Burgess, S.A., Sellers, J.R., Wang, F., Hammer, J.A., Trinick, J., and Knight, P.J. (2000). Two-headed binding of a processive myosin to F-actin. Nature. **405,** 804-7.

Walker, R.A., O'Brien, E.T., Pryer, N.K., Soboeiro, M.F., Voter, W.A., Erickson, H.P., and Salmon, E.D. (1988). Dynamic instability of individual microtubules analyzed by video light microscopy: rate constants and transition frequencies. J. Cell Biol. **107,** 1437-1448.

Walker, R.A., Salmon, E.D., and Endow, S.A. (1990). The Drosophila claret segregation protein is a minus-end directed motor molecule. Nature. **347,** 780-782.

Wang, D.Y., Kumar, S., and Hedges, S.B. (1999). Divergence time estimates for the early history of animal phyla and the origin of plants, animals and fungi. Proc. R. Soc. Lond. B. Biol. Sci. **266,** 163-171.

Wang, W., Takezawa, D., Narasimhulu, S.B., Reddy, A.S.N., and Poovaiah, B.W. (1996). A novel kinesin-like protein with a calmodulin-binding domain. Plant Mol. Biol. **31,** 87-100.

Waters, E.R., and Vierling, E. (1999). The diversification of plant cytosolic small heat shock proteins preceded the divergence of mosses. Mol. Biol. Evol. **16,** 127-139.

White, O., Soderlund, C., Shanmugan, P., and Fields, C. (1992). Information contents and dinucleotide compositions of plant intron sequences vary with evolutionary origin. Plant Mol. Biol. **19,** 1057-1064.

Wick, S.M. (1991). Spatial aspects of cytokinesis in plant cells. Curr. Opin. Cell Biol. **3,** 253-260.

Woehlke, G., and Schliwa, M. (2000). Directional motility of kinesin motor proteins. Biochim. Biophys. Acta. **1496,** 117-127.

Wolenski, J.S. (1995). Regulation of calmodulin-binding myosins. Trends Cell Biol. **5,** 310-316.

Wolenski, J.S., Hayden, S.M., Forscher, P., and Mooseker, M.S. (1993). Calcium-calmodulin and regulation of brush border myosin-I MgATPase and mechanochemistry. J. Cell Biol. **122,** 613-621.

Wolfe, K., Gouy, M., Yang, Y., Sharp, P., and Li, W. (1989). Date of the monocot-dicot divergence estimated from chloroplast DNA sequence data. Proc. Natl. Acad. Sci. USA. **86,** 6201-6205.

Wolfe, K.H., Morden, C.W., and Palmer, J.D. (1992). Small single-copy region of plastid DNA in the non-photosynthetic angiosperm *Epifagus virginiana* contains only two genes. Differences among dicots, monocots and bryophytes in gene organization at a non-bioenergetic locus. J. Mol. Biol. **223,** 95-104.

Woods, C.M., Polito, V.S., and Reid, M.S. (1984). Response to chilling stress in plant cells. II. Redistribution of intracellular calcium. Protoplasma. **121,** 17-24.

Yamamoto, A.H., Komma, D.J., Shaffer, C.D., Pirrotta, V., and Endow, S.A. (1989). The claret locus in Drosophila encodes products required for eye color and for meiotic chromosome segregation. EMBO J. **8,** 3543–3552.

Yang, J.T., Laymon, R.A., and Goldstein, L.S.B. (1989). A three-domain structure of kinesin heavy chain revealed by DNA sequence and microtubule binding analyses. Cell. **56,** 879-889.

Yang, J.T., Saxton, W.M., Stewart, R.J., Raff, E.C., and Goldstein, L.S.B. (1990). Evidence that the head of kinesin is sufficient for force generation and motility *in vitro*. Science. **249,** 42-47.

Yang, T., Segal, G., Abbo, S., Feldman, M., and Fromm, H. (1996). Characterization of the gene family in wheat: structure, chromosomal location, and evolutionary aspects. Mol. Gene. Genet. **252,** 684-694.

Yokota, E., Muto, S., and Shimmen, T. (1999). Inhibitory regulation of higher-plant myosin by Ca^{2+} ions. Plant Physiol. **119,** 231-240.

Yoon, C. (1999). Evolutionary biologists have at least answered a question so difficult that Darwin himself called it the "abominable mystery". New York Times, A1, A26.

Zhang, D.H., Callaham, D.A., and Hepler, P.K. (1990). Regulation of anaphase chromosome motion in *Tradescantia* stamen hair cells by calcium and related signaling agents. J. Cell Biol. **111,** 171-182.

Zhang, D.H., Wadsworth, P., and Hepler, P.K. (1992). Modulation of anaphase spindle microtubule structure in stamen hair cells of Tradescantia by calcium and related agents. J. Cell Sci. **102,** 79-89.

Zhou, Y.H., and Ragan, M.A. (1995). The nuclear gene and cDNAs encoding cytosolic glyceraldehyde-3-phosphate dehydrogenase from the marine red alga *Gracilaria verrucosa*: cloning, characterization and phylogenetic analysis. Curr. Genet. **28,** 324-32.

Zielinski, R.E. (1998). Calmodulin and calmodulin-binding proteins in plants. Ann. Rev. Plant Physiol. Plant Mol. Biol. **49,** 697-725.